Indian Journal of Natural Sciences www.tnsroindia.org.in ©IJONS

Vol.8 / Issue 49 / August /2018 *International Bimonthly* *ISSN: 0976 – 0997*

REVIEW ARTICLE

Marker Assisted Selection (MAS), A New Hope for Modern Breeding

Kanaka K K[1]*, Chethan Raj R[1], Jeevan C[2], Bhanuprakash A G[1], N G Sagar[1], Rajendra Prasad[1], Balraj S[1], Sneha Smitha Panda[1] and Mitek Tarang[1]

[1]Indian Veterinary Research Institute, Izatnagar, Utter Pradesh, India.
[2]National Dairy Research Institute, Karnal, Haryana, India.

Received: 09 May 2018 Revised: 15 Jun 2018 Accepted: 19 July 2018

***Address for Correspondence**
Kanaka K K
Indian Veterinary Research Institute,
Izzatnagar, Utter Pradesh, India.
Email : kkokay07@gmail.com

ABSTRACT

Marker assisted selection or marker aided selection (MAS) is an indirect selection process where a trait of interest is selected based on a marker linked to a trait of interest (e.g. productivity, disease resistance, a biotic stress tolerance, and quality), rather than on the trait itself. This process has been extensively researched and proposed for plant and animal breeding. Here we combine marker information and conventional selection to select the elite individual for further breeding programme. The majority of MAS work in the present era uses DNA-based markers which includes microsatellites, restriction fragment length polymorphism (RFLP), random amplification of polymorphic DNA (RAPD), amplified fragment length polymorphism (AFLP), and single nucleotide polymorphisms (SNPs). Here we dealt different types, methods and other aspects of marker assisted selection.

Key words: Marker, Selection, Linkage, Polymorphism.

INTRODUCTION

The potential benefits of using marker linked to genes of interest in breeding programmers' thus moving from phenotype based selection to genotype based selection have been obvious for many decades, however, the realization of this potential has been limited by the lack of markers .Before the advent of the molecular techniques we have made a larger improvement in the potentialities of our livestock, by the conventional breeding programmers'. But they have some limitations which we can address by the application of molecular based techniques and thus accelerating the gains we obtain through selection. Selection with the help of markers turned to be one of the recent developments in selection and breeding of livestock, in which we combine both conventional selection and marker information. DNA level, molecular genetics has given us the tools to make those opportunities a reality.

Selection is the process of giving preference to a certain individual in a population to reproduce than other individuals that are denied the opportunity to produce their next generation i.e., 'non random differential mating' (Lerner, 1958).**'**Marker assisted selection' which is also known as 'Marker aided selection' is the process whereby a marker (molecular, biochemical, or molecular marker) is used for the indirect selection of a genetic determinant or determinants of a trait of interests (economic traits). Most of the genes of economic interest are quantitative genes which most likely are controlled by many genes. A chromosomal region that contains one or more genes that influence a multi factorial trait is known as Quantitative Traits Loci (QTL) (Crosses, 2001). They contain genes that differentially affected a continuous phenotypic expression. The genes on QTL with large effects are called major genes and a QTL also have many polygene's with minor effect and additive effect of all these will determine the trait if interest.

CONCEPT OF MARKER

The gene of interest causes production of RNA that produce a desired trait or phenotype through proteins, whereas markers which may be a DNA sequence or the morphological or biochemical markers produced due to that DNA are genetically linked to the gene of interest. The gene of interest and the marker tend to move together during segregation of gametes due to their proximity on the same chromosome and concomitant reduction in recombination (chromosome crossover events) between the marker and gene of interest (Botstein, 1980). When markers are used there may be some inaccurate results due to inaccurate tests for the marker. There also can be false positive results when markers are used, due to recombination between the marker of interest and gene (or QTL). A perfect marker would elicit no false positive results. The term 'perfect marker' is sometimes used when tests are performed to detect a SNP or other DNA polymorphism in the gene of interest, if that SNP or other polymorphism is the direct cause of the trait of interest (Lander, 1995). The term 'marker' is still appropriate to use when directly assaying the gene of interest, because the test of genotype is an indirect test of the trait or phenotype of interest.The principle of MAS as that there may be many genes with significant importance which can be targeted specifically in selection. For such genes close association with a marker is determined, since these genes of interests are not easy to visualise. In using markers, we follow the inheritance pattern of these marker alleles instead of visualising the genes as such (Johnson, 2003).

Genetic marker can be defined as any stable and inherited variation that can be measured or detected by a suitable method, and can be used subsequently to detect the presence of a specific genotype or phenotype other than itself, which otherwise is non measurable or very difficult to detect. Such variations occurring at different levels, i.e. at the morphological, biological, chromosomal, biochemical or DNA level can serve as the genetic markers. The markers that reveal variations at the DNA level are referred to as the molecular markers. Based on the techniques used for their detection, they have been classified into two major categories: Hybridization-based markers, and PCR-based markers (Mitra, 1999).

Biological Markers

Different pathogen races or insect biotypes based on host pathogen or host parasitic interaction can be used as a marker since the genetic constitution of an organism can affect its susceptibility to pathogens or parasites.

Morphological Markers

Marker loci available that have obvious impact on morphology of animals. Genes that form colorations, male sterility etc are included here

Biochemical Markers

Here a gene that encodes a protein is characterized and observed.

Cytological Markers

In these markers we make use of cytological techniques like banding.

DNA Base Markers

They are also called molecular markers. They are unique DNA sequences that are occurring in the proximity to the gene or locus of interest. These include many types of molecular markers, via RFLPs, RAPDs, SNP, AFLP, microsatellites etc (Phillips, 2013).

Important Properties of Ideal Markers

A marker to be consider as ideal, it should be easy recognition in all possible phenotypes, i.e., they should be co-dominant. It must demonstrate measurable difference in expression between trait types and gene of interest and has no effect on the trait of interest and pose a low or no interaction among the markers that allowing the use of many at the same time in a segregating population. It also be abundant in the population hence it can be considered as polymorphic. Thus there are two types of markers base on its distance and type of association with the gene of interest. They are direct markers and Linked markers. If there is no recombination between the marker and the QTL then such markers are called direct markers i.e., the marker exactly identifies the gene and then, finding the marker implies finding the gene of interest. Linked markers also called indirect markers are not located within the gene of interest. They may be in linkage disequilibrium or linkage-equilibrium with the gene (Sunnucks, 2000).

Direct Markers

Direct markers are the loci for which the functional polymorphism can be genotyped. The molecular marker is located within the gene of interest. They are the most convenient markers in the sense that the marker genotype will directly inform us about the genotype. But only few direct genetic markers for economically important traits have been developed hitherto. Examples for such markers are halothane gene in pigs, double muscling in a cattle which is due to myostatin gene (Dekkers, 2004). The greatest benefit with these markers is that they can be even used without trait measurements and pedigree recording. The possible risks with the direct markers are, there can be more mutations causing the desired effects and thus if we test for only a few mutations it will fail to pick up all the animals with desired effects. Thus they may result in false negative results. There is also some possibility for false positive results by incorrectly identifying a candidate gene as major gene incorrectly identifying as a major gene affecting the trait of interest. Thus the gene we pick may turn out to be a negative gene (Sunnucks, 2000).

Linked Markers

Linked marker occurs only near QTL on the genome and not the causative mutation in the gene concerned. For the identification of the markers we need pedigree data and records of phenotype. If the marker and markers in population-wide linkage disequilibrium with the functional it is called a linkage dis-equilibrium. In linkage dis equilibrium case the recombination percentage is very less because they are linked closer (Jorde,1995). With the knowledge of pedigree and phenotype these markers are equally useful as direct markers. There are two strategies to find markers that are in population-wide LD with QTL. In one case, the candidate gene approach knowledge from species that are rich in genome information (e.g., human, mouse) and/or knowledge of the physiological basis of

traits is used to identify genes that are thought to play a role in the physiology of the trait. Using this information, the candidate genes are identified in the species of interest and polymorphisms (genetic variants) are identified. It is then determined whether there is an association between the genotype for the candidate gene with the phenotype for the trait. In another case a genome scan using a high-density marker map, with a marker every 0.5 to2 cM (Dekkers and Hospital, 2002). In genome scan approach to QTL detection uses random genetic markers spread over the genome to identify genes affecting quantitative traits. Using statistical methods QTL can then be identified and their position and effect estimated by associating marker data to phenotypic records (Thompson, 1988). The precision of estimates of QTL position that can be obtained from these approaches is, however, limited and large population sizes are needed. If the marker locus is in population-wide linkage equilibrium with the functional mutation then they are called Linkage equilibrium markers (LE markers). It is the most difficult situation for applying MAS. The implementation of LE-MAS requires large amounts' of genotyping and advanced analysis to keep track of the QTL. For LE-MAS a detected QTL can be directly implemented because the linkage phase between marker and QTL varies between the families, the QTL effect has to be re-assessed continuously and within each family in MAS process. This requires genotyping for several markers not only for the selected genes (Ollivier, 1998).

Level of Marker Assisted Selection

Gene Assisted Selection (Gas)

The marker is located within the gene of interest (GAS). This is the most favorable situation for MAS since, by following inheritance of the marker alleles, inheritance of the QTL alleles is followed directly. On the other hand, these kinds of markers are the most uncommon and are thus the most difficult to detect because causality is difficult to prove and, as a result, a limited number of examples are available, except for single-gene traits. It denotes application of marker-trait associations determined via association genetics, which we anticipate will be based on poly morphisms associated with expressed genes. Prerequisites for successful application include suitable populations for detecting linkage disequillibrium; powerful quantitative genetic and bioinformatic capabilities; large EST libraries, if not whole genomic sequences, to identify candidate genes; and other capabilities for studying functional genomics; as well as a mix of quantitative genetics, tree breeding, and molecular biology skills(Wilcox *et al.,* 2007).

Linkage Disequilibrium MAS (LD-MAS)

Where a marker (or marker haplotypes) is in population-wide disequilibrium with a QTL. Occurrence of some combinations of alleles or genetic markers in a population more often or less often than would be expected from a random formation of haplotypes from alleles based on their frequencies. One requirement for the most effective use of LD mapping and of LD markers in MAS is that marker density is high enough that at least one marker is in sufficiently high LD with any putative QTL. With the availability of whole-genome sequences and large numbers of single-nucleotide polymorphisms (SNPs) in several agricultural species, high-density marker studies have become possible. The cost associated with genotyping, however, leads to an interest in using the smallest required number of markers for LD mapping and MAS. Because the required marker density depends directly on the extent of LD, which varies between populations, an important step prior to any association analysis is to ascertain the extent of LD in the populations of interest (Andreescu*et al.,* 2007).

Linkge Equiliberium (MAS)

The markers that are in population wide linkage equilibrium with functional mutation in outbred populations. The LE markers can be detected on a genome-wide basis by using breed crosses or analysis of large half-sib families within the breed. Many examples of successful applications of this methodology for detection of QTL regions are

available in the literature.It requires extensive genotyping and fairly complicated statistical procedures. Selection on these three types of markers will be referred to as gene-assisted selection (GAS), LD markers-assisted selection (LD-MAS), and LE marker-assisted selection (LE-MAS) (Dekkers 2004).

Genomic Selection

Genomic selection is a form of marker-assisted selection in which genetic markers covering the whole genome are used so that all quantitative trait loci (QTL) are in linkage disequilibrium with at least one marker. This approach has become feasible thanks to the large number of single nucleotide polymorphisms (SNP) discovered by genome sequencing and new methods to efficiently genotype large number of SNP. Simulation results and limited experimental results suggest that breeding values can be predicted with high accuracy using genetic markers alone but more validation is required especially in samples of the population different from that in which the effect of the markers was estimated. The ideal method to estimate the breeding value from genomic data is to calculate the conditional mean of the breeding value given the genotype of the animal at each QTL (Neves *et al.,* 2012). Genomic selection, which refers to selection decisions based on genomic breeding values (GEBV). The GEBV are calculated as the sum of the effects of dense genetic markers, or haplotypes of these markers, across the entire genome, thereby potentially capturing all the quantitative trait loci (QTL) that contribute to variation in a trait (Schaeffer*et al*., 2006). The QTL effects, inferred from either haplotypes or individual single nucleotide polymorphism markers, are first estimated in a large reference population with phenotypic information. In subsequent generations, only marker information is required to calculate GEBV (Hayes *et al.,* 2009) Genomic selection can result in lower costs and increased rates of genetic gain.

Steps for Marker Assisted Selection

MAS is likely to complement rather than replace the conventional breeding systems leading to increased rate of genetic improvement through higher selection intensity, reduction of generation interval and increase in the accuracy of prediction. Furthermore, selection based on markers is possible in early life or in individuals of both sexes for sex-limited traits. However, there is a risk of reduced genetic response if the marker association information is inaccurate, as MAS is a form of indirect selection (Ribaut *et al,* 1997). The association between the markers and the QTL is a function of distance between the markers and target traits, type of linkage phase, and degree of linkage disequilibrium. Therefore, a high-density gene map with closer linkage is a prerequisite for successful implementation of MAS55. It is estimated, that an average.

Marker density of 10 cm (5–20 cm), with about 200–250 makers, should be sufficient for the detection of marker–QTL association23. Till recently, gene maps with average marker interval exceeding 5cM (Walling*et al.,* 1998) in are available. However, currently high resolution maps with 2.5 cM or even less marker density have been published (Ihara*et al.,*2004).Thus MAS involves two steps viz., Identification of marker loci linked to the QTL and use of this information by incorporating it in existing breeding programmes suitably.

Identification of Marker QTL Linkage

Molecular markers are capable of exposing the genetic variations at QTL can be located in either coding sequence or non coding sequence. In livestock, there are basically four design possibilities for marker QTL linkage analysis (Ron and Weller, 2007).

1. Using F2 populations crossing two similar F1 populations, or a backcross between the F1 and one of the original populations.

2. Using a half sib sire design on which heterozygous sires for the markers are mated to a random sample of females and all the progeny is genotyped.
3. Using instead a granddaughter design on which a sire and their sons evaluated by progeny testing are genotyped.
4. Using crosses of individuals with extreme phenotypes for one trait or trait combination.

Animals from divergently selected lines or from populations with wide variation for important traits are also used. There are two approaches for the identification of molecular markers that are associated with the QTL.

Polymorphism in the coding sequence: DNA polymorphisms that occur in and around the structural and/or regulatory sequences of a gene of physiological significance (e.g. hormone genes, milk protein genes, MHC) may directly affect gene expression and thereby contribute to the phenotypic variations among the individuals in terms of productivity and health (disease resistance/susceptibility). Consequently, such DNA polymorphisms, occurring in the genes which already have a priori possibility to be associated or closely linked with the performance trait of importance, can be selected as markers (Beckmann and Soller, 1990).

Polymorphism in the non coding sequence: In this approach, the variations occurring in noncoding sequences (e.g. flanking regions or intergenic regions) are utilized indirectly as markers for linkage analysis (Smith and Simpson, 1986) Microsatellite markers, which are often highly polymorphic, are presently being exploited to identify QTL economically important traits.

Incorporating MAS in Selection Programmes

Molecular information can be used to enhance both the processes of integrating superior qualities of different breeds and within breed selection (Collard and Mackill, 2008). The strategies are discussed below.

Between Breed Selection

Using both direct and linked markers between breed selections can be done. It the difference between the two breeds in the trait of interest is due to small number of genes then marker assisted introgression can be can be used. Introgression is the movement of the target gene from the donor breed into the gene pool of the second breed, recipient by repeated crossing of the hybrid with the recipient breed. There will multiple back crossing followed by 1 or 2 intercrossing. These inter crossing will fix the QTL in the recipient. Examples: naked neck gene in low body weight poultry into broiler (Cahaner *et al., 1993*).

Within Breed Selection

Selection on QTL or marker information alone ignores information that is available on all other genes (polygenes) that affect the trait and is expected to result in the lowest response to selection unless all genes that affect the trait are included in the QTL EBV. This strategy does not, however, require additional phenotypes other than those that are needed to estimate marker effects, and can be attractive when phenotype is difficult or expensive to record (e.g. disease traits, meat quality, etc.). Selection on the sum of the QTL and polygenic EBV is expected to result in maximum response in the short term, but may be suboptimal in the longer term because of losses in polygenic response. Indexes of QTL and polygenic EBV can be derived that maximize longer-term response (Dekkers and van Arendonk, 1998) or a combination of short- and longerterm responses (Dekkers and Chakraborty, 2001). However, if selection is on multiple QTL and emphasis is on maximizing shorter-term response, selection on the sum of QTL and polygenicEBV is expected to be close to optimal. Optimizing selection on a number of EBVs, indexes and genotypes,

While also considering inbreeding rate and other practical considerations is not a trivial task. Mate selection approach could be used to handle such problems, and it can be expected that with more widespread use of genotypic information for a larger number of regions, specific knowledge about individual QTL becomes less interesting and will simply contribute to prediction of whole EBV or whole genotype.

Situations that are Favorable for Molecular Marker Selection

There are several indications for the use of molecular markers in the selection of a genetic trait. In such situations that:

- The selected character is expressed late in plant development, like fruit and flower features or adult characters with a juvenile period (so that it is not necessary to wait for the organism to become fully developed before arrangements can be made for propagation).
- The expression of the target gene is recessive (so that individuals which are heterozygous positive for the recessive allele can be crossed to produce some homozygous offspring with the desired trait).
- There is requirement for the presence of special conditions in order to invoke expression of the target gene(s), as in the case of breeding for disease and pest resistance (where inoculation with the disease or subjection to pests would otherwise be required). This advantage derives from the errors due to unreliable inoculation methods and the fact that field inoculation with the pathogen is not allowed in many areas for safety reasons. Moreover, problems in the recognition of the environmentally unstable genes can be eluded.
- The phenotype is affected by two or more unlinked genes (epistasis). For example, selection for multiple genes which provide resistance against diseases or insect pests for gene pyramiding.

The cost of genotyping (an example of a molecular marker assay) is reducing while the cost of phenotyping is increasing particularly in developed countries thus increasing the attractiveness of MAS as the development of the technology continues (Ribaut and Ragot, 2006).

CONCLUSION

The developments in the molecular genetics hitherto enable us to reveal many QTLs and stable constituents called markers associated with them. The use of markers help in selection is called marker assisted selection or MAS. Thus we have GAS, LD-MAS, LD-MAS based on the association of marker with the QTL. The knowledge about the markers is incorporated into the conventional breeding point and thus MAS cannot occur in vacuum. Molecular marker assisted selection aids us to address the situations where the conventional breeding fails. Now the concept of MAS is changing to genomic selection where SNPs associated with the gene of interest is used in selection criteria. Finally above all the researches we should be guided by economic motive. MAS involves huge expenses, and thus without monetary benefits it would become a failure.

REFERENCES

1. Andreescu, C., Avendano, S., Brown, S., Hassen, A., Lamont, S.J. and Dekkers, J.C., 2007. Linkage disequilibrium in related breeding lines of chickens. *Genetics*.
2. Beckmann, J.S. and Soller, M., 1990. Toward a unified approach to genetic mapping of eukaryotes based on sequence tagged microsatellite sites. *Nature Biotechnology*, *8*(10), p.930.
3. Botstein, D., White, R.L., Skolnick, M. and Davis, R.W., 1980. Construction of a genetic linkage map in man using restriction fragment length polymorphisms. American journal of human genetics, 32(3), p.314.
4. Cahaner, A., Deeb, N. and Gutman, M., 1993. Effects of the plumage-reducing naked neck (Na) gene on the performance of fast-growing broilers at normal and high ambient temperatures. Poultry Science, 72(5), pp.767-775.

5. Collard, B.C. and Mackill, D.J., 2008. Marker-assisted selection: an approach for precision plant breeding in the twenty-first century. Philosophical Transactions of the Royal Society of London B: Biological Sciences, 363(1491), pp.557-572.
6. Crosses, E., 2001. Review of statistical methods for QTL mapping in experimental crosses. Lab animal, 30(7).
7. Dekkers, J.C.M. and Van Arendonk, J.A.M., 1998. Optimizing selection for quantitative traits with information on an identified locus in outbred populations. *Genetics Research*, *71*(3), pp.257-275.
8. Dekkers, J.C. and Hospital, F., 2002. Multifactorial genetics: The use of molecular genetics in the improvement of agricultural populations. Nature Reviews Genetics, 3(1), p.22.
9. Dekkers, J.C.M. and Chakraborty, R., 2001. Potential gain from optimizing multigeneration selection on an identified quantitative trait locus. *Journal of Animal Science*, *79*(12), pp.2975-2990.
10. Dekkers, J.C., 2004. Commercial application of marker-and gene-assisted selection in livestock: Strategies and lessons 1 2. *Journal of animal science*, *82*(13_suppl), pp.E313-E328.
11. Hayes, B.J., Chamberlain, A.J., McPartlan, H., Macleod, I., Sethuraman, L. and Goddard, M.E., 2007. Accuracy of marker-assisted selection with single markers and marker haplotypes in cattle. *Genetics Research*, *89*(4), pp.215-220.
12. Ihara, N., Takasuga, A., Mizoshita, K., Takeda, H., Sugimoto, M., Mizoguchi, Y., Hirano, T., Itoh, T., Watanabe, T., Reed, K.M. and Snelling, W.M., 2004. A comprehensive genetic map of the cattle genome based on 3802 microsatellites. *Genome Research*, *14*(10a), pp.1987-1998.
13. Johnson, R., 2003. Marker-assisted selection. *Plant Breeding Reviews: Part 1: Long-Term Selection: Maize*, *24*, pp.293-309.
14. Lerner, I.M., 1958. The genetic basis of selection. The genetic basis of selection.
15. Mitra, A., Yadav, B.R., Ganai, N.A. and Balakrishnan, C.R., 1999. Molecular markers and their applications in livestock improvement. *Current Science*, *77*(8), pp.1045-1053.
16. Neves, H.H., Carvalheiro, R. and Queiroz, S.A., 2012. A comparison of statistical methods for genomic selection in a mice population. BMC genetics, 13(1), p.100.
17. Ollivier, L., 1998. The accuracy of marker-assisted selection for quantitative traits within populations in linkage equilibrium. *Genetics*, *148*(3), pp.1367-1372.
18. Phillips, R.L.and Vasil, I.K. eds., 2013. DNA-based markers in plants (Vol. 6). Springer Science & Business Media.
19. Ribaut, J.M., Jiang, C., Gonzalez-de-Leon, D., Edmeades, G.O. and Hoisington, D.A., 1997. Identification of quantitative trait loci under drought conditions in tropical maize. 2. Yield components and marker-assisted selection strategies. Theoretical and Applied Genetics, 94(6-7), pp.887-896.
20. Ribaut, J.M. and Ragot, M., 2006. Marker-assisted selection to improve drought adaptation in maize: the backcross approach, perspectives, limitations, and alternatives. Journal of experimental botany,58(2), pp.351-360.
21. Ron, M. and Weller, J.I., 2007. From QTL to QTN identification in livestock–winning by points rather than knock-out: a review. Animal genetics, 38(5), pp.429-439.
22. Schaeffer, L.R., 2006. Strategy for applying genome-wide selection in dairy cattle. *Journal of animal Breeding and genetics*, *123*(4), pp.218-223.
23. Smith, C. and Simpson, S.P., 1986. The use of genetic polymorphisms in livestock improvement. *Journal of Animal Breeding and Genetics*, *103*(1-5), pp.205-217.
24. Sunnucks,P.,2000. Efficient genetic markers for population biology. *Trends in ecology & evolution*,*15*(5), pp.199-203.
25. Thompson, E.A., Deeb, S., Walker, D. and Motulsky, A.G., 1988. The detection of linkage disequilibrium between closely linked markers: RFLPs at the AI-CIII apolipoprotein genes. *American journal of human genetics*, *42*(1), p.113
26. Walling, G.A., Archibald, A.L., Cattermole, J.A., Downing, A.C., Finlayson, H.A., Nicholson, D., Walker, C.A., Haley, C.S. and Visscher, P.M., 1998. Mapping of quantitative trait loci on porcine chromosome 4. *Animal genetics*, *29*(6), pp.415-424.
27. Wilcox, P.L., Echt, C.E. and Burdon, R.D., 2007. Gene-Assisted Selection Applications of Association Genetics for Forest Tree Breeding. In *Association Mapping in Plants* (pp. 211-247). Springer, New York, NY.

Indian Journal of Natural Sciences www.tnsroindia.org.in ©IJONS

Vol.8 / Issue 49 / August /2018 *International Bimonthly* *ISSN: 0976 – 0997*

RESEARCH ARTICLE

Evaluation of Drinking Water Quality in Al Wathba Treatment Plant in Baghdad City- Iraq

Dalya R.Mohammed Ali and Hind S.Abdulhay*

Department of Biology, College of Science, University of Baghdad, Baghdad, Iraq.

Received: 02 Apr 2018 Revised: 05 May 2018 Accepted: 07 Jun 2018

***Address for Correspondence**
Hind S.Abdulhay
Department of Biology,
College of Science,
University of Baghdad, Iraq.
Email: hind442@yahoo.com

ABSTRACT

The study was carried out to assess the quality of drinking water in Al Wathba plant in Baghdad city by determined some physicochemical and biological characteristics. The samples (raw water, water plant and drinking water) were collected from the study areas during the period from September 2016 to July 2017. Three replicates seasonally distribute into two months (autumn, winter, spring and summer).The physical and chemical tests of raw and drinking water (plant water and houses neighbor the plant) showed that the mean value of (the overall range) water temperature maximum in July 2017 (summer season) and minimum in December 2016 from 14- 27 ˚C respectively. The means value of water pH was minimum in summer 2017 reached 6.35 and the maximum in winter 2016-2017 to 8.2.Turbidity was 1.22 - 53 NUT in spring 2017 and autumn 2016 respectively. Biological oxygen demand (BOD5) was 0.001-4.6 mg/ml in spring 2017 and summer 2017 respectively. orthophosphate (PO4) 0.02-13.67mg/ml in autumn 2016 –summer 2017, total Trihalomethanes (TTHMs) 35.23-63.1ppb in summer 2017- winter 2016-2017 respectively, in addition to pesticide ranged 0.095- 17.5µg/l in autumn 2016- spring 2017 respectively. The statically analysis showed highly significant differences ($p \leq 0.01$) between raw Tigris river water samples and Al Wathba wastewater treatment plant water samples and houses drinking water with all physicochemical and biological parameters in the study, while have variety significant correlation between all type of water samples and season in addition parameters in this study. The mean value of all parameters in the study was within the permissible limits for Iraqi criteria and standards for drinking water and river water and drinking water. However the assessments of exposure were calculated to THMs concentrations in the distribution network of Al-Wathba plant. The WHO index for additive toxicity approach in compliant with the WHO guideline value, and does not pose any adverse toxic health impacts. The results of bacteriological tests of raw water showed varied with increasing and decreasing in APC, TC, FC and *E. coli* through seasons, as compared to those of the other seasons for raw

water plants and drinking water. The APC, FC and *E. coli* did not exceed the allowable limit for drinking water, for all samples of water plant.

Key word: Drinking water; Tigris River; Water quality; physicochemical properties.

INTRODUCTION

About 75% of the earth's surface is covered with water. Water forms more than (60 %) of the total weight of living cells and tissues, therefore it represents a good media for the biological reactions to take place in the cell, it is a critical requirement in the maintenance of metabolic functions and homeostasis in living cells, which is the ability to maintain stable body conditions [1]. Human health is closely related to drinking water quality, and access to safe, reliable drinking water in sufficient quantities is fundamental for good health and well-being [2]. The water quality class is defined depending on the measured physical, biological and chemical parameters besides the purposes for water used such as; drinking water, water used in agriculture, or water used in industry [3].The consumption of poor quality drinking water causes several health risks to the community, and ultimately, it increases the amount of healthcare budget [4].The increasing negative effects of water pollution have put more people at risk of carcinogenic diseases, potentially contributing to 'cancer villages' [5].

Among all the hazardous pollutants, pesticides and heavy metals are the most abundant in soil, water and agricultural products. They are environmental concern because of their toxic nature and their extensive usage and consequent pollution. Different biological methods, biosorption and bioaccumulation have been conducted to replace conventional methods for the removal of pollutants [6,7]. Imported taken care of the safety and supplying healthy portable water from World Health Organization (WHO) and United States Environment Protection Agency (USEPA) which must meet the following standards: Should be colorless, tasteless, and without smell. Should not contain heavy metals with ratios exceeding the allowable limit, not containing any polluted radiations, and Should be clear of any kind of microbes, especially the colonial bacteria and should not exceed the allowable limit. The aim of the study is investigating the quality of drinking water in AL-Wathba in Baghdad city through examination the chemical, physiological and biological properties of the station water. Also, the presence of THMs and some pesticides in tap water which supplied from this station were recorded.

MATERIALS AND METHODS

Preparation of Solutions

Stock phosphate anddiluting buffer, magnesium chloride, sodiumthiosulphate solution were perpetrated according [6].

Bacteriological Culture Media

The azide glucose broth media used in raw water and drinking water tests. The volume was duplicated when adding 10 ml of sample to the deferent media (Brilliant Green Bile Lactose Broth- BGBL, E.C. Broth, E.C MUG Broth and Nutrient Agar- N agar).Put a dirham tube in LSB, BGBL and E.C. broth media tubes for indicator to gas formation due to lactose fermentation by bacterial activity. Add the promo cresol purple to the LSB broth tube to recognize the positive results.

Methods

Study Area Description

Tigris river water is the only source of drinking water for the Baghdad city, and the river divides the city into two sides Karkh and Rusafa with a flow direction from north to south. At Baghdad city there are seven water treatment plants located along Tigris River starting from Al Karkh water treatment plant to the north of Baghdad.
The tests in this research were carried out at the Al Wathba water plants located in the Baghdad city/ Ayawadiyah area/ sectors 118 / street 1. The area of the plant is 15 dunums located on the Tigris River between latitudes 33° 21'03.90° N and longitudes 44°22'27.18" E, 30.5 to 34.85 m at sea level (a.s.l).. The plant consists of three main lines to filter out water is as follows:

- The first line (project struggle) design card 40560 m/ day (The project was established in 1935).
- The second line (old expansion) design card 68400 m/ day (Created 1976).
- The third line (new expansion) design card76800 m/ day (Created 2006).

Al Wathba water plant serves all areas and all the neighborhood of the center of Rusafa side and parts of Adhamiya neighborhoods, AL Kifah, Al-Rasheed Street, AL Sadriyah neighborhoods, the third line (new expansion) design card 76,800 m/ day (figure 1).

Water Sampling

The study was carried out from September 2016 to July 2017, for determined physicochemical and microbial (using serialized bottles) characteristics of raw water, drinking water and water of the Al-Wathba water treatment plant in Baghdad city depending on the standard methods for examination of water and waste water [8]. The water samples are taking from this two water treatment Al Wathba plant in addition to its network. Sites within the plant included: River intakes with three replicate seasonally WR. W= Al-Wathba, R= Raw water. After chlorination (treated water-outlet).Sites were distributed among residential areas fed by the plant. Distribution based on the distance from the plant from the nearest to the farthest point which feeding from the plant with drawn to cover plant. The points covered Al-Wathba plant is: W2 the beginning point of water distribution network, W3 the middle point of water distribution network and W4 the farthest point of water distribution network from the plant. All samples collected with three replicates monthly, every two months represents a season: autumn, winter, spring and summer.

Bacteriological Tests

To examine the validity of drinking water, conducted these testing by detecting bacteria that may be contaminate the water depending on the Standard Methods for examination of water and waste water 22st edition 2012. Included Aerobic Plate Count (APC), fecal coliform and *Escherichia coli* (F.C/100ml), (*E. coli*/ 100 ml), MPN of F.C/ 100 ml, *E. coli*/ 100ml Test for raw and drinking water [8].

Physiochemical Measurement

The parameters of physiochemical measurment were imported to determined by deference methods according to [8]. included (Water Temperature, Hydrogen Ion (pH), Turbidity, Biological Oxygen Demand BOD, Orthophosphate (PO4), Total Trihalomethanes (TTHMs) and Pesticides.

Statistical analysis

Statistical analysis was conducted using SPSS 21.0 (SPSS). Simple correlation analysis was performed as well to test for the significance of the linear relationship among continuous variables; ($p \leq 0.01$) was considered to indicate statistical significance. Differences in water pollutants concentrations between plants and periods of collection were determined using analysis of variance (one way ANOVA). Finally, Tukey's honestly significant difference test is applied in order to quantitatively compare the mean water pollution levels.

RESULTS AND DISCUSSION

Physicochemical properties

Water Temperature

Temperature cause a significant impact on water chemistry; the increase in chemical reaction rates of water causes high temperature that melts minerals in rocks, thus the higher electrical conductivity and biological effectiveness and growth of aquatic organisms, insects, phytoplankton, fauna and other aquatic species will be charged.The water temperature during different months and seasons of sampling were found to vary from 17 to 26.5 °C in Tigris River. While, the Al Wathba plant water temperature values were varied between 15– 24 °C, meanwhile ranged between 13.917– 26.83 °C in drinking water in houses neighbor plant. The overall range in water temperature was at its minimum levels in December 2016 and its maximum levels were recorded in July 2017 (Table 1).

These values followed almost identical seasonal cycles. However, the variations in temperature may be due to different timings of collection, influence of the season and the effect of atmospheric temperature. Temperature is known to influence the pH, alkalinity and DO concentration in the water [9].The statistical analysis showed that there was a no significant difference in water temperature among months and season ($P \leq 0.05$) (Table 1).The temperature showed changes between the samples of the group because they were in close geographical locations and the timing difference in the collection of samples (collected some samples in the morning and others collected at noon when the sun was vertical to the water surface). The preferred temperature of each species varies when temperatures change to above or below the preferred grade as the number of individual's decreases until the species is extinct [10].

Hydrogen ion (pH)

The pH value represents the instantaneous hydrogen ion activity which affects biological and chemical reactions in a water body, a measure of base acid balance and in most natural waters [11]. pH value change in Tigris River (Raw Water) varied between7.55 – 8.5, whereas in plants water samples it varied from 6.65 to 7.35, and there was a high significant difference ($P \leq 0.01$) found among study samples were observed (Table 1). In the same time the drinking water neighbor the plant 6.35- 7.68 found high significant difference with raw water samples from Tigris River and water samples from plant. The pH of the water samples tended to be higher in autumn and lower in winter (Figure 2). Alkaline pH is considered to be good for promoting high primary productivity.

The minimum and maximum pH values recorded in present study were within the permissible limits of Iraqi standards for drinking water according to the Iraqi Criteria and Standards of water's chemical limits, ICS /13.060.20 number 417/2009, second update, which was 6.5-8.5.The statistical analysis showed that there was no significant difference in water temperature among months and seasons ($P \leq 0.05$) (Table1). The high negative correlation was observed between pH and TRI and PES (r= - 0.33, r= -0.35). The positive significant correlation between pH and (*E. coli*, F coli and FST), BOD (r=0.24, r=0.24, r= 0.23 and r= 0.23) respectively (Table 4).

The increase in pH in rivers can be related to photosynthesis and the growth of aquatic plants, where photosynthesis consumes carbon dioxide and changes pH values and pH plays a key role in the survival of aquatic organisms and affects their distribution in water. Temperature affects equilibrium and acidity, and the toxicity of many pollutants depends on pH [12].

Turbidity

Turbidity is an optical measurement that indicates the presence of particles suspended in water which cannot seen by naked eye. These particles can be algae, dirt, metals, proteins, oils, or even bacteria, measured by highlighting through a sample, and determining the concentration of suspended particles. The greater the concentration of particles in the solution; the greater is the turbidity [13].Analysis of variance of these data (Table 1) has shown that the Al-Wathba water plant (1.8- 3.6) NTU and drinking water1.37- 4.13 NTU, with different seasons had clear effects ($P \leq 0.01$) comparison with raw water from Tigris River (18.1 -51.0) NTU. In general all the examined sites of the water plants showed low mean turbidity value apart from many sites which had high mean value. The statistical analysis showed high significant differences among months at ($P<0.01$), as well as there were significant differences among sampling sites (Table 4). The results of present research showed the high negative correlation was observed between Turbidity and phosphate and TRI (r= - 0.51 and r= - 0.74). The positive high significant correlation between turbidity and APC, *E. coli*, F. coli, FST, BOD and PES(r= 0.87, r= 0.90, r= 0.83, r= 0.71, r= 0.66and 0.69) respectively, while no significant correlation between turbidity and pH, temperature (r=0.17, r=0.04) respectively.

The high mean values of raw water turbidity in winter, especially in January, could be due to the increasing of rain fall proportion which led to soil erosion in the nearby catchment and domestic sewage water near Al- Wathba plants as well as vegetable oil plant discharge water which leads to increase the level of organic materials and other materials that increase turbidity. In the other hand the mild temperatures leads to increase the rate of algae growth and when they died, the rate of decomposers will increase because of the abundance of organic materials. The high levels of turbidity of houses water may due to their distance from the plant and the lack of water pressure in the pipeline leads to mix of drinking water with the surrounding environment especially when the pipes network occur have breaks and cracks. The maximum turbidity in plants water and drinking water recorded in present study were exceeding the permissible limits for Iraqi standards for drinking water according to the Iraqi Criteria and Standards of water's chemical limits, ICS /13.060.20 number 417/2009, second update, which was (0-5)NTU.

Chemical Characteristics

Biological Oxygen Demand (BOD_5)

Variations in DO can occur seasonally, or even over 24 hour periods, in relation to temperature and biological activity (i.e. photosynthesis and respiration). Fast moving water, lower temperature and lower salinity all result in the availability of more dissolved oxygen. [14] considered that DO is one of the one of most important parameters in water quality assessment and reflects the physical and biological processes prevailing in the water. [15] reported that high levels of BOD5 can indicate a decrease in DO, because oxygen in water is consumed by microorganisms, resulting in the inability of fish and other aquatic organisms to live in the river.

Data of BOD at the present study area are shown in figure (2) and the listed values in Table (2) show that Al- Wathba water plants 0.005 mg/l and drinking water0.0- 0.005 mg/l, with different seasons had clear effects comparison with raw water (Tigris River) (1.44- 4.60) mg/l and have high significant ($P \leq 0.01$). In general all the examined sites in the water plants showed low mean of BOD apart from most samples, which had high means value in raw water. The high BOD5 value during autumn and winter was probably linked to the level of organic matter load from sewage, industrial discharges. Generally the increase of BOD in Tigris River returned to the river affect by agriculture area which surround the river especially in study area, this agriculture area enriched by organic matter. On the other

hand, BOD revealed high positive correlations with all bacteriological parameters (P<0.01), and a weak significant negative correlation to P (r = -0.53) (Table 4). Mainly due to removal of free oxygen by microorganisms during decomposition of organic matter particularly in winter months. Higher water flow is suggested to contribute significantly in elevating dissolved oxygen concentrations the disturbance of water could lead to the increase of dissolved oxygen in water [16].

Phosphate ($PO4^{-3}$)

Phosphorus is one of the essential elements necessary for the growth of plants and animals. Phosphates can be found in water in two forms. Either in a particle or in melting phase. Particles include living and dead plankton, phosphorus deposits, adsorbed phosphorus and particulate matter. The dissolved phase includes inorganic phosphorus, organic phosphorus produced by living organisms, and molecular phosphorus. Orthophosphate is produced through normal processes such as decomposition and is present in wastewater [17]. Phosphate comes from fertilizers, pesticides, industry and cleaning compounds. Any increase in the levels of any of this nutrient will increase the risk of experiencing eutrophication [18].Phosphate levels were relatively high in drinking water from houses neighbor to the Al Wathba plants varying from 12.33– 14.67 mg/l. It ranged in n Al Wathba plant water samples in ranged from 0.01- 0.137 mg/l, while ranged from 0.035- 0.105 in raw water from Tigris river neighbor to the plant (Fig 3, Table 2).

The statistical analysis revealed high negative significant correlation between phosphate and bacteriological tests (APC, *E coli*, F. coli, FST), (r= -0.38, r = -0.50, r= -0.50 and r= -0.55),respectively (Table 4).Agricultural runoff containing phosphate fertilizers increase phosphate concentrations in Tigris River during winter months. While, the decline during summer months due to consume by plants and phytoplankton in photosynthesis and increase soil particles adsorption [19]. The highest phosphate content was recorded in drinking water which undoubtedly reflects the discharge of sewage effluent from the treating Al Wathba plant.

Total Trihalomethanes (TTHMs)

During the decontamination, the organic matter in the water will react with chlorine and bromine, resulting in the formation of carcinogenic and hazardous by-products human. These by-products are divided into two main groups: Haloic acids (HAA) and trihalomethanes (THM). Some studies have shown that acute toxicity of chloroform can cause depression in the central nervous system and cardiac effects. The US Environmental Protection Agency (EPA) recommends that concentrations of THMs should not exceed 100 μg /l in tap water to customers [20].The table (2) showed the mean value of total trihalomethanes in water sampled from seven sites of Al Wathba water plants, three sites during houses neighbor the plant and two sites of Tigris River in four seasons (two months every season). Total trihalomethanes level were relatively high in drinking water from houses neighbor to the Al-Wathba plant varying the means from 40.5– 48.4 ppm, where in Al Wathba plant the mean ranged from 41.66- 61.7 ppm, and no TTHM found in raw water of Tigris river (Fig 3, Table 2).The statistical analysis revealed high significant differences (P<0.01) in TTHM among months and seasons (Table 2).The high negative significant correlation between TTHM and bacteriological tests (APC, *E coli*, F. coli, FST),BOD and TOC (r= -0.58, r = -0.75, r= -0.76 and r= -0.84) , (r= -80) and (r= -0.87)respectively except phosphate will have high positive significant correlation (r= 0.45), respectively (Table 4).

Pesticides

The health effects of pesticides depend on the type of pesticide, such as the organophosphates including diazinon and chlorpyrifos, are insecticides that contain phosphorus and carbamates, affect the nervous system. Others may irritate the skin or eyes and some pesticides may be carcinogens [21]. The table (3) showed the mean value ± standard deviation of pesticide in water sampled from seven sites of Al Wathba water plant, three sites from houses neighbor

the plant and two sites of Tigris River in four seasons. Pesticide levels were relatively high in Tigris River water samples and varying the means from 10.36- 17.30 µg/l from sites neighbor the Al-Wathba plant and the moderate levels from drinking water from houses neighbor to the plant Al Wathba plant varying the means from 0.88– 7.36 µg/lm, while in Al Wathba plant water samples the mean ranged from 0.09- 0.88 µg/l(Figure3, Table 2).The statistical analysis revealed high significant differences (P<0.01) in pesticide concentration among months and seasons. The high positive significant correlation between pesticide and bacteriological tests (APC, *E coli*, F. coli, FST) and BOD(r= 0.46 , r = 0.61, r= 0.64 and r= 0.67) and (r= 0.69) respectively except phosphate and TRI will have high negative significant correlation (r= - 0.41, and r= -0.63) respectively was observed (Table 4). Agricultural streams recorded a high occurrence of some type of pesticide in surface waters with detection rates as high as 78% in some catchments [22]. Also, [23] concluded glyphosate and AMPA concentrations in streams and groundwater are not always measured because of the cumbersome analytical procedure. However, glyphosate is the most sold chemical used for weed control in agricultural, silvicultural and urban environments revealed that despite its high degradability under aerobic conditions, it can pose a threat to groundwater.

Bacteriological Characteristics

Coliform bacteria are present in the environment and feces of all warm-blooded animals and humans. Coliform bacteria are unlikely to cause illness. However, their presence in drinking water indicates that disease-causing organisms (pathogens) could be in the water system [22].

Total Bacterial Count (T.B.C)

The total bacterial (APC, Fecal Coliform (FC), *Escherichia coli* (*E.coli*) in this study ranged between19.85- 77.5 cfu/ ml, 28.5 x 103 to 185.5 x103 CFU/100ml and 18.5 x 103 to 57 x103CFU/100ml in Tigris River neighbor Al Wathba plant. While the mean number no growth in plant water samples. The distribution and seasonal variation of the total bacterial count in Tigris river, Al Wathba plant and Drinking water are shown in the Figure(4) and Table 3. The highest number of total bacterial count was recorded in December and January 2016- 2017 in Tigris River, while the lowest number of total bacterial count was recorded in summer (Jun and July) 2017 in Tigris River and no growth recorded in plant water. The statistical analysis revealed high significant differences (P≤0.01) in APC among months and all sites of samples were found and the statistical analysis revealed high significant differences (P<0.01) in F.C between months and seasons (table 3).The high positive correlation between F.C and APC and *E. coli* (r=0.74; r= 0.89) respectively, While the statistical analysis revealed high significant differences (P<0.01) in E. coli between some months and seasons (Table 3).The positive correlation between E. coli and APC (r= 0.89) (Table 4).

High number of total aerobic bacteria and fecal coliform and *E. coli* count in Tigris river was recorded during winter months, which might be because the high numbers of bacterial level of this rivers due to receiving the large amounts of sewage, as well as increase the agricultural activities have led to increase bacteria number in the waters of the river [25]. In addition the low number of bacteria during summer months may be due to flood period which dilutes the organic matter which used as food for the bacteria, as well as high temperature that caused kills of large number from the bacteria [26].The increase in numbers of FC in Tigris River may be due to the low temperature and effluent discharged enriched with organic matter from (RTP) which leading to increase in BOD5 value. The E.coli uses many interesting ways to avoid this change. E. coli can sense changes in temperature, pH, certain chemicals, and osmolarity, with many possibilities to adapt physically and live in a various habitats which have some kinds of pollution, as well as to compete with the large amount of other bacteria that are present in its habitat [27].

Fecal streptococci are a bacterial group that has been used as an index of fecal pollution in recreational water; however, the group includes species of different sanitary significance and survival characteristics. In addition, streptococci species prevalence differs between animal and human feces. Furthermore, the taxonomy of this group has been subject to extensive revision [28]. Current results revealed as shown in the figure (4) and table 3, the mean of

fecal streptococcus in this study varied between 385 to 960CFU/100ml and mean range between 390 to 895 in Tigris River neighbor Al Wathba plant, while the results showed no growth in water samples from plant and drinking water samples from houses neighbor Al Wathba plant. High values of fecal streptococcus recorded in spring 2017 at Tigris River sites neighbor Al Wathba plant which were 895 cfu/100ml. While the lowest value was recorded during autumn 2016 at Tigris River sites which was 390 cfu/100ml. These results lower than the levels were exceeded from local and international guidelines ranges [29].

The statistical analysis revealed high significant differences ($P<0.01$) in fecal *Streptococcus* between some months and seasons (Table 3).The high positive correlation between fecal *Streptococcus* and APC, *E. coli* and fecal coliform ($r= 0.51$, $r= 0.73$ and $r= 0.72$) (Table 4).The results showed that the high variability in the levels and number of fecal streptococcus in Tigris Rivers may be due to the variation of environmental conditions such as solar radiation, turbidity, temperature, salinity, dissolved oxygen and organic matter [30].

CONCLUSION

From the previous results we can concluded that Tigris River is suitable source of drinking water and the studied parameters were within the acceptable limits compared with the Iraqi standard, despite of discharge of a large amount of pollutant to the river without treatment. In addition the weather changes during the four seasons play an important role in terms of influencing the physicochemical and microbial variables under study in the water purification plants. The concentration levels of THMs in drinking water samples from houses neighbors of both plant are generally within the allowable concentration recommended by the WHO and the Iraqi standards.

REFERENCES

1. Mushini, V., Subba, R., Dhilleswara, R.V., and Andrews, B.S.A. (2012). Assessment of Quality of Drinking Water at Srikurmam in Srikakulam District, Andhra Pradesh, India, International Research Journal of Environment Sciences, 1: 13-20.
2. Bain, R.E.S., Wright, J.A., Christenson, E., and Bartram, J.K. (2014). Rural: urban inequalities in post 2015 targets and indicators for drinking-water. Science Total Environ. 490: 509–513.
3. Sargaonkar, A., and Deshpande, V. (2003). Development of an overall index of pollution for surface water based on a general classification scheme in Indian context. Environ. Monit. Assess. 89:43–67.
4. Chowdhury, S. (2012). Heterotrophic bacteria in drinking water distribution system: a review. Environ. Monit. Assess. 184:6087–6137.
5. Lu, Y.L., Song, S., Wang, R.S., Liu, Z.Y., Meng, J., Sweetman, A.J., Jenkins, A., Ferrier, R.C., Li, H., Luo, W., and Wang, T.Y. (2015). Impacts of soil and water pollution on food safety and health risks in China. Environ. Int. 77:5-15.
6. Hameed, Q. A. and Abdulhay, H. S. (2016). Bioremoval of chromium by local isolates of *pseudomonas aeruginosa* in respect to its genotype. Iraqi J. Science. 57(1B): 367-375.
7. Al-Shammary, M.A. and Abdulhay, H.S. (2016). Bioremoval of copper and zinc by filamentous alga *Oscillatoria limnetica*. World J. Exp. Biosci. 4(1): 37-39.
8. APHA, AWWA, and WEF. (2012). Standard Methods for the Examination of Water and Wastewater. 22st edition. Washington, DC: American Public Health Association, American Water Works Association, Water Environment Federation.
9. Ashbolt, N.J. (2004). Microbial contamination of drinking water and disease outcomes in developing regions. Toxicology 198: 229–238.
10. Al-Aney, I.A.M. (2012). Evaluation of potable water of both East Tigris and Al-Karama purification plant in Baghdad. M.Sc. Thesis. Baghdad University. Iraq.

11. Abdallah, K.J. and Abdulhay, H.S. (2017). The adsorption of cadmium and lead ions from aqueous solutions using non living biomass of *Phragmites australis*. Iraqi J. Science. 58(1C): 427-434.
12. Al-Zubaidi, A.N.H. (2011). A study of Al-Kut and Al-Karama water treatment plants efficiency to purify the drinking water in Al-Kut city. M.Sc. Thesis. College of Science, Baghdad University, Iraq.
13. Lako, V., Zhuri, E., Babani, F., and Karaja, T. (2012). Characterization of turbidity of some water ecosystems in southwestern Albania (Vlora region). Balwois- Ohrid, Republic of Macedonia.
14. Bhattacharya, T., Chakraborty, S., and Tuck, N. (2012). Physico chemical characterization of ground water of Anand district, Gujarat, India, I. Research J. University Science.1: 28-33.
15. Vaishali, P., and Punita, P. (2013). Assessment of seasonal variation in water quality of River Mini, at Sindhrot , Vadodara. Int. J. Environ. Science. 3:0976 - 4402.
16. Tobin, M., Yakub, G., Buys, M., Mccartney, B., Meyer, S., and Earth, E. (2001). Three rivers –second nature water quality report. Retrieved March 5th 2005, from the college of Fine Arts, Carnegie Mellon University website.
17. Flores, M.J.L., and Zafaralla, M.T. (2012). An assessment of the physicochemical parameters of mananga River, Cebu, Philippine. Intern. P. Rev. J., ISSN 2244-1581.
18. Jayalakshmi, V., Lakshmi, N., and SigaraCharya, M.A. (2011). Assessment of physico-chemical parameters of water and waste waters in and around Vijayawada. Int. J. Research Pharm. Biomed. Science. 2:1040-1046.
19. Lind, O.T. (1979). Handbook of Common Methods in Limnology. C. V. Mosby Co., st. Louis.
20. Elshorbagy, W. (2000). Kinetics of THM Species in Finished Water , J. Water Resour. Plng. and Mgmt., ASCE, 126:21-28.
21. USEPA (United State Environmental Protection Agency). (2003). Drinking Water Advisory: Consumer Acceptability Advice and Health Effects Analysis on Sulfate. Health and Ecological Criteria Division, Washington, D.C20460.
22. Kolpin, D., Thurman, E., Lee, E., Meyer, M., Furlong, E., and Glassmeyer, S. (2006). Urban contributions of glyphosate and its degradateampa to streams in the United States.Science Total Environ.354:191–197.
23. Scribner, E.A., Battaglin, W.A., Gilliom, R.J., and Meyer, M.T.(2007). Concentrations of Glyphosate, its Degradation Product, Aminomethyl-phosphonic Acid, and Glufosinate in Ground- and Surface Water, Rainfall, and Soil Samples Collected in the United States, 2001-06. Technical Report. United States Geological Survey.
24. Matteson, A.R., Graves, A.K., Hall, A.M., Matthew, D.K., and Polizzotto, L. (2016). Fecal contamination and Microcystis in drinking-water sources of rural Cambodia using PCR and culture-based methods water sanitation and hygiene for development, 6 : 353-361.
25. Adams, S.B., and Kolo, R.J. (2006). Public Health Implications of Gurara River around Izam Environs, Niger State, Nigeria. Fisheries Society of Nigeria (FISON). Conference Proceedings.
26. Abdo, M.H., Sabae, S.Z., Haroon, B.M., Refaat, B.M., and Mohammed, A.S. (2010). Physico-chemical characteristics, microbial assessment and antibiotic susceptibility of pathogenic bacteria of Ismailia Canal Water, River Nile, Egypt. J. American Science 6: 243-250.
27. Rowan, J. (2011). Defining established and emerging microbial risks in the aquatic environment: current knowledge, implications, and outlooks. Inter. J. of Micro. 1, article ID 462832, 15.
28. Leclerc, H., Devriese, L.A., and Mossel, D.A.A. (1996). Taxonomical changes in intestinal (faecal) enterococci and streptococci: consequences on their use as indicators of faecal contamination in drinking water. Journal of Applied Bacteriology, 81: 459–466.
29. WHO (World Health Organization). (1996). Guide lines for Drinking Water Quality. Recommendation, 1, Geneva.
30. Yehia, H.M., and Sabae, S.Z. (2011). Microbial Pollution of Water in El-Salam Canal, Egypt. American-Eurasian J Agric and Environ Science 11: 305-309.

Table 1.Results of river and drinking water physical characterization for Al Wathba plants and during four seasons

Variables	Season	Mean ± Standard deviation					
		Al-Wathbaplant					
		R.W	P.W	H1	H2	H3	P-value
pH	Autumn	8.05 ±0.15	7.35 ±0.25	7.50 ±0.10	7.45 ±0.05	7.50 ±0.10	0.001 **
	Winter	7.80 ±0.10	7.20 ±0.10	7.15 ±0.05	7.50 ±0.00	7.50 ±0.10	0.001 **
	Spring	7.55 ±0.25	6.65 ±0.55	7.55 ±0.05	7.60 ±0.10	7.20 ±0.00	0.001 **
	Summer	7.65 ±0.15	7.00 ±0.10	4.24 ±3.16	7.50 ±0.00	7.30 ±0.00	0.001 **
Temp. (C)	Autumn	17.30 ±0.60	15.50 ±1.50	17.00 ±3.00	17.00 ±5.00	18.50 ±0.50	0.001 **
	Winter	26.50 ±2.50	24.00 ±2.00	25.50 ±0.50	28.00 ±0.00	27.00 ±0.00	0.001 **
	Spring	24.50 ±3.50	23.50 ±3.50	25.00 ±0.00	25.00 ±2.00	21.00 ±5.00	0.001 **
	Summer	17.00 ±6.00	15.00 ±5.00	11.75 ±4.25	16.00 ±3.00	14.00 ±2.00	0.001 **
Turbidity	Autumn	53.00 ±18.00	2.00 ±0.50	2.35 ± 0.30	2.30 ±1.40	2.60 ±0.20	0.001 **
	Winter	46.00 ±15.00	1.80 ±0.40	2.57 ±1.43	1.450 ±0.10	2.81 ±1.09	0.001 **
	Spring	33.00 ±5.00	2.10 ±0.10	2.50 ±0.08	0.735 ±0.08	0.865 ±0.41	0.001 **
	Summer	18.10 ±0.90	3.60 ±0.50	7.74 ± 6.25	2.39 ±0.51	2.27 ±0.82	0.001 **

****: Highly significant**

Table 2.Chemical characterization of river and drinking water from Al-Wathba plant during four seasons

Variables	Season	Mean ± Standard deviation					
		R.W	D.W	H1	H2	H3	P-value
PO4-P. (mg/L)	Autumn	0.035 ±0.002	0.015 ±0.01	11.50 ±1.50	14.00 ±0.00	12.50 ±0.50	0.001 **
	Winter	0.105 ±0.01	0.137 ±0.01	13.50 ±1.50	16.00 ±3.00	14.50 ±2.50	0.001 **
	Spring	0.090 ±0.09	0.020 ±0.01	15.50 ±1.50	15.00 ±1.00	10.50 ±0.50	0.001 **
	Summer	0.085 ±0.07	0.010 ±0.00	11.00 ±0.00	12.50 ±0.50	13.50 ±0.50	0.001 **
BOD	Autumn	2.15 ±0.05	ND	0.005 ±0.002	0.005 ±0.002	0.005 ±0.002	0.001 **
	Winter	2.37 ±0.03	ND	ND	ND	0.005 ±0.002	0.001 **
	Spring	1.44 ±0.19	ND	0.005 ±0.002	ND	ND	0.001 **
	Summer	4.60 ±0.20	ND	0.005 ±0.002	ND	0.005 ±0.002	0.001 **
Free Residual chlorine (ppm)	Autumn	ND	2.77 ±0.38	1.63 ±0.67	2.170 ±0.37	1.95 ±0.05	0.001 **
	Winter	ND	3.60 ±0.04	1.05 ±0.15	1.855 ± 0.15	1.91 ±0.02	0.001 **
	Spring	ND	3.69 ±0.41	1.82 ±0.28	0.765 ±0.24	1.67 ±0.32	0.001 **
	Summer	ND	2.39 ±0.15	1.56 ±0.45	1.275 ±0.42	1.31 ±0.49	0.001 **
TTHMS (ppb)	Autumn	ND	42.50 ±15.20	38.50 ±2.10	42.10 ±1.10	40.90 ±0.00	0.001 **
	Winter	ND	61.70 ±5.10	40.95 ±2.15	45.25 ±7.55	49.05 ±9.25	0.001 **
	Spring	ND	41.66 ±2.36	51.60 ±2.20	46.45 ±3.85	47.15 ±3.05	0.001 **
	Summer	ND	43.91 ±13.79	54.60 ±0.60	41.90 ±4.00	41.95 ±2.85	0.001 **
Pesticide (µg/l)	Autumn	17.30 ±0.60	0.095 ±0.08	0.970 ±0.01	0.905 ±0.02	0.875 ±0.15	0.001 **
	Winter	10.36 ±0.54	0.150 ±0.02	0.810 ±0.02	0.910 ±0.03	0.920 ±0.00	0.001 **
	Spring	12.35 ±0.55	0.105 ±0.02	1.01 ±0.22	1.025 ±0.09	0.890 ±0.00	0.001 **
	Summer	14.50 ±0.30	0.880 ±0.82	19.93 ±18.96	0.945 ±0.11	1.205 ±0.02	1.01 **

Table 3: Biological characterization of river and drinking water from Al-wathba plant during four seasons

Variables	Season	Mean ± Standard deviation					
		Al-Wathbaplant					
		R.W	D.W	H1	H2	H3	P-value
APC cfu/ ml	Autumn	1100000 ±900000	ND	13.00 ±7.50	30.00 ±12.00	49.50 ±48.50	0.001 **
	Winter	1550000 ±550000	ND	49.00 ±40.00	15.00 ±14.00	14.00 ±7.00	0.001 **
	Spring	210000 ±90000	ND	52.50 ±48.50	81.50 ±65.50	98.50 ±90.50	0.001 **
	Summer	150000 ±50000	ND	34.50 ±9.50	17.50 ±8.50	7.50 ±6.50	0.001 **
E. coli cfu/ 100ml	Autumn	44500 ±9500	ND	ND	ND	ND	0.001 **
	Winter	57000 ±22000	ND	ND	ND	ND	0.001 **
	Spring	28500 ±6500	ND	ND	ND	ND	0.001 **
	Summer	18500 ±5500	ND	ND	ND	ND	0.001 **
F. coliform cfu/ 100ml	Autumn	29500 ±5500	ND	ND	ND	ND	0.001 **
	Winter	35000 ±0.00	ND	ND	ND	ND	0.001 **
	Spring	28500 ±6500	ND	ND	ND	ND	0.001 **
	Summer	185500 ±5500	ND	ND	ND	ND	0.001 **
F. streptococcus cfu/100 ml	Autumn	390.00 ±10.00	ND	ND	ND	ND	0.001 **
	Winter	690 ±90	ND	ND	ND	ND	0.001 **
	Spring	895 ±25	ND	ND	ND	ND	0.001 **
	Summer	805.00 ±175.00	ND	ND	ND	ND	0.001 **

Table 4. Correlation coefficient between difference parameters

Parameters	**APC**	**E. Coli**	**F. Coli**	**FST**	**P**	**BOD**	**TRI**	**PES**	**PH**	**Temp.**	**Turbidity**
APC	-										
E. Coli	0.89 **	-									
F. Coliform	0.74 **	0.89 **	-								
F. Strepto.	0.51 **	0.73 **	0.72 **	-							
P	-0.38 **	-0.50 **	-0.50 **	-0.55 **	-						
BOD	0.50 **	0.69 **	0.70 **	0.85 **	-0.53 **	-					
TTHMS	-0.58 **	-0.75 **	-0.76 **	-0.84 **	0.45 **	-0.80 **	-				
Pesticide	0.46 **	0.61 **	0.64 **	0.67 **	-0.41 **	0.69 **	-0.63 **	-			
PH	0.18 NS	0.24 *	0.24 *	0.23 *	-0.09 NS	0.23 *	-0.33 **	-0.35 **	-		

Temp	0.13 NS	0.11 NS	0.05 NS	0.11 NS	0.05 NS	-0.07 NS	-0.01 NS	- 0.19 NS	0.18 NS	-
Turbidity	0.87 **	0.90 **	0.83 **	0.71 **	- 0.51**	0.66 **	- 0.74**	0.69 **	0.17 NS	0.04 NS
* Refer into significant results ** high significant										

Figure (1): The study area that fed by Al Wathba plant within the confines of Baghdad www.lib.utexas.edu.

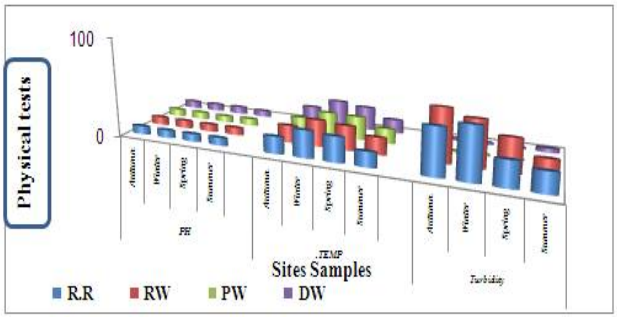

Figure (2) Mean seasonal physical values within different sites (Tigris River, Al Wathba plants and houses neighbor of plant).

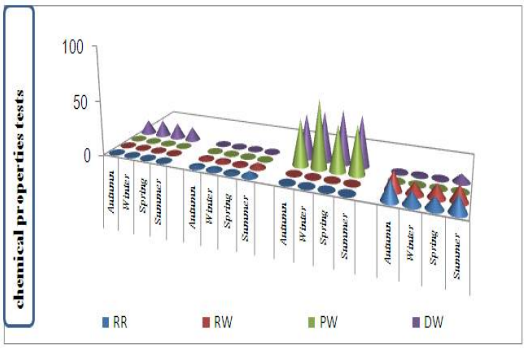

Figure 3: Mean seasonal physical values within different sites (Tigris River, Al Wathba plants and houses).

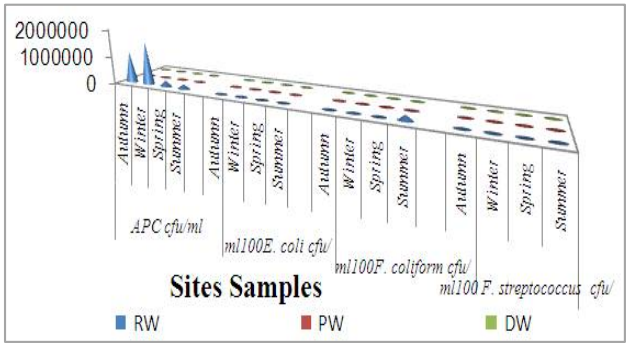

Figure (4) mean of fecal streptococcus seasonal values within different sites (Tigris River, Al Wathbaplant, Houses neighbor of plant).

Indian Journal of Natural Sciences www.tnsroindia.org.in ©IJONS

Vol.8 / Issue 49 / August /2018 *International Bimonthly* *ISSN: 0976 – 0997*

RESEARCH ARTICLE

Annealing Effects on the Structure and Morphological Character of CuO Thin Film Prepared By PLD

Kadhim A. Aadim[1]*, Ali A. Yousif[2] andf Radea H. Al-Shammari[2]

[1]Department of Physics, College of Science, University of Baghdad, Baghdad, Iraq.
[2]Department of Physics, College of Education, Almustansiriya University, Baghdad, Iraq.

Received: 06 Apr 2018 Revised: 04 May 2018 Accepted: 12 Jun 2018

***Address for Correspondence**
Kadhim A. Aadim
Department of Physics,
College of Science,
University of Baghdad, Iraq.
Email: kadhim_adem@yahoo.com

ABSTRACT

Copper oxide thin films were prepared on Indium tin oxide (ITO) substrate by pulse laser deposition. The copper oxide film was grown on aIndium tin oxide substrate by pulas laser deposition.Laser Nd:YAG ($1.064\mu m$, 9 ns) Q-switch Nd-YAG laser with 900 mJ/cm^2 laser energy's. The effects of annealing on the structural properties and morphological character of copper oxide thin films were studied. The films were annealed in ambient for different temperature ranging from (473,573 and 673)K . An X-ray diffraction pattern reveals that the films as-deposited and annealed at 573K and 673K are of CuO structure with composition Cu_2O, Annealing at 573K andabove became mix these films to Cu_2O phase and cuo . The atomic force microscopy results show the average particles diameter increasing with mix phase.

Key words. Thin films, Pulsed laser deposition, CuO, Indirect Phase.

INTRODUCTION

Pulsed laser deposition (PLD) is now increasingly used in the preparation of thin film companies with various materials. In the most basic configuration of the PLD, the flux of the material to be deposited is generated by irradiating the appropriate target with a high intensity pulsed laser beam, and a film is grown by collecting this flux on a nearby substrate [1] The efforts to produce high-quality thin layers of these materials worldwide have led to a wide range of available technical studies. Among them, PLD ranked firstIt has been reported that copper oxide is classified as a transition metal oxide group of p-type semiconductors since copper vacancies are the most stable defect in copper-rich and rich O environments. As p-type semiconductors, copper form two types of oxides, which are known as lead and cuprous copper oxide (CuO) Oxides (Cu_2O) are copper salts [2]. The mantle and chalcopyrite

have different physical properties, different colors, Crystal structure and electrical properties. Compared with Cu_2O, CuO is a more thermally stable material the stability of CuO with high oxidation number [3].Copper oxide (CuO) is a promising non-toxic and low cost semiconductor with potential applications in photovoltaic devices and sensor applications, CuO has bandgap energy of 1.21 eV to 1.51 eV, with a brown black appearance [4]. CuO also has a lattice constant a = 4.6859A, b = 3.4283, c = 5.1232 and β = 99.541o [5] monoclinic crystal structure. CuO is unique in a single oxide of 3d transition elements coordinated to a square plane with copper Oxygen in monoclinic structures. At the same time, cuprous oxide (Cu_2O) is brown the appearance of the p-type semiconductor as the second stable phase of the copper oxide compound. Cu_2O is direct Band gap of 2.0 eV to 2.60 eV, can absorb up to the visible area [6].Cu_2O have both ionic and covalent structure which belongs to the cubic structure with a lattice constant of 4.2696 Å [7]. It has been used in photovoltaic devices, p-n junction diodes, power supplies, microwave dielectrics, solid state gas sensors and catalysts for several environmental processes. CuO films have been grown by various techniques such as thermal oxidation, electrodeposition, molecular beam epitaxy, induced physical vapor deposition, RF magnetron sputtering and pulsed laser deposition [8,9].In this study, the influence of annealing in the(473,573 and 673)K range onthe structural (XRD) and morphological (AFM) properties of CuO thin films was investigated.

MATERIALS AND METHODS

The target of the deposition was CuO bulk with purity 99.999%, shaped liked disc with a diameter of 1cm .Using the deposition method (PLD), CuO film on substrate Indium tin oxide, the laser energy was900m J /cm^2.The substrate and target inside vacuum at a pressure of 10^{-3}mbar. The substrate was placed at 3cm from the CuO target, the CuO target it is bombarded by 650 pulses by (10-30) second to obtain a one layer offilm.During the deposition, was fired using a Nd: YAGlaser operating under specific energy, The Nd: YAG laser with a fundamental harmonic frequency (λ=1064nm, 10ns, 6Hz) is focused on a CuO target with a quartz lens. The laser beam is focused on the target by an angle of incidence of 45°. The ablated material of CuO is ejected on the substrate with high kinetic energy, the annealing temperature changes from (473,573,673) K to study their influence on the phase of CuO and properties of the deposited film.

RESULTS AND DISCUSSION

This study focused on thestructure and morphology of CuO films deposited at substrateIndium tin oxide than annealing temperatures to determine the annealing effect on phase of CuO and properties of copper oxide films prepared bypulas laser deposition.An atomic force microscopy (AFM) image of the CuO film annealing at different temperatures (473,573, 673) K as shown in and table (1), Fig (2).

The surface nanostructure of copper oxide films was carried out by AFM. Fig(2) indicates the three dimension (3D) AFM imagesof copper oxide films at different annealing temperature varied at 473K, 573K and 673K. The root mean square (RMS) surface roughness, obtained from AFM images corresponding to copper oxide films, is listed in Table1.The AFM results show that the size of the grains increased as theannealing temperature increased to 573K The grains size of the films has increased from 80 nm at 300K to124.50nm at 573K.

Annealing temperature to 91.5 nm at 673K annealing temperature, this is due to the phase stability of the oxide. It was observed that larger grain structure wasobtained at films annealed at 573K.This is due to the increases of surface energy at high temperature [10]. The graingrowth mechanism happens due to the transfer of atoms at higher temperature have sufficient diffusion activation energy to occupy the crystal lattice and induced the small grains by grain boundary diffusion thus the grains form inlarger size [11]. Meanwhile,the surface roughness of the copper oxide films was The maximum value 2.47 nm onannealing at 573K.The surface roughness was decreasedto a minimum value of1.1nm as the annealing temperature increased to673K This behavior can be attributed tothe random distributions of the grains and also due to the phase change. Based on the results obtained, it can beconcluded that low roughness of copper oxide films was at high annealing temperatures. The results AFM were

consistent with the results of X-ray, where the peaks are clear at temperature (673K)a phase shift CuOWhere it is included Cu_2O.Table (2) shows the results of X-RD of thin film. We can see through the mix phase CuO and Cu_2Ofilm annealing at two temperatures (573,673) K, Where the top is very clear at a temperature 673K of Cu_2Otemperature room and 473k shows amorphous, similar behaviour was reportedearlier by Fei Wu, et al [12].

CONCLUSION

Copper oxide film prepared pulsed by laser deposition andannealing temperatures (473, 573 and 673)K. The morphology, roughness and grain size were studied by atomic force microscopy (AFM). The AFM results show an increase in grain size. The surface roughness increases as the substrate temperature increases. The film of CuOwhen annealing temperature 573K occur indirect phase transformation of CuO to Cu_2O**.**

REFERENCES

1. Ali A. Yousif and Kadhim A. Aadim, Nanoparticle dopants TiO_2 films for structure, optical and gas sensing properties prepared by PLD technique, Journal of Multidisciplinary Engineering Science Studies (JMESS), Vol. 2 Issue 9, September, pp.879-891,(2016).
2. K. Khojier, H. Savaloni and Z. Sadeghi, J. Theor. Appl. Phys. 8, 116 (2014).
3. P. Samarasekara, GESJ Phys. 2(2), 3–8 (2010).
4. L. Armelao, D. Barreca, M. Bertapelle, G. Bottaro, C. Sada and E. Tondello, Thin Solid Films 442(03), 48–52 (2003).
5. F. Marabelli, G. B. Parravicini, and F. Salghetti-Drioli, Phys. Rev. B 52(3), 1433–1436 (1995).
6. A. S. Zoolfakar, "Tuning and Engineering of ZnO and Cu_xO for Sensor , Solar Cells and Memory Devices,(2013).
7. Q. Zhang, K. Zhang, D. Xu, G. Yang, and H. Huang, Prog. Mater.Sci. 60, 208–337 (2014).
8. Darma, T.; Ogwu, A. and Placido, F. Effects of Sputtering Pressure on Properties of Copper Oxide Thin Films Prepared by RF Magnetron Sputtering, Materials Technology: Advanced Performance Materials 26, 28–31(2011),.
9. Lu, H.; Chu, C., Lai, C. and Wang, Y. Property Variations of Direct-Current Reactive Magnetron Sputtered Copper Oxide Thin Films Deposited at Different Oxygen Partial Pressures, Thin Solid Films, 4408–4412,(2009).
10. K. Khojier, Int. J. Nano Dimens. 2(3), 185–190 (2012).
11. Z. Huda, T. Zaharinie, H. S. C. Metselaar, S. Ibrahim, and G. J. Min, Arch. Metall. Mater. 59(3), 1–5 (2014.
12. Fei Wu, Sriya Banerjee, Huafang Li, Yoon Myung, and Parag Banerjee" Indirect Phase Transformation of CuO to Cu2O on a Nanowire Surface"*Washington University in St. Louis, St. Louis, MO 63130, USA*(2016).

Table 1: AFM Parameters of Cuo Films at Different Temperature

Temperature	Average Diameter (nm)	RMS roughness (nm)	Peak-peak (nm)
RT(300k)	80.84	1.5	5.2
473k	86.63	1.09	4.16
573K	124.50	2.47	10.8
673k	91.51	1.1	3.83

Table 2: Structural parameters for as deposited Cuo thin films onIndium tin oxide substrate and treated with temperature

Ta(K)	2θ (Deg.)	FWHM (Deg.)	d_{hkl} Exp.(Å)	G.S (nm)	d_{hkl} Std.(Å)	Phase	hkl	card No.
RT	Amourphus							
473	Amourphus							
574	35.4094	0.8818	2.5330	9.5	2.5216	CuO	(11-1)	96-410-5686
	36.3751	0.3358	2.4679	24.9	2.4644	Cu_2O	(11-1)	96-900-7498
	38.5584	1.0917	2.3330	7.7	2.3158	CuO	(111)	96-410-5686
673	32.3863	0.5878	2.7622	14.1	2.7460	CuO	(110)	96-410-5686
	35.4094	0.4199	2.5330	19.9	2.5216	CuO	(11-1)	96-410-5686
	36.2491	0.3359	2.4927	35.5	2.4644	Cu_2O	(11-1)	96-900-7498
	38.6004	0.6718	2.3306	12.5	2.3158	CuO	(111)	96-410-5686
	48.7614	0.5039	1.8660	17.3	1.8679	CuO	(20-2)	96-410-5686
	67.7817	0.4619	1.3814	20.7	1.3730	CuO	(220)	96-410-5686

Figure(1) shows system of PLD

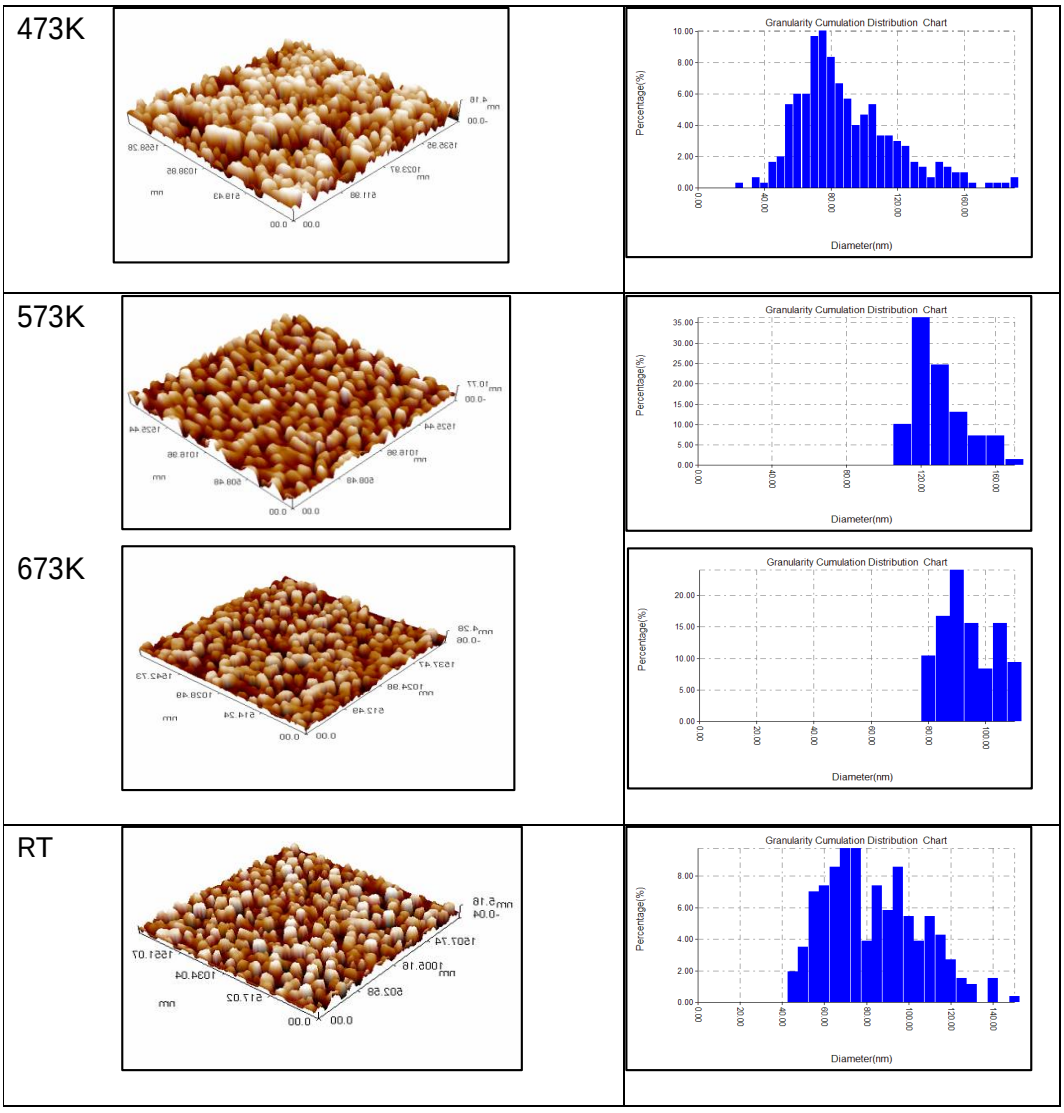

Figure(2) shows AFM of film Cuo annealing temperature (473,573,673and300 K) on series

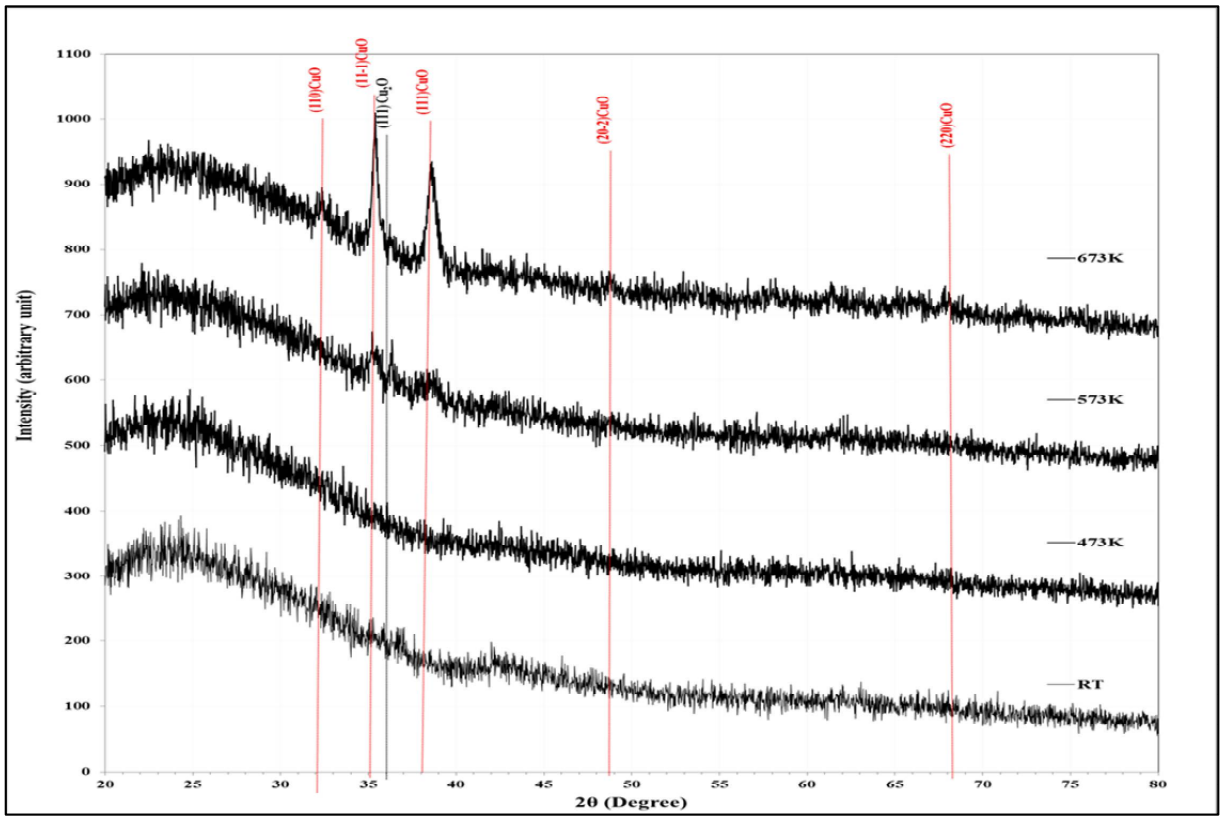

Figure 3 Shows XRD of Film Cuo at Different Annealing Temperatures

Indian Journal of Natural Sciences *www.tnsroindia.org.in ©IJONS*

Vol.8 / Issue 49 / August /2018 *International Bimonthly* *ISSN: 0976 – 0997*

RESEARCH ARTICLE

Laser Energy Impact on CdO NPs Prepared By PLD Technique

Ayad Z. Mohammad [1*], Kadhim A. Aadim [2] and May A. Abduljabbar [1]

[1]Laser Engineering Department, Laser and Optoelectronics Engineering Department, University of Technology, Baghdad, Iraq.
[2]Department of Physics, College of Science, University of Baghdad, Baghdad, Iraq.

Received: 05 Apr 2018 Revised: 06 May 2018 Accepted: 12 Jun 2018

[*]**Address for Correspondence**
Ayad Z. Mohammad
Laser Engineering Department,
Laser and Optoelectronics Engineering Department,
University of Technology, Baghdad, Iraq.
Email: ayad_1967_2005@yahoo.com

ABSTRACT

PLD technique was used in this work to synthesize CdO NPs at different laser energies (171, 201 and 263 mJ/pulse). Nd:YAG laser is used with 1064 nm wavelength for 200 pulses for each sample. The structural, optical and morphological properties were inspected for the produced thin films. As the laser energy increase, the band gap energy increase from 1.85 to 2.84 eV. XRD patterns showed the domination of polycrystalline nature of cubic structure. AFM results demonstrated the increase of particle size as the laser energy increase from 60.52 nm to 72.21 nm.

Key words: PLD, CdO, NPs.

INTRODUCTION

Cadmium oxide nanostructures have emerged as one of the most popular materials for various applications. Cadmium oxide (CdO) is an n-type semiconductor that has an interesting features, like low electrical conductivity, large band gap ~ 2.2eV, highly transmitting in the visible region of the spectrum [1]. Due to these attractions, CdO nanoparticles are desired in many optoelectronic applications like optoelectronic devices, gas sensors, photocatalytic activity, photodiodes, biosensors and solar cells[2–6]. CdO NPs can be synthesized in many techniques, such as sputtering, thermal evaporation, sol-gel, chemical bath deposition, and pulsed laser ablation[7–11].

Pulsed laser deposition is widely used method to synthesize crystalline NPs thin films of different materials of high quality, in one step, with lower cost than any other method [12]. In this work, we study the effect of laser energy at the optical, structural and morphological properties of cadmium oxide nanoparticles synthesized by pulsed laser deposition PLD technique.

MATERIALS AND METHODS

Materials

A pure CdO powder (99%) was purchased from BDH chemicals Ltd Poole, England.

Experimental Setup

2g of CdO powder was pressed into a circular pellet with a diameter of 16mm, 3mm high using hydraulic compressor under the pressure of 10Tons. Pulse laser deposition technique was used to prepare the CdO Nps in one step directly to the glass substrate that is placed above the pellet inside the vacuum chamber of the PLD system, operating with background pressure of $2.5*10^{-2}$ mbar. The CdO pellet was radiated with 1064 nm Q-switched Nd:YAG laser (Model HF -301, Huafei technology, China) at different energies for 200 pulses. Table (1) lists the laser parameters used in this work. The laser beam was focused on the pellet surface using a lens that has a focal length of 120mm, fig. (1) Shows a schematic diagram for the PLD system.

Measuring Techniques

The optical properties of the samples were measured using SP-8001 UV/Visible Spectrophotometer, Metertech, Taiwan. The crystalline structure of prepared samples were examined using XRD (D2 phaser, Bruker, Karlsruhe, Germany) operating with CuKa1 radiation at wavelength= 0.154060 nm, generated at 30 KV and 10 mA; for 2θ values between -3º to 160º. The surface morphology of CdO NPs was imaged by atomic force microscope (AFM) (CSPM-Scanning probe microscope).

RESULTS AND DISCUSSION

Optical Properties

Fig. (2) Shows the absorption spectrum as a function of wavelength. When increasing the laser energy, particles ablated from the pellet surface more rapidly. This causes the thin films thickness deposited on the glass substrate to increase. This leads to higher absorption.

From Tauc's relation of direct transitions, CdO NPs optical band gap is estimated graphically [13] :

$$(\alpha h\upsilon)^2 = A^2(h\upsilon - E_g)$$

Where:
E_g: optical energy gap.
α: absorption coefficient.
hυ: photon energy of incident radiation.
A: constant.

Laser energy has a significant effect on the band gap energy. As sown in fig.(3) as the energy increases, the band gap shifts towards higher energy. This can be due to the decrease in particle size and new quantum confinement effects [14]. Table 2 shows the increase in band gap energy as the laser energy increase:

Structural Properties

Fig.(3) presents the XRD patterns at different energies. These patterns exhibit peaks centered at 2θ= 33.0º, 38.283º, 55.25º, 65.9º and 69.28º, which corresponds to (111), (200), (220), (311) and (222) planes, that are the same as in pure CdO (JCPDS No. 05-0640) card. In other words, pure nanoparticles are obtained. Crystal growth at (200) plane indicate the domination of polycrystalline nature of cubic structure. the interplaner separation and crystalline size value of synthesized samples were calculated according to Scherrer's equation [15], and listed in table (2-a,b,c).

Morphological Properties

Fig. (4) Shows the size distribution and surface morphology of CdO NPs prepared at different energies. The AFM results displayed an increase in nanoparticles grain size as the laser energy increase, due to cluster formation as reported previously by Happy [16], S. Beke [17], and R. Myerlas [18].

CONCLUSION

In this paper, CdO NPs are prepared by PLD technique. The optical, structural and morphological properties were studied at different energies. XRD results showed the domination of polycrystalline nature of cubic structure with high purity peaks. AFM studies showed that the particle size increase with increasing laser energy, and it ranged from 60.52 nm to 72.21 nm. The optical properties indicate the increase in band gap energy due to reduction of particle size compared with the bulk material.

REFERENCES

1. A. S. Lanje, R. S. Ningthoujam, S. J. Sharma, and R. B. Pode, "Luminescence and electrical resistivity properties of cadmium oxide nanoparticles," *Indian J. Pure Appl. Phys.*, vol. 49, no. 4, pp. 234–238, 2011.
2. R. Ferro, J. a. Rodriguez, I. Jimenez, a. Cirera, J. Cerda, and J. R. Morante, "Gas-sensing properties of sprayed films of $(CdO)_x(ZnO)_{1-x}$ mixed oxide," *IEEE Sens. J.*, vol. 5, no. 1, pp. 48–52, 2005.
3. A. K. Barve, S. M. Gadegone, M. R. Lanjewar, and R. B. Lanjewar, "Synthesis , Characterization and Photocatalytic capability of CdO Nanoparticle for methyl red Abstract :," no. April, pp. 35–38, 2014.
4. M. Negahdary *et al.*, "Direct Electron Transfer of Cytochrome c on ZnO Nanoparticles Modified Carbon Paste Electrode," *ISRN Biophys.*, vol. 2012, pp. 1–6, 2012.
5. A. A. Yousif and M. H. Hasan, "Gas Sensitivity and Morphologically Characterized of Nanostructure CdO Doped In2O3 Films Deposited by Pulsed Laser Deposition," *J. Biosens. Bioelectron.*, vol. 6, no. 4, pp. 4–10, 2015.
6. N. F. Habubi, M. H. Jadduaa, and A. Z. Ckal, "Fabrication And Characterization Of CdO 2 Nanoparticles For Solar Cells Applications," vol. 3, no. 8, pp. 5427–5433, 2016.
7. R. A. Hammoodi, A. Prof, A. K. Abbas, and P. A. K. Elttayef, "Structural and optical properties of CuO thin films prepared via R . F . magnetron sputtering," vol. 3, no. 7, pp. 1–7, 2014.
8. R.-V.L.E and O. M. de la L, "Growth of CdO films from CdO 2 films by chemical bath deposition: Influence of the concentration of cadmium precursor," *Superf. y Vacío*, vol. 28, no. 1, pp. 25–29, 2015.
9. A. Firdous and U. Hameed, "The Synthesis and Characterization of Nano Composites of CdO and Its Applications for the Treatment of Simulated Dye Wastewater," *Am. Chem. Sci. J.*, vol. 13, no. 1, pp. 1–10, 2016.
10. N.M.Al-Hada,E.Saion,Z.A.Talib, and A.H.Shaari,"The impact of polyvinylpyrrolidone on properties of cadmium oxide semiconductor nanoparticles manufactured by heat treatment technique," *Polymers (Basel).*,vol.8,no.4, 2016.
11. S.C. Singh, R. K. Swarnkar, and R. Gopal, "Laser ablative approach for the synthesis of cadmium hydroxide-oxide nanocomposite," *J. Nanoparticle Res.*, vol. 11, no. 7, pp. 1831–1838, 2009.
12. H. Zeng *et al.*,"Nanomaterials via laser ablation/irradiation in liquid: A review," *Adv. Funct. Mater.*, vol. 22, no. 7, pp. 1333–1353, 2012.

13. A.M.Mostafa,S.A.Yousef,W.H.Eisa,M.A.Ewaida,andE.A. Al-Ashkar, "Synthesis of cadmium oxide nanoparticles by pulsed laser ablation in liquid environment," *Optik (Stuttg).*, vol. 144, no. July, pp. 679–684, 2017.
14. L. Filipponi and D. Sutherland, *Nanotechnologies: Principles, Applications, Implications and Hands-on Activities*. Luxembourg: Publications Office of the European Union, 2012.
15. S. Z. H. Shah, U. Khan, S. Riaz, and S. Naseem, *Effect of pH on Iron Oxide Nanoparticles*, vol. 2, no. 10. Elsevier Ltd., 2015.
16. Happy *et al.*, "Effect of deposition parameters on morphology and size of FeCo nanoparticles synthesized by pulsed laser ablation deposition," *Appl. Surf. Sci.*, vol. 252, no. 8, pp. 2806–2816, 2006.
17. S. Beke, S. Giorgio, L. Korosi, L. Nanai, and W. Marine, "Structural and optical properties of pulsed laser deposited V2O5 thin films," *Thin Solid Films*, vol. 516, no. 15, pp. 4659–4664, 2008.
18. R. Myerlas, "Key Parameters of Pulsed Laser Deposition for Solid Electrolyte Thin Film Growth," 2017.

Table 1: Nd:YAG laser properties

E (mJ/pulse)	Freq. (Hz)	λ (nm)	Pulse duration (nm)	Pulse diameter (mm)
171,201, 263	1	1064	10	2.2

Table 2: The Optical Band Gap of CdO NPs Prepared at Different Energies

Laser energy (mJ)	Optical energy gap (eV)
171	1.85
201	2.08
263	2.84

Table 2-A: The Crystalline Size of Cdo Nps Prepared at 171 Mj/Pulse

2θ (deg.)	(hkl)	d_{hkl} Theo.(Å)	d_{hkl} Exp.(Å)	FWHM (deg.)	Crystalline size (nm)
33	111	2.712	2.7122	0.173	85.26
38.2	200	2.349	2.3541	0.248	60.35
55.25	220	1.661	1.4306	0.211	75.65
65.9	311	1.416	1.4162	0.249	67.68
69.28	222	1.355	1.3552	0.253	67.94

Table 2-B: The Crystalline Size Value of Cdo Nps Prepared at 201 Mj /Pulse

2θ (deg.)	(hkl)	d_{hkl} Theo.(Å)	d_{hkl} Exp.(Å)	FWHM (deg.)	Crystalline size (nm)
33	111	2.712	2.7122	0.166	88.59
38.2	200	2.349	2.3541	0.273	54.82
55.25	220	1.661	1.6613	0.163	97.93
65.9	311	1.416	1.4162	0.291	57.91

Table 2-C: The Crystalline Size Value of Cdo Nps Prepared at 263 Mj/ Pulse

2θ (deg.)	(hkl)	d_{hkl} Theo.(Å)	d_{hkl} Exp.(Å)	FWHM (deg.)	Crystalline size (nm)
33	111	2.712	2.7122	0.171	86.26
38.2	200	2.349	2.3541	0.248	60.35
55.25	220	1.661	1.6613	0.258	61.87
65.9	311	1.416	1.4162	0.163	10.34
69.28	222	1.355	1.3552	0.261	65.86

Table 3: The Average Diameter and Roughness of Cdo Nps Prepared Under Different Laser Energies

Laser energy(mJ/pulse)	Average diameter (nm)	Roughness (nm)
171	60.52	3.87
201	68.16	2.21
263	72.21	0.692

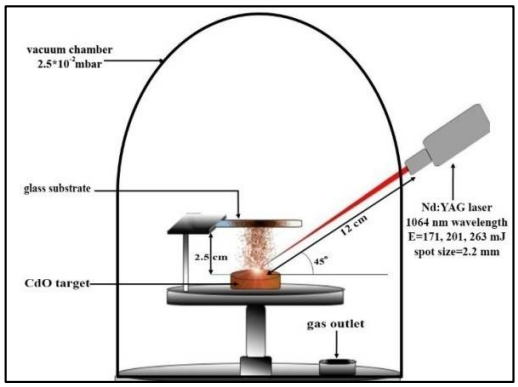

Fig.1: Experimental Representation of Technique

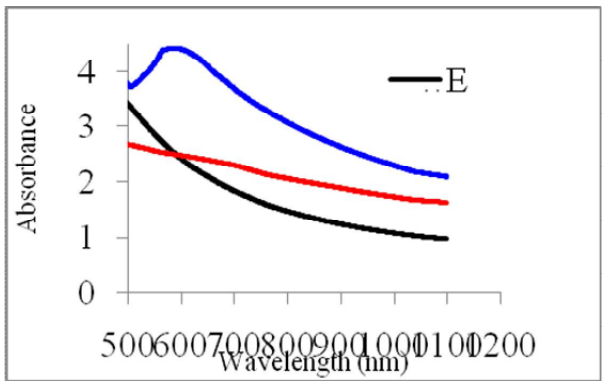

Fig.2: Absorption Spectrum as a Function of PLD Wavelength of CdO/NPs at Different Energies

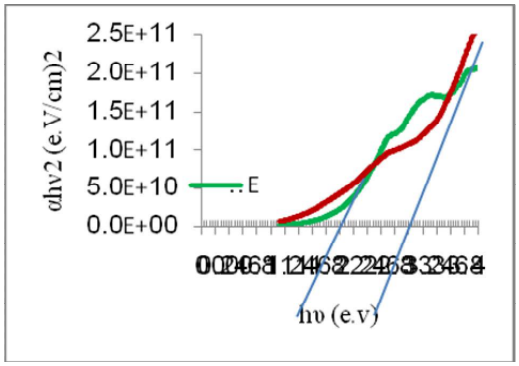

Fig.3: The $(\alpha h\upsilon)^2$ versus $h\upsilon$ Plot for CdO NPs Prepared at Different Energies

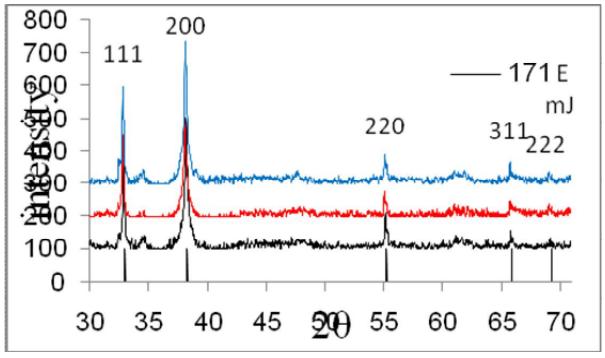

Fig.(4): X-Ray Diffraction (XRD) Spectra of CdO NPs Prepared at Different Laser Energies

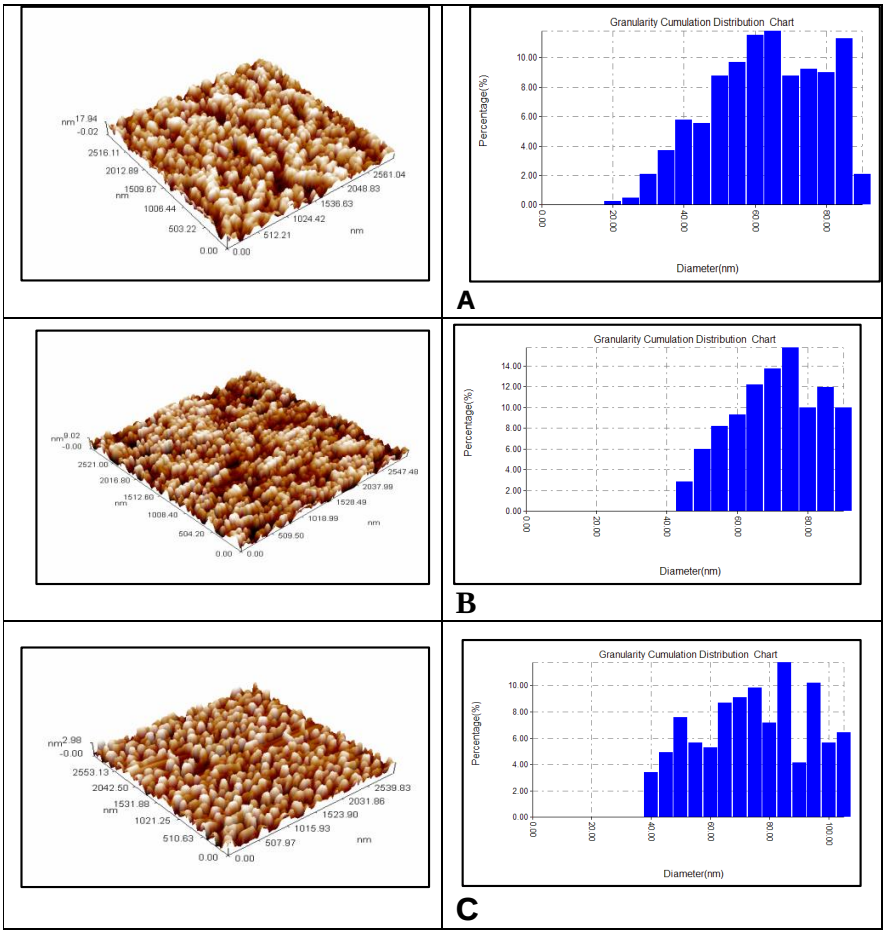

Fig.5: 3D AFM images and Size Distribution of CdO NPs Prepared at Different Laser Energies (a) 171 mJ/pulse, (b) 201 mJ/pulse, (c) 263 mJ/pulse.

Indian Journal of Natural Sciences www.tnsroindia.org.in ©IJONS

Vol.8 / Issue 49 / August /2018 *International Bimonthly* *ISSN: 0976 – 0997*

RESEARCH ARTICLE

Clinical and Biochemical Study of Maternal Blood Serum during Different Stages of Pregnancy in Local Iraqi Cows

AL-Ali. A. A[1]*, Al-Yasiri. E. A[2].

[1]College of Veterinary Medicine, University of Baghdad, Baghdad, Iraq.
[2]Assistant Professor, Dr.Department of Surgery and Obstetrics, College of Veterinary Medicine, University of Baghdad, Baghdad, Iraq.

Received: 02 Apr 2018 Revised: 06 May 2018 Accepted: 15 Jun 2018

*Address for correspondence
AL-Ali. A. A
College of Veterinary Medicine,
University of Baghdad, Iraq.

ABSTRACT

Sixty healthy local Iraqi cows were used to investigate the changes in ions and hormones of maternal blood serum during pregnancy. The data were collected from December 2017 to April 2018. The ages of cows selected between (3-6) years at Al-Muthanna Province. Samples included maternal blood serum divided into three groups according to stages of pregnancy and fourth group non-pregnant. These groups were 1st group (n=10) cows in 1st Trimester (1-3) months, 2nd group (n=14) cows in 2nd Trimester (4-6) months, and 3rd group (n=17) cows in 3rd Trimester (7-9) months of pregnancy and four group (n=19) non-pregnant. The result observed that the concentration of calcium (Ca) and phosphorus (P) ions in maternal blood serum Significantly increased ($p<0.01$) recorded in 1st and 2nd trimesters of pregnancy compared with 3rd trimesters and non-pregnant, but potassium (K) recorded significantly ($P < 0.01$) in 2nd trimester compared with other groups and sodium (Na) ion concentrations recorded significantly higher ($p<0.01$) in 3rd trimesters of pregnancy compared with 1st, 2nd trimesters and non-pregnant. Progesterone hormone recorded superior significantly ($P < 0.01$) in 2nd trimester compared with other groups. Finally, cortisol hormone recorded best significant increase ($P < 0.01$) during 3rd trimester of pregnancy compared with other groups. In conclusion, there were changes in ions and hormones concentrations in maternal blood serum, these changes possible considered as one method of pregnancy diagnosis.

Key words. Hormones, blood serum, pregnancy, serum, parameters.

INTRODUCTION

The health of the cows can be evaluate and depends on hematologic and biochemical profile of blood (1). Measurement of these parameters provide a practical diagnostic tool for evaluating pathological conditions in live animals or for monitoring the health status of animals (2). Reference values are of great importance for the correct

interpretation of biochemical data (3). Standard serum biochemical parameters provide information that serves as the basis for the diagnosis, treatment, and prognosis of diseases. Recently, major and trace elements have been recognized as essential for the maintenance of normal metabolic states and productivity in animals (4). Pregnancy is physiological status considered to modify metabolism in animals (5). All animals require minerals such as calcium (Ca) and phosphorus (P) and other ions for growth, reproduction and lactation which often affect specific requirements, and serve as catalytic components of enzymes or regulate several mechanism involved just in pregnancy and lactation (5,6,7). Serious changes during the Pregnancy period were observed in other blood metabolites in cows, including hematological, mineral, enzymatic and hormonal profiles, as well as some variables related to protein metabolism (8,9,10). The present study recorded changes in, ions and hormones in maternal blood serum to compare of blood biochemical profile of pregnant and non pregnant local Iraqi cows to help in pregnancy diagnosis.

MATERIALS AND METHODS

This study conducted on 60 healthy local Iraqi cows at Al-Muthanna Province for the period from December 2017 to April 2018. Ages of cows selected between (3-6) years. The cows divided into three groups according to stages of pregnancy and fourth non-pregnant. These groups were 1st group (n=10) cows in 1st Trimester (1-3 months), 2nd group (n=14) cows in 2nd trimester (4-6 months), 3rd group (n=17) cows in 3rd Trimester (7-9 months) of pregnancy and fourth group (n=19) non-pregnant**.** The blood samples were collected from jugular vein and analysis was completed in the laboratories of the Department of Technical Animal Production/Technical institute /Al-Mussiab/ Al-Forat Al-Awsat Technical University.The blood collected by vacutainer tubes (6 ml) without anticoagulant for accumulate the maternal blood for analysis the blood compositions (ions and hormones) after serum separated by centrifuge in 3600 rpm for 10 minutes and aspirated by eppendorf tube by using micropipette and stored at −20◦C until assayed. Statistic analysis for data included mean, chi–squar, standard error and F-test (one way) was done by (11)

RESULTS

The results of ions concentrations showed in table-1and figure-1. Concentrations of Ca ion in maternal blood serum in different stages of pregnancy, were (12.04 ± 2.34, 13.46 ± 1.86 and 9.35 ± 1.64 mmol/L) in 1st, 2nd and 3rd trimesters from pregnancy respectively, and 7.54 ± 0.16 mmol/L in non-pregnant. Concentrations of P were (8.52 ± 0.27,8.25 ± 0.68,and 5.33 ± 0.12 mmol/l) in 1st, 2nd and 3rd trimesters from pregnancy respectively, and 4.87 ± 0.23 mmol/l in non-pregnant. The results showed that the concentrations of Ca and P ions in maternal blood serum were significantly increased ($p<0.01$) in 1st and 2nd trimesters of pregnancy compared with 3rd trimesters and non-pregnant.

Concentrations of K ion were (4.23 ± 0.21, 6.35 ± 0.62 and 4.56 ± 0.17 mmol/L) in 1st, 2nd and 3rd trimesters from pregnancy respectively, and 1.36 ± 0.02 mmol/L in non-pregnant. It was recorded superior significantly ($P < 0.01$) in 2nd trimesters compared with other groups. The results observed that the concentrations of Na ion were (3.34 ± 0.16, 4.52 ± 0.23 and 5.22 ± 0.14) mmol/L in 1st, 2nd, and 3rd trimester respectively and 1.36 ± 0.02 mmol/L in non-pregnant, that recorded significantly ($P < 0.01$) in 2nd and 3rd trimesters with superior increase in 3rd trimesters compared with other groups, also significantly ($P < 0.01$) related with1**st** trimesters of pregnancy compared with non-pregnant (group- 4).

Concentrations of hormones showed in table-2 and figure-2. Progesterone hormone concentrations recorded (8.56 ± 1.43, 14.63 ± 1.84 and 11.45 ± 2.23 ng/ml) in 1st, 2nd, and 3rd, trimesters of pregnancy respectively and 5.63 ± 0.65 ng/ml in non-pregnant, which recorded superior significantly ($P < 0.01$) related with 2nd compared with 1st, 3rd trimester of pregnancy and non-pregnant, as well as significant difference ($P < 0.01$) related with 3rd compared with 1st, trimester of pregnancy and non-pregnant, also best significantly ($P < 0.01$) related with 3rd trimester compared with non-pregnant. finally, the results of cortisol hormone concentrations were (11.54 ± 0.09, 10.23 ±1.26, and 16.45 ±1.58

(ng/ml)) in 1st, 2nd, 3rd, trimester of pregnancy respectively and 14.62 ± 1.56 ng/ml in non-pregnant that recorded significant difference ($p < 0.01$) related with 3rd trimester and non-pregnant compared with 1st and 2nd trimesters of pregnancy.

DISCUSSION

The results of ions concentrations (table -1) showed that the concentration of Ca ion in maternal blood serum was increased significantly ($p<0.01$) in 1st and 2nd trimesters of pregnancy, as a result of the precipitation of Ca from blood circulation of dam to the skeletal of fetus and absorption from the gastrointestinal tract are required to re-establish homeostasis (12). The decrease in Ca level in late pregnancy may also be associated with haemodilution which has been reported in cows (13). During pregnancy advances, the serum calcium level depletes which corroborated with the finding of (14) and (15). The significant ($p<0.01$) decrease in the phosphorus level during the 3rd trimester might be due to increased utilization of Phosphorus at this stage and to enhance carbohydrate metabolism of pregnancy or might be due to meeting requirement of the P for the secretion of colostrums (16). The present results are in accordance with (4), (15), (14) and (17)

Concentration of Na ion in maternal blood serum was recorded best significantly ($p<0.01$) in 2ndand 3d trimesters of pregnancy compared with other groups due to indicating very efficient reabsorption capacity in the collecting of kidney lead to hypotonic of fetal urine compared with blood plasma and the sodium absorption by renal of fetus at the last period of pregnancy was highly percentage of the filtered load (18, 19). The higher sodium level in the pregnant animal with an increasing trend as pregnancy advanced may be due to the accumulation of fluid in pregnant animals, which is facilitated by reabsorption of sodium from the renal tubules (20) and also may be due to an increased demand of this element by the fetus (21). These results agreement with (22, 21, 23).

The concentration of potassium in maternal serum recorded best significantly ($P < 0.01$) in 2nd trimester of pregnancy, after that decrease in third trimester. The requirement of potassium has been found to be increasing during pregnancy (24). This may be because potassium located mostly within cells is needed for maintenance of acid-base balance in the body and for normal tissue protein synthesis calcium dependent- big potassium channel in protein depleted animals during the advanced pregnancy (25). Our results were similar to (26). The results of the hormones concentrations in maternal blood serum observed in table -2 and figure -2**,** the progesterone hormone was noted higher significantly ($P < 0.01$) in second trimester of pregnancy compared with other groups. This result agreement with (27) and (28) who found progesterone level was significantly increased with the progress of gestation and at the end of the 3rd trimester of gestation; progesterone decreased and reached its minimum level during the period from 6 to 1 day before parturition.

The cortisol hormone concentration recorded best significantly ($P < 0.01$) in 3rd trimester of pregnancy. These results agreement with (14,17).This response indicates that pregnancy constitutes a physiological stress, particularly in the 3rd trimester (14) and (29) who mentioned that late pregnancy may constitute a source of additional stimulus that activates the hypothalamic- pituitary –adrenal axis causing increased secretion of cortisol in cows. Cortisol levels peak in the late pregnancy because of placental production of corticotrophin releasing hormone and fall abruptly at delivery (30).

REFERENCES

1. Roland, L.; Drillich, M. and Iwersen, M. (2014). Hematology as a diagnostic tool in bovine medicine. Journal of Veterinary Diagnostic Investigation 26(5), 592-598.
2. Verheyen, A.J. M.; Maes, D.G.D.; Mateusen, B.; Deprez, P.; Janssens, G. P. J.; de Lange, L. and Counotte, G.(2007). Serum biochemical reference values for gestating and lactating sows. The Veterinary Journal, 174, 92 – 98.

3. Garcia, M. J.; Alegria,A. R.; Barbera.; Farre R. and Lagarda, M. J. (2000). Selenium, copper, and zinc indices of nutritional status: influences of sex and season on reference values, Biol. Trace Element Res. 73(1), 77–83
4. Yokus, B. ana Cakir, U.D. (2005). Seasonal and physiological variations in serum chemistry and mineral concentrations in cattle. Biological Trace Element Research,109 (3), 255-266.
5. Tanritanir, P. Dede, S. and Ceylan.; E. (2009). Changes in some macro mineral and biochemical parameters in female healthy siirt hair goats before and after parturition. J Anim Vet Adv 8(3), 530-533.
6. Brzezinska, M.; and Krawczyk, M. (2009). Changes of the mineral profile of Serum of goats in various physiological states. Journal of Elementology14(3), 649–656.
7. Samardzjia, M.; Dobranic, T.; Lipar, M.; Harapin, I.; Prvanovic, N.;Girzelji, J.; Greguric Gracner, G.; Dobranic, V.; Radisic, B. and Duricic, D. (2011). Comparison of blood serum macromineral concentrations in meat and dairy goats during puerperium. Veterinarski Ahriv. T. 81. P. 1–11.
8. Tóthová, c.; nagy, o. and kováč, g. (2014). Relationship between some variables of protein profi le and indicators of lipomobilization in dairy cows after er carving. Archiv Tierzucht, 57(1), 1–9.
9. Hagawane, S. D.; Shinde, S. B. and Rajguru, D. N. (2009). Haematological and blood biochemical profile in lactating buffaloes in and around Parbhani city. Veterinary World, 2(12), 467-469.
10. Peterson, R.G. and Waldern, D.E. (1981). Repeatabilities of serum constituents in Holstein-Friesians affected by feeding, age, lactation and pregnancy. J. Dairy Sci.; 64, 822-831.
11. Steel, R. G. D. and Torrie, J. H. (1986). Principles and procedures of Statistics, A biometrical approach. 4th Ed., McGraw Hill Book Co., New York, USA.
12. Kaneko, J.J.; Harvey, J.W. and Bruss, M.L. (2008). Clinical Biochemistry of Do- mestic Animals. 6th ed. Academic Press, Burlington, MA.
13. Hassan, G.A. and El-Nouty, F.D. (1985). Thyroid activity in relation to reproductive status, seasonal variation and milk production in buffaloes and cow heifers during their first lactation. Indian J. Dairy Sci.; 38: 129-136.
14. Alameen, A. O. and Abdelatif, A. M. (2012). Metabolic and endocrine responses of crossbred dairy cows in relation to pregnancy and season under tropical conditions. *American-Eurasian Journal of Agricoltural & Environmental Science*, *12*(8), 1065-1074.
15. Habasha, H. A. S. F. G. (2015). Total protein and some minerals in late stage of gestation and early lactation in dairy cows. AL-Qadisiya Journal of Vet. Med. Sci.14(2), 8-11.
16. Roussel, J. D.; Aranas, T. J. and Seybt, S. H. (1982). Metabolic profile testing in Holstein cattle in Louisiana: reference values. American journal of veterinary research, 43(9), 1658-1660.
17. Mohammad.A (2011). A Study of some Haematological and Biochemical Parameters in Late Pregnancy, Parturition and early Lactation in Crossbred Cows. PHD.V.Sc Thesis, College of Vet Med. University of Basrah.
18. Robillard, J. E. and Nakamura, K. T. (1988). Neurohormonal regulation of renal function during development. American Journal of PhysiologyRenal Physiology, 254(6), 771-779.
19. Oliveira, F. R.; Barros, E. G. and Magalhaes, J. A. (2002). Biochemical profile of amniotic fluid for the assessment of fetal and renal development. Brazilian journal of medical and biological research, 35(2), 215-222
20. Rakesh, K.; Sharma, I. J.; Rao, M. L. V.; & Quadri, M. A. (2001). Status of haemogram, plasma protein, minerals and electrolytes during pregnancy, anorexia and sub-clinical ketosis in cows and buffaloes. Indian J. Anim. Sci, 71(2), 118-121.
21. Deshpande, S.M.; Mantri, A.M, Talvelkar, B.A. and Deshmukh, B.T. (1998). Studies on microelements during gestation and early postpartum period in Gir and crossbred cows. Indian J Dairy Sci,51(5), 275- 279.
22. Padodara, R. J.; Arya, J. S. and Jacob, N. (2012). Assessment of serum mineral profile at different stages of gestation in triple crossbred cattle. Wayamba J Anim Sci, 26, 1-5.
23. Jacob, S. K. (2000). Assessment of mineral status during pregnancy in crossbred cattle. M.V.Sc. Thesis, Kerala Agricultural University, Mannuthy, Thrissur, Kerala.
24. Sikka, P. (1992). Role of minerals in reproduction -A Review. Indian J Dairy Sci,45(4), 159-167.
25. Choudhury, S.; Garg, S. K.; Singh, T. U.; & Mishra, S. K. (2011). Functional and molecular characterization of maxi K+-channels (BKCa) in buffalo myometrium. Animal reproduction science, 126(3), 173-178.

26. Tabatabaei, S. and Mamoei, M. (2012). Changes in the biochemical composition of fetal fluids and maternal blood serum during different days of gestation in cattle. Comparative Clinical Pathology, 21(5), 1005-1012.
27. Ashmawy, N. A.(2015). Changes in Peripheral Plasma hormone Concentrations and metabolites during the last trimester of pregnancy and around Parturition in the Egyptian Buffalo and Baladi cows. International Journal of Advanced Research,3(11), 1377 – 1390.
28. El-Fouly, H. A.; EL-Masry, K. A.;and Gamal. M. H. (1998). Physiological studies related to some productivity traits in Baladi cows. Zag. Vet. J. 26:69-78.
29. Lacetera, N.; U. Bernabucci, D. Scalia, B. Ronchi, G. Kuzminsky and A. Nardone, (2005). Lymphocyte functions in dairy cows in hot environment. Int. J. Biometeorol.; 50: 105-110.
30. Hendrick V, M.D.; Lori, L.; Altshuler, M.D. and Rita Suri, M.D. (1998). Psychosomatics. Academy of Psychosomatics Medcine 39:93-101.

Table1. Ions Concentration in Blood Serum in Different Physiological Status of Animal of Local Iraqi Cows

Groups	Physiological status of animal	Calcium (mmol/l) Mean ± SE	Phosphorus (mmol/l) Mean ± SE	Potassium (mmol/l) Mean ± SE	Sodium (mmol/l) Mean ± SE
1st group	10 pregnant cows 1st Trimester (1-3 months)	12.04 ± 2.34 b	8.52 ± 0.27 b	4.23 ± 0.21 a	3.34 ± 0.16 a
2nd group	14 pregnant cows 2nd Trimester (4-6 months)	13.46 ± 1.86 a	8.25 ± 0.68 a	6.35 ± 0.62 a	4.52 ± 0.23 a
3rd group	17 pregnant Cows 3d Trimester (7-9 months)	9.35 ± 1.64 b	5.33 ± 0.12 b	4.56 ± 0.17 b	5.22 ± 0.14 a
4th group	19 non pregnant Cows	7.54 ± 0.16 b	4.87 ± 0.23 b	3.81 ± 0.26 b	1.36 ± 0.02 c

Table.2 Hormones Concentration in Blood Serum in Different Physiological Status of Local Iraqi Cows

Groups	Physiological status of animal	Progesterone (ng/ml) Mean ± SE	Cortisol (ng/ml) Mean ± SE
1st group	10 pregnant cows 1st Trimester (1-3 months)	8.56 ± 1.43 c	11.54 ± 1.09 b
2nd group	14 pregnant cows 2nd Trimester (4-6 months)	14.63 ± 1.84 a	10.23 ±1.26 b
3th group	17 pregnant Cows 3d Trimester (7-9 months)	11.45 ± 2.23 b	16.45 ±1.58 a
4th group	19 non pregnant Cows	5.63 ± 0.65 d	14.62 ± 1.56 a

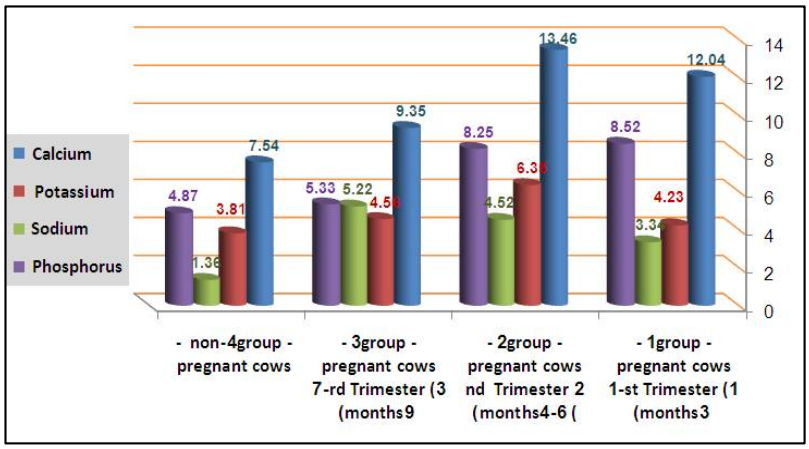

Figure-1 Ions Concentration (Mmol/L) in Blood Serum in Different Physiological Status of Animal of Local Iraqi Cows

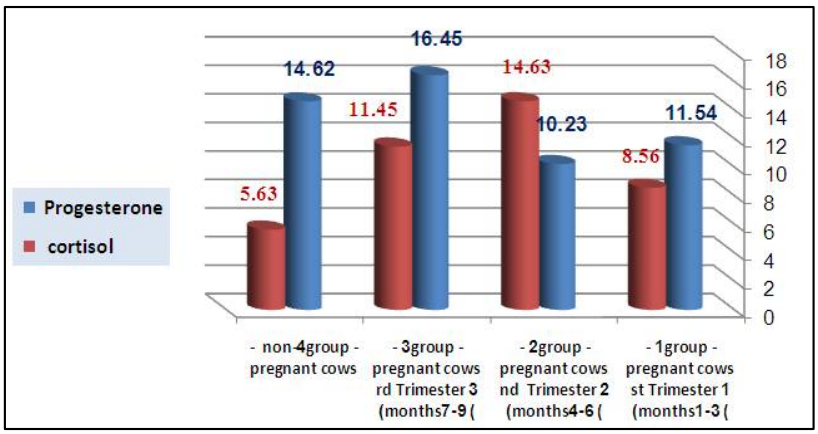

Figure-2 Hormones Concentration (ng/ml) in Blood Serum in Different Physiological Status of Local Iraqi Cows

Indian Journal of Natural Sciences www.tnsroindia.org.in ©IJONS

Vol.8 / Issue 49 / August /2018 *International Bimonthly* *ISSN: 0976 – 0997*

RESEARCH ARTICLE

Effect of Age and Breeding Season Upon Testicular and Epididymal Parameters in Relation to Spermatozoa Abnormality in Iraqi Ram

Wafir M. Saleh*

Department of Surgery and Obstetrics, College of Veterinary Medicine, University of Baghdad, Iraq.

Received: 06 Apr 2018 Revised: 08 May 2018 Accepted: 15 Jun 2018

*Address for correspondence
Wafir M. Saleh
Department of Surgery and Obstetrics,
College of Veterinary Medicine,
University of Baghdad, Iraq.

ABSTRACT

This study was conducted to evaluate the effects of age and breeding season upon testicular and epididymal parameters (testicular weight and size, epididymal weight, size and length) in Iraqi rams in relation to spermatozoa validity and abnormalities. Sheep is a short day breeder, its breeding season started from late September to early November with a tendency for ewes to give birth at February to March. 40 ram testicular pairs aged between 6-24 months are collected from Al-Shoàalla slaughter house each season (within and out of breeding season) starting from the end of September 2017 to the beginning of November 2017 (within breeding season) and from February 2018 till March 2018 (out of breeding season). Age of donor rams were recorded (6, 9, 12, 18, 24 month), testicular weight (87±0.22gm, 104.8±1.75gm, 210.3±4.55gm, 230.2±5.36gm, 280.5±6.78gm.), size were (35.5±2.74mm, 40.6±3.087mm, 60.8±3.66mm, 68.8±4.22mm, 76.6±4.88mm), while epididymal parameters were; weight (12.7 ±1.19gm, 14.2±2.07gm, 16.8±2.22gm, 17.4±2.87gm, 18.4±3.22gm.), size (12.2±1.2, 12.8±1.45, 13.1±1.67, 13.6±2.08, 13.8±2.11 mm) and length (13.2±1.08, 13.6±1.22, 14±1.54, 14.2±1.69, 14.7±1.82 cm.). Testicular and epididymal parameters in relation to the incidence of season were divided to within season WS (September, October, and November) and out of season OS (January, February, and March). WS testicular weight were (210.3±4.55, 208.3±4.34, 210.8±4.35 gm.) and size WS (60.8±3.66, 61.3±3.78, 60.3±3.50mm). Epididymal parameters WS were; wt (14.2±2.07, 15.1±2.21, 14.6±2.13 gm.), length (14.8±1.88, 14.6±1.66 15±1.78 cm.) and caudal wt (4.8±0.76, 5.2±0.82, 5.1±0.89gm). Out of season parameters were; testicular wt (211.2±4.60, 211.8±4.45, 209.4±4.43gm.), TS (62.1±3.78, 60.8±3.09, 61.6±3.11 mm), while those for epididymis were; wt (15.2±2.11, 14.8±2.09, 15±2.22 gm.), length (14.7±2.22, 14.7±2.20, 14.8±2.30 cm) and caudal wt (4.8±0.67, 5.3±0.74, 5.1±0.822gm). Effect of season on total sperm motility, viability, dead and alive percentage, were WS(viability%, 80-85, total motility 85%, dead 18-20% alive 78-80%), OS (viability 40%, total motility 35-40%, dead 60-65% and alive 35-40%). On conclusion there was a noticeable effect of season on ram reproductive parameters, but age significantly has more effect on those parameters in regarding to the healthy status of the ram as well as its breed.

Wafir M. Saleh

Keywords: Spermatozoa, Testicle, Epididymis, Season, Ram.

INTRODUCTION

Sheep gonadal activity cycle is a well-documented event in many breeds reared and controlled by photoperiod effect (1).Numerous evidences already exist in the literatures to support that gonadal function of high-latitude rams is regulated by changes in the day-length throughout a synchronization process involving the circadian system (2) which drives the melatonin-production and leads to the annual restriction of reproduction (3). Photoperiod may itself have better and significant effect on semen volume, motility and percentage dead or abnormal cells if accompanied with the Breed of ram (4).There is a tendency to keep in relation the animal (ram) total weight gain with the development and enlargement of the testicle in direct proportion way, the more weight gain is the more testicular organ weight, that is mean the breeding season mainly happened with most suitable period for the well pasture (raining season) and more grazing time (5,6).

Seasonal reproduction in ram is controlled by the pineal hormone melatonin which is the common link between photoperiod and reproduction (7). An increase in the daily diurnal period of melatonin secretion is associated with a decrease in GnRH release in long-day breeders, while an increase in GnRH release in short-day breeders (8). Melatonin influences GnRH release within or close to the mediobasal hypothalamus. Prolactin concentrations are consequently low during the breeding season of sheep and high during the breeding season of horses and hamsters (long-day breeder), Prolactin stimulates testicular function in rams. Seasonal changes in GnRH release in the horse are regulated by changes in a GnRH-inhibitory opioidergic tone. Opioids are at least, in part, responsible for the decrease in testicular function during winter. An opioidergic inhibition of LH release is present during the breeding season in rams; but dopaminergic pathways inhibit LH release during long daylight hours. A dopaminergic inhibition of LH release does not exist in stallions (9).

The effects of seasonal variations on the scrotal circumference and semen characteristics were analyzed by(10) in which; largest production of semen was recorded mainly in spring, whereas the lowest semen volume was produced in summer, seminal pH was slightly alkaline and significantly lower in autumn than in spring, the highest value of the total number of sperm per ejaculate was observed in spring for both breeds, and mass motility increased significantly in autumn compared with winter, spring, and summer while progressive motility was significantly lower during the months of summer and spring. Scrotal circumference, semen quality and the concentration of total protein in seminal plasma were relatively constant during the year, while total lipid and cholesterol concentrations increased in winter and summer, progressive motility was higher in winter and summer (11).

(12) described the effect of summer and spring season on testicles histological picture of ram, this effect involved some changes occurred on the wall of the arterioles that supplied the testicles, physiological increase in testicular vascularization was more in summer time if compared with spring time, the diameter and thickness of arterioles wall in summer time was higher than in spring.

MATERIALS AND METHODS

This study is designed to evaluate the effect of age and season on testicular size and weight, epididymal long, weight, cauda weight, size and spermatozoa mass motility, viability and abnormality within and out-season in ram.20 testicular pairs of 6-24months old donor rams, were collected from Al-Shoàalla slaughter house each season (within and out of breeding season) starting from the end of September 2017 to the beginning of November 2017 (within breeding season) and from February 2018 till March 2018 (out of breeding season).

Preparation of the testicles is accomplished as described by(13). Testicular abattoir specimens after collected soon after slaughtering at the abattoir preserved in cool boxes and transported to the lab. Testicles specimens were refreshed by removing all surrounding tissue by curved surgical scissors thoroughly washed twice with water then cleaning out with normal saline. Epididymal separation from the entire testicular organs using curved surgical scissors, separated epididymis was subjected to long, weight and caudal size calculation, all results were recorded. Cauda of epididymis then separated from the whole epididymal organ, injected with warm normal saline and subjected for slicing by surgical blade. By a plastic syringe, we aspirate o.5 ml of the fluid (the consistency of this fluid is the injectable normal saline which mixed and diluted caudal secretion and spermatozoa, this 0.5 ml were conducted for evaluation the spermatozoa parameters (massive motility, viability and abnormalities). All results will be recorded for further evaluation

RESULT

Effect of Donor Ram Age Upon Testicular and Epididymal Parameters

Result showed that; age of donor ram had a direct proportion effects on testiculat weight and size, epididymal weight, length and size, in which, an older donor rams supplied more large and bigger size testicular samples, and this elevated testicular samples relected the elevated epididymal parameters as shownen in table (1).

Effect of Breeding Season Upon Testicular and Epididymal Parameters

Result showed that; season had a proportional or even relative effect upon testicular and epididymal parameters, in which; testicular weight remain unchanged or even slightly changed which is related mainly to the age. Same results are collected with the epididymal parameters as showen in table(2). Age of donor ram is not envolved with this parameters and from a practical and more scintific veiw we fixed the 18 months is the age of donor ram that the other parameters are followed.

Effect of Breeding Season Upon Spermatozoa Motility and Viability Inrelation to Dead or Alive Spermatozoa

Result showed that; there is a marked effect of season on dead or alive spermatozoa percentage, number of dead spermatozoa is increased with the samples that collected on breeding season. This finding is reflected the effect of season upon spermatozoa vaibility inrelation to. Total motality, is decreased as the donor ram out of breeding season according to the collected samples at that period, while these activities appeared more bronounced in the samples collected within breeding season (table. 3)

Effect of Breeding Season on Abnormalities Percentage and Type

Result showed that; The more spermatozoa abnormality incidance is the protoplasmic droplets (distal), in a way, it is appeared in both season but with more and clearly obvious when the samples are collected out of season (January, February and March). The incidence of the other abnormalities as detached head, double tail and coiled tail is with relatively low within season appositing to a moderate or slightly elevated out of season as showen in (table.4).

DISCUSSION

The main objective results of this study areto confirm ; whether the breeding season has a relatively to moderate factor that affects ram reproduction or the effect of age and other environmental factors have more affected incidence than that of the breeding season.

Effect of Donor Ram Age Upon Testicular and Epididymal Parameters

Sheep is a seasonal breeder animals (short-day light) in which reproduction in this species are eliminated by the effect of day light upon its minimized period. Results of this study showed that; although there is an effect of season upon testicular stimulations but the effect of the age is more dominant. This is may be due to sexual maturity modulation by age or the increase effect of androgen hormone in relation to age factor. (14) put his approval in which ram has the ability to produce semen of high quality all over the year not at restricted period (breeding period) (6) not agree with result of this study, because; unlike most domestic livestock species, sheep are widely known as an animal with marked seasonality of breeding activity..The annual cycle of daily photoperiod has been identified as the determinant factor of this phenomenon, while environmental temperature, nutritional status, social interactions, lambing date and lactation period are considered to modulate it.

The importance of seasonal breeding as a reproductive strategy for the survival of species, given to the neuroendocrine base of photoperiodic regulation of seasonal breeding. (15)put his agreement on the age factor,testicular parameters, semen quality and production improved and stabilized up to at the age of 3 years, in which testicular parameters as weight, size, spermatozoa production as well as epididymal parameters all are improved as the rams being older. (16) Approved the results of this study, testicular size, weight and testosterone concentration increased with age. Furthermore, semen quality was fairly independent of age except for some morphological abnormalities.

Despite the seasonal variations affecting sperm quality and quantity, these parameters were within the range regarded as satisfactory for normal fertility. (17) Agreed with the results but he concludes that neither the age itself nor the season alone can arranged the reproductive status of the ram especially those ram chosen for breeding purposes, in which; there is a marked effect and control of the season on the reproductive performances but ram age has more effect on ram reproduction and mainly if we can put both season and age on consideration.

Effect of Season on Testicular and Epididymis Parameters

Sheep are important animals in many tropical and subtropical countries, and have a seasonal controlling in their reproductive status. In subtropical areas, as in Iraq; ewes are generally bred during the late summer to lamb during the winter, mainly at rain period to have excessive food, thus increasing the need at parturition for milk production (18). (19) Not agree with the results of this study and put her approved in which; sheep breed is known to display a clear seasonal reproductive response orchestrated by the significant annual variation in photoperiod related to its latitude of origin. However, in the low latitudes of the tropical and subtropical environments the magnitude and timing of these responses in rams has been well investigated.

Rams were monitored during 1 year for testicular size, seminal parameters and serum testosterone, from autumn to winter, under shortening daylength, rams underwent a significant gonadal involution. Testicular size increased in spring and reached a peak in summer, similar to the latitude of which this breed originates. Parallel to scrotal circumference, other parameters such as testicular volume, serum testosterone concentration, ejaculate volume and sperm concentration followed a seasonal profile. Testosterone levels followed the same seasonal pattern as testicular size. Ejaculate volume was significantly lower during autumn and winter and higher values of sperm concentration

were detected in spring. Sheep native to temperate climates are usually quite seasonal in their breeding habits, though rams are less affected than ewes. A ram's testicular size, sperm production, and mating capacity will vary according to the season of the year, being highest during the normal fall breeding season .Some breeds are much less seasonal in their breeding behavior: Dorset, Rambouillet, Merino, Polypay, Finnsheep, Romanov, and hair sheep. (Special communication). (20) put his approval that; the main affected factor on ram reproduction is its seasonality more than the effect of the age in which testicular endocrine activity concerned serum testosterone concentration, no statistically significant effect of age on the testosterone concentration, while seasonal variations were statistically significant in ram ages with higher values during spring and autumn and lower values during summer and winter. (21) put his approval that the age factor influenced ram reproductive activities more than the season, result of his study showed that no significant different found for semen quality parameters at different ages of ram, sperm motility of local ram semen was influenced by age oldest age of 25-36 months produces highest motility of sperm and viability.

Effect Season on Abnormalities Percentage and Spermatozoa Viability

Seasonal changes in semen volume and quality in ram semen obviously influence ejaculate volume, semen pH, sperm concentration, sperm motility, percentage live and normal sperm and sperm abnormalities. (22) Agree with this if age of ram doesn't influence, ram was found to be a seasonal breeder (late summer through autumn) and produced semen only during this period. Semen volume differed between months, with the highest production in autumn and the lowest in summer. Semen pH increased linearly from autumn through spring, and lower early (February) and late (August) in the breeding season, the percentage of normal sperm was higher during winter than in summer and autumn. (23) Approved that; if age not involved, ram was under seasonal effect in a way this factor influence the semen quality and volume as well as spermatozoa validity, winter season is not generally recommended for semen collection, especially when this semen used in AI processes seminal quality is not recommended. (24) Add his statement that; the magnitude of the seasonal effects which involved ram production was not sufficient to prevent it from being used for breeding throughout the year. However, the existence of differences among rams within each breed in semen quality and quantity makes it necessary to perform a semen evaluation on individual basis in order to select the best males before they are used for breeding, that is mean season in not the main factor t involved ram reproduction, there is an individual variation that need to follow when we select rams for breeding purposes, ram can bred all over the year. (25) mentioned his statement that; ram reproductive status is controlled mainly by two main factors with some degrees of variations, those factors are age and season, in which, the volume of ejaculate was highly influenced by the season but not by the age, it was more important in spring and autumn than in winter and summer. The mass motility did not show seasonal variation, but showed significant variation with age, the sperm concentration was not influenced by the season but it varied significantly with the age category.

REFERENCES

1. Gómez-Brunet, J. Santiago-Moreno, A. del Campo, B. Malpaux, P. Chemineau, D.J. Tortonese, A. Gonzalez-Bulnes, A. López-Sebastián (2008). Endogenous circannual cycles of ovarian activity and changes in prolactin and melatonin secretion in wild and domestic female sheep maintained under a long-day photoperiod. Biol. Reprod., 78 (2008), pp. 552-562.
2. LincolnG.A; Clarke, I.J; Hut, R.A; and Hazlerigg, D.G.(2006). Characterizing a mammalian circannual pacemaker.Science, 314, pp. 1941-1944.
3. Arendt, J; Symons, A.M; English, J.; A.L. Poulton, A.L. and I. Tobler, I. (1988). How does melatonin control seasonal reproductive cycles .Reprod. Nutr. Dev., 28, pp. 387-397

4. Blond, M.P.; Al-Kamali, A.A.; Crosby, T.F.; Haynes, N.B.; Howles, C.H.; Kelleher, D.L and Gorden, I. (1988). The influence of breed, season and photoperiod on semen characteristics, testicular size, and libido and plasma hormone concentrations in rams. Animal Reproduction Science. Volume 9, Issue 3, October 1985, Pages 241-252.
5. Allaoui, A.; B. Safsaf, B.; W. Laghrouand Tlidjane, M. (2014). Factors Affecting Scrotal Measurements and Weight of Oule-Djellal Rams in Eastern and South-Eastern Algeria.2013 4th International Conference on Agriculture and Animal Science (CAAS 2013).APCBEE Procedia 8 (2014) 260 – 265.
6. Rosa, H.J.D. and Brynat, M.J. (2003).Seasonality of reproduction in sheep.Small Ruminant Research. Volume 48, Issue 3, June 2003, Pages 155-171.
7. Bielli, A; Pedrana, G; Gastel, MT; Castrillejo, A**;** Morana, A; Lundeheim, N; Forsberg, M and Rodriguez-Martinez, H (1999). Influence of grazing management on the seasonal change in testicular morphology in Corriedale rams.Anim. Reprod. Sci., 56: 93-105.
8. Lincoln, GA; Lincoln, CE and McNeilly, AS. (1990). Seasonal cycles in the blood plasma concentration of FSH, inhibin and testosterone, and testicular size in rams of wild, feral and domesticated breeds of sheep. J. Reprod. Fertil, 88: 623-633.
9. Gerlach, T and Aurich, JE (2000).Regulation of seasonal reproductive activity in the stallion, ram and hamster.Anim. Reprod. Sci., 58: 197-213.
10. Al-Anazi, Y; M Al-Mutary, M. G.; Al-Ghadil, M.; M. M. Alfuraiji, M.M.; Al-himaidi, A.R.; Ammari, A (2017). Seasonal variations in scrotal circumference and semen characteristics of Naimi and Najdi rams in Saudi Arabia.South African Journal of Animal Science.On-line version ISSN 2221-4062. Print version ISSN 0375-1589.
11. Benmoula A; Badi A,; El Fadili M,; El Khalil K.; Allai L.;, El Hilali , A. and El Amiri B. (2017).Effect of season on scrotal circumference, semen characteristics, seminal plasma composition and spermatozoa motility during liquid storage in INRA180 rams.Anim Reprod Sci. 2017 May;180:17-22.
12. Saleh, W. M. (2016). Role of Epididymal Spermatozoa *In Vitro* Fertilization and Embryo Transfer in Iraqi Sheep. PhD dissertation submitted to the Council of the College of Vet. Med.\ University of Baghdad in Partial Fulfillment of the Requirement for degree of Doctor of Philosophy in Vet. Med.\ Theriogenology. August 2016.
13. Hassan, M.R.; Pervage, S.; Ershaduzzaman, M. and M. Talukder, M.A.I. (2009) Influence of age on the spermiogramic parameters of native sheep.J. Bangladesh Agril. Univ. 7(2): 301–304, 2009 ISSN 1810-3030.
14. Belkhiri, Y.; Bouzebda-Afri, F.; Bouzebda, Z. and Mouffok, C. (2017).Age and Season Effects on Sexual Parameters in Mature Rams Used in Artificial Insemination Centre (Algeria) Global Veterinarian 18 (1): 31-40, 2017.
15. Zamiri, M.J., B. Khalili, M. Jafaroghli and Farshad T. (2010).Seasonal variation in seminal parameters, testicular size and plasma testosterone concentration in Iranian Moghani rams. Small Ruminant Research, 94(1-3): 132-136.
16. Degen AA, Benjamin RW.(2003). Milk intake and growth rate of Awassi lambs sucking ewes grazing on natural pasture in the semiarid Negev. Anim Sci, 76:455-460
17. Viviane Milczewskia; Samira Chahad-Ehlersa; Katherine Maria Spercoskib; Rosana Nogueira Moraisb; and VaneteThomaz Soccola (2015).Quantifying the effect of seasonality on testicular function of Suffolk ram in lower latitude. Small Ruminant Research Volume 124, March 2015, Pages 68-75
18. Benia, A. R.; Taibi, K.; Ait-Amrane, A.; Belhamiti, T.; Hammoudi, S. M. and Kaidi, R.(2013). Study of seasonal sexual activity variations in Algerian rams: Sexual behavior, testosterone concentration control and environmental factors. African Journal of Biotechnology. Vol. 12(41), pp. 6042-6048.
19. Solihati N; Rasad SD; Setiawan R, and Alvionita C. (2016).Quality and Viability of Javanese Local Ram Semen at Different Age. DOI: http://dx.doi.org/10.14334/Proc.Intsem.LPVT-2016-p.265-270.
20. Loubser, P.G. and van Niekerk, C.H.(1983).Seasonal changes in sexual activity and semen quality in the Angora ram. 2. Semen volume, quality and freezability. S. Afr.Tydskr. Veek, 1983 13(3).
21. Malejane, C.M.; Greyling, J.P.C. and M.B. Raito. (2014).Seasonal variation in semen quality of Dorper rams using different collection techniques. South African Journal of Animal Science 2014, 44 (No. 1).
22. Karagiannidisa, A.; Varsakelib, S.; Alexopoulosa, C. and Amarantidis, I. (2000).Seasonal variation in semen characteristics of Chios and Friesian rams in Greece.Small Ruminant Research 37 (2000) 125±130.

23. Benia, A.R.; Saadi, M.A.; Ait-Amrane, A.; Belhamiti, T.B.; Selles, S, M. A. and R Kaidi, R. (2018). Effect of season and age on main characteristics of sperm production in the Ouled-Djellal rams. Livestock Research for Rural Development, 30 (1) 2018

Table1: Effect of Age of Donor Upon Testicular and Epididymal Parameters

Age (Month	Testicle				Epididymis					
	Weight (gm)	SE	Size (mm)	SE	Weight (gm)	SE	Size (mm)	SE	Length (cm)	SE
6	87	±0.22	35.5	±2.74	12.7	±1.19	12.2	±1.2	13.2	±1.08
9	104.8	±1.74	40.6	±3.087	14.2	±2.07	12.8	±1.45	13.6	±1.22
12	210.3	±4.55	60.8	±3.66	16.8	±2.22	13.1	±1.67	14	±1.54
18	230.2	±5.36	68.8	±4.22	17.4	±2.87	13.6	±2.08	14.2	±1.69
24	280.5 ±6.78		76.6 ±4.88		18.4 ±3.22		13.8 ±2.11		14.7 ±1.82	

Table 2: Effect of Breeding Season Upon Testis and Epididymis Parameters

Parameter	Within season			Out of season		
	Sptember	October	November	January	Fabruary	March
Testis wt. gm	210.3±4.55	208.3±4.34	210.8±4.35	211.2±4.60	211.8±4.45	209.4±4.43
Testis size mm	60.8 ±3.66	61.3±3.78	60.3±3.50	62.1±3.78	60.8±3.09	61.6±3.11
Epididymal wt gm	14.2 ±2.01	15.1±2.21	14.6±2.31	15.2±2.11	14.8± 2.09	15± 2.22
Epididymal length cm	14.8±1.68	14.6±1.66	15±1.78	14.7± 2.22	14.7± 2.20	14.8± 2.30
Caudal wt gm	4.8± 0.76	5.2±0.82	5.1± .89	4.8± 0.67	5.3±0.74	5.1±0.822

Table 3: Effect of Season on Total Motility and Viability of Spermatozoa Inrelation to the Dead or Alive Spermatozoa

Season	Viability (%)	Total motility(%)	Dead (%)	Alive (%)
Within season	80-85	85	18-20	75-80
Out of season	40	35-40	60-65	35 - 65

Table 4: Type and Incidence of Spermatozoa Within and Out of Season

Season	Distal droplet %	Detached head %	Double tail %	Coiled tail %
Within season	8	3	2	3
Out of season	15	11	8	11

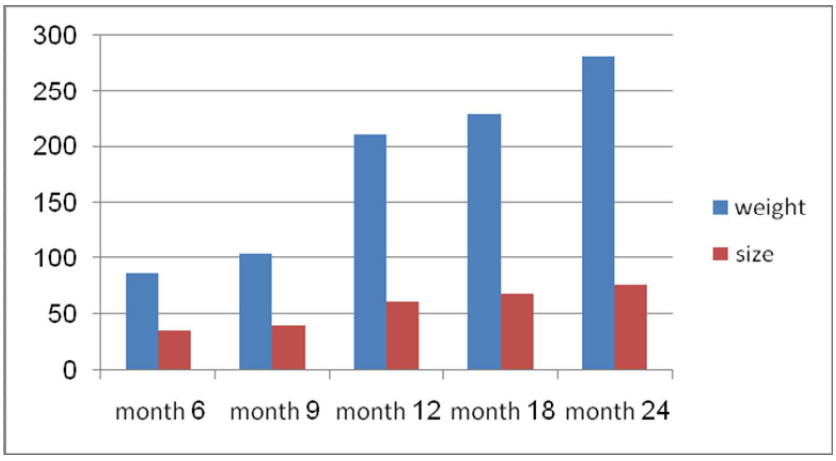

Diagram 1: Effect of Age (Month) Upon Testicular Weight (gm) and Size (mm)

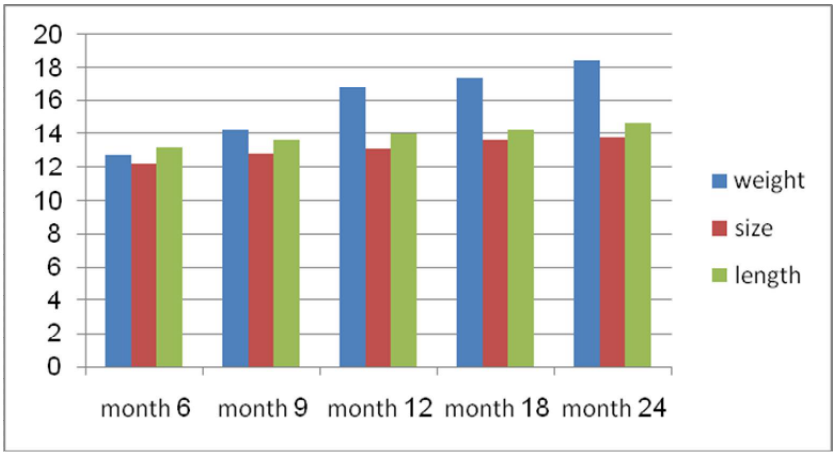

Diagram 2: Effect of Age (Month) Upon Epididymis Weight (gm.), Size (mm) and Length (cm)

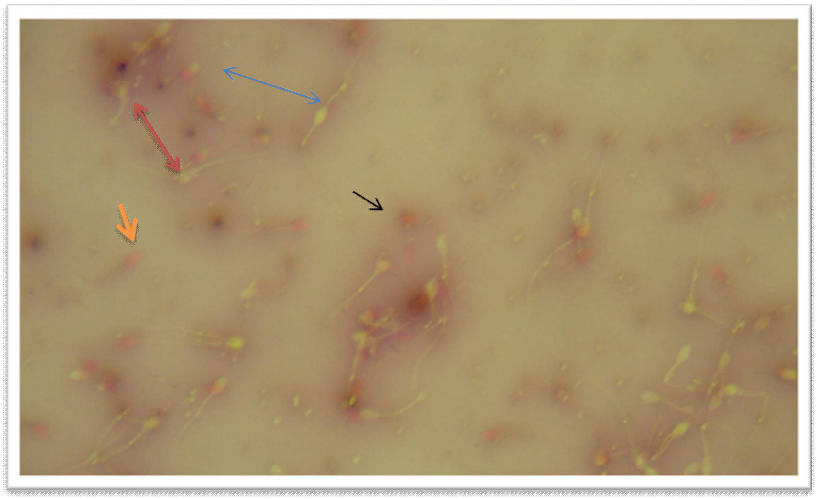

Diagram 3:Stained Slide for Out Season Collected Sample Shows the Moderate Sperm Cells with Some Abnormalities, Distal Protoplasmic Droplet (bule), Alive Sperm Shows as Uncolor Head (green), Detached Head (black) and Dead Sperm with Stained Head (orange).

Indian Journal of Natural Sciences www.tnsroindia.org.in ©IJONS

Vol.8 / Issue 49 / August /2018 *International Bimonthly* *ISSN: 0976 – 0997*

RESEARCH ARTICLE

The Prevalence of H. Pylori in Wait Province, Iraq

Adil Abdul Razzaq Waheeb Al Shammari [1], Mustafa Khudhair Abbas [2] and Khawlah Abdulamer Abed [3]*

[1]Department of Medicine, College of Medicine, University of Wasit, Kut, Iraq.
[2,3]Department of Microbiology, College of Medicine, University of Wasit, Kut, Iraq.

Received: 04 Apr 2018 Revised: 09 May 2018 Accepted: 15 Jun 2018

***Address for Correspondence**
Khawlah Abdulamer Abed
Department of Microbiology,
College of Medicine,
University of Wasit, Kut, Iraq.

ABSTRACT

Helicobacter pylori is considered as main cause of gastro-intestinal infections. The current study was done in Al-Kut city, from January 2016 to January 2017. A total of 100 patients were joined our study and all patients were having symptoms of gastrointestinal infection. All 100 samples were examined for detection of H. pylori infection by H. pylori antigen assay and for the lipid profile test. It was found that the mean serum values were considerably higher for cholesterol, triglyceride and LDL; whereas it was lower for HDL. There is no significant association between H. pylori infection and lipid profile, Cholesterol, triglyceride, HDL and LDL was lower in H. pylori positive than in negative samples. This study revealed the prevalence rate of *H. pylori* infection and the lipid profile according to gender in Iraq.

Key words: - H. Pylori,

INTRODUCTION

Helicobacter pylorus was depicted in 1984 (1). It is a gram-negative winding or helix molded, microphilic urease-delivering bacterium and motile (2, 3). It colonizes and develops in abdominal mucosa and in zones of abdominal biennial in the duodnum; it can enter the mucoid covering in the stomach (3). It is a standout amongst the most well-known unending bacterial contaminations in human's world– wide (4, 5). The greater part of the total populace harbor H. pylori in their upper gastrointestinal plot; in this way it is the most pervasive disease on the planet (4, 6). The contamination frequency of H. pylori varies as indicated by area; it is more typical in creating nations, and diminished in European nations (5, 7, 8). The hatching span for H. pylori separation has been proposed to be 2-7 days (9). A few examinations set up that it causes a few upper gastrointestinal maladies, for example, ceaseless gastritis, plot and duodenal ulceration, and peptic ulcers and it is engaged with the malignancies (gastric carcinoma and lymphoma) (3,10). Moreover, H. pylorus is related with other malady not identified with stomach related framework, for example, Myocardial Infection, Coronary Heart illness and Insulin subordinate diabetes (11, 12). The most widely recognized colonized individuals still asymptomatic and sound and just 15% have ailment (11). The event of fiery Pathogenesis relies upon have hereditary powerlessness, strain destructiveness and ecological cofactors (13). For

ideal development, H. pylori serotypes needs complex basal medium with enhancements, for example, entire blood of pony or sheep, corn starch, egg yolk emulsion, charcoal or serum. These supplements may fill in as nourishing substrates or detoxify medium or ensure H. pylori development (12, 14). The exact method off conveyance is dubious however intra-familial grouping proposes individual to-individual spread for the most part in adolescence (15). The contamination chance with H. pylori is related with living conditions financial status (5, 11). Potential dietary relations with H. pylori have been examined in people and interminable over the top salt utilization has been appeared to enhance the colonization of H. pylori in mice and people (13). Different methods of transmission for H. pylori are assumed and no particular pathway has been distinguished obviously.

These pathways might be individual to individual, oraloral and fecaloral transmission by which salivation, Feces or regurgitation can spread the life form (14). Additionally, it can spread from mother to infant either in pregnancy or on a level plane by bosom drain in the postnatal period (13). Also, it can be transmitted mechanically by housefly (15), therefor poor sanitation can give its transmission. Individual to individual approach is the most conceivable method of transmission. Extra course of conveyance is iatrogenic in which endoscopes or tubes in contact with gastric mucosa of one patient are utilized for someone else. Another conceivable method of transmission is oral-fecal and H. pylori have been found in dung of contaminated youngsters (3, 11). Water dirtied with excrement is a fundamental disease sources too the ingesting of uncooked vegetables washed with debased water (9). Defiled open water supply has more odds of spreading H. pylori disease contrasted and private water supply (15). Disease is more continuous in early youth in creating nations contrasted and western populaces as sign of H. pylori is uncommon before 10 years of age while increments too 10 % in ages 18-30 years of age and too 50 % in individuals more established than 60 years of age maybe in light of the poor clean conditions, possibly connected with bring down anti-toxins treatment for irrelevant pathologies (12).

In numerous creating nations, there is a high pervasiveness rate of disease (80-95%) (5). More prominent than half of kids with 10 years of age are contaminated with H. pylori with the occurrence of contamination more than 80% in youthful grown-ups (3, 6). The period of contamination with this bacterium is impact the potential pathologic result of the disease: Acquisition of this bacterium at youth are conceivable to grow more separate irritation which might be trailed by atrophic gastritis related with a higher danger of gastric tumor, gastric ulcer, or both (15). Individuals who tainted with this bacterium at a more established age create diverse gastric changes that are more conceivable to cause duodenal ulcer (11). The contamination with H. pylori followed through procedures off carcinogenesis which are: Chronic dynamic gastritis, gastric decay, intestinal metaplasia, dysplasia and gastric tumor. Systems of H. pylori disease conclusion include microbiological strategies, hereditary, immunological, neurotic, and finding by the identification of bacterial urease. Methodologies are either intrusive requiring biopsy with endoscopy or non-obtrusive (3, 7).

MATERIALS AND METHODS

Study Population

100 unwell enrolled from Al-Kut city in Iraq. Stool samples (20 gm) were collected from each unwell for detection of *H. pylori infection* by *H. pylori antigen* assay. Additionally, blood (1 ml) samples were obtained from every patient for the lipid profile test. This study was continued from January 2016 to January 2017.

Sample Preperation

After gathering, blood was centrifuged for10 min at 1500 rpm. At that point the serum was isolated and utilized for the lipid profile examine. For stool antigen test, the top of the example tube was untie, at that point the example accumulation utensil was arbitrarily wounded into fecal example in 3 unique positions to acquire around 40 mg of

defecation. At that point the tool was returned again into the tube and shut. Accumulation tube was shaken mphatically by vortex blender, at that point centrifuged at 4000 rpm for 5 minutes. At last, supernatant was prepared for the test.

H. Pylori Stool Antigen Assay

The examples analyzed for H. pylori antigen by ABON one stage H. pylori antigen test gadget (Inverness Medical Innovation Hong Kong Limited). It is a sidelong stream chromatographic immunoassay. Assay expert as indicated by the maker directions. Right off the bat, two drops of extricated stool were acquainted with the example well of the test unit. The outcome was watched 10 min after example expansion. The measure is sure once the test line (a purple-pink line) showed up with the control line, and considered negative if just the control line showed up. Nonappearance of control line uncovered invalid outcome.

The Lipid Profile Detection

Triglycerides were. HDL.Total cholesterol. Serum samples were tested for the lipid profile. Test was performed according to manufacture's, measured using direct enzymatic assy. The Friedewald equation was used to calculate L.D [Tunisia, Biomagherb] ruction by kits inst. Statistics collected were analyzed using SPSS package.L serum levels (to) 20 version conclude the variance magnitude 0.05>P value of under ROC curve ratio and area odd regarded magnitude.

RESULTS

100 unwell enrolled in this study. Tables (1) illustrate the Demographic data of the patients enrolled in this study. The male patients were 65 (65%), while the female were 35 (35%). Survey set up no connection *H. pylori* infection and sex. Totally, the smoking data in these patients was 24 (24%) smoking and 76 (76%) don't smoking.

Lipid Profile in *H. Pylori* Infection

It was founded that in patients infected who are positive for *H. pylori* the mean serum values were lower for [LDL 112.9286 mg/dl; HDL 36.486 mg/dl; P=0.000], cholesterol [0], triglyceride [302.8571mg/dl; P=0.037] than in *H. pylori* negative samples [LDL=141.6209 mg/dl; HDL= 37.756 mg/dl; cholesterol= 0 mg/dl; triglyceride =235.0581 mg/dl]. Nevertheless, VLDL mean serum value was higher [59.2714 mg/dl P=0.000] in H. pylori positive cases than in those negative [46.8012], (Table- 2, 3).

DISCUSSION

The contamination with H. pylori was related with physiological adjustments in human (16, 17). This investigation demonstrated that there was an essential change in lipid profile H. pylori samples. It was discovered that the serum esteems were extensively higher for cholesterol, triglyceride and LDL; while it was bringing down for HDL. There is no critical relationship between H. pylori contamination and lipid profile, Cholesterol, triglyceride, HDL and LDL was bring down in H. pylori proven than in negative examples. A few investigations built up that H. pylori may be related in incitement different changes in serum lipid profile and play as hazard component for atherosclerosis (18,19,16). However, different explores not set up these discoveries (20, 21). An investigation of Ansari et al had expressed that mean levels of triglyceride, cholesterol, LDL notwithstanding LDL/HDL and cholesterol/HDL extent in 40 patients with gastritis caused by H. pylori contamination were significantly expanded contrasted with controls, though HDL was diminished extensively. Kim et al (20). Demonstrate that cholesterol and LDL was expanded in

patients tainted with H. pylori, yet HDL and triglyceride not have such outcome. Furthermore, it was appeared in a Jordanian report (22), which included 350 examples, showed that 77% of tests were H. pylori sure, while in this present examination the inspiration rate was 14%. Likewise, other investigation uncovered energy of 73% in Turkey (23). The serum cholesterol, cholesterol/HDL and triglyceride were extensively low in unwell contaminated with H. pylori in contrast with H. pylori sure (23). Foundational incendiary reaction to H. pylori animates changes in lipid and lipoprotein digestion (24). In spite of the fact that past examinations on the connection between lipid profiles and H. pylori contamination displayed conflicting outcomes, there is a typical assertion that H. pylori contamination changes serum lipid profiles (25,26). H. pylori contaminated patients demonstrated an atherogenic lipid profile which increment in LDL cholesterol or diminished HDL cholesterol in correlation with uninfected patients (27, 28). H. pylori disease was built up by the presence of serum H. pylori-particular neutralizer in a large portion of the earlier examinations on the relationship between H. pylori disease and lipid profile (25,27). By and by, the H. pylori disease serological determination has a high exactness; it is considered as a roundabout strategy. In this manner, histological determination stills the standard for the identification of H. pylori disease (28).

CONCLUSION

The relevance through H. pylori disease and LDL cholesterol levels requires more examinations to endorse our outcomes. Estimating LDL cholesterol when H. pylori annihilation can be an appropriate case.

ACKNOWLEDGMENTS

I am very grateful to my team for their help in following up patients' thank you for all your technical and emotional support.

REFERENCES

1. Marshall BJ, Warren JR. Unidentified curved bacilli in the stomach of patients with gastritis and ulceration. Lancet 1984; i: 1311-1315.
2. Pounder RE, Ng D. The prevalence of Helicobacter pylori infection in different countries" Aliment Pharmacol Thera 1995; Volume (Suppl 2): 33-39.
3. Pounder RE, Ng D. The prevalence of Helicobacter pylori infection in different countries. Alimentary Pharmacology & Therapeutics. 1995; 9(2):33-39.
4. Segal I, Ally R, Mitchell H. Helicobacter pylori--an African perspective. QJM. 2001; 94(10):561-565.
5. Perez-Perez GI, Rothenbacher D, Brenner H. Epidemiology of Helicobacter pylori infection. Helicobacter. 2004; 9(1):1-6.
6. Cave DR. Transmission and epidemiology of Helicobacter pylori. Am J Med. 1996; 100(5A):12S-17S.
7. McColl KEL. Helicobacter pylori, clinical aspects. Journal of Infection 1997; 34: 7-13.
8. Pounder RE, Ng D. The prevalence of *Helicobacter pylori* infection in different countries. Aliment Pharmacol Ther 1995; 9 Suppl 2: 33-9.
9. Pounder RE, Ng D. The prevalence of Helicobacter pylori infection in different countries" Aliment Pharmacol Thera 1995; Volume (Suppl 2): 33-39.
10. McGee DJ, May CA, Garner RM, Himpsl JM, Mobley HL. Isolation of Helicobacter pylori genes that modulate urease activity. J Bacteriol. 1999; 181(8):2477-2484.
11. McGee DJ, May CA, Garner RM, Himpsl JM, Mobley HL. Isolation of Helicobacter pylori genes that modulate urease activity. J Bacteriol. 1999; 181(8):2477-2484.
12. Yin, Y.; He, L. and Zhang,J. Successful isolation of *Helicobacter pylori* after prolonged incubation from patient with failed eradication therapy, *World J Gastroenterol.* Vol. 15, No. 12, 1528-1529 (2009).

13. Labigne A; de Reuse H. Determinants of Helicobacter pylori pathogenecity. Infectious Agents and Diseases1996; 5: 191-202.
14. Riegg SJ, Dunn BE, Blaser MJ. Microbiology and pathogenesis of Helicobacter pylori.. Infections of the gastrointestinal tract. New York. Raven Press. 1995; 535-550.
15. Pounder RE, Ng D. The prevalence of Helicobacter pylori infection in different countries. Alimentary Pharmacology & Therapeutics. 1995; 9(2):33-39.
16. Titeman TL, Morris J. Beyond the stomach: an updated view of Helicobacter pylori pathogenesis, diagnosis and treatment. World J Gastroenterol, 2014; 20: 12781-12808.
17. Franceschi F, Annalisa T, Teresa DR, Giovanna D, Ianiro G, Franco S, Viviana G, Valentina T, Riccardo LL, Antonio G. Role of Helicobacter pylori infection on nutrition and metabolism. World J Gastroenterol, 2014; 20(36): 12809-12817.
18. Buzas GM. Metabolic consequences of Helicobacter pylori infection and eradication. World J Gastroenterol, 2014; 20: 5226-5234.
19. Ansari MH, Omrani M, Sayyah B, Ansari SK. Effect of Helicobacter pylori infection on the lipid, lipoproteins, Apolipoprotein-A1, lipoprotein (a) and Apolipoprotein-B in patients with gastritis. African J Microbiol Res, 2010; 4: 84-87.
20. Danesh J, Peto R. Risk factors for coronary heart disease and infection with Helicobacter pylori: meta-analysis of 18 stud- ies. BMJ, 1998; 316: 1130-1132.
21. Zhu J, Quyyumi AA, Muhlestein JB, Nieto FJ, Horne BD, Zalles-Ganley A, Anderson JL, Epstein SE. Lack of association of Helicobacter pylori infection with coronary artery disease and frequency of acute myocardial infarction or death. Am J Cardiol, 2002; 89: 155-158.
22. Erdogan AF, Asma S, Gereklioglu C, Turan I, Abaci K. Association between Helicobacter pylori infection and low density lipoprotein cholesterol. Turkish J Family Med Pri Care, 2014; 8: 19-24.
23. Al-Fawaeir S, Zaid MA, Awad AA, Alabedallat B. Serum lipid profile in Helicobacter pylori infected patients. J Investig Biochem, 2013; 2: 132-135.
24. Gallin JI, Kaye D, O'Leary WM. Serum lipids in infection. N Engl J Med. 1969;281:1081–1086.
25. Jia EZ, Zhao FJ, Hao B, Zhu TB, Wang LS, Chen B, Cao KJ, Huang J, Ma WZ, Yang ZJ, Zhang G. Helicobacter pylori infection is associated with decreased serum levels of high density lipoprotein, but not with the severity of coronary atherosclerosis. Lipids Health Dis. 2009;8:59.
26. Kucukazman M, Yavuz B, Sacikara M, Asilturk Z, Ata N, Ertugrul DT, Yalcin AA, Yenigun EC, Kizilca G, Okten H, Akin KO, Nazligul Y. The relationship between updated Sydney System score and LDL cholesterol levels in patients infected with Helicobacter pylori. Dig Dis Sci. 2009;54:604–607.
27. Takashima T, Adachi K, Kawamura A, Yuki M, Fujishiro H, Rumi MA, Ishihara S, Watanabe M, Kinoshita Y. Cardiovascular risk factors in subjects with Helicobacter pylori infection. Helicobacter. 2002;7:86–90.
28. Hoffmeister A, Rothenbacher D, Bode G, Persson K, März W, Nauck MA, Brenner H, Hombach V, Koenig W. Current infection with Helicobacter pylori, but not seropositivity to Chlamydia pneumoniae or cytomegalovirus, is associated with an atherogenic, modified lipid profile. Arterioscler Thromb Vasc Biol. 2001;21:427–432.

Table-1: Demographic Data of the Patients

Sex of the patients		
Male	65	65%
Female	35	35.0%
H. pylori test results		
Positive	14	14%
Negative	86	86%
Smoking history		
Yes	24	24%
No	76	76%

Table 2: Correlation between H. *pylori* Test and Laboratory Finding

Item	Result Code	N	Mean	Std. Deviation	P Value
HDL	Positive	14	36.486	18.4348	0.6
	Negative	86	37.756	6.8889	
LDL	Positive	14	112.9286	57.30816	0.08
	Negative	86	141.6209	56.96176	
VLDL	Positive	14	59.2714	42.06315	0.06
	Negative	86	46.8012	17.98163	
Triglyceride	Positive	14	302.8571	230.86655	0.05
	Negative	86	235.0581	90.34670	

Table3: Age and Laboratory Finding of the Patients

Item	N	Minmum	Maximum	Mean	Std. devition
Age	100	18	90	48.29	14.588
HDL	100	18.1	96.1	37.578	9.2503
LDL	100	17.00	317.50	137.6040	57.59502
VLDL	100	13.20	179.00	48.5470	22.99695
Triglyceride	100	66.00	987.00	244.5500	120.69039
Cholesterol	100	70.00	410.00	223.9300	59.71485

Indian Journal of Natural Sciences www.tnsroindia.org.in ©IJONS

Vol.8 / Issue 49 / August /2018 *International Bimonthly* *ISSN: 0976 – 0997*

RESEARCH ARTICLE

Irrigation Water Quality and Soil Salinization in the Eastern Ziban Region (Algeria): Intelligent Analysis

Salah BELGHEMMAZ[1*], Mohamed FENNI[1], Saddek BOUHARATI [2] and Yacine LOUADJ[3]

[1]Laboratory of Valorization of Biological and Natural Resources, Ferhat Abbas Setif-1 University, Algeria.
[2]Laboratory of Intelligent Systems, Ferhat Abbas Setif-1 University, Algeria.
[3]Department of Agronomic Sciences, Ferhat Abbas Sétif-1 University, Algeria.

Received: 06 Apr 2018 Revised: 07 May 2018 Accepted: 18 Jun 2018

[*]**Address for Correspondence**
Salah BELGHEMMAZ
Laboratory of Valorization of Biological and Natural Resources,
Ferhat Abbas Setif-1 University, Algeria.
Email: sbelghemmaz@yahoo.fr

ABSTRACT

Land degradation and desertification are recurring problems in the world. These phenomena affect in particular the arid zones (the Eastern Ziban region – Algeria) and can have repercussions on the food demand of the populations. Water quality and soil salinization are aspects to be addressed especially in arid regions. However, the interaction of different factors such as soil properties, climate, and irrigation water quality and crop type can affect the risk of soil degradation. Analyzing such factors using classical mathematical models becomes very difficult given the complexity of the system. In this study, an analysis model using artificial intelligence techniques including the principles of fuzzy logic is proposed. Since fuzzy logic deals with uncertainty and imprecision, its application in this field is adequate. The variables analyzed are considered imprecise given their nature. By this mode of reasoning, the result is as precise as possible. A system is constructed with three input variables (water irrigation composition, soil chemical composition, climatic conditions, and crop species). An output variable of the system expresses the growth rate of the plant species cultivated. A base rule connecting the inputs to the output is established. The system adjusts the variables at the input to automatically predict the growth rate at the output. Depending on the factorsthatcharacterize the soilsconsidered as input variables to the system, the farmercanreaddirectly the impact thatthis has on the soildegradation and thus the growth rate of the cultivated plants. This thenmakesit possible to adapt the appropriate plant species for a betteryield.

Keywords: Soil, Water, land degradation, irrigation, salinization, fuzzy logic.

INTRODUCTION

The study area (the Eastern Ziban region – Algeria) is characterized by its arid climate. The impact of global warming only aggravates the situation. This is accompanied by frequencies of extreme events. A characteristic of the Mediterranean climate in these conditions is the increase of the temperature in winter and a change of the frequencies of the precipitations in spatial and temporal distributions in quantity [1]. These fluctuations in rainfall and the resulting drought increase the demand for waterand threaten agricultural production in the region. The solution of crop irrigation is threatened by salinity. Salt and sodic soils pose a threat to irrigated agriculture because of the accumulation of these in the soil [2]. Also, when there is a shortage of fresh water, irrigation with even saline water becomes an alternative [3]; and it has even become inevitable in these regions [4]. It should be noted, however, that the use of saline water increases the risk of salt accumulation in root zones [5].

In this case, it is necessary to increase the frequency and quantity of irrigation in order to avoid these accumulations [6]. All of this has a direct effect on the productivity of farmland including the impact on small farmers [7] [8]. Add to this, the poor quality of irrigation water has a direct impact on the effectiveness of pesticides while modifying the physical structure of the soil [9]. Depending on the composition of the irrigation water, the effect is noted. This composition takes into account the pH, the electrical conductivity, the sodium absorption rate and the adjusted residual sodium.

These rates are combined with those already existing in the land and so the soil properties are to be taken into account. This can be accentuated by the effect of climate change. From there, appears the complexity of the system. This study addresses the analysis of these factors and their effect on plant growth. It should be noted that the cultivated species is also related to this. Classical mathematical methods are very difficult. An artificial intelligence technique is proposed in this data analysis. The fuzzy logic deals with uncertainty and imprecision, its application in this area is adequate. After a global overview of the factors involved, a fuzzy system is built. Four input variables related to an output variable expressing the growth rate of the plant in question. A base of the rules is established. The system predicts the growth rate from the random input of input values.

Effect of Water Composition

The quality of the water is defined by several parameters. These parameters include the acidity or alkalinity of water expressed in pH and the content of salts dissolved in water (TDS). These salts have an effect on the variability of electrical conductivity (EC). This factor is also to be considered. Also, what influences the growth of the vegetation by their complex interaction is the rate of absorption of sodium and adjusted residual sodium (adj RNA). Other chemical element interacts with the soil composition and makes the system become very complex [10]. The chemical composition of the water combined with that of the soil has a direct impact on the physiological culture [11]. The effect of saltwater irrigation on maize is proven and results in decreased water potential, transpiration and photosynthesis [12]. The same effects are also proven on wheat [13]. Although salt-tolerant plants adapt, they remain sensitive to the effective water used [14]. The effect of saline water on plants is also manifested by its soil accumulation and its impact on root growth as well as the distribution of these in the soil is a function of the ionic distribution [15]

MATERIALS AND METHODS

Analysis and Modeling of the Water-Salt Dynamics

The distribution of salts in irrigated soil and its dynamics have been the subject of a large literature. [16-19]. Also, different techniques are used in the analysis of the data relating to the water-salt dynamics which make it possible to

define an irrigation strategy [20]. Generally, the performance response factor (Ky) is an indicator of stress performance. This factor expresses the quantification of the tolerance level of vegetation. [21];[22]. This proves that there is an interaction between this factors and the efficient use of water [23].

In our study, the effect of irrigation water quality is analyzed in terms of the risk of soil salinization. This study is carried out on the eastern *Ziban* region (case of *Zeribet El-Oued* in Biskra region (Algeria) and the surveys are done in December 2010. We find that the parameters taken are soil and irrigation water. It is then necessary to analyze the effect of these factors on the melon and watermelon cultures over the study period.

By Analyzing the Effect of Each Parameter on the Crop, We can predict its Growth Rate. Knowing that

- A pH below 5.5 affects the plant by a decrease in roots and leaves
- Lack of water with Ca and Mg deficiency affects air movement and root growth.
- pH greater than 7 may affect some alkaline hydrolysis-sensitive pesticides
- When the high HCO_3 concentration (high alkalinity) can increase buffer capacity and therefore pH variation.
- HCO_3^- compounds combine with calcium and manganese. Depending on the nature of the soil, when it is a sandy Soil there is a risk of closing the porosity.
- There is also biological activity that causes pH fluctuation in surface water. From the foregoing, we find that it is Very difficult to analyze such parameters using conventional mathematical techniques. The application of fuzzy Inference supports such complexity.

Fuzzy Logic Inference

The classical (binary) logic considers only two states (true or false). On the other hand, fuzzy logic imitates human reasoning and introduces different levels between the true and the false with degrees of belonging to the true or false function. As for the place of processing the numeric variables, linguistic variables are treated. In this way the uncertainties and imprecision is taken care of. Here, fundamental notions are presented to facilitate the understanding of the application.

The constructed system includes an input space that contains the variables that influence the growth of the plant and an output space that expresses the growth rate of the plant. These two spaces are connected in a processing module in the form of inference rule (If ... Then). Each input or output variable is fuzzyfied [24].

Input Fuzzyfication

This operation consists in the conversion of numerical variables into linguistic variables. Quantification of input variables (water irrigation composition, soil chemical composition, climatic conditions, and crop species) is translated into linguistic variables.

Water Irrigation

This variable expresses the degree of influence of the physicochemical properties of the irrigation water on the cultivated plant. Referring to the effect of each composition cited above and referring to the composition of the water analyzed (Table 1 and 2), the effect is expressed by linguistic variables (no effect, average effect and great effect). To compensate for the inaccuracy of the complexity of the system, fuzzy intervals are created between two neighboring functions.

Soil Effect

In the same way, the effect of the physicochemical properties of the soil as well as its pedological nature is translated in degree of effect on the vegetal growth (not very favorable, moderately favorable and very favoring). Also, fuzzy intervals are created to compensate for the uncertainty.

Climate Changes Effect

As climate change has a direct effect on the amount of water in terms of fluctuation and precipitation. This variable is expressed by its degree of effect. Difficult to quantify in numeric, it is expressed in symbolic values by (low impact, average impact and high impact).

Plant Species

Each plant species planted differs from the other in terms of adaptability and resistance to water stress and water salinity. It is clear that this property is impossible to express in numerical terms. Its fuzzyfication in symbolic terms is of the form: (weak resistance, average resistance, very resistant)

Output Fuzzyfication

The output variable expresses the synthesis of all the effects of the input variables on the growth of the crop. This variable expresses the growth rate of the plant under given conditions. Given the imprecise nature of calculating this growth rate, this variable is fuzzyfied in three fuzzy intervals (low, medium and high).

Rule Base

This is to do the correspondence between the inputs and the output. The general form of a rule is of the form (If ... Then). The basis of the rules is established from the recorded experimental data of the composition of irrigation water and soil (Table 1 and 2) in relation to their effects on the cultivated plant namely melon and watermelon.

Example

If “Water irrigation” Is “no effect” and “Soil effect” Is “moderately favorable” and “Plant species” Is “very resistant” Than “growth rate” Is “high”. The base of the rules must contain all possible combinations. The system operates by aggregating the set of rules to extract a symbolic result in linguistic and also numeric terms by a defuzzyfication process.

Proposed System

The overall scheme of the proposed system includes four inputs and one output. Each input and output is considered a fuzzy variable. (Figure1).

Creating Membership Functions

```
[System]
Name='Salt irrigation'
Type='mamdani'
MF2='Moderately.Favorable':'trimf',[1 2 3]
MF3='Very.Favoring':'trimf',[2 3 4]
```

```
Version=2.0
NumInputs=4
NumOutputs=1
NumRules=31
AndMethod='min'
OrMethod='max'
ImpMethod='min'
AggMethod='max'
DefuzzMethod='centroid'

[Input1]
Name='Water.Irrigation'
Range=[0 4]
NumMFs=3
MF1='No.Effect':'trimf',[0 1 2]
MF2='Average.Effect':'trimf',[1 2 3]
MF3='Great.Effect':'trimf',[2 3 4]

[Input2]
Name='Soil.Composition'
Range=[0 4]
NumMFs=3
MF1='Not.Very.Favorable':'trimf',[0 1 2]

[Input3]
Name='Climate.Changes'
Range=[0 4]
NumMFs=3
MF1='Low.Impact':'trimf',[0 1 2]
MF2='Average.Impact':'trimf',[1 2 3]
MF3='High.Impact':'trimf',[2 3 4]
[Input4]
Name='Cultivated.Species'
Range=[0 4]
NumMFs=3
MF1='Weak.Resistance':'trimf',[0 1 2]
MF2='Average.Resistance':'trimf',[1 2 3]
MF3='Great.Resistance':'trimf',[2 3 4]

[Output1]
Name='Growth.Rate'
Range=[0 4]
NumMFs=3
MF1='Low':'trimf',[0 1 2]
MF2='Medium':'trimf',[1 2 3]
MF3='High':'trimf',[2 3 4]
```

RESULTS AND DISCUSSION

Given the complex nature of the system to be analyzed, the application of the principles of fuzzy inference has proved adequate. Considering each factor as uncertain and imprecise, by fuzzying each factor, it makes it possible to take into account these inaccuracies. We ignore the exact effect of each parameter on plant growth. Several factors are combined starting with the concentration of water in mineral salts up to the plant species itself and its degree of adaptability through the chemical properties of the soil. The introduction of the inference rules from the real values recorded experimentally makes it possible to take into account all possible combinations and thus the result obtained is as accurate as possible. The established system randomly introduces the symbolic values to the input variables to instantly read the output result in terms of the growth rate of the crop species. (Fig.2). the system also makes it possible to display the variations in the growth rate of the cultivated plant species according to the input parameters fixed (Fig. 3) By randomly varying the input variables, the farmercan directly read the growth rate of the crop species according to these factors. Despite the complexity of the system, the analysis used makes it possible to overcome this. For example, by setting a crop species and varying other factors that influence growth such as irrigation water quality, soil composition or the effect of climate change, the expected growth rate of this species is directly displayed. By combining all the input variables, it makes it possible to choose the species best adapted to these extrinsic factors and thus to optimize the yield under given conditions.

CONCLUSION

Each plant species has intrinsic properties as regards its resistance to the amount of irrigation water and its chemical composition including salinity. So the chemical composition of the soil influences the growth of the crop. The

environment in which the plant develops is very complex. Trying to model these factors by conventional mathematical techniques whether by differential equations proves very difficult if not impossible. The statistical tool remains imprecise and is always in the domain of the probable. The proposed system allows us to resume human reasoning by taking into account approximations related to the uncertainties inherent in the nature of the variables. By this, it is possible to predict the growth rate of each species grown according to the nature of irrigation water, soil, climate change and the crop itself. By reasoning thus, the resulting value at the output is more accurate possible. Also, the proposed system remains extensible to other variables that have an effect and are not considered in this study. The proposed system allows selection of the crop species best suited to a given environment for better yield. However, each environment is characterized by its specificity. The proposed model supports some of the most important factors in our case. Although the system supports the inaccuracies related to the other parameters that are not considered here, nevertheless, for more precision it is necessary to add other factors specific to each region. For this, the system remains extensible to other input factors that affect the yield of a crop species.

ACKNOWLEDGMENTS

The authors declare they have no conflict of interest.

REFERENCES

1. Mimi Z. A. & Jamous S. A. (2010). Climate change and agricultural. Water demand: impacts and adaptations. . African Journal of Environmental Science and Technology Afr. J.Environ. Sci. Technol. 4, 183–191.
2. Batakanwa F.J., Mahoo H.F., Kahimba F.C. (2015). Influence of irrigation water quality on soil salinization in semi-arid areas: A case study of Makutopora, Dodoma-Tanzania. International Journal of Scientific & Engineering Research, Volume 6, Issue 9. 1435-46
3. Jiang J., Huo Z.and Feng S. (2012). Effect of irrigation amount and water salinity on water consumption and water productivity of spring wheat in Northwest China, Field Crops Research, vol.137, pp.78-88,
4. J. Letey and G .L. Feng. (2007). Dynamic versus steady-state approaches to evaluate irrigation management of saline waters. Agricultural Water Management. Vol.91, pp.1-10,
5. Pereira L.S., Oweis T. and Zairi A. (2002). Irrigation management under water scarcity. Agric. Water Manage., vol.57, no.3, pp.175-206
6. Corwin D.L., Rhoades J.D., and Simunek J. (2007). Leaching requirement for soil salinity control, Steady-state versus transient models, Agricultural Water Management. Vol.90, pp.165-180
7. Sharma D.P., Rao, K.V.G.K. (1998). Strategy for long term use of saline drainage water for irrigation in semi-arid regions. Soil and Tillage Research,48(4), 287–295.
8. Tanwir F., Saboor A., Nawaz, N. (2003). Soil salinity and the livelihood strategies of small farmers: A case study in Faisalabad district, Punjab, Pakistan. Int. J. Agric. Biol. 5(4), 440–441.
9. Sanchez C.A. & Silvertooth J.C. (1996). Managing saline and sodic soils for producing horticultural crops. HortTechnology. 6(2), 99-107
10. Dara M. Park, Sarah A. White, Nick M. (2014). Assessing Irrigation Water Quality for pH, Salts, & Alkalinity. Journal of Exetention. Volume 52. N6.
11. Katerji N., Van Hoorn J.W., Hamdy A., Karam F., Mastrorilli M. (1996). Effect ofsalinity on water stress, growth, and yield of maize and sunflower. Agric.Water Manage. 30 (3), 237–249.
12. Van Hoorn J.W., Katerji N., Hamdy A., Mastrorilli M. (1993). Effect of saline wateron soil salinity and on water stress, growth, and yield of wheat and potatoes.Agric. Water Manage. 23 (3), 247–265.)
13. Katerji N., Van Hoorn J.W., Hamdy A., Mastrorilli M. (2003). Salinity effect on cropdevelopment and yield, analysis of salt tolerance according to severalclassification methods. Agric. Water Manage. 62 (1), 37–66.)
14. Hamdy, A., Mastrorilli, M., 2000. Salt toleranceclassification of crops according to soil salinity and to water stress day index.Agric. Water Manage. 43 (1), 99–109.

15. Ashraf M., Leary J.W.O. (1996). Responses of newly developed salt-tolerant genotype of spring wheat to salt stress. 1. Yield components and ion distribution. J. of Agron. Crop Sci., 176, 91–101
16. Wang Y-R, Kang S-Z, Li F-S, Zhang L, Zhang J-H. (2007). Saline Water Irrigation Scheduling Through a Crop-Water-Salinity Production Function and a Soil-Water-Salinity Dynamic Model. Pedosphere; 17(3):303±17. http://dx.doi.org/10.1016/S1002-0160(07)60037-X.
17. Kumar P, Sarangi A, Singh DK, Parihar SS, Sahoo RN. (2015). Simulation of salt dynamics in the root zone and yield of wheat crop under irrigated saline regimes using SWAP model. Agricultural Water Management. 148(0):72±83. http://dx.doi.org/10.1016/j.agwat.2014.09.014.
18. Kanzari S, Hachicha M, Bouhlila R, Battle-Sales J. (2012). Characterization and modeling of water movement and salts transfer in a semi-arid region of Tunisia (Bou Hajla, Kairouan)±Salinization risk of soils and aquifers. Computers and Electronics in Agriculture.86 (0):34±42. http://dx.doi.org/10.1016/j.compag.2011.09.010.
19. Yao R-j, Yang J-S, Zhang T-j, Hong L-z, Wang M-w, Yu S-p, et al. (2014). Studies on soil water and salt balances and scenarios simulation using SaltMod in a coastal reclaimed farming area of eastern China. Agricultural Water Management. 131(0):115±23. http://dx.doi.org/10.1016/j.agwat.2013.09.014.
20. Kumar P, Sarangi A, Singh DK, Parihar SS, Sahoo RN. (2015). Simulation of salt dynamics in the root zone and yield of wheat crop under irrigated saline regimes using SWAP model. Agricultural Water Management.148 (0):72±83. ttp://dx.doi.org/10.1016/j.agwat.2014.09.014.

Table 1. Physicochemical Characterization of Soils before Planting Crops (December 2010)

Sample	Depth (cm)	Granulometric fractions (%)					Org. C. (%)	O M. (%)	$CaCO_3$ (%)	Gypsum (%)
		C	F.S	C.L	F.S	G.S				
M	0-30	15.20	37.10	29.80	13.8	4.10	0.47	0.81	20.1	0.50
	30-70	30.70	33.40	28.34	5.34	1.70	0.47	0.81	31.0	0.80
	70-120	21.30	40.60	32.90	4.50	0.65	0.17	0.30	34.6	0.5
W	0-30	17.30	25.00	38.10	13.40	6.2	0.98	1.70	25.6	0.5
	30-70	28.20	35.20	25.90	6.83	3.85	0.42	0.72	33.7	0.7
	70-120	26.00	38.90	29.80	3.50	01.7	0.29	0.50	35.0	0.96
Witness	0-30	17.10	40.20	28.30	10.5	3.9	0.70	1.20	20.2	1.10
	30-70	39.00	24.90	23.40	8.3	4.30	0.58	1.00	26.4	2.3
	70-120	21.3	38.30	35.00	4.5	0.85	0.29	0.50	30.8	0.74

M: Melon; **W**: Watermelon; **C**: Clay; **F.S**: Fine silt; **C.L**: Coarse Silt; **F.S**: Fine sand; **G.S:** Coarse Sand;
Org.C: Organic carbon; OM: Organic mater; **$CaCO_3$**: Total limestone; **$CaSO_4$**: Gypsum

Table 2. Evolution of Physicochemical Properties of Irrigation Water from February to July 2011

Physicochemical Settings		Sampling Periods			
		December	February	April	July
pH		7.63	7.70	7.84	7.92
E C $_{25\,°c}$ (dS/m)		2.85	2.80	3.20	3.30
Cations (mEq/L)	Ca^{++}	9.3	10.5	9.9	12.4
	Mg^{++}	4.8	5.60	6.3	6.70
	Na^{+}	7.60	7.10	8.50	9.8
	K^{+}	0.20	0.20	0.35	0.40
Anions (mEq/L)	HCO_3^{-}	3.20	3.30	3.50	4.6
	Cl^{-}	12.90	13.2	13.7	15.6
	SO_4^{--}	7.70	8.80	8.60	10.1
S.A.R		2.5	2.2	2.5	2.7
Adj.R.Na		3.0	2.6	3.0	3.4
Anionic facies		$Cl.SO_4$	$Cl.SO_4$	$Cl.SO_4$	$Cl.SO_4$
Cationic facies		Ca.Na	Ca.Na	Ca.Na	Ca.Na
Alkalinity classes		C4.S1	C4.S1	C4.S1	C4.S1

EC: Electrical conductivity; **mEq/L**: Milliequivalents per Litre; **S.A.R**: Sodium Adsorption Ratio; **Adj.R.Na**: Adjusted Sodium Adsorption Ratio

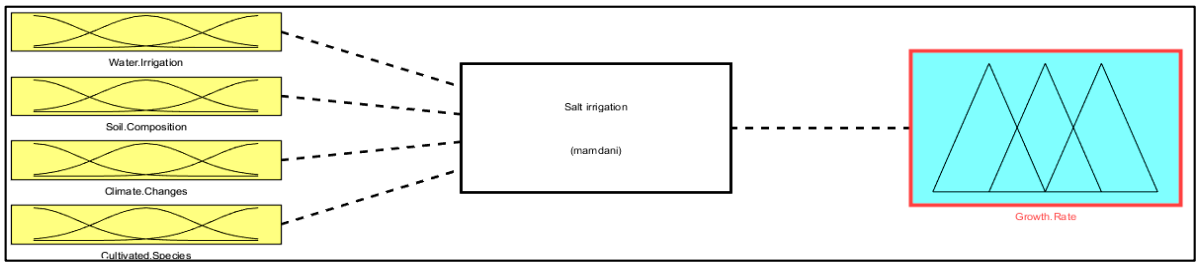

Figure 1. System block diagram

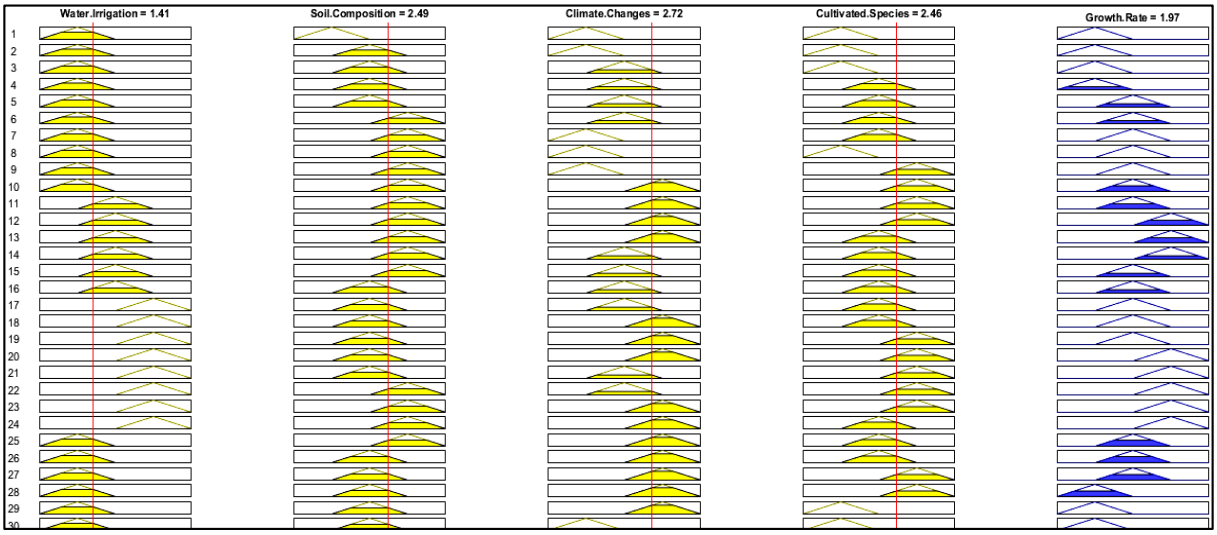

Figure 2. Application example

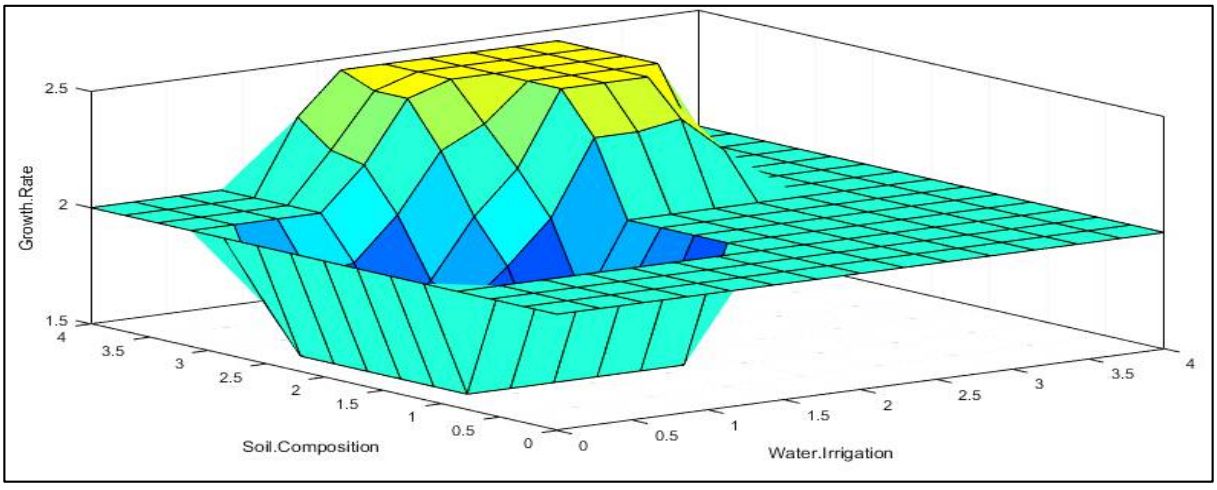

Figure 3. 3D Function of Growth Rate

Indian Journal of Natural Sciences www.tnsroindia.org.in ©IJONS

Vol.8 / Issue 49 / August /2018 *International Bimonthly* *ISSN: 0976 – 0997*

RESEARCH ARTICLE

The Measuring of Ionizing Radiation and CO_2 Gas Emanation in the Residential Areas of Baghdad City

Naseer A. Ahmed and Asia H. Al-Mashhadani*

Department of Physics, College of Science, University of Baghdad, Iraq.

Received: 05 Apr 2018 Revised: 08 May 2018 Accepted: 18 Jun 2018

***Address for Correspondence**
Asia H. Al-Mashhadani
Department of Physics,
College of Science,
University of Baghdad, Iraq.
Email: assia19662006yahoo.com

ABSTRACT

In this work the large ionizing radiation and environmental measurement has been achieved in residential areas, hundreds of readings have been collected in many cities of Baghdad. The huge data was processed by new way of data visualization which makes all the data looked on the map by using software named Google Earth Pro. The lowest average exposure of nuclear radiation in air for peoples is in Al-Tobji city 1.226mSv/y, while the highest one is 2.803mSv/y in Jisr Diyala city, the average of radiation exposure in the air for people's is1.615mSv/y.

Keywords: Ionizing radiation, CO_2 gas emanation, detectors.

INTRODUCTION

External exposure may happen when the radioactive materials such as liquid, dust and some other things are put on skin or wears. This type of radioactive materials can regularly be removed from the body by simply washing [1]. Over the last few decades' man has artificially formed several hundred radionuclides. And he has learned to use the power of the atom for a wide variety of purposes, from medicine to weapons, from the detection of fires to the making of energy [2]. Exposure to ionizing radiation can also produce from irradiation by an external source like medical radiation exposure from x-rays [3]. External irradiation stops when the radiation source is isolated or when the person transfers outside the radiation. When ionizing radiations of alpha, beta, gamma and x-rays pass through matter they pass on some or all of their energy to the material by ionizing and exciting the atoms of the material [4,5].

MATERIALS AND METHODS

Baghdad consists of many cities and the people who live in these areas. There are many factories in these places, power stations of electricity and oil sites. The study checked many thousands of sites all over Baghdad by measuring

the emanation of the carbon dioxide in air and readings of nuclear radiation detection of gamma, beta and x-ray in air. All that achieved by new modern device GMC-520

Al-Bayaa City, Jihad City and Saidiya City

The level of gamma and beta radiation alters from 0.06uSv/h to 0.21uSv/h in the small gardens, streets and many sections as shown in Figure (1).

The readings of CO_2 change from site to site but all these records are within 397ppm to 484ppm as shown in the Table (1).

Al-Sadr City

This is the largest city in Baghdad, it includes main market of flour and foods which is called the market of Jameela. The device GMC-520 is design also for scientific testing on samples like building material, food and water [6]. In this market of the Al-Sadr City the readings which appeared is about 0.04uSv/h to 0.18uSv/h in some stores of flour, oil and other foods as shown in Figure (2).

The readings of CO_2 are between 391ppm to 573ppm in different sections and streets in the Al-Sadr city as shown in the Table (2).

Baghdad Al-Jadeeda and Al-Dora Cities

This area includes many sections as shown in Figure (3). The readings of nuclear radiation in air are 0.04uSv/h to 0.25uSv/h around the schools and markets.

The levels of CO_2 in many sites is within the range of 315 ppm to 445ppm.

Al-Mansour City

There are no factories and power stations in this area as shown in Figure (4). The reading of CO_2 is within 426ppm to 534ppm in different sites of this city.

The levels of nuclear radiation are also between the stages 0.05uSv/h to 0.19uSv/h.

Al-Tobji City

The readings of nuclear radiation inside the market of this area is 0.04uSv/h to 0.14uSv/h and among the houses, too. The CO_2 levels among small shops in this place is between 429ppm to 556ppm.

Al-Ameria City

The records of CO_2 in the streets and many houses in this place is from 397ppm to 504ppm as shown in Figure (5).

The reading of nuclear radiation in different sites is about 0.05uSv/h to 0.18uSv/h.

Al-Yarmouk and Al-Qadisiyah Cities

This area includes many sections which stretches to the Tigris river, as shown in Figure (6).

The detecting of nuclear radiation in all these places is between 0.05uSv/h to 0.17uSv/h. The reading of CO_2 among gardens, in the streets and between many schools is about 417ppm to 503ppm.

AL-Ghazaliya City

The reading of nuclear radiation in many sections of this area altered between 0.05uSv/h to 0.18uSv/h, as shown in Figure (7).

The CO_2 level among many squares and large shops is about 497ppm to 583ppm.

Al-Khadra City

The reading of nuclear radiation among the houses and the streets is 0.06uSv/h to 0.16uSv/h. The readings of CO_2 by device GMC-520 is from 426ppm to 544ppm.

Jisr Diyala City

This area including location of the previous Iraqi Atomic Energy Commission as shown in Figure (8). Some readings in this area represent the largest among all other readings in Baghdad; it is 0.32 uSv/h, also the minimum readings were 0.09uSv/h which considers the largest among the all places.

The reading of CO_2 is about 357ppm for the low emanation and 451ppm for the high emanation in this area.

RESULTS AND DISCUSSION

Visualization is chief the approach to help Big Data to obtain a complete view of data and determine data values [6]. The chief issue is how to represent these massive data to understand and extract knowledge from kept information, which is a global task. In simple words, the collection of data is no longer a problem but its extracting of valuable knowledge from the collected data is a big problem [7]. Visualization methods are considered to be very important for the users because it provides mental models of the information [8]. Visualization methods make vast and complex data intelligible. Information visualization is a visual user interface that offers insight of information to the user [9]. The average of radiation exposure in the air for people in many sectors in Baghdad city illustrated by the small reading 1.2264mSv/y for AL-Tobji city while the large one is the reading of Baghdad Al-Jadeeda and Al-Dora cities 2.19mSv/y, as shown in the Table (3).

The fifth green column illustrates that Al-Tobji city has small reading of the average of radiation exposure 1.2264mSv/y, but the third green column of Baghdad Al-Jadeeda and Al-Dora cities has 2.19mSv/y which is the largest one. The average of radiation exposure in the air for people in residential areas illustrates by the orange column 1.615mSv/y, as shown in the Figure (9).

CONCLUSION

It is very clear that the highest reading of the average exposure of ionizing radiation for persons in air is in Jisr Diyala city 2.803mSv/y where there is the previous Iraqi power nuclear reactor project situated, while the lowest reading of the average exposure of ionizing radiation for persons in air is in the is in Al-Tobji city 1.226mSv/y.

The average of ionizing radiation exposure in the air for Baghdad city is 1.734mSv/y, while for Jisr Diyala 2.803mSv/h; those two readings are within the ordinary limits [10,11].

The readings of the carbon dioxide CO_2 in many cities and large streets in Baghdad is about 315ppm as a smallest reading in Baghdad Al-Jadeeda and Al-Dora cities to a 583ppm as a largest reading in The AL-Ghazaliya city.

REFERENCES

1. United Nations Scientific Committee on the Effects of Atomic Radiation. Sources and Effects of Ionizing Radiation. New York 2010.
2. Margaret MacDonell, Michelle Raymond, David Wyker, Molly Finster, Young-Soo Chang, Thomas Raymond, Bianca Temple, and Marcienne Scofield. Mobile Sensors and Applications for Air Pollutants. 31 October 2013.
3. Richard Lawson, An Introduction to Radioactivity, Nuclear Medicine Department Manchester Royal Infirmary. October 1999.
4. Turner, J. E. Atoms, Radiation, and Radiation Protection. 2nd ed. New York: John Wiley & Sons; 1995.
5. UNSCEAR. Report, United Nations Scientific Committee on the Effects of Atomic Radiation. Sources and Effects of Ionizing Radiation:Exposures from Natural Sources of Radiation.NewYork: UnitedNationsPublication, (1993).
6. V. Sucharitha, S.R. Subash and P. Prakash, Visualization of Big Data: Its Tools and Challenges, International Journal of Applied Engineering Research, 9(18), 2014.
7. I.B.Otjacques,UniGR Workshop: Big Data- The challenge of visualizing big data, Report, Gabriel Lippmann, 2013
8. Syed Mohd Ali, Noopur Gupta, Gopal Krishna Nayak, Rakesh Kumar Lenka Department of Computer Science and Engineering International Institute of Information Technology, Bhubaneswar, India. Big Data Visualization: Tools and Challenges. Oct 22, 2017
9. B. Porter, Visualizing Big Data in Drupal: Using Data Visualizations to Drive Knowledge Discovery, Report, University of Washington, October 2012.
10. Sohrabi M. High radon levels in nature and in dwellings: remedial actions. In: Ilic R, Durrani SA, editors. Radon Measurements by Etched Track Detectors. Applications in Radiation Protection, Earth Sciences and the Environment. 1997. Singapore: World Scientific.
11. Sohrabi M. The state-of-the-art on worldwide studies in some environments with elevated naturally occurring radioactive materials (NORM) Appl. Radiat. Isot. 49, 169–188, 1998.

Table 1: Data of measuring of the Bayaa, Jihad and Saidiya cities

Date	CPM	ACPM	uSv/h	Latitude	Longitude	Altitude	Air Pressu	CO2	Temperat	Humidity
10/10/2017 12:29	14	16.58	0.09	33.30873	44.29619	35	1005	450	34.35	17
10/10/2017 12:28	11	16.58	0.07	33.31047	44.3024	29	1006	445	34.23	17
10/10/2017 12:27	32	16.58	0.21	33.30915	44.30351	20	1006	425	32.95	18
10/10/2017 12:26	10	16.58	0.06	33.30085	44.30624	23	1005	413	33.38	18
10/10/2017 12:25	16	16.58	0.1	33.29406	44.30856	11	1005	397	33.45	17
10/10/2017 12:24	14	16.58	0.09	33.28617	44.3102	21	1005	404	34.17	18
10/10/2017 12:23	13	16.58	0.08	33.28108	44.31352	16	1006	428	35.39	17
10/10/2017 12:22	16	16.58	0.1	33.28202	44.31863	26	1006	439	35.24	17
10/10/2017 12:21	17	16.58	0.11	33.28236	44.32018	25	1006	422	33.98	19
10/10/2017 12:20	14	16.58	0.09	33.28463	44.32062	26	1006	431	32.8	18
10/10/2017 12:18	18	16.58	0.12	33.2889	44.31933	17	1006	434	33.43	20
10/10/2017 12:17	12	16.58	0.08	33.28426	44.32077	25	1006	434	33.67	18
10/10/2017 12:16	16	16.58	0.1	33.27948	44.32237	28	1006	453	34.48	17
10/10/2017 12:15	17	16.58	0.11	33.27556	44.32357	26	1006	448	34.89	17
10/10/2017 12:14	23	16.58	0.15	33.27353	44.32581	16	1006	454	34.71	17
10/10/2017 12:13	9	16.58	0.06	33.27424	44.32924	28	1006	461	34.72	20
10/10/2017 12:12	15	16.58	0.1	33.27632	44.32874	28	1006	461	34.09	21
10/10/2017 12:11	21	16.58	0.14	33.2763	44.32874	28	1006	457	33.78	19
10/10/2017 12:10	15	16.58	0.1	33.27886	44.32791	21	1006	440	32.86	19
10/10/2017 12:09	17	16.58	0.11	33.28464	44.32604	21	1006	441	32.45	19
10/10/2017 12:08	17	16.58	0.11	33.28525	44.32598	19	1006	442	32.63	19
10/10/2017 12:07	17	16.58	0.11	33.27899	44.32787	63	1006	472	33.65	18
10/10/2017 12:06	13	16.58	0.08	33.2768	44.32861	21	1006	439	34.05	18
10/10/2017 12:05	18	16.58	0.12	33.27778	44.33346	22	1006	429	33.33	19
10/10/2017 12:04	12	16.58	0.08	33.28161	44.33179	28	1006	423	33.12	19
10/10/2017 12:03	10	16.58	0.06	33.28569	44.33005	51	1006	430	33.45	18
10/10/2017 12:02	16	16.58	0.1	33.28551	44.33002	55	1006	413	32.86	19
10/10/2017 12:01	20	16.58	0.13	33.28197	44.33168	34	1006	421	33.55	19
10/10/2017 12:00	15	16.58	0.1	33.27807	44.33346	27	1006	427	34.28	18
10/10/2017 11:59	14	16.58	0.09	33.2786	44.33577	16	1006	426	33.77	19
10/10/2017 11:58	14	16.58	0.09	33.27966	44.33653	18	1006	454	33.17	18
10/10/2017 11:57	20	16.58	0.13	33.27792	44.33427	20	1006	465	33.39	18
10/10/2017 11:56	23	16.58	0.15	33.27714	44.33111	22	1006	460	33.58	18
10/10/2017 11:55	15	16.58	0.1	33.27539	44.32912	28	1006	442	33.53	18
10/10/2017 11:54	10	16.58	0.06	33.27101	44.33048	39	1006	437	33.67	17
10/10/2017 11:53	17	16.58	0.11	33.26802	44.33255	27	1007	434	33.66	18
10/10/2017 11:52	19	16.58	0.12	33.26606	44.33624	22	1006	436	32.91	19
10/10/2017 11:51	16	16.58	0.1	33.26801	44.33079	20	1006	448	33.17	18
10/10/2017 11:50	11	16.58	0.07	33.26404	44.32887	34	1006	452	34.34	17
10/10/2017 11:49	17	16.58	0.11	33.26304	44.33055	27	1007	446	32.97	18
10/10/2017 11:48	18	16.58	0.12	33.26071	44.33506	23	1006	432	33.18	18
10/10/2017 11:47	16	16.58	0.1	33.2581	44.34118	24	1005	437	32.22	18
10/10/2017 11:45	15	16.58	0.1	33.25105	44.34531	25	1006	443	32.56	18
10/10/2017 11:44	17	16.58	0.11	33.24502	44.34515	23	1006	438	32.7	18
10/10/2017 11:43	22	16.58	0.14	33.23819	44.34536	34	1006	433	33.61	17
10/10/2017 11:42	16	16.58	0.1	33.23549	44.35055	31	1006	441	33.85	17
10/10/2017 11:41	21	16.58	0.14	33.236	44.35899	27	1006	432	33.64	17
10/10/2017 11:40	18	16.58	0.12	33.23658	44.36658	28	1006	436	33.04	18
10/10/2017 11:39	19	16.58	0.12	33.24348	44.37006	27	1006	444	33.27	18

Table 2: Data of Measuring of the Al-Sadr City

Date	CPM	ACPM	uSv/h	Latitude	Longitude	Altitude	Air Pressu	CO2	Temperat	Humidity
11/1/2017 10:33	22	17.4	0.14	33.36813	44.43392	5	1012	425	26.89	26
11/1/2017 10:31	27	17.4	0.18	33.37256	44.43861	21	1012	451	28.79	23
11/1/2017 10:30	14	17.4	0.09	33.37515	44.43947	30	1012	465	30.1	21
11/1/2017 10:29	17	17.4	0.11	33.37579	44.43863	33	1012	603	31.55	20
11/1/2017 10:28	18	17.4	0.12	33.37632	44.43791	37	1012	559	31.22	24
11/1/2017 10:27	14	17.4	0.09	33.37652	44.43774	44	1012	490	30.81	24
11/1/2017 10:26	10	17.4	0.06	33.37649	44.43772	44	1012	494	31.17	20
11/1/2017 10:26	20	17.4	0.13	33.37629	44.4377	41	1012	564	31.1	21
11/1/2017 10:24	20	17.4	0.13	33.37701	44.43702	55	1012	573	30.39	26
11/1/2017 10:23	16	17.4	0.1	33.37745	44.43648	49	1012	521	29.77	26
11/1/2017 10:22	16	17.4	0.1	33.37769	44.43607	47	1012	486	29.12	26
11/1/2017 10:21	19	17.4	0.12	33.37769	44.43607	47	1012	466	27.88	26
11/1/2017 10:20	13	17.4	0.08	33.37764	44.43613	49	1012	459	28.01	26
11/1/2017 10:19	6	17.4	0.04	33.37754	44.43635	48	1012	444	27.43	26
11/1/2017 10:18	17	17.4	0.11	33.30408	44.29765	0	1012	426	27.37	27
11/1/2017 10:17	16	17.4	0.1	33.37771	44.43601	28	1012	436	27.27	25
11/1/2017 10:16	18	17.5	0.12	33.3791	44.43443	27	1012	434	27.66	24
11/1/2017 10:15	19	17.5	0.12	33.37797	44.43601	26	1012	418	27.42	26
11/1/2017 10:14	18	17.5	0.12	33.37775	44.4363	33	1012	414	27.54	26
11/1/2017 10:13	11	17.5	0.07	33.37761	44.43655	38	1012	425	27.18	26
11/1/2017 10:12	25	17.5	0.16	33.37732	44.43686	33	1012	428	26.52	26
11/1/2017 10:11	20	17.5	0.13	33.37561	44.43902	32	1012	437	26.7	27
11/1/2017 10:10	21	17.5	0.14	33.37495	44.43986	24	1012	446	26.34	26
11/1/2017 10:09	19	17.4	0.12	33.37401	44.4413	17	1012	444	26.24	28
11/1/2017 10:08	23	17.4	0.15	33.37409	44.44131	13	1012	446	25.67	29
11/1/2017 10:07	25	17.4	0.16	33.37308	44.44244	21	1012	451	25.23	28
11/1/2017 10:06	12	17.4	0.08	33.37027	44.4453	31	1012	427	25.82	28
11/1/2017 10:05	16	17.4	0.1	33.36824	44.44316	28	1012	417	25.23	28
11/1/2017 10:04	21	17.4	0.14	33.36549	44.44013	20	1012	415	25.49	27
11/1/2017 10:03	12	17.4	0.08	33.36273	44.43707	19	1012	436	25.94	27
11/1/2017 10:02	15	17.4	0.1	33.36058	44.43693	20	1012	441	25.9	27
11/1/2017 10:00	13	17.4	0.08	33.35745	44.44106	42	1012	442	27.18	26
11/1/2017 9:59	26	17.4	0.17	33.35561	44.44338	39	1012	498	28.34	26
11/1/2017 9:58	19	17.4	0.12	33.35225	44.4484	43	1012	508	27.79	26
11/1/2017 9:57	17	17.4	0.11	33.34988	44.45073	33	1012	506	27.27	27
11/1/2017 9:56	13	17.4	0.08	33.34942	44.45124	31	1012	572	26.47	29
11/1/2017 9:55	14	17.4	0.09	33.34933	44.45132	39	1012	548	26.13	30
11/1/2017 9:54	14	17.4	0.09	33.34901	44.45179	34	1012	434	25.4	30
11/1/2017 9:53	15	17.4	0.1	33.34752	-5328.48	0	1012	437	24.58	31
11/1/2017 9:52	23	17.4	0.15	33.34408	44.45815	27	1012	438	24.29	30
11/1/2017 9:51	11	17.4	0.07	33.34308	44.45846	22	1012	439	24.86	38
11/1/2017 9:50	12	17.4	0.08	33.34382	44.45862	30	1012	434	24.41	31

The residential Areas	The largest reading in uSv/h unit	Average exposure of people to ionizing radiation in air per year uSv/y	Average exposure of people to ionizing radiation in air per year mSv/y.
The Al-Bayaa city, Jihad city and Saidiya cit	0.21	1839.6	1.8396
The Al-Sadr City.	0.18	1576.8	1.5768
The Baghdad Al-Jadeeda and Al-Dora	0.25	2190	2.19
The Al-Mansour	0.19	1664.4	1.6644
The Al-Tobji (Al-Salam city).	0.14	1226.4	1.2264
The Al-America	0.18	1576.8	1.5768
The Al-Yarmouk and Al-Qadisiyah.	0.17	1489.2	1.4892
The AL-Ghazaliya city.	0.18	1576.8	1.5768
The Al-Khadra city	0.16	1401.6	1.4016
The Jisr Diyala City.	0.32	2803.2	2.8032
Average			1.73448

Table 3: The Average of Radiation Exposure in the Residential Areas

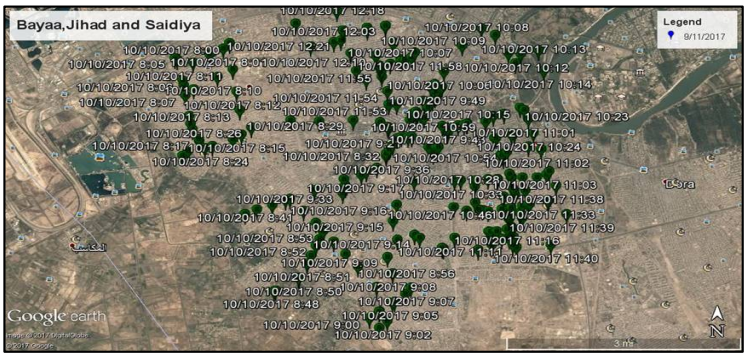

Saidiya

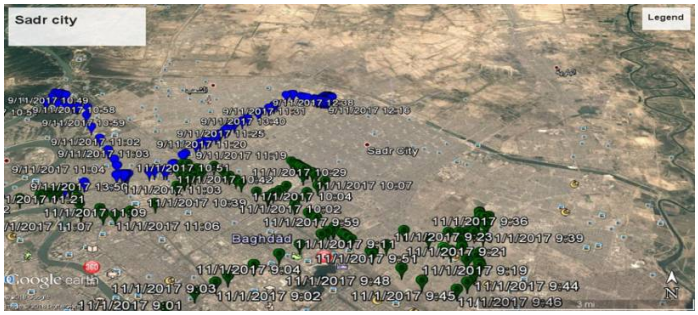

Figure 2: The Measuring of Concentration of CO_2 and Nuclear Radiation for Al-Sadr City

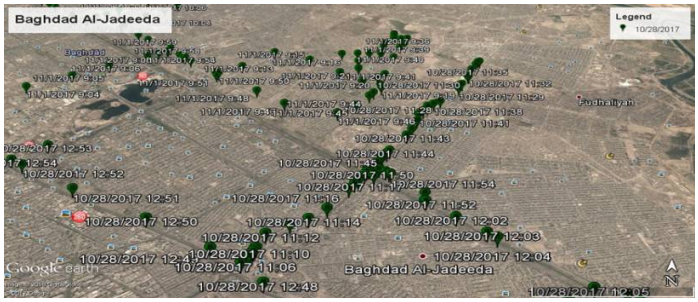

Figure 3: The Measuring of Concentration of CO_2 and Nuclear Radiation Levels in Babhdad Al-Jadeeda

Figure 4: The Measuring of Concentration CO_2 and Nuclear Radiation in Al-Mansour City

Figure 5: The Measuring of Concentration of CO_2 and Nuclear Radiation in Al-Ameria Ciy

Figure 6: The Measuring of Concentration of CO_2 and Nuclear Radiation for the Al-Yarmouk and Al-Qadisiyah Cities

Figure 7: The Measuring of Concentration of CO_2 and Nuclear Radiation in Al-Ghazaliya City

Figure 8: The Measuring of Emanation of CO_2 and Nuclear Radiation in Jisr Diyala City

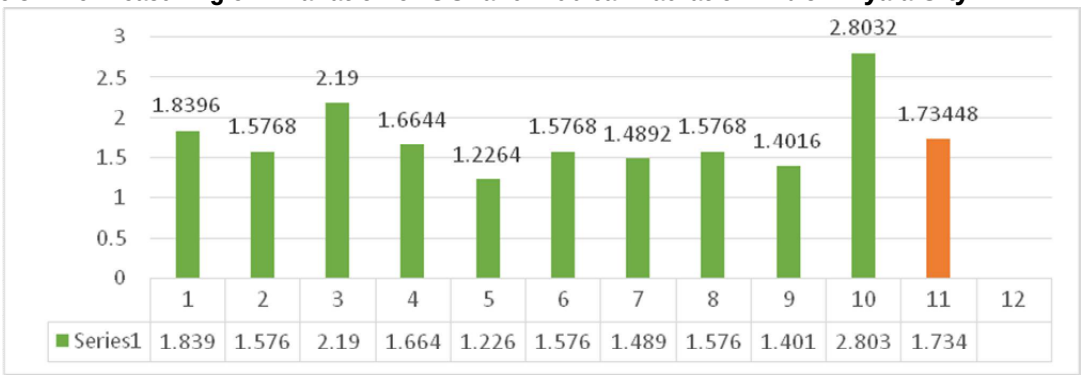

Figure 9: The Distribution of the Average Radiation Exposure in the Residential Areas

Indian Journal of Natural Sciences www.tnsroindia.org.in ©IJONS

Vol.8 / Issue 49 / August /2018 *International Bimonthly* *ISSN: 0976 – 0997*

RESEARCH ARTICLE

Study of the Coronal Mass Ejections for the Down Phase of the Solar Cycle 24, the Events, Verifications and Simulation of the Plasma speed in the Sheath and ICME

Hamza A. Ali[1*], Alaa F. Ahmed[1] and Wafa H. Zaki[2]

[1]Department of Physics, College of Science, University of Baghdad, Baghdad, Iraq.
[2]Department of Physics, College of Science, University of Kirkuk, Kirkuk, Iraq.

Received: 22 Jan 2018 Revised: 20 Feb 2018 Accepted: 24 Mar 2018

[*]**Address for correspondence**
Hamza A. Ali
Department of Physics,
College of Science,
University of Baghdad,
Baghdad, Iraq.
Email : hrhhalove@gmail.com

ABSTRACT

Coronal mass ejections CMEs are large amount ejections of plasma and magnetic field from solar corona which propagate through interplanetary space, and usually it affects Earth and other planets of solar system , In our study, we've identified all the events and sun activities through the global Labs, SOHO LASCO, (2014-2015), then we've filtered all the events that could reach the earth, the events that have more the 500 km/s as a speed of the coronal mass ejections, after identifying the events in SOHO LASCO and filtering the events, we did compare the results of the proposed events with other Lab (ERNE) in order to figure out if these events are clear showed with ERNE or not, for the clear event, will be considered as real events, other events will be neglected, once comparing done, we worked on mathematical methods for tripled check and verifications, between the times evaluated and the times assumed, and this was the last method to identify where the events are earth reaching or not, using lognormal model to study the probability of the speed distributions in the sheath and ICME.

Kew words: Coronal mass, ICME, SOHO, Plasma speed, solar cycle.

INTRODUCTION

The investigation of solar activity is a very important part of space physics because of the significant impact on Earth technological systems. The effective part of solar activity is solar storm which include The Coronal Mass Ejections (CMEs), the output of X-ray and UV-variation are various with solar cycle and all of these are related to the transients

released from large amount of energy from Sun [1]. Occasionally eruptions are directed toward the Earth change the conditions of near-Earth space in several ways, including a cut in the electricity power in high latitudes on the Earth and damaged of some satellites [2]. All observations for this study were taken from Large Angle and Spectroscopic Coronagraph (LASCO), which provide the first ever CMEs database to cover a full solar cycle with a single instrument, thus opening investigations to the solar cycle dependence on CME properties [3]. By using the photometric scale observations of LASCO, so there will be able to find the speed of Coronal Mass Ejections (CMEs), angular width (AW) and the Central Position Angle (CPA), as for finding the intensity-time profile, the energy and the shape of the events which can be obtained from ERNE detectors system. LASCO and ERNE are scientific instruments boarded on SOHO [4]. The main objective of this study is to detect and analyze when and where SEPs take place by finding the location of CMEs and find the time of the events as well as find a simulation for the down phase of solar cycle (24) for years selected by taking high speed events CMEs with velocities >500 (km/s) and angular width with Halo (dig).The fastest CMEs erupt from large sunspot active regions, powered by the strongest magnetic field concentrations on the Sun. These fast CMEs can reach Earth in a little time as ~14 - 17 hours and caused major geomagnetic storms. It is well-known that the most solar cycles show a double peak due to the out-of-phase activity in the two hemispheres [6]. The double peak in SSN during solar cycle 24 is the second peak is larger than the first one by ~20%. Such a behavior was observed only a few times since the 1800s [7]. In order to address the fundamental problem of prediction of geomagnetic storms, it is important to examine the Halo CMEs first observed by Howard [8]. A Halo CMEs appears to surround the occulting disk of the observing coronagraph in sky plane projection. Halo CMEs constitute only approximate 3% of all CMEs and represent an energy population because most of the CMEs that produce major geomagnetic storms are Halo [9], There only 11 CMEs that caused major storms during cycle 24 until the end of period 2014 [10]. CMEs number shows a double peak and similar to seen in sunspot number [11].

MATERIALS AND METHODS

Research activity has been related to the observation of big solar eruptions. In big solar events, before the magnetic storm hits the Earth, SEPs bombard Earth earlier, and may be both (storm and particles) come from the eruption which is called CME. Observed eruptions are associated with different composition and energy spectra. So the investigation of their source is very important to learn SEPs [5]. SOHO which placed into the whole orbit close to lagrangian point L1 carries twelve scientific instruments; LASCO & ERNE are some of these devices that data were obtained by them for this study. ERNE provide an opportunity to analyze protons and helium nuclei intensity-time profile with high resolution and LASCO give information about acceleration, CPA, and AW, the speed of CME and their basic attributes which cataloged in a data base known as the SOHO/LASCO catalog Figure 1. The logarithmic intensity-time Profile of SEP associated to CME for the down phase nof solar cycle (24) for years (2014-2015) were provided by ERNE detectors [6]. From this profile the injection time, speed, width, acceleration, CPA and onset time were estimated. The Injection time (T_{inj}) representing the time of particles that Injected from the Sun and it gives the acceleration time for the particles [5]:

$T_{inj} = (t_0 - t_f) + 8.3$ min……..... (1)

Equation (1) gives the observer to set a real time at the detector, the flight time can be realized by using beta equation, and this cannot be done without finding the ratio of the velocity of the particles of velocity of light which called the relativistic velocity coefficient (β)

$\beta = v/c$……..... (2)

Where v= the speed of particles = S/t_f ,c= the speed of the light

(t_0) is the onset time observed by the detectors, (8.3 min) have been added to represent the time of light to teach the earth from the sun, and the filght time (t_f) given by equation (3)

$T_f = s/\beta c$…… (3)

Where (s) is the fixed path length for the particles which equal the distance between the sun and the detector

$\beta = [1-(p/ (E+p))^2]^{1/2}$ …..…….…….. (4)

In this study all selected observations for the down phase of solar cycle (24) (2014-2015) have been analyzed; on this basis the most important events will be analyzed. So for this study 8 event were selected and provided that its speed (v > 500 km/s) and of (AW > Halo). The analysis of the data related to logarithmic intensity-time profile of proton for resolution time of 45 hour from ERNE for 8 significant event filtered from the long list of event were represented in (Figures 2-7) and this is filtered based on events which have the highest number of CME for each year of the down phase of solar cycle (24). By using equations (1, 2, 3, 4) for the adopted events, onset time have been created with the fixed path length method, the flight time of the non-scattered protons along the Archimedean field line of nominal length (1.2 AU) has been calculated so the injection time will be extracted. While the characteristics of the CMEs in C2 for all events have been taken from LASCO and analyzed which is shown in Table 1.

Also below table (2) is the table present the final all events reached the earth magnetosphere for the down phase of solar cycle 24

In this table shows the time flight and the time injection comparing with the LASCO time of the event for the events who has more than 45 min different will be neglected, then the 8 significate events are shown in the table above

RESULTS AND DISCUSSION

Fig (1) For the first event in 6-January-2014 it was identified by SOHO/LASCO the event with criteria of high linear speed more than or equal to 500 km/s with Halo PAC,Time: 8:00 am

In order to simulate the distribution of the CME Speed, we used the lognormal model for simulation using the matlab program to present the simulations in (2-3) D

In figure (4) we will observe the probability of the CME speed distribution within the Sheath and the ICME

REFERENCES

1. Lang, K. the Sun from Space. Springer-Verlag, Berlin Heidelberg, 1-251. (2009)
2. Kallenrode, M.B. Current Views on Impulsive and Gradual Solar Energetic Particle Events. Journal of Physics G: Nuclear and Particle Physics, 29, 965-981. PII: S0954-3899(03)53935-4.(2003)
3. Gopalswamy, N., Yashiro, S., Michalek, G., Stenborg, G., Vourlidas, A., Freeland, S. and Howard, R. The SOHO/LASCO CME Catalog. Earth Moon and Planets, 104, 295-313. (2009) http://dx.doi.org/10.1007/s11038-008-9282-7
4. The coronal Mass ejections catalog in the SOHO LASCO Lab,http://cdaw.gsfc.nasa.gov/CME_list/
5. Al-Sawad, A. Multi Eruption Solar Energetic Particle Events Observed by SOHO/ERNE. Ph.D Thesis, Turku University, Turku, Finland, (2009)

6. Singh, P.R., Ahmad, S., Pandey, A.C., Saxena, A.K., Tiwari, C.M. and Mishra, A.P. Cosmic Ray Associated with Coronal Index and Solar Flare Index during Solar Cycle 22-23. International Journal of Astronomy and Astrophysics, 7, B. Nigam et al. (2017)
7. Gopalswamy, N., et al. The Peculiar Behavior of Halo Coronal Mass Ejections in Solar Cycle 24. The Astrophysical Journal, 804, L23. (2015)
8. Howard, R.A., et al. The Observation of a Coronal Transient Directed at Earth. The Astrophysical Journal Letters, 263, L101.(1982) https://doi.org/10.1086/183932
9. Gopalswamy, N., Yashiro, S., Krucker, S., Stenborg, G. and Howard, R.A. Intensity Variation of Large Solar Energetic Particle Events Associated with Coronal Mass Ejections. Journal of Geophysical Research, 109, 12105. https://doi.org/10.1029/2004JA010602 (2004)
10. Gopalswamy, N., et al. Short-Term Variability of the Sun-Earth System: An Overview of Progress Made during the CAWSES-II Period. In: Zank, G., Ed., Proc. IAC, in the Press. (2015)
11. Gopalswamy, N., et al. CMEs during the Two Activity Peaks in Cycle 24 and Their Space Weather Consequences.(2015)

Table (1) Shows the Coronal Mass Ejection Who Matching the Criteria While Being Analyzed and Verified with ERNE in Order to Identify the Intensity Time Profile

First C2 Appearance Date Time [UT]		Central PA [deg]	Angular Width [deg]	Linear Speed [km/s]	2nd-order Speed at final height [km/s]	2nd-order Speed at 20 Rs [km/s]	Accel [m/s²]	Remarks
1/4/2014	21:22:38	Halo	360	977	1188	995	49.3*1	Only C3/not clear in erne
1/6/2014	8:00:05	Halo	360	1402	1360	1385	-7.1	clear in crne
1/29/2014	0:36:05	Halo	360	640	608	607	-3.5	not clear in erne
1/30/2014	16:24:05	Halo	360	1087	821	940	-39.1	not clear in erne
1/7/2014	18:24:05	Halo	360	1830	1569	1714	-60.8	clear in erne
1/20/2014	15:24:05	Halo	360	675	575	551	-12	not clear in erne
1/20/2014	22:00:05	Halo	360	721	700	707	-2.1	not clear in erne
2/9/2014	16:00:06	Halo	360	908	797	846	-12.7	not clear in erne
2/10/2014	21:36:06	Halo	360	557	452	343	-13.6	Poor Event/ not clear in erne

Table (2) Present the Final All Events Reached the Earth Magnetosphere for the Down Phase of Solar Cycle 24

Event Date	ERNE time	Intensity	Energy	Tf	T injection	LASCO Time
6-Jan-14	8:45	1.07588	15.4	55.86285079	7:57	8:00
7-Jan-14	19:25	3.855	72	26.96873956	19:06	18:24
20-Feb-14	8:15	5.64532	72	26.96873956	7:56	8:00
18-Apr-14	13:35	5.7	72	26.96873956	13:16	13:25
10-Sep-14	19:25	1.08218	72	26.96873956	19:06	18:00
22-Sep-14	7:55	2.734	15.4	55.86285079	7:07	8:48

21-Feb-15	11:15	1.4332	23.3	45.69663257	10:37	9:24
1-Jul-15	16:05	5.924	15.4	55.86285079	15:17	14:36
20-Sep-15	18:35	7.07774	15.4	55.86285079	17:47	18:12
4-Nov-15	15:05	5.9	18.9	50.56412597	14:23	14:48
28-Dec-15	13:25	2.239	15.4	55.86285079	12:37	12:12

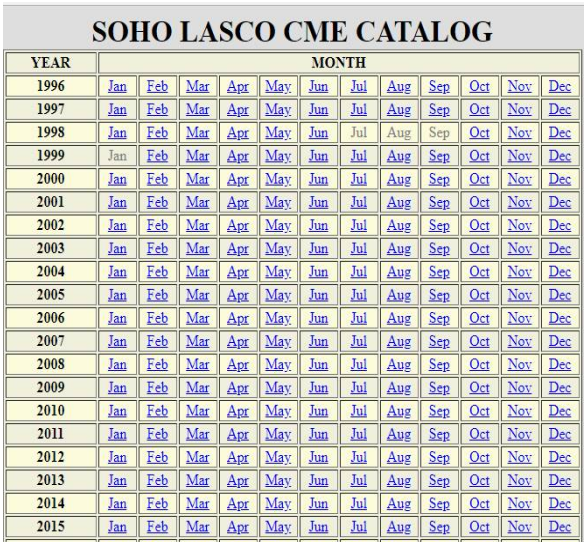

SOHO LASCO CME CATALOG

YEAR	MONTH											
1996	Jan	Feb	Mar	Apr	May	Jun	Jul	Aug	Sep	Oct	Nov	Dec
1997	Jan	Feb	Mar	Apr	May	Jun	Jul	Aug	Sep	Oct	Nov	Dec
1998	Jan	Feb	Mar	Apr	May	Jun	Jul	Aug	Sep	Oct	Nov	Dec
1999	Jan	Feb	Mar	Apr	May	Jun	Jul	Aug	Sep	Oct	Nov	Dec
2000	Jan	Feb	Mar	Apr	May	Jun	Jul	Aug	Sep	Oct	Nov	Dec
2001	Jan	Feb	Mar	Apr	May	Jun	Jul	Aug	Sep	Oct	Nov	Dec
2002	Jan	Feb	Mar	Apr	May	Jun	Jul	Aug	Sep	Oct	Nov	Dec
2003	Jan	Feb	Mar	Apr	May	Jun	Jul	Aug	Sep	Oct	Nov	Dec
2004	Jan	Feb	Mar	Apr	May	Jun	Jul	Aug	Sep	Oct	Nov	Dec
2005	Jan	Feb	Mar	Apr	May	Jun	Jul	Aug	Sep	Oct	Nov	Dec
2006	Jan	Feb	Mar	Apr	May	Jun	Jul	Aug	Sep	Oct	Nov	Dec
2007	Jan	Feb	Mar	Apr	May	Jun	Jul	Aug	Sep	Oct	Nov	Dec
2008	Jan	Feb	Mar	Apr	May	Jun	Jul	Aug	Sep	Oct	Nov	Dec
2009	Jan	Feb	Mar	Apr	May	Jun	Jul	Aug	Sep	Oct	Nov	Dec
2010	Jan	Feb	Mar	Apr	May	Jun	Jul	Aug	Sep	Oct	Nov	Dec
2011	Jan	Feb	Mar	Apr	May	Jun	Jul	Aug	Sep	Oct	Nov	Dec
2012	Jan	Feb	Mar	Apr	May	Jun	Jul	Aug	Sep	Oct	Nov	Dec
2013	Jan	Feb	Mar	Apr	May	Jun	Jul	Aug	Sep	Oct	Nov	Dec
2014	Jan	Feb	Mar	Apr	May	Jun	Jul	Aug	Sep	Oct	Nov	Dec
2015	Jan	Feb	Mar	Apr	May	Jun	Jul	Aug	Sep	Oct	Nov	Dec

Figure 1. The Top Page of the SOHO/LASCO CME Catalog. One Row Corresponds to All the Months In the Year. Months Not Underlined (No Link) have no Data [10]

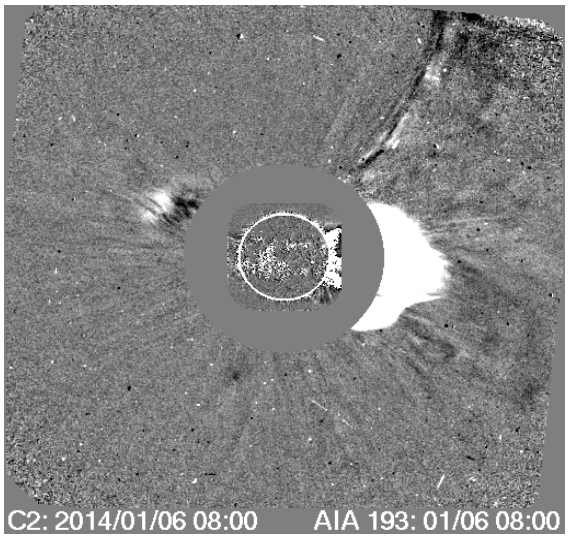

Figure 2. For the Same Event Happened in 6-January-2014 it was detected and Observed Clearly in ERNE

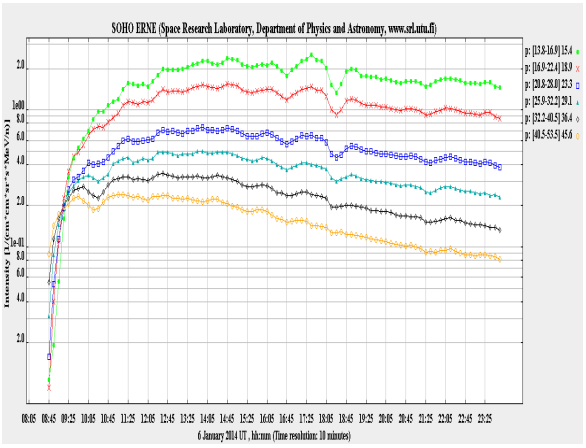

Figure 3. For the Event Happened in 6-January 2014 Clearly Observed in ERNE Detectors

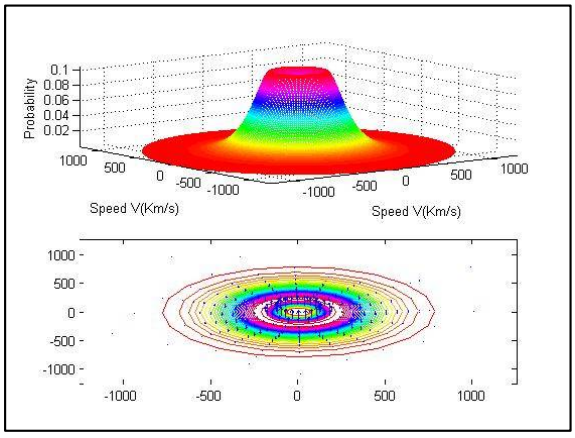

Figure 4. The above Present the 3D Probability Versus Speed v (Km/s) for the Coronal Mass Ejection in the Sheath and ICME,the Below Shape Shows the 2D Probability Versus Speed v (Km/s) for the Coronal Mass Ejection in the Sheath and ICME

Indian Journal of Natural Sciences *www.tnsroindia.org.in ©IJONS*

Vol.8 / Issue 49 / August /2018 *International Bimonthly* *ISSN: 0976 – 0997*

RESEARCH ARTICLE

Socio-Demographic and Diagnostic Features of Patients Attending Psychiatric Unit in Wasit Province

Mahdi Abdulkarim Abdulhussain*

Head of Psychiatric Unit, Al-Zahraa Teaching Hospital, Wasit, Iraq.

Received: 15 Apr 2018 Revised: 18 May 2018 Accepted: 21 Jun 2018

***Address for correspondence**
Dr.Mahdi Abdulkarim Abdulhussain
Head of Psychiatric Unit,
Al-Zahraa Teaching Hospital,
Wasit, Iraq.

ABSTRACT

There is no previous epidemiological study specified for Wasit mental morbidity. A cross sectional study conducted to view the demographic and clinical profiles of patients attending psychiatric unit in Wasit province. It is locating about 180 km to the south of Iraqi capital Baghdad. One million and thirty hundred thousand (1368000) people live in, males to female's ratio was 1:1, rural-urban distribution was 39.7% - 60.3% respectively. Life expectancy at birth in Wasit was 72.2 for males and 75.6 for females. The main aims of the present study are to establish the socio demographic characteristics of attendees at the psychiatric clinic during about 5 years' period. Moreover, to put a basis for future planning for mental health services in our province**.** The main aims of the present study are to establish the socio demographic characteristics of attendees at the psychiatric clinic during about 5 years' period.Moreover, to put a basis for future planning for mental health services in our province.

Keywords: - Socio-demographic, diagnostic, psychiatric unit.

INTRODUCTION

Mental illnesses affect the functioning and thinking processes of the individual, greatly diminishing his or her social role and productivity in the community. In addition, because mental illnesses are disabling and last for many years, they take a tremendous toll on the emotional and socio-economic capabilities of relatives who care for the patient, especially when the health system is unable to offer treatment and support at an early stage (1). The burden of mental disorders continues to grow with significant impacts on health and major social, human rights and economic consequences in all countries of the world (2). Concerned that millions of people worldwide are affected by mental disorders (3). A recent systematic review estimated that 14.3% of deaths worldwide, or about eight million deaths each year, are attributable to mental disorders. Five types of mental illness appear in the top 20 causes of global burden of disease (GBD): major depression (second), anxiety disorders (seventh), schizophrenia (11th), dysthymia (16th), and bipolar disorder (17th) were leading causes of years lived with disability (YLDs) in 2013 (4,5). The

economic consequences of these health losses are equally large: the cumulative global impact of mental disorders in terms of lost economic output will amount to US$ 16.3 billion between 2011 and 2030 (3). The number of specialized and general health workers dealing with mental health in low-income and middle-income countries is grossly insufficient. Almost half the world's population lives in countries where, on average, there is one psychiatrist to serve (200 000) or more people; other mental health care providers who are trained in the use of psychosocial interventions are even scarcer. Similarly, a much higher proportion of high-income countries than low income countries reports having a policy, plan and legislation on mental health; for instance, only 36% of people living in low income countries are covered by mental health legislation compared with 92% in high-income countries (3). Mental health services in Iraq have historically been highly centralized in urban areas and hospital based (6), the national rate of psychiatrist served people is 0.36 per 100000 populations while in Wasit 0.07 per 100000 populations (7); however, in Wasit there is one psychiatrist to serve 650 000 or more people.

For a number of people with severe mental disorders, hospitalization is required at some point in their lives. District general hospitals provide an accessible and acceptable location for 24-hour medical care and supervision of people with acute worsening of mental disorders, in the same way that these facilities manage acute exacerbations of physical health disorders. Mental health services provided in district general hospitals also enable 24-hour access to services for any physical health problems that might arise during the course of inpatient stays. Ideally, district general hospitals will have wards dedicated to the treatment of mental disorders and these wards will have layouts that support good observation and care, thereby minimizing the risk of neglect and suicide. To minimize the risk of human rights violations, facilities should adhere to clear policies and guidelines that support the treatment and management of mental disorders within a framework that promotes human rights and dignity and uses evidence-based clinical practice (8). Eight units of community-based psychiatric facilities were rehabilitated in Baghdad Russafa, Baghdad Karkh, Baquba, Kerbela, Mosul, Basra, Sulaimaniya and Babylon centres. Six new psychiatric facilities have been developed in Erbil and Al Najaf, Nasiriya, Wasit and Kirkuk and Baghdad Russafa since 2006 (9), for more details about the history of mental health services in Iraq please read the report of mental health policy in Iraq since 2003 [(10)]. Only 2% of all health research in Iraq was on mental health (10). The Iraq Mental Health Survey (IMHS) 2006/7 report provides valuable and previously unavailable information regarding the prevalence of mental disorders in Iraq, the relationship between trauma exposure and mental disorders, the family burden, prevalence of mental disorders in different regions of Iraq and the percentage of treatment utilization by people suffering from mental disorders and substance use. The results of the World Mental Health Survey in Iraq (with an overall response rate of 95.2%) indicate an overall lifetime prevalence of mental disorders of 16.56%, and an overall 12-month prevalence of 11.09% (9).

MATERIALS AND METHODS

Study Design and Sampling Technique

A cross-sectional study involved all patients diagnosed to be suffering from mental and behavioral disorders who were recorded according to a file system started with the initiation of the psychiatric unit in Al-zahraa Teaching Hospital/ established in 2006/ Wasit province. For research purposes since 2015 to date the socio-demographic, economic data and diagnosis routinely recorded by using SPSS.

Instrument, Measurement, and Data Collection

Information was elicited from the computerized records of socio-demographic, economic profiles (age, gender, marital status, education, occupation, residence) and diagnosis of the patients attended the outpatient clinic of the psychiatric unit from July 2011 to December 2017. The recorded signs and symptoms of 10 major groups were classified according to the International Statistical Classification of Diseases and Related Health Problems 10th

Revision (ICD-10)-WHO Version for; 2016 [11]. Ethical consent sought from appropriate committee of the hospital/ health directorate and the National Mental Health Advisor/ MOH.

Inclusion and Exclusion Criteria

The inclusion criteria included all attendees for psychiatric consultation regardless of whether it was their first visit or they were coming for follow up. Exclusion criteria included those who are not diagnosed yet and those who referred for medico-legal purposes or known medical cases referred to the psychiatric unit as part medical management.

Statistical Analysis

Descriptive and inferential statistics were performed using the Statistical Package for Social Sciences (SPSS) software (Version 0.22, IBM, and Chicago, Illinois, USA), p-value of less than 0.05 considered statistically significant.

RESULTS

A sample of 2175 attendants in psychiatric unit included, based on ICD-10 criteria 33%, 25%, 11.4%, and 10% of attendants diagnosed with schizophrenia, depression, stress and mental retardation respectively (table 1). Mean age of patients was 38 yrs. (range from 4 to 107 yrs.) 60% of them present in age group 15-44 yrs. (figure 1). Male patients were 60.7% (1320) of sample and 39.3% (855) were females. Distribution of mental disorders vary according to patient's sex with highly statistically significant (p-value <0.05) as explained in table 2. Most of patients (70%) reside in urban areas and (30%) of them reside in rural areas. In addition, the majority of patients (95%) live in Wasit province and (5%), coming from neighbor provinces (Baghdad, Nasiriya, and Maysan). Social status findings indicated that half of patients 18 yrs. and above were single, and 43% married (figure 2), of those under 18 yrs., only two were married.

DISCUSSION

There were a lot of studies of mental illnesses in Iraq with a different diagnostic profile (9). In spite of multiple programs performed under the supervision and support of WHO, mental health services are still below the expected level in the national health policy and priority in Iraq (9). To our knowledge, this is the first sociodemographic study performed in Wasit Province. In developed countries where the provision of health is the responsibility of the government, like in Iraq, studies in mental health caries a special significance to formulate any plan regarding mental health, since the mental disorders are the leading cause of disease burden is this sector of the world (12). Mental disorders are a leading cause of disease burden in developed countries therefore studies in this field becomes important mainly to formulate any plan regarding mental health development especially when the provision of health is the responsibility of government like Iraq Heath System. Epidemiological studies have indicated that in terms of services there is one mental health professional per million population in spite the fact that there are 680 million people who are likely to exposed to psychiatric disorder, (13) Attendance to the psychiatric clinic was affected by many factors like social stigma; the extent of stigma varies according to the cultural and sociological backgrounds of each society and by cultural understanding of mental illness and tendency to seek help from traditional healers instead of health professionals (14). Male patients were overrepresented among the consultees in proportion to their ratio in the total population, which is concomitant with a study performed in Baghdad teaching hospital at December 2010 (7, 14). It is well known that Gender is an important factor in mental illness predisposition with predominance to female gender but because of social and ethical consideration in our community are unlikely to seek help or to be seen at the psychiatric clinic, this might reverse the equation (15). Social status findings indicated that half of

patients, 18 years and above, were single, and 43% married (figure 2), of those under 18 years, only two were married.

CONCLUSION

It is notable that Gender is a vital factor in psychological sickness inclination with transcendence to female sexual orientation but since of social and moral thought in our locale are probably not going to look for help or to be seen at the mental facility, this may turn around the condition Social status findings indicated that half of patients 18 yrs. and above were single, and 43% married of those under 18 yrs., only two were married.

ACKNOWLOGEMENT

I am very grateful to my team for their help in following up patients' thank you for all your technical and emotional support.

REFERENCES

1. World health organization. Mental health problems: the undefined and hidden burden, WHO 2018.
2. World health organization (WHO). Mental disorders Fact sheet, WHO 2016.
3. World health organization(WHO). Mental health action plan 2013-2020. WHO 2013.
4. Walker ER, McGee RE, Druss BG. 2015. Mortality in mental disorders and global disease burden implications: a systematic review and meta-analysis. JAMA Psychiatry.72: 334–41.
5. Daniel V, Graham T, Rifat A. 2016. Estimating the true global burden of mental illness, Lancet Psychiatry. 3: 171–78
6. Sadik et al. 2010. Public perception of mental health in Iraq. International Journal of Mental Health Systems 2010 4:26.
7. Ministry of health/ environment (MOH). 2016. Annual statistical report.
8. World Health Organization and World Organization of Family Doctors (WHO). 2008. Integrating mental health into primary care: a global perspective, Wonca.
9. World health organization (WHO), Iraq Mental Health Survey (MOH). 2006, 2009.
10. Sonali S et al, Mental Health Policy in Iraq since 2003, 2012.
11. International Statistical Classification of Diseases and Related Health Problems 10th Revision (ICD-10)-WHO Version for ;2016.
12. Vos T and Mathers CD. 2007. The burden of mental disorders. Bulletin of the World Health Organization, 78 (4)
13. Prince M, Patel V, Saxena S, Maj M, Maselko J, Phillips MR, et al. 2007. No health without mental health. Lancet, 370(9590):859-877.
14. Maha S. Y. Clinical and Demographic Profile of Attendees at Baghdad's Walk-in Psychiatric Clinic.
15. Toksoz BK, Robert P, Robert I, Stein M, Hope C and Barbara S. 2006. Patterns of Psychiatric Consultation in a General Hospital.

Table 1: Mental and Behavioral Disorders According to ICD-10 Diagnosis

ICD-10 Mental and behavioural disorders (F00-F99)	No.	%
F00-F09 Organic, including symptomatic, mental disorders	**58**	**2.7**
F10-F19 Mental and behavioral disorders due to psychoactive substance use	**13**	**0.6**
F20-F29 Schizophrenia, schizotypal and delusional disorders	**722**	**33.2**
F30-F39 Mood [affective] disorders	**544**	**25.0**
F40-F48 Neurotic, stress-related and somatoform disorders	**248**	**11.4**
F50-F59 Behavioural syndromes associated with physiological disturbances and physical factors	**40**	**1.8**
F60-F69 Disorders of adult personality and behaviour	**94**	**4.3**
F70-F79 Mental retardation	**229**	**10.5**
F80-F89 Disorders of psychological development	**86**	**4.0**
F90-F98 Behavioural and emotional disorders with onset usually occurring in childhood and adolescence	**36**	**1.7**
F1X01 Substance abuse	**31**	**1.4**
G40 Epilepsy	**74**	**3.4**
Total	**2175**	**100.0**

Table 2: Distribution of mental disorders according to patient's sex (N=2175)

Females	ICD-10	Males
36 (62.9%)	F00-F09	22 (37.9%)
0 (0%)	F10-F19	13 (100%)
275 (38.1%)	F20-F29	447 (61.9%)
294 (54%)	F30-F39	250 (46%)
103 (41.5%)	F40-F48	145 (58.5%)
13 (32.5%)	F50-F59	27 (67.5%)
6 (6.4%)	F60-F69	88 (93.6%)
75 (32.8%)	F70-F79	154 (67.2%)
13 (15.1%)	F80-F89	73 (84.9%)
5 (13.9%)	F90-F98	31 (86.1%)
5 (16.1%)	F1X01	26 (83.9%)
30 (40.5%)	G40	44 (59.5%)
855 (39.3%)	Total	1320 (60.7%)

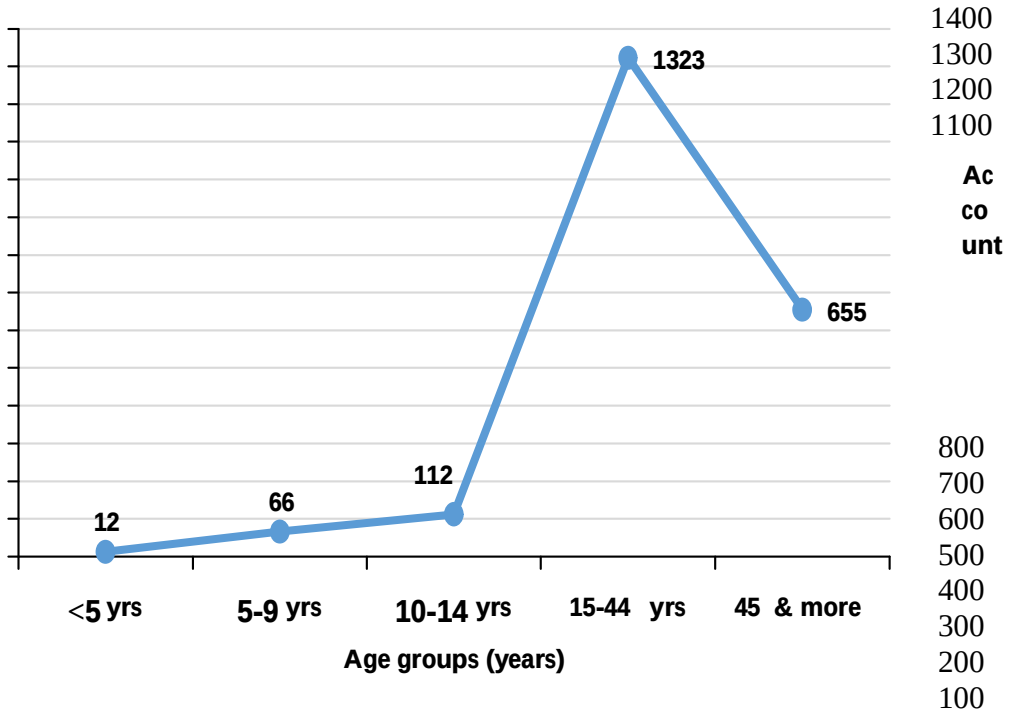

Figure 1: Description of Patients According to their Ages (n=2168).

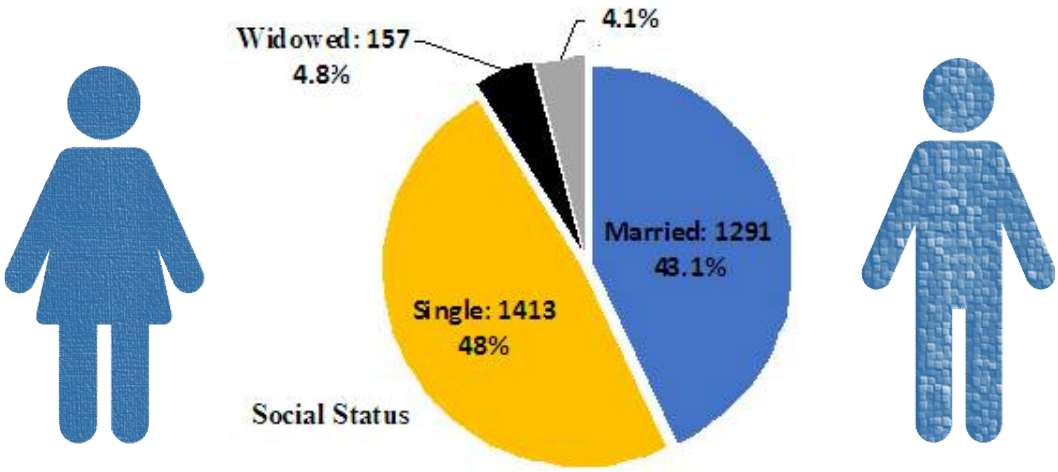

Chi-square: 156.986, df: 11, sig. 0.0001
Divorced: 119

Figure 2: Description of Patients According to Their Social Status (N=2174)

Indian Journal of Natural Sciences www.tnsroindia.org.in ©IJONS

Vol.8 / Issue 49 / August /2018 *International Bimonthly* *ISSN: 0976 – 0997*

RESEARCH ARTICLE

Study the Physical Properties of Laser Induced Sodium Oxide Plasma

Hasan Ali Tawfeeq*

Physics Teacher at the Ministry of Education, Iraq.

Received: 20 Apr 2018 Revised: 23 May 2018 Accepted: 25 Jun 2018

***Address for correspondence**
Hasan Ali Tawfeeq
Physics Teacher,
Ministry of Education, Iraq.
E Mail: almodars@yahoo.com

ABSTRACT

In this work; Sodium Oxide (Na_2O) plasma plume was prepared by laser induced plasma (LIP). The electron number density, plasma frequency and Debye length were calculated by reading the data of I-V curve of Langmuir probe which was used as a diagnostic method of measuring plasma properties. Pulsed Nd: YAG laser was used for measuring the electron number density of Na_2O plasma plume under vacuum environment with varying both vacuum pressure and axial distance from the target surface. Some physical properties of the plasma generated such as electron density, plasma frequency and Debye length have been measured experimentally and the effects of vacuum pressure and Langmuir probe distance from the target were studied on those variables. An inverse relationships between electron density, Debye length and plasma frequency with axial distance from the target were observed as well direct proportionality between both plasma density and plasma frequency with vacuum pressure while the exception is true in case of Debye length which is proportional inversely with vacuum pressure.

Keywords: Sodium Oxide, measuring, effects, plasma, pressure.

INTRODUCTION

Pulsed laser ablation (PLA) has different applications making it as attractive field of fundamental research. One of the applications of PLA is laser-induced plasma (LIP) [1]. Due to various key applications in material processing, thin film deposition, environmental monitoring, biomedical studies, military safety usage, art restoration/conservation and metal analysis, the pulsed laser-induced plasmas (LIPs) created as a result of laser irradiance is of a great importance. In this method a highly intense laser pulse interacts with a target material leading to the formation of a micro-plasma in nanosecond due to high intensity plume propagate. The initial part of the plasma is re-heated by the inverse bremsstrahlung (IB) absorption [2]. Dependence of the propagation and expansion behavior of the plasma on the laser pulse parameters is due to post-ablation interaction of the generated plasma plume [3].

In LIPS method, a micro-plasma is generated in nanosecond when highly intense laser pulse interacts with a target material; vaporization take place and thus plasma produced expand in the form of vapor plume. During the expansion process of vapor plume the Inverse Bremsstrahlung (IB) absorption also happened repeatedly which is considered as heat loss through plasma routine applications [4]. During ablation process, laser energy is used in dissipation into the sample target through heat conduction, melting and vaporization of the target material to create plasma plume [5]. In the process of pulsed laser ablation of solid target, highly energetic species are ejected from the target surface. The energy reaches up to several hundreds of eV. The ejected species compose a plasma plume. In the plume, the ablated species undergo various chemical reactions by themselves and also with ambient species. By using these species, thin films or fine particles can be obtained [6].Laser-generated plasma characteristics are strongly dependent upon different key parameters, such that laser intensity, pulse duration and wavelength, target material and geometry, and the nature and pressure of any ambient gas [7,8]. The key parameters of laser ablated plumes are density and temperature. The characteristics of the plasma plume are controlled initially by electron contributions to temperature and density. There are various diagnostic techniques employed for the determination of these parameters including Langmuir probe, mass spectroscopy, optical emission spectroscopy, laser absorption spectroscopy, microwave interferometry, laser interferometry, Thomson scattering, laser-induced fluorescence, beam deflectometry, etc.[8,9]. Langmuir probes have been widely used to diagnose the low-temperature plasmas generated by laser ablation. These probes have been used to measure the plasma density and temperature, the plasma flow velocity and the shape of the ablation plume expansion [8,10]. The probe measurements are based on the I–V curve of a circuit consisting of metallic electrode that is immersed in the plasma under study. Electron density of laser-induced plasma can be computed by the relation given below:

$$n_e = I_0/Ae\sqrt{2\epsilon_0 kT_e} \quad (1)$$

Where "I0" is probe current at zero biasing voltage, A is the area of the probe tip inside the plasma .Debye's length can be calculated by the formula:

$$\lambda_D = \sqrt{\epsilon_0 kT_e/e^2 n_e} \quad (2)$$

Plasma frequency can be calculated as:

$$\omega_p = \sqrt{n_e e^2/\epsilon_0 m_e} \quad (3)$$

Where „me" is the mass of electron

In this research some physical properties of Sodium Oxide (Na_2O) laser induced plasma like electron density; plasma frequency and Debye length have been investigated as a function of vacuum pressure and Langmuir probe axial distance from the target surface [8].

MATERIALS AND METHODS

The target of the laser induced plasma (LIP) process was Na_2O powder with purity 99.999%, and compressed under the pressure (8 tons) in order to make it shaped liked disc with a diameter of 3cm and then sintered in oven to temperature (350 ^oC) for 2 hours. LIP experiment was achieved under vacuum pressure (0.2mbar by using Varian DS219 Rotary pump).The beam of Nd: YAG laser with fundamental harmonic frequency (λ=1064nm, 9ns, 5Hz) was focused onto Na_2O target with quartz lens (f=10cm), the target was kept onto rotating motor (speed 5 rev/min) to prevent fast drilling. The cylindrical Langmuir probe distance from the target was fixed at 1cm. The LIP experiment was performed at room temperature. LIP setup scheme with the electric circuit of the Langmuir probe has been

shown in Figure- 1. Electron density of the Na_2O ablated atoms were calculated by analyzing the I-V data of the Langmuir probe. The Na_2O target was ablated by 800 pulses. The vacuum pressure was varied from (0.03-0.15) mbar, also the distances between the Na_2O target and the tip of the Langmuir probe was changed from (0.45-1.6) cm to study their effects on the value of electron density hence on the plasma frequency and Debye length.

RESULTS AND DISCUSSION

Electron density in laser induced plasma depends strongly on the vacuum background pressure for Na_2O target. In order to measure electron density (n_e) laser pulse energy has been set constant at 500mJ and vacuum pressure has been altered. Electron density has been calculated by using eq.(1) after getting Te values from I-V curve of Langmuir probe data as in Figure-2.

The electron temperature Te can be obtained from the slopes of the electron saturation part of the I-V characteristic curve at different background vacuum pressure by using the relation Te=1/Slope. Electron density ne against vacuum pressure ranged from $4x10^{-2}$ to $2x10^{-1}$ mbar using fundamental wavelength of Nd: YAG laser has been illustrated in Figure -3.

Obviously from the Figure -3 that the electron density ne increases exponentially with increasing vacuum pressure. This is because of the increasing pressure will lead the plasma to be confined in small volume and hence increasing the collisions between the plasma species (electrons, ions, atoms and molecules), consequently the neutral atoms and molecules will be ionized by the liberated electrons and ions due to that collision and more electrons will be produced and there will be increment in their number and density. The curve fitting of the electron density as a function of vacuum pressure has been performed with fitting equation

$$n_e = 4.5x10^{10} - 2x10^{10}/(1 + e^{(P-0.08)/0.019})$$

Figure- 4 shows also the inverse relationship between the electron density and the axial distance from the Na_2O target, it is noted that the experimental data coincide with the fitting data.

As the axial distance from the Na_2O target surface increases the electron density decreases. When the axial distance from the target increases the plasma plume continue propagation and the recombination process between the ionized atoms and molecules with electrons happens at large distance to form a neutral atoms which leads to decrease number of free electrons hence decreasing the electron density (ion-electron recombination at large distances from the target surface), The curve fitting equation is

$$n_e = 3.31x10^{10}(1 + 0.35d)^{-1} \quad (4)$$

In Figures -5and 6 the relationship between Debye length and vacuum pressure and axial distance from target are shown respectively.

From the figures above, we observe that Debye length decreases with increasing both vacuum pressure and axial distance from the surface of Na_2O target, and the reason for this is due to equation (2), in Figure-5 the reason of this behavior of Debye length versus vacuum pressure belongs to the inverse relationship between the Debye length with the electron density ne. Since electron density is direct proportional with vacuum pressure so as a result, the Debye length decreases exponentially with vacuum pressure.The plasma frequency depends on both vacuum pressure and axial distance from the target surface as shown in Figures -7 and 8 below.

It is clear in Figure-7 that as vacuum pressure increase, the plasma frequency exponentially increases too because of dependence of the plasma frequency on electron density according to the equation (3), which is in turn depends on the pressure. So consequently the plasma frequency increases with increasing the pressure while in Figure- 8 the plasma frequency decreases linearly with the distance from the target because of the electron density is inversely proportional to the distance from the target surface (d) Therefore, the plasma frequency ωp is inversely proportional to the distance from the target surface (d).

CONCLUSION

It has been concluded from the results that the electron density, Debye length and plasma frequency of laser induced plasma of Na_2O target depend clearly on the LIP conditions such as vacuum pressure and axial distance from the target surface. The electron density increased exponentially with increasing vacuum pressure and decreased with increasing the distance from the Na_2O target. This is due to the recombination processes of the constituents of plasma plume and confinement phenomena. Debye length is proportional inversely with both vacuum pressure and the axial distance from the target because of the dependence on the electron temperature. The plasma frequency is related directly with vacuum pressure and inversely with the distance from the target. This behavior of plasma frequency can be explained in term of the dependence on the electron density in the plasma plume of Na_2O target.

REFERENCES

1. Hussein, A.E., Dwakar, P.K. ,Harilal, S.S. and Hassanein , A. **2013** The role of laser wavelength on plasma generation and expansion of ablation plumes in air, *Journal of applied physics* 113,pp:143305-1 -143305-10.
2. Naeem , M.A., Iqbal, M., Amin, N., Musadiq, M. , Jamil Y. and Cecil, F. 2013, Measurement of Electron Density and Temperature of Laser-Induced Copper Plasma, *Asian Journal of Chemistry* ,25,pp:2192-2198.
3. Xueshi Bai, Qianli Ma, Vincent Motto-Ros, Jin Yu, David Sabourdy,Luc Nguyen, and Alain Jalocha,2013, Convoluted effect of laser fluence and pulse duration on the property of a nanosecond laser-induced plasma into an argon ambient gas at the atmospheric pressure, *Journal of applied physics* ,113,pp:013304-1 – 013304-10.
4. Muhammad Musadiqa, Nasir Amina, Yasir Jamila, Munawar Iqbalb, M. Asif Naeema and Hafiz Akif Shahzada ,2013, Measurement of electron number density and electron temperature of laser-induced silver plasma, *International Journal of Engineering and Technology* , 2,pp:32-43.
5. Hanif, M., Salik, M.and Baig, M. A. 2012, Diagnostic Study of Nickel Plasma Produced by Fundamental (1064 nm) and Second Harmonics (532 nm) of an Nd: YAG Laser, *Journal of Modern Physics*, 3,pp:1663-1669.
6. Hideki Furusawa, Tetsuo Sakka, and Yukio H. Ogata,2004, Characterization of ablated species in laser-induced plasma plume, *Journal of applied physics* ,96,pp:975-982.
7. Harilal, S. S., Beau O¨Shay, and Mark. Tillack, S. 2005, Spectroscopic characterization of laser-induced tin plasma, *Journal of applied physics* ,98,pp: 013306-1 – 013306-7.
8. Bhatti, K.A. , Khaleeq-ur-Rahman, M., Rafique, M.S., Shahzad, M.I. Latif, A. and Parveen, 2 N. 008, Electrical diagnostics of laser ablated platinum plasma, *Vacuum* ,82,pp:1157-1161.
9. Marko Cvejić, Sonja Jovićević, Emilien Mothe, Laurent Mercadier, Nikola Konjević, and Jörg Hermann,2010, Electron density diagnostics of laser induced plasma in helium ,*Publ. Astron. Obs. Belgrade* ,89,pp:189-192.
10. Doggett , B., Budtz-Joergensen , C., Lunney , J.G. , Sheerin , P. and Turner, M.M. 2005, Behaviour of a planar Langmuir probe in a laser ablation plasma ,*Applied Surface Science* , 247,pp:134-138.

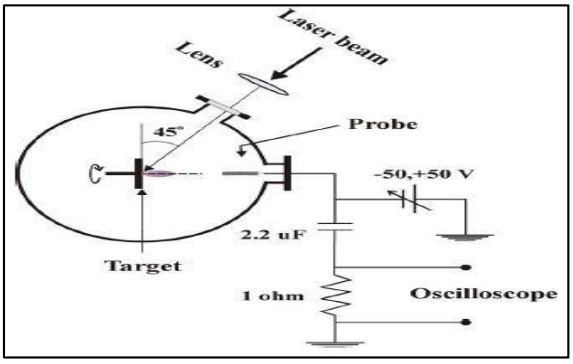

Figure 1- Schematic Diagram of the LIP Experimental Setup

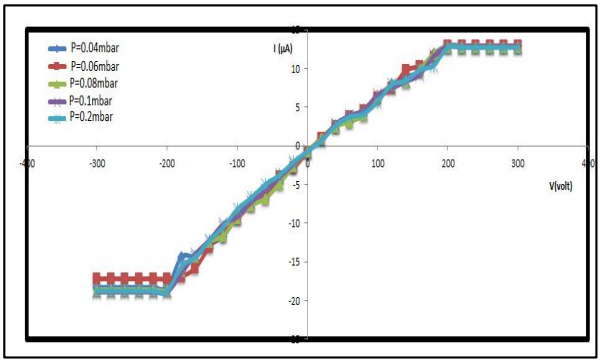

Figure 2- I-V chart of Langmuir Probe at Different Background Vacuum Pressure

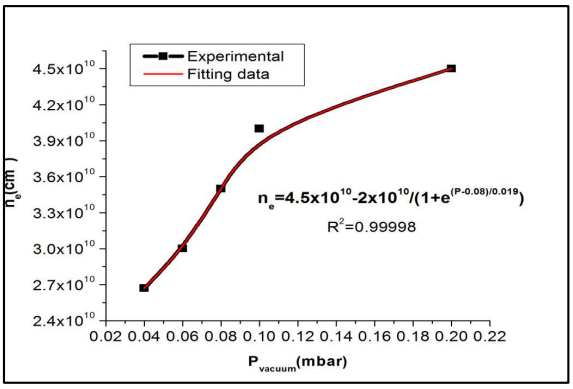

Figure 3- Electron density versus different vacuum pressure by using Nd:YAG laser wavelength 1064nm , laser pulse energy 600mJ

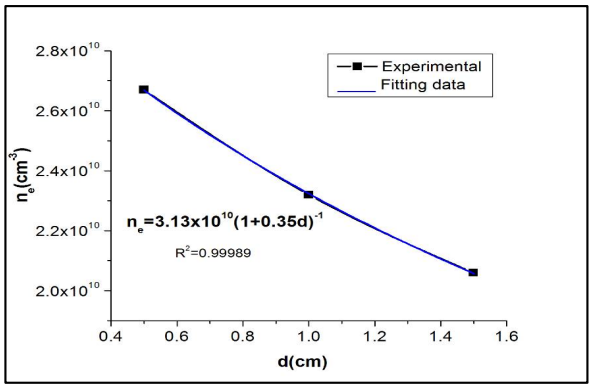

Figure 4- Electron density as a function of different axial distance from the target by using Nd:YAG laser wavelength 1064nm , laser pulse energy 600mJ

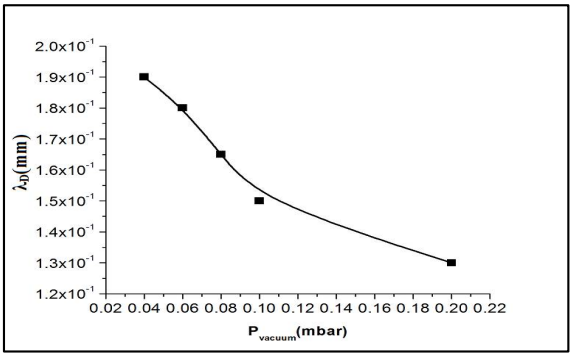

Figure 5- Debye length versus different vacuum pressure by using Nd:YAG laser wavelength 1064nm , laser pulse energy 600mJ.

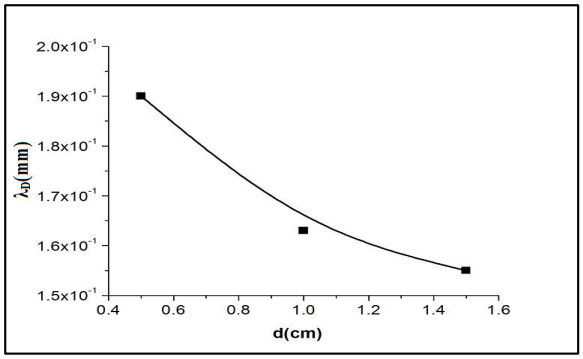

Figure 6- Debye length as a function of different axial distance from the target by using Nd:YAG laser wavelength 1064nm , laser pulse energy 600mJ

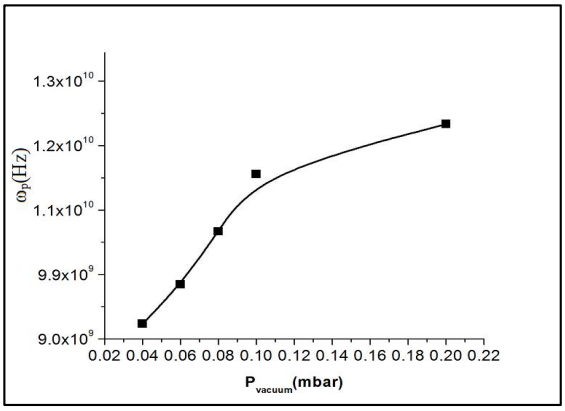

Figure 7- The variation of plasma frequency as a function of pressure at distance 0.4cm.

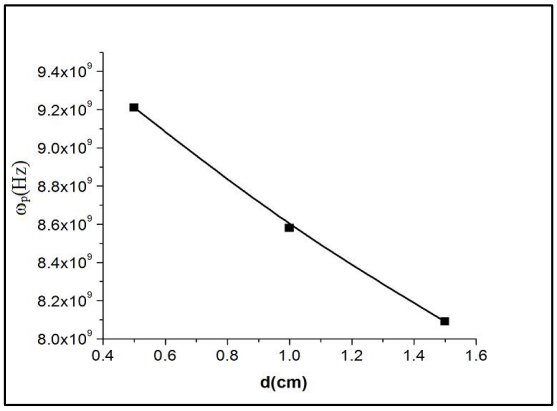

Figure 8- The variation of plasma frequency as a function of distance from the Na_2O target at pressure 0.03mbar.

Indian Journal of Natural Sciences www.tnsroindia.org.in ©IJONS

Vol.8 / Issue 49 / August /2018 *International Bimonthly* *ISSN: 0976 – 0997*

RESEARCH ARTICLE

Organic Source of Silica, Flower Extracts and Essential Oils to Enhance Resistance of Tomato Plants to Fruit Borers, *Helicoverpa armigera* (Hubner), *Spodoptera litura* (Fabricius) and *Tuta absoluta* (Gennadius)

Chandramani .P*

Professor, Agricultural College and Research Institute, Kudumiyanmalai, Pudukkottai Dist., Tamil Nadu, India.

Received: 25 May 2018 Revised: 28 Jun 2018 Accepted: 30 July 2018

*Address for correspondence
Chandramani .P
Professor,
Agricultural College and Research Institute,
Kudumiyanmalai, Pudukkottai Dist.,
Tamil Nadu, India.
E Mail: pcento12@gmail.com

ABSTRACT

Experiments were conducted to study the effect of spraying of flower extracts, essential oils, plant growth regulators along with basal application of rice husk ash and silicate solubilising bacteria or *Pseudomonas fluorescens* on the occurrence of borer pests of tomato *viz.,* fruit borer, *Helicoverpa armigera*; tobacco caterpillar, *Spodoptera litura* and tomato pin worm, *Tuta absoluta*. The results revealed that the tomato plants treated with basal application of rice husk ash 1t, with silica solubilizing bacteria followed by foliar spray of 2% *Chrysanthemum* flower extract, plant growth regulator NAA alternated with GA_3 10 ppm and essential oils (lemongrass oil alternated with rosemary oil) 0.2% significantly reduced the incidence and damage by fruit borer, tobacco caterpillar and tomato pin worm. The per cent reduction recorded with regard to *S.litura* was 70.56; tomato pin worm 73.60 over untreated check. The per cent fruit damage by *H. armigera* was significantly less in the treatments with basal application of RHA1t + SSB and foliar spray of 2% CFE along with NAA alternated with GA_3 and essential oils @ 0.2% and PF along with azophos and foliar spray of LFE 2% along with NAA alternated with GA_3 and essential oils @ 0.2%. Lab experiment conducted with various concentrations of essential oils to test the efficiency of food utilization of *S. litura* revealed that consumption index of *S. litura* was significantly less in lemongrass oil and rosemary oil applied at 0.4 and 0.5%. Similarly, approximate digestibility of *S. litura* was significantly less in the treatment with lemongrass oil at 0.4 and 0.5% and rosemary oil at 0.3, 0.4 and 0.5%. While testing the efficiency of flower extracts, consumption index of *S. litura* was significantly less in the treatments *Chrysanthemum* flower extract at 3 % and *Lantana* flower extract at 5%. Similarly, approximate digestibility of *S. litura* was significantly less in the treatment with CFE at 4 and 5%, LFE at 5%.

Key words: silica, flower extracts, essential oil, *Helicoverpa, Tuta, Spodoptera*.

INTRODUCTION

India ranks fourth in the world tomato production in terms of area (57.1 lakh million hectares) and production (10.2 million tones) and the productivity being 17.9 t/ hectare. Among all the known factors attributed for low yield of tomato, the insect pests are of prime biotic factors which significantly affect the production, almost during all the stages of crop growth right from nursery to maturity. Among the various insect pests attacking tomato, tomato fruit borer, *H. armigera* (Hubner) is very important pest which causes 40-50 percent damage to the tomato crop (Pareek and Bhargava, 2003). *H. armigera* is a charismatic insect pest in agriculture accounting for the consumption of over 55 percent of total insecticides used in India (Puri, 1995). This is a key pest as it attacks fruits and makes fruits unfit for human consumption causing considerable crop loss up to 55 percent in yield (Selvanarayanan, 2000).

Leaf caterpillar *Spodoptera litura* (Fabricius.) is one of the predominant polyphagous pest and the larvae cause significant damage to the foliage and cause fruit damage ranging from 11.8 to 23.01 per cent in rainy season and 9.4 to 27.4 per cent in winter (Patnaik, 1998). Similarly, tomato leafminer, *Tuta absoluta* (Gennadius) is a most destructive pest in tomato. Larva attack all the parts of the plants *viz*, leaves, flowers, stems and both green and red fruit. The infestation may cause 50-100% losses in the tomato crop (Saad Moussa *et al*., 2013).

In recent years, the use of synthetic insecticides in crop protection programmes around the world has resulted in disturbances of the environment, resurgence and resistance of insects to pesticides and lethal effect to non target organisms in the agro-ecosystems in addition to direct toxicity to users. Therefore, it has now become necessary to search for the alternative means of pest control, which can minimize the use of synthetic pesticides. Organic products are the important alternatives to minimize or replace the use of synthetic pesticides as they possess an array of properties including toxicity to the pest, repellency, antifeedance, insect growth regulatory activities against pests of agricultural importance (Prakash and Rao, 2003). The increasing concern for environmental safety and global demand for pesticide residue free food has evoked interest of ecofriendly methods of pest management *viz.,* plant derivatives, plant growth promoting rhizobacteria, plant growth regulators and microbials as important components in the organic pest management.

MATERIALS AND METHODS

A field experiment was conducted during December to March 2016 (Rabi season) at Vaigasipatti village of Alanganallur block, Madurai. The design adopted was Randomized block design (RBD) using a variety PKM 1 with fourteen treatments as indicated in the table, each replicated twice. All the agronomic practices were followed uniformly in all the plots with plot size of 5 x 4 m^2. The incidence of major pest's *viz.,* fruit borer, tobacco caterpillar and leaf miner/ tomato pin worm was recorded in 5 randomly selected plants in each plot at weekly interval.

Note

- Rice husk ash (RHA), silica solubilizing bacteria (SSB), *Pseudomonas fluorescens* (PF) and Azophos were applied as basal
- Spraying of flower extract *chrysanthemum* flower exract (CFE); *Lantana* flower extract (LFE) , PGR and essential oil were taken up as mentioned in the treatment schedule

Assessment of pest population

Fruit borer, *Helicoverpa armigera*

The Fruit borer *H.armigera* incidence was assessed by recording larval population and fruit damage. For larval population, five plants were selected at random and the number of larvae present in each plant was recorded and mean number of larvae per plant was worked out.

The Fruit damage was recorded by counting the number of healthy and infested fruits in five randomly selected plants and per cent fruit damage was worked out. A post treatment observation was recorded on 1, 3 and 5 days.

$$\text{Fruit damage (\%)} = \frac{\text{Number of fruits damaged / plant}}{\text{Total number of fruits / plant}} \times 100$$

Tobacco Caterpillar, *Spodoptera litura*

The tobacco caterpillar, *S.litura* incidence was assessed in five randomly selected plants and the number of larvae present in each plant was recorded and the mean number of larvae per plant was worked out. Post treatment observations were recorded on 1, 3 and 5 days after each spray.

Tomato Pin Worm, Leaf Miner, *Tuta Absoluta*

The leaf miner, *T. absoluta* incidence was assessed by recording larval population per plant. Five plants selected randomly and total number of larvae was counted using the magnifying lens in five leaves per plant.

Laboratory Experiment

The effect of flower extracts and essential oils were studied in the laboratory against the insect pests namely *S.litura*. *Chrysanthemum* and *Lantana* flower extracts each at 1, 2, 3, 4 and 5% concentrations and the essential oils at 0.1, 0.2, 0.3, 0.4 and 0.5% concentrations were studied.

Toxicity Study for *S.litura* (Jeyarajan Nelson, 1996)

Uniform sized tomato fruit slices were sprayed with flower extracts and essential oils for 60 sec, shade dried for 5 min and placed in petridishes lined with moistened filter paper. Three replications were maintained. In each treatment, 5 uniform sized thrid instar larvae pre straved for 4hr were introduced into the petridishes. Tomato fruit slices sprayed with water served as check. Initial larval weight and the weight of the fecal pellets voided out after 72hr of feeding were also recorded and calculated consumption index and approximate digestability.

$$\text{Consumption index} = \frac{\text{Fresh weight of food eaten}}{\text{Duration of feeding} \times \text{mean fresh wt of insect during feeding period}}$$

$$\text{Approximate digestability} = \frac{\text{Wt of food ingested - Wt of faeces}}{\text{Wt of food ingested}}$$

The data on per cent values and insect population counted in numbers were transformed into arcsine and square root values respectively. Duncan's (1995) Multiple Range Test (DMRT) was applied for comparing the treatment means. Correlation coefficients were worked out as per Singh and Chaudhary (1979).

RESULT AND DISCUSSION

The population of fruit borer, tobacco caterpillar and tomato pin worm were observed in the field at seven and fifteen days intervals starting from 30 DAT to 104 DAT.The results revealed that the incidence of fruit borer, *H.armigera* was significantly less in plants treated with the basal application of rice husk ash1t + SSB with foliar application of *Chrysanthemum* flower extract 2% + NAA/ GA_3 10 ppm + lemongrass oil + rosemary oil 0.2% sprayed during critical phases of the crop (**Fig 1**). The per cent fruit damage was also significantly less in the same treatment but it was on par with the application of PF with azophos and foliar spray of *Lantana* flower extract 2% along with NAA alternated with GA_3 and lemongrass oil 0.2% alternated with rosemary oil 0.2%.

This is in endorsement with the findings of Arti Prasad and Sujoita Purohit (2006) who compared the efficacy and feasibility of herbal (leaf and flower extracts of *L. camara* L.) and fungal (*Beauveria bassiana*) bio pesticides with synthetic chemicals against *H. armigera* in chick pea and tomato crops. This is again in confirmation with finding of Murugan *et al*. (2005) who reported that the application of PGPR, *P. fluorescens* (strain pf1) to seed, soil and plant has reduced fruit borer complex in tomato. Similarly Murugan (2003) reported that application of *P. fluorescens* in tomato and okra reduced the incidence and damage of *Helicoverpa armigera* and also reduced the fecundity. The relative growth rate, consumption rate and digestibility of food by *H. armigera* have been affected when larvae fed on cotton plants treated with *Pseudomonas gladioli* due to an increase in their polyphenol and terpenoid content (Qingwen *et al*. 1998).

Tobacco Caterpillar

In the field experiment conducted, the incidence of tobacco caterpillar was significantly less in plants treated with basal application of rice husk ash1t + SSB with foliar application of *Chrysanthemum* flower extract 2% + NAA/ GA_3 + lemongrass oil + rosemary oil 0.2% sprayed during critical phases of the crop (**Fig 1**).This is in confirmation with the findings of Meena *et al*. (2013) who reported that application of Si to corn affected the infestation of the *Spodoptera*. Oral toxicity of gibberellic acid (GA_3) was evaluated on *S. littoralis* larvae. The insects were exposed to various concentrations of GA_3 incorporated into the diet. GA_3 significantly reduced food consumption of insect species leading to larval weight loss (Khemais Abdellaoui *et al.,* 2009).

The present finding is in confirmation with the finding of Mourad *et al*. (2008) who reported that the flower extract of *Chrysanthemum coronarium* L. and their fractions have shown insecticidal effect on the cotton leaf worm *Spodoptera littoralis.* Tripathi *et al*. (2009) reported the toxicity of essential oil of *Aegle marmelos* by topical application to *S. litura* larvae with LD50 value of 116.3 μg/ larvae. Essential oil of *Lippia alba* induces growth inhibition (GI50 = 6.9–11.0 mg/g diet), where both relative growth and feeding consumption rates of *S.litura* were conspicuously reduced.

Kaur and Rup (2002) reported that GA_3 concentration applied at 125, 625 and 3125 ppm significantly decreased the food intake of *Spodoptera littoralis* larvae by 44, 65 and 64% respectively compared to the control. Goussain *et al*. (2002) proved that *Spodoptera frugiperda* (J. E. Smith) larvae displayed increased mortality, cannibalism and mandibular wear after feeding on corn plants fertilized with Si.

This is again in consonance with finding of Bernays and Bargeman (1987) who stated that most of the plant silicon occurs in the epidermis, which might dislodge young larvae before they can establish in the stem. The application of nano silica to the tomato plants may minimize the problems caused by *Spodoptera littoralis*. Coors (1987) showed that high levels of silica decreased digestibility in *Spodoptera eridania* and promoted increased consumption rates. Final-instar *Spodoptera eridania* larvae fed on artificial diet with powdered silicic acid at 10 - 20 per cent dry weight showed reduced ability to digest the diet, leading to increased consumption rates.

Tomato Pin Worm

In the present study, the incidence of tomato pin worm was significantly less in the basal application of rice husk ash1t + SSB with foliar application of *Chrysanthemum* flower extract 2% + NAA/ GA_3 + lemongrass oil + rosemary oil 0.2% sprayed during critical phases of the crop (**Table 1**)**.** This is in line with the findings of Dos Santos *et al*. (2015) who stated that the foliar application of silicon-containing compounds at 0.50% was found to be effective against the attack of *T. absoluta* caterpillars causing detachment of midgut cells from the basal membrane, which may result in digestion difficulties and larval mortality. *T. absoluta* reared on tomato plants accumulating silicon show decrease in larval and pupal survival and male and female weight (Santos *et al.,* 2012).

Cote-Beaulieu *et al.* (2009) confirmed the efficiency of silicon-containing products for the control *T. absoluta* and it was due its toxic and anti-feeding effect to the larval stage, playing a role as the activator of tomato plants resistance. One of the effects caused by the application of silicon in the leaves was the detachment of the midgut epithelium from the basal membrane, which leads to the reduction of digestive capacity in insects (Almeida *et al.,* 2009).

This is in line with the findings of Goussain *et al.* (2002) and Kvedaras *et al.* (2009) who stated that the deleterious effects of silicon on *Tuta absoluta* larvae that fed on tomato plants treated with calcium silicate was due to the damages in the incisor teeth of the mandibles, affecting the insect nourishment and development.

Lab experiment conducted with various concentrations of essential oils and flower extracts to test the efficiency of food utilization of *S. litura* revealed that consumption index of *S. litura* was significantly less in the treatments CFE at 3 % and LFE at 5%, lemongrass oil at 0.4 and 0.5%, and rosemary oil at 0.4 and 0.5%. Similarly, approximate digestibility of *S. litura* was significantly less in the treatment with CFE at 4 and 5% , LFE at 5% , lemongrass oil at 0.4 and 0.5% and rosemary oil at 0.3, 0.4 and 0.5% (**Fig 2 & 3**). This is in confirmation with the findings of Tripathi *et al*. (2009) who reported that essential oil of *Lippia alba* induces growth inhibition in *S. litura* (GI50 = 6.9–11.0 mg/g diet) where, both relative growth and feeding consumption rates of *S.litura* were conspicuously reduced. Similarly Coors (1987) reported that high levels of silica decreased digestibility in *Spodoptera eridania* and promoted increased consumption rates.

To conclude, the present study clearly indicated that foliar spray of flower extracts, alternated with growth regulators and essential oils along with basal application of RHA/ *Pseudomonas* in field condition greatly reduced the incidence of fruit borers of tomato as evidenced through reduced consumption index and approximate digestibility of insects in the lab experiment and it is concluded that the effect might be due to systemic acquired resistance. This study reflects that use of organic sources is a very good alternate option for reducing the insect menace in tomato without pesticides and pesticide residue.

REFERENCES

1. Almeida, G.D., D. Pratissoli, J.C.Zanuncio, V.B.Vicentini, A.M.Holtz and J.E. Serrao. 2009. Calcium silicate and organic mineral fertilizer increase the resistance of tomato plants to *Frankliniella schultzei*. Phytoparasitica, 37: 225-230.
2. Arti Prasad and Sujoita Purohit. 2006. Study on incidence of key pest, *Helicoverpa armigera* (Hubner) in Udaipur district of South Rajasthan. Pestology, 30 (8):31-38
3. Bernays and Bargeman. 1987. Nutritional ecology of grass foliage chewing insects. Nutritional ecology of insects, mites, spiders and related invertebrates. pp 147-175.
4. Coors, J.G. 1987. Resistance to the European corn borer, *Ostrinia nubilalis* (Hubner), maize, *Zea mays*as affected by soil silica, plant silica, structural carbohydrates and lignin. Genetic aspects of plant mineral nutrition, 16-20 June, 1985, Madison, USA, 445-456 pp.

5. Cote-Beaulieu, C., F.Chain , J.G. Menzies, S.D. Kinrade and R.R. Belanger.2009. Absorption of aqueous inorganic and organic silicon compounds by wheat and their effect on growth and powdery mildew control. Environmental and. Experimental Botany, 65:155-116.
6. Dos Santos, M.S., A.M. Resende Junqueira, V.G. Mendes de Sá, J.C. Zanúncio and J.E. Serrao. 2015. Effect of silicon on the morphology of the midgut and mandible of tomato leafminer *Tuta absoluta* (Lepidoptera: Gelechiidae) larvae .Department of Entomology, Federal University of Viçosa, 12: 158-165pp.
7. Duncan, D.B. 1995. Multiple Range and Multiple F–Test. Biometrics, 11: 1–43.
8. Goussain, M.M., J.C. Moraes, J.G. Carvalho, N.L. Nogueira and M.L. Rossi. 2002. Efeito da aplicacao de silicio em plantas de milho no desenvolvimento biologico da lagarta-do-cartucho *Spodoptera frugiperda* (J.E. Smith) (Lepidoptera: Noctuidae). Neotropical Entomology, 31: 305 – 310.
9. Jeyarajan nelson. 1996. Evaluation of plants for their anti- insect activites with special references to *Acorus calamus* and *Cymbopogon martini.* Ph.D thesis, Tamil Nadu agricultural university, Coimbatore.
10. Kaur, R., and P.J. Rup. 2002. Evaluation of regulatory influence of four plant growth regulators on the reproductive potential and longevity of melon fruit fly *Bactrocera cucurbitae*. Phytoparasitica, 30:1-7.
11. Khemais Abdellaoui Monia Ben Halima and Kamel. 2009. Insecticidal Activity of Gibberellic Acid against *Spodoptera littoralis* (Lepidoptera, Noctuidae) and *Locusta migratoria migrator ia* (Orthoptera, Acrididae). Pest Technology, 3 (1), 28-33.
12. Kvedaras, O.L., M.J.Byrne, N.E.Coombes and M.G.Keeping. 2009. Influence of plant silicon and sugarcane cultivar on mandibular wear in the stalk borer *Eldana saccharina.* Agriculture and Forest Entomology, 11: 301-306.
13. Meena, R. S., O. P. Ameta and B. L. Meena. 2013. Population Dynamics Of Sucking Pests And Their Correlation With Weather Parameters In Chilli, Capsicum Annum L. Crop. The Bioscan., 8(1): 177 – 180.
14. Mourad L S, Salama and Ayoub. 2008. Insecticidal effect of Chrysanthemum coronarium L. flowers on the pest *Spodoptera littoralis* Boisd and its parasitoid *Microplitis rufiventris* Kok. with identifying the chemical composition. Journal of Applied Sciences, 8: 1859-1866.
15. Murugan, M. 2003. Role of induced resistance in the management of major insect pests of tomato (*Lycoporsicon esculentum* Mill.) and okra (*Abelmoschus esculentus* L.) Moench). Ph.D. Thesis, Tamil Nadu Agriculture University, Coimbtore, India. 302 pp.
16. Murugan, M., N. Dhandapani and M. Devanathan. 2005. Bottom up and top down effect of induced resistance in okra against insect pests. Annals of Plant Physiology, 19: 106-113.
17. Patnaik, H. P., 1998, Pheromone trap catches of *Spodoptera litura,* F. and extent of damage on hybrid tomato in Orissa. Reddy. P. P., N. K. K. Kumar and A. Varghese (Eds) Proc. I. Natl. Symp. On Advances in IPM. For Horticultural crops, Environmental implications and Thrusts, Bangalore Oct 15-17, 68-72.
18. Pareek, P. L. and M.C. Bhargava. 2003. Estimation of avoidable losses in vegetables caused by borers under semi arid condition of Rajasthan. Insect Environment, 9: 59-60.
19. Prakash, A., and Rao. 2003. Management of rice storage incest. CRRI, Technical Bulletin, 174 PP.
20. Puri, S. N. 1995. Present status of IPM in India. Proceeding of National Seminar on Integrated Pest Management in Agriculture, Nagpur, Maharashtra.
21. Qingwen Z., L. Ping, W. Gang and C. Qingnian. 1998. On the biochemical mechanism of induced resistance of cotton to cotton bollworm by cutting off young seedling at plumular axis. Acta Phytolacca Sinica, 25: 209–212.
22. Saad Moussa, Fatina baomy, Anil Sharma and Fathi eid el-adl. 2013. The Status of tomato leafminer; *Tuta absoluta* (Meyrick) (Lepidoptera: Gelechiidae) in Egypt and potential effective pesticides . Academic Journal of Entomology, 6 (3): 110-115.
23. Santos, M.C., A.M.R.Junqueira , J.C. Zauncio and J.E. Serrão . 2012. Efeito do silício em aspectos comportamentais e na história de vida de *Tutaabsoluta* (Meyrick) (Lepidoptera: Gelechiidae).Rev. Brasil. Agropec. Sust., 2: 76-88.
24. Selvanarayanan, V. 2000. Host plant resistance in tomato against fruit borer, *Helicoverpa armigera* (Hub.). M.Sc., (Ag) Thesis, Annamalai University, Annamalainagar, India.
25. Singh, R. K. and B. D. Chaudhary. 1979. Biometrical Methods in Quantitative Genetic Analysis. Kalyani Publ., New Dehli. 33 pp.

26. Tripathi, A. K., S. Upadhyaya, MantuBhuiyan and P. R .Bhattacharya. 2009. A review on pros pects of essentialoils as biopesticde in insect- pest management. Journal of Pharmovcologonosy and Phytrohteraphy, 1: 52-63.

Table 1. Effect of Organic Source of Silica, Rhizobacteria, Flower Extracts, PGR and Essential Oils Against Pin Worm, Leaf Miner, *Tuta absoluta* in Tomato in Field Experiment

S.No	Treatments	*Tuta absoluta* – (Number of larvae/ plant)*								% reduction over control
		Pre count	Vegetative stage		Flowering stage		Fruiting and ripening stage			Grand mean
			30 DAT	37 DAT	44 DAT	59 DAT	74 DAT	89 DAT	104 DAT	
T_1	RHA 1t + SSB + CFE 2% thrice	2.57	2.46 (1.57)^{ed}	2.27 (1.51)^{cd}	3.35 (1.83)^{f}	3.08 (1.75)^{f}	3.86 (1.96)^{i}	3.21 (1.79)^{e}	4.28 (2.07)^{f}	3.22 (1.79)^{e}	39.11
T_2	RHA 2t + SSB +CFE 2% thrice	3.42	3.04 (1.74)^{e}	2.88 (1.70)^{f}	3.57 (1.89)^{f}	2.99 (1.73)^{f}	3.01 (1.73)^{g}	3.43 (1.85)^{f}	4.44 (2.11)^{f}	3.34 (1.83)^{e}	36.81
T_3	PF+ Azophos+ CFE 2% thrice	2.62	2.41 (1.55)^{bc}	2.36 (1.54)^{d}	4.73 (2.17)^{g}	3.54 (1.88)^{g}	3.66 (1.91)^{hi}	4.12 (2.03)^{g}	4.57 (2.14)^{f}	3.63 (1.90)^{f}	31.32
T_4	RHA1t + SSB+ CFE 2% thrice + NAA/GA_3+ LO+ RO 0.2%	2.41	2.02 (1.42)^{a}	1.93 (1.39)^{a}	1.76 (1.33)^{a}	1.47 (1.21)^{a}	1.04 (1.02)^{a}	0.98 (0.99)^{a}	0.56 (0.75)^{a}	1.39 (1.18)^{a}	73.60
T_5	RHA2t + SSB+ CFE 2%thrice + NAA/GA_3+ LO+ RO 0.2%	3.45	2.99 (1.73)^{e}	2.54 (1.59)^{e}	2.16 (1.47)^{c}	1.78 (1.33)^{bc}	1.52 (1.23)^{cd}	1.46 (1.21)^{c}	0.88 (0.94)^{c}	1.90 (1.38)^{d}	63.94
T_6	PF+ Azophos+ CFE 2% thrice + NAA/GA_3+ LO+ RO 0.2%	2.87	2.56 (1.60)^{d}	2.37 (1.54)^{e}	2.22 (1.49)^{c}	1.85 (1.36)^{cd}	1.67 (1.29)^{e}	1.07 (1.03)^{a}	0.74 (0.86)^{b}	1.78 (1.34)^{d}	66.24
T_7	RHA 1t + SSB + LFE 2% thrice	2.57	2.47 (1.57)^{cd}	2.32 (1.52)^{d}	2.99 (1.73)^{e}	2.25 (1.50)^{e}	3.58 (1.89)^{h}	4.53 (2.13)^{h}	5.43 (2.33)^{g}	3.37 (1.83)^{ef}	36.25
T_8	RHA 2t + SSB + LFE 2% thrice	2.69	2.48 (1.57)^{cd}	2.27 (1.51)^{cd}	2.59 (1.61)^{d}	2.43 (1.56)^{e}	3.47 (1.86)^{h}	5.87 (2.42)^{j}	6.51 (2.55)^{h}	3.66 (1.91)^{g}	30.70
T_9	PF+ Azophos+ LFE 2%	2.65	2.51 (1.58)^{cd}	2.22 (1.49)^{cd}	3.56 (1.89)^{f}	2.99 (1.73)^{f}	3.47 (1.86)^{h}	4.93 (2.22)^{i}	5.64 (2.37)^{g}	3.62 (1.90)^{fg}	31.51
T_{10}	RHA1t+ SSB+ LFE 2% thrice + NAA/GA_3 + LO+ RO 0.2%	2.71	2.39 (1.55)^{b}	2.29 (1.51)^{cd}	2.07 (1.44)^{bc}	1.89 (1.37)^{cd}	1.59 (1.26)^{de}	1.33 (1.15)^{c}	1.03 (1.01)^{d}	1.80 (1.34)^{d}	65.95
T_{11}	RHA2t+ SSB+ LFE 2% thrice + NAA/GA_3 + LO+ RO 0.2%	2.53	2.31 (1.52)^{c}	2.15 (1.47)^{bc}	1.87 (1.37)^{a}	1.76 (1.33)^{bc}	1.42 (1.19)^{c}	1.24 (1.11)^{b}	0.93 (0.96)^{cd}	1.67 (1.29)^{c}	68.41
T_{12}	PF+ Azophos+ LFE 2% thrice + NAA/GA_3 + LO+ RO 0.2%	2.32	2.24 (1.50)^{b}	2.02 (1.42)^{ab}	1.91 (1.38)^{a}	1.64 (1.28)^{ab}	1.21 (1.10)^{b}	1.09 (1.04)^{a}	0.61 (0.78)^{a}	1.53 (1.24)^{b}	71.00
T_{13}	Standard check- Panchakavya 2%	2.51	2.35 (1.53)^{cd}	2.24 (1.50)^{cd}	2.08 (1.44)^{bc}	2.02 (1.42)^{d}	1.95 (1.40)^{f}	1.78 (1.33)^{d}	1.43 (1.20)^{e}	1.98 (1.41)^{d}	62.54
T_{14}	Untreated check	2.81	3.44 (1.85)^{f}	3.61 (1.90)^{g}	5.28 (2.30)^{h}	6.52 (2.55)^{h}	4.26 (2.06)^{j}	6.54 (2.56)^{k}	7.32 (2.71)^{i}	5.28 (2.30)^{h}	-
SEd		-	0.03	0.03	0.03	0.03	0.02	0.03	0.03	0.03	-
CD(0.05)		-	0.07	0.06	0.06	0.07	0.05	0.06	0.07	0.07	-

*Mean of two replications, First 3 sprays given at 7 days intervals, 30, 37, 44 DAT ; subsequent sprays were given at 15 days intervals, 59, 74, 89, 104 DAT Values in parentheses are square root transformation, In a column, mean followed by same letters are not significantly different at P=0.05 as per LSD

Table 2.Growth Stages of Tomato

S.No.	DAT	GROWTH STAGES
1.	1-40	Establishment and vegetative stage
2.	40-60	Flowering stage
3.	60-80	Fruiting stage
4.	80-100 & upto 120	Ripening and harvesting stage

Table 3 Spray Schedule

S.No	Organic sources	Spraying done on
1.	Flower extract	30 DAT, 37 DAT and 59 DAT
2.	PGR	44 DAT and 74 DAT
3.	Essential oil	89 DAT and 104 DAT

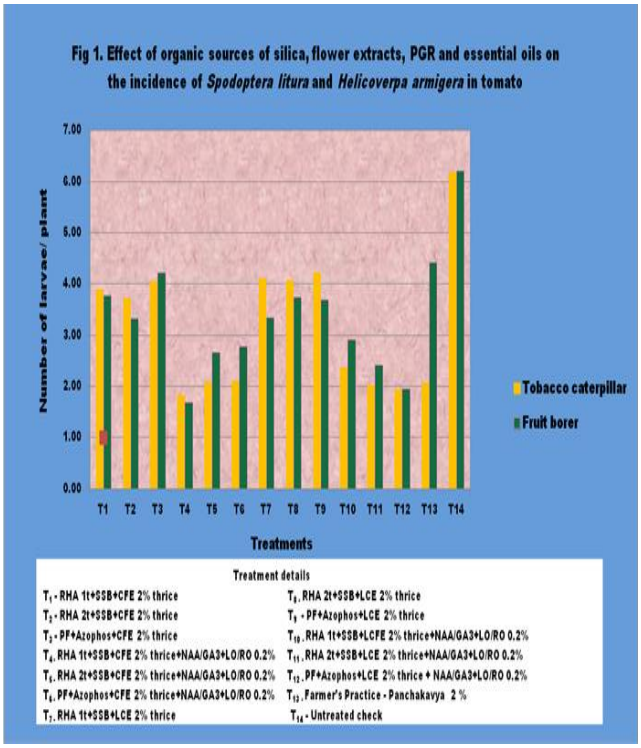

Figure 1 Effect of organic source of silica, flower extracts, PGR and essential oils on the incidences of *Spodoptera litura Helicoverpa armigera* in tomato

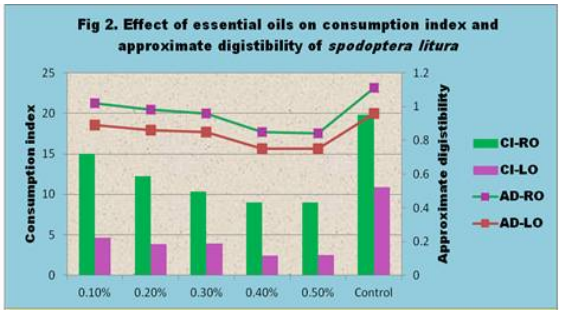

Figure 2 Effect of essential oils on Consumption index and approximate digistibillity of *Spodoptera litura*

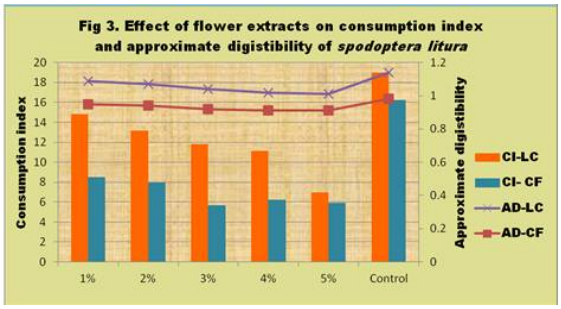

Figure 3 Effect of flower extracts on consumption index and approximate digistibillity of *Spodoptera litura*

Indian Journal of Natural Sciences www.tnsroindia.org.in ©IJONS

Vol.8 / Issue 49 / August /2018 *International Bimonthly* *ISSN: 0976 – 0997*

RESEARCH ARTICLE

Molecular identification and phylogenetic tree analysis of *Enterobius vermicularis* from Children in Wasit City of Iraq

Russul Wassit Kadhum*, Nawar Jaber Hussein Al–Asadi and May Naji Alkhanaq

Department of Biology, College of Science, Wasit University, Kut, Iraq.

Received: 24 Apr 2018 Revised: 22 May 2018 Accepted: 26 June 2018

*Address for correspondence
Russul Wassit Kadhum
Department of Biology,
College of Science,
Wasit University, Kut, Iraq.

ABSTRACT

This study was designed to molecular identification and studies the genetic characterization of *E. vermicularis* through polymerase-chain-reaction expansion, DNA sequencing which in view of the phylogenetic tree analysis of 18S ribosomal RNA gene in *E. vermicularis*. The PCR was performed by using specific PCR primers that designed in this study using NCBI-Gen-bank (HQ646164.1) to amplified 667bp PCR product. The PCR results have shown 39 (78%) positive stool samples out of 50 stool samples. The negative samples were 11 (22%) out of 50 stool samples. The multiple sequence alignment analysis and neighbor joining phylogenetic tree analysis (MEGA 6.0 version). The analysis revealed that local Enterobius vermicularis isolates IQ-K1 into IQ-K5 were show different and less related to NCBI-Blast *E. vermicularis* isolate from different countries that show different and out of tree. Our isolated were deposited in NCBI-GenBank. This study represents the explained the highly specific and sensitive molecular detection method and is considered the first report which used the molecular phylogeny *E. vermicularis* in wasit province, Iraq.

Keywords: - Molecular identification, phylogenetic tree, *Enterobius vermicularis*.

INTRODUCTION

Albeit most parasitic irresistible sicknesses have vanished in created nations, enterobiasis (pinworm disease) has still frequently been accounted for in numerous created nations (1– 3), which is the most widely recognized intestinal parasites in created nations in mild atmospheres (4). People are the main characteristic of *E.vermicularis*, and kids which regularly influenced through infection, which is spread from the rear-end to mouth. Despite the fact that it is viewed as a safe contamination, serious illness such as "colitis, perianal boil, ectopic diseases" in femals, and an infected appendix can happen (4, 5, 6). While destruction is accomplished by anthelmintics much of the time, repetitive or diligent oxyuriasis going on for quite a long time regardless of a few treatment courses is found in a few

patients (6). Intestinal disease is transmitted by direct contact with contaminated persons (or with eggs) or questions. E. vermicularis transmission occurs by eating irresistible pinch eggs. The eggs move from the back to the fingers, nails, or hands when someone scratches an area around the anus where female worms attract and store eggs. Eggs are spread in clothing and night clothes and move more into different materials including feeding, books, work areas and seats (7). At this point, when asked questions, eggs can enter the mouths and nose of another person, in this way they are addressed (7,8). Because of this move procedure, the proximity of young people and their theories, for example, thumb sucking, overcrowded conditions and lack of sanitation, increases the prevalence of intestinal disease in primary schools, where close contact occurs between children (9,10,11). Drugs against *E. Vermiculares*, for example, Albindazole, are exceptionally strong in the treatment of intestinal disease (6). However, the injury again is normal, regardless of treatment, because pharmaceuticals only work on the execution of mature worm, but not small worms (7). The critical angle of disappointment in one-size-fits-all chemotherapy is an irresistible approach to the Earth, which encourages rapid return of infection. In this way, people with gastrointestinal disease need revised measurements of pharmaceuticals to cover the time it takes for eggs to end up with bloated worms. Semi-atomic devices can understand transmission cycles and recognize their stability from reconstituted diseases. However, the order of data on E. vermicularis is restricted (12, 13). Hence, the study was conducted to molecular detect the probable presence of *E. vermicularis* among the children and the most phylogeny obtained in Wasit, province, Iraq.

MATERIALS AND METHODS

Samples Collections

50 stool samples have been collected from patients with clinical symptoms for enterobiasis in Wasit hospital, Iraq. 10 gm of sample was placed to a clean, dry plastic container and transported to the laboratory for analysis.

Flotation Method

The flotation method was done by using sheather's solution, 5gm feces samples were mixed with small amounts (10ml) of D.W. Than feces mixture was filtered by using sieve (40 ange) to discarded from large particles. After that, filtrates were collected in sterile plastic tubes and placed in centrifuge at.1000.rpm for 3 minutes. The supernatant was disposed of and small amount off sheather's solution was added into precipitate and mixed well by using wood sticks. After that placed in centrifuge at 1000 rpm for 2 minutes. Plastic tests tubes were place on holder and stand vertical and drops of sheather's solution were added by pipette until fill the tubes. Than glass cover slide was placed on up end of tubes for 2-5 minutes. The glass cover slide was lifted carefully and placed under at (10X, 40X, and 100X) Magnification power under microscope to observe the Eimeria oocyst.

Stool DNA Extraction

DNA was removed of excrement tests by utilizing (Stool DNA extraction Kit, Bioneer. Korea). The extraction was finished by organization guidelines by utilizing stool lysis convention technique with Proteinase K (14). From that point forward, the separated gDNA was checked by Nanodrop spectrophotometer, and after that put away at - 20C at icebox until utilized as a part of PCR intensification.

Polymerase Chain Reaction (PCR)

The PCR technique was performed for detection and identification of *E. vermicularis*. The PCR examine was done by utilizing particular groundworks inner translated spacer 1 (ITS-1) region of 18S ribosomal RNA gene in Enterobius vermicularis (15). Primers were designed by using NCBI-Gen-bank data base (HQ646164.1) (Bioneer-Company-Korea) (Table-1).

The PCR ace blend was set up bu utilizing (AccuPower® PCR PreMix kit. Bioneer. Korea). The PCR premix tube contains solidify dried pellet of (Taq DNA polymerase 1U, dNTPs 250µM, Tris-HCl (pH 9.0) 10mM, KCl 30mM, MgCl2 1.5mM, stabilizer, and tracking dye) and the PCR ace blend response was set up as indicated by pack directions in 20 ul aggregate volume by included 5 ul of decontaminated genomic DNA and 1.5 ul of 10 pmole of forward preliminary and 1.5 ul of 10 pmole of invert groundwork, at that point finish the PCR premix tube by deionizer PCR water into 20 ul and quickly blended by exispin vortex rotator (Bioneer. Korea).

The response done in a thermos-cycler by set up the accompanying thermos-cycler conditions; beginning denaturation temperature of95°C for 5min; trailed by30cycles at denaturation95°Cfor30.sec., toughening58°Cfor30sec., and expansion72°C for30 s. and after that last augmentation at72°C for5 min. The PCR items were analyzed by electrophoresis in a 1 % agarose gel, recolored with ethidium bromide, and envisioned under UV-transilluminator.

DNA Sequencer Method

DNA sequencing method was performed to study the genetic characterization relationship between local E. pyrimicularis isolates and NCBI was introduced by Enterobius vermuscalate isolates in the eyes of the 18S ribosome RNA gene. Using a tree-tree analysis. Small rRNA gene. A PCR product of agarose gel was purified using EZ-10 Spin Column DNA Extraction Kit, Biobasic. Samples of a purified ribosome RNA 18R RNA product were sent to Korea's Macrogen Company to perform DNA sequencing using the ribosome RNA 18S primer by DNA sequence (AB DNA sequence). The examination was carried out in light of the verification of interference identified by NCBI-Blast and the search for the Hungarian tree (Mega version 6).

Statistical Analysis

The measurable investigation done through SAS (Statistical Analysis System – version.9.1) (16).

RESULT

Polymerase Chain Reaction (PCR)

The PCR was made in a total of50 stool samples, the results were 39 (78 %) stool samples were positive, where 19 (22 %) were negative for *E. vermicularis*. The Polymerase-Chain-Reaction test technique were in view of exposure off 18S ribosomal RNA gene for detect of *E. vermicularis* which which showed the size of demonstrative sections of PCR items that was (667 bp), Table (3), Figure (1).

DNA Sequencing Results

Multiple sequence alignment analysis of the partial small-subunit rRNA gene sequence in local *E. vermicularis* isolates IQ-K1 into IQ-K5 based ClustalW alignment analysis through (MEGA 6.0, multiple alignment analysis tools). That demonstrate the different arrangement investigation closeness (*) and differences in 18S rRNA gene nucleotide sequences (Figure 2).

Phylogenetic tree analysis in view of the 18S rRNA quality fractional grouping that utilized for evaluation of genetic relationship between local *E. vermicularis* and NCBI-BLAST isolates. The evolutionary way were calculated through the possible composition maximum method by the reproductive tree UPGMA method (MEGA 6.0 version). The local *E. vermicular* is isolates IQ-K1 into IQ-K5 were show not related to NCBI-Blast *E. vermicular* is isolate from different countries that show different and out of tree (Figure 3).

DISCUSSION

Molecular techniques like PCR analysis have been developed to improve the detection of pathogens in both human and veterinary medicine. PCR-based testing is now advocated as an adjunct to traditional health-monitoring programs (17, 18), which are not easily transmitted to sentinels by soiled bedding (19,20,21). For some agents, PCR testing can be more sensitive than traditional methods used to survey pathogens in sentinels. Like any other large-scale diagnostic methodology, PCR assays are subject to false-positive and -negative results. As such, any outcomes must be deciphered mindfully with a general comprehension of the PCR method, the inborn controls, and every other variable that may influence comes about including groundwork plan and specificity and additionally control and handling of the example in the home office, amid transport, and at the reference research center (22).

Validating a PCR assay for diagnostic purposes is challenging (23) in both human and veterinary medicine. The first step is to design primers by computer modeling to optimize PCR conditions, specificity, and sensitivity. Diagnostic laboratories typically use primers that target ubiquitous housekeeping genes or ribosomal RNA common to several species to identify pathogens at the genus level, whereas primers complimentary to specific elements within the genome are used for organism speciation. The specificity of the chosen primers must then be compared with all available sequences in genome databases, such as Gen-bank (22). The 18S quality is by and large found an eukaryotes. As is notable, the 18S-rDNA district isn't appropriate for phylogenetic examination as it opens up a very monitored area (24). For our situation, the PCR test focused on an area of the 28S rRNA quality normal, our opened up section secured a large portion of the 5′ half of the 18S quality, where much arrangement inconstancy has a tendency discovered, considered a helpful district for the DNA-barcoding approach. Results from this case report suggest that the PCR assay was not specific despite the stringent validation performed by the first reference laboratory.

One possible explanation is that the databases used to design the primers were flawed or incomplete at the time of the validation process. Indeed, genome databases such as Gen-bankare known to contain unverified, incomplete, and inaccurate sequences (25), as well as entries from genetically different organisms under the same species name (26). In addition, large numbers of microorganisms are discovered every year and are classified phylogenetically according to the genome sequence. The nematode phylum is especially rich in species and is biologically diverse, with plant and animal parasites as well as free-living organisms (22).

The examination has demonstrated the nearness of *E. vermicularis* in Wasit, whereas 39 (78 %) stool samples were positive out of 50 stool samples by PCR. Our result is agreeing with (27) which showed that *E. vermicularis* obtained in 20 (54 %) samples out of 37 by PCR and also agree with (28, 29) which observed the maximum number of the sick individuals founded in the Warmia-Masuria province, enterobiasis was diagnosed in children under 7 years of age (preschoolers), 36.7%orphans and in 30.6 %of7-year-old children. Our observation is also in comfort with (30, 31, 32, 33, 34) which found the *E. vermicularis* infections rate ranges from7.3% (Greece) to28% (Sweden) in examinedchildren populations. The local *E vermicular* IQ-K1 to IQ-K5 isolated were show not related to NCBI-Blast this consider is the first obtained in Wasit, Iraq. Our result was in agreement with (35, 36), which found a new haplotype of E. vermicularis unregistered in Gen- Bank, was detected.

CONCLUSION

PCR is considered as an alternative tool in epidemiological studies and the diagnosis of *E. vermicularis.* The results showed that the local *E. vermicularis* isolates IQ-K1 into IQ-K5 were show not related to NCBI-Blast *E. vermicularis* isolate from different countries.

ACKNOWLEDGEMENT

Authors sincerely wish to acknowledge the members of the Laboratory of the College of Science, Wasit University for supporting.

REFERENCES

1. Degerli S, Malatyali E, Ozcelik S, Celiksoz A. (2009). Enterobiosis in Sivas, Turkey from past to present, effects on primary school children and potential risk factors. Turkiye Parazitol Derg 33: 95–100.
2. Kang IS, Kim DH, An HG, Son HM, Cho MK, et al. (2012) Impact of health education on the prevalence of enterobiasis in Korean preschool students. Acta Trop 122: 59–63.
3. Bager P, Vinkel Hansen A, Wohlfahrt J, Melbye M .(2012). Helminth infection does not reduce risk for chronic inflammatory disease in a population-based cohort study. Gastroenterology 142: 55–62.
4. Ariyarathenam et al. (2010). *Enterobius vermicularis* infestation of the appendix and management at the time of laparoscopic appendectomy: case series and literature review. Int. J. Surg. 8:466–469.
5. Craggs B et al. (2009). *Enterobius vermicularis* infection with tuboovarian abscess and peritonitis occuring during pregnancy. Surg. Infect. 10:545–547.
6. Georgiev V. (2001). Chemotherapy of enterobiasis (oxyuriasis). Expert Opin. Pharmacother. 2:267–275.
7. Roberts LS, Schmidt GD, Janovy J. (2009). Foundations of parasitology. Boston: McGraw-Hill Higher Education. xvii, 701 p.
8. Cook GC. (1994). Enterobius vermicularis infection. Gut 35: 1159–1162.
9. Kang IS, Kim DH, An HG, Son HM, Cho MK, et al. (2012). Impact of health education on the prevalence of enterobiasis in Korean preschool students. Acta Trop 122: 59–63.
10. Song HJ, Cho CH, Kim JS, Choi MH, Hong ST. (2003). Prevalence and risk factors for enterobiasis among preschool children in a metropolitan city in Korea. Parasitol Res 91: 46–50.
11. Kim DH, Son HM, Kim JY, Cho MK, Park MK, et al. (2010). Parents'knowledge about enterobiasis might be one of the most important risk factors for enterobiasis in children. Korean J Parasitol 48: 121–126.
12. In˜iguez, A. M., A. C. Vicente, A. Arau´j, L. F. Ferreira, and K. J. Reinhard. 2002. *Enterobius vermicularis*: specific detection by amplification of an internal region of 5S ribosomal RNA intergenic spacer and *trans*-splicing leader RNA analysis. *E. vermicularis*: specific detection by PCR and SL1 RNA analysis. Exp. Parasitol. 102:218–222.
13. Kang S, et al. (2009). The mitochondrial genome sequence of *Enterobius vermicularis* (Nematoda: Oxyurida)–an idiosyncratic gene order and phylogenetic information for chromadorean nematodes. Gene 429:87–97.
14. Haque R, Ali IKM, Akther S, Petri WA. (1998). Comparison of PCR, isoenzyme analysis and antigen detection for diagnosis of Entamoeba histolytica infection. Journal of Clinical Microbiology. 36: 449-452.
15. Ulrike E. Z, Ralf B and Michael W. (2011). Molecular Phylogenetic Analysis of *Enterobius vermicularis* and Development of an 18S Ribosomal DNA-Targeted Diagnostic PCR. Journal of clinical microbiology. p. 1602–1604
16. SAS. SAS/STAT Users Guide for Personal Computer. Release 9.13.SAS Institute, Inc., Cary, N.C., USA.2010
17. Artwohl JE, Cera LM, Wright MF, Medina LV, Kim LJ. (1994). The efficacy of a dirty-bedding sentinel system for detecting Sendai virus infection in mice: a comparison of clinical signs and seroconversion. Lab AnimSci 44:73–75.
18. Dillehay DL, Lehner ND, Huerkamp MJ. (1990). The effectiveness of a microisolator cage system and sentinel mice for controlling and detecting MHV and Sendai virus infections. Lab Anim Sci 40:367–370.
19. Jensen ES, Allen KP, Henderson KS, Szabo A, Thulin JD. (2013). PCR testing of a ventilated caging system to detect murine fur mites. J Am Assoc Lab Anim Sci 52:28–33.
20. Macy JD, Paturzo FX, Goodrich LJB, Compton SR. (2009). A PCRbased strategy for detection of mouse parvovirus. J Am Assoc Lab Anim Sci 48:263–267.
21. Shek WR. (2008). Role of housing modalities on management and surveillance strategies for adventitious agents of rodents. ILAR J 49:316–325.

22. Mathias L, Kristina B, Sandy G, Brandon B, and Jon D R. (2014). False-Positive Results after Environmental Pinworm PCR Testing due to Rhabditid Nematodes in Corncob Bedding Vol 53, No 6 November 2014 Pages 717–724 Journal of the American Association for Laboratory Animal Science.
23. Dieffenbach CW, Lowe TM, Dveksler GS. (1993). General concepts for PCR primer design. PCR Methods Appl3:S30–S37.
24. Floyd RMA, Rogers D, Lambshead JD, Smith CR. (2005). Nematode specific PCR primers for the 18S small subunit rRNA gene. Mol Ecol Notes 5:611–612
25. Clarridge JE. (2004). Impact of 16S rRNA gene sequence analysis for identification of bacteria on clinical microbiology and infectious diseases. Clin Microbiol Rev 17:840–862.
26. Clayton RA, Sutton G, Hinkle PS, Bult C, Fields C. (1995). Intraspecific variation in small-subunit rRNA sequences in GenBank: why single sequences may not adequately represent prokaryotic taxa. Int J Syst Bacteriol 45:595–599
27. Ulrike E, Zelck R and Michael W. (2011). Molecular Phylogenetic Analysis of Enterobius vermicularis and Development of an 18S Ribosomal DNA-Targeted Diagnostic Pcr Journal of Clinical Microbiology. p. 1602–1604.
28. Kubiak K, Wrońska M, Dzika E, Dziedziech M, Poźniak H, Leokajtis M. Dzisko J. (2015). The prevalence of intestinal parasites in children in preschools and orphanages in the Warmia-Masuria province (North-Eastern Poland). Przegl. Epidemiol. 69: 483 – 488, 601 – 604.
29. Bitkowska E, Wnukowska N, Wojtyniak B, Dzbeński T H. (2004). The occurrence of intestinal parasites among children attending fi rst classes of the elementary schools in poland in the school year 2002/2003. Przegl. Epidemiol. 58: 295 – 302 (In Polish)
30. Patsantara G G, Piperaki E T, Tzoumaka-Bakoula C, Kanariou M G. (2015). Immune responses in children infected with the pinworm Enterobius vermicularis in central Greece. J. Helminthol.
31. Değerli S, Malatyali E, Ozçelik S, Celiksöz A. (2009): Enterobiosis in Sivas, Turkey from past to present, effects on primary school children and potential risk factors. Turkiye Parazitol. Derg. 33: 95 – 100
32. Kang S, Jeon H K, Eom KS, Park JK. (2006). Egg positive rate of Enterobius vermicularis among preschool children in Cheongju, Unauthenticated Download Date | 3/29/18 10:12 PM 291 Chungcheongbuk-do, Korea. Korean J. Parasitol. 44: 247 – 249.
33. Bøås H, Tapia G, Sødahl J, Rasmussen T, Rønningen K. (2012). Enterobius vermicularis and risk factors in healthy Norwegian children. Pediatr. Infect. Dis. J. 31: 927 – 930.
34. Remm M. (2006). Distribution of enterobiasis among nursery school children in SE Estonia and of other helminthiases in Estonia. Parasitol. Res. 99: 729 – 736.
35. Ferrero M R, Röser D, Nielsen H V, Olsen A, Nejsum P. (2013). Genetic variation in mitochondrial DNA among Enterobius vermicularis in Denmark. Parasitology, 140: 109 – 114.
36. Kang S, Sultana T, Eom K S, Park Y C, Soonthornpong N, Nadler S A, Park J K. (2009). The mitochondrial genome sequence of Enterobius vermicularis (Nematoda: Oxyurida) – An idiosyncratic gene order and phylogenetic information for chromadore an nematodes. Gene, 429(1 – 2): 87 – 97. DOI: 10.1016/j. gene.2008.09.011.

Table 1. The List of Primers

Primers	Sequence ofthe Primers		PCR product size
18SrRNA	F	GGCCGTTCTTAGTTGGTGGA	667 bp
	R	ATAGAAGCCATACGTGCCCTT	

Table 2. The Compound of PCR Master Mix in PCR Run

PCR-master mix	Volume
DNA-template	5µl
Entamoeba sp. Forward-primer (10pmol)	1.5µl
Entamoeba sp. Reverse-primer (10pmol)	1.5µl
PCR-water	12µl
Total	20µl

Table 3: The Thermocycler-Conditions Cycles

PCR-step	Temperature	Time	Repeat cycle
Initial-Denaturation	95-°C	5-m	1
Denaturation	95-°C	30-s	30
Annealing	58-°C	30-s	
Extension	72-°C	1-m	
Final Extension	72-°C	5-m	

Table 4: The Results of PCR (Polymerase Chain Reaction)

Result	Samples	Percentage %
Positive	39	78 %
Negative	19	22 %
Total	50	100 %

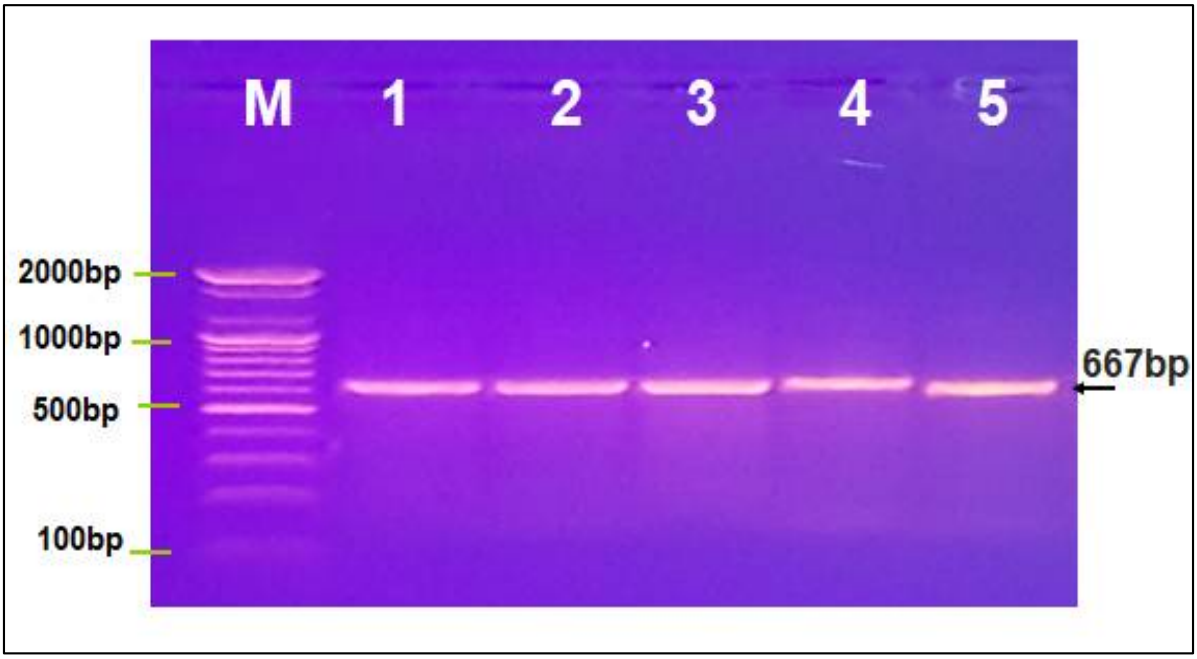

Figure1: Agarose-gel-electrophoresis photo shown the PCR-product off 18S rRNA gene that using to exposure *E. vermicularis*. Where (M) Marker (100-2000 bp), lane (1-5) some positive *E. vermicularis* stool samplse that send to DNA sequencing technique at 667bp PCR product size.

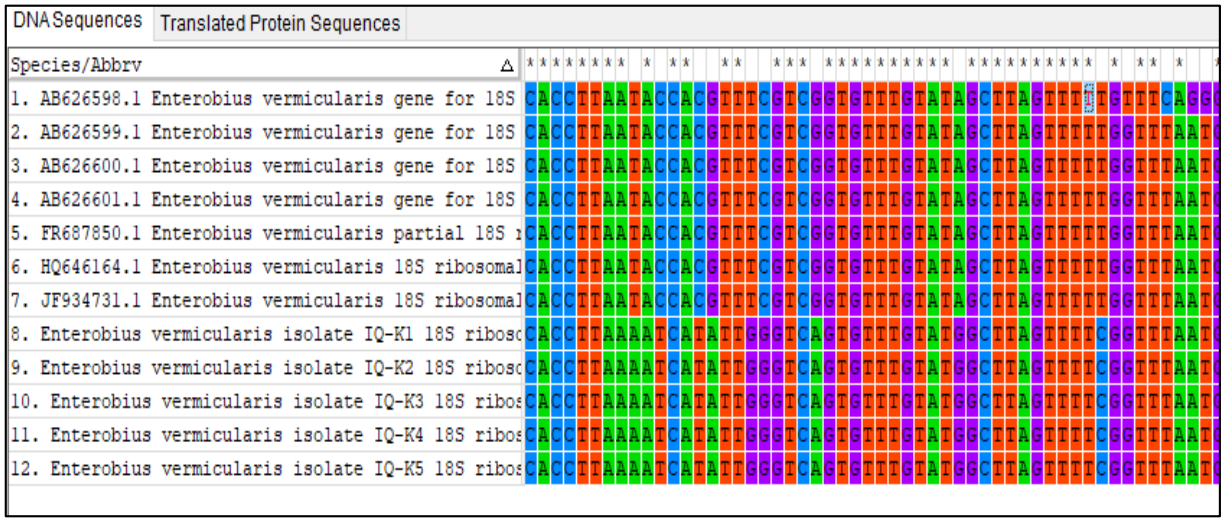

Figure 2: The DNA Sequencing Results

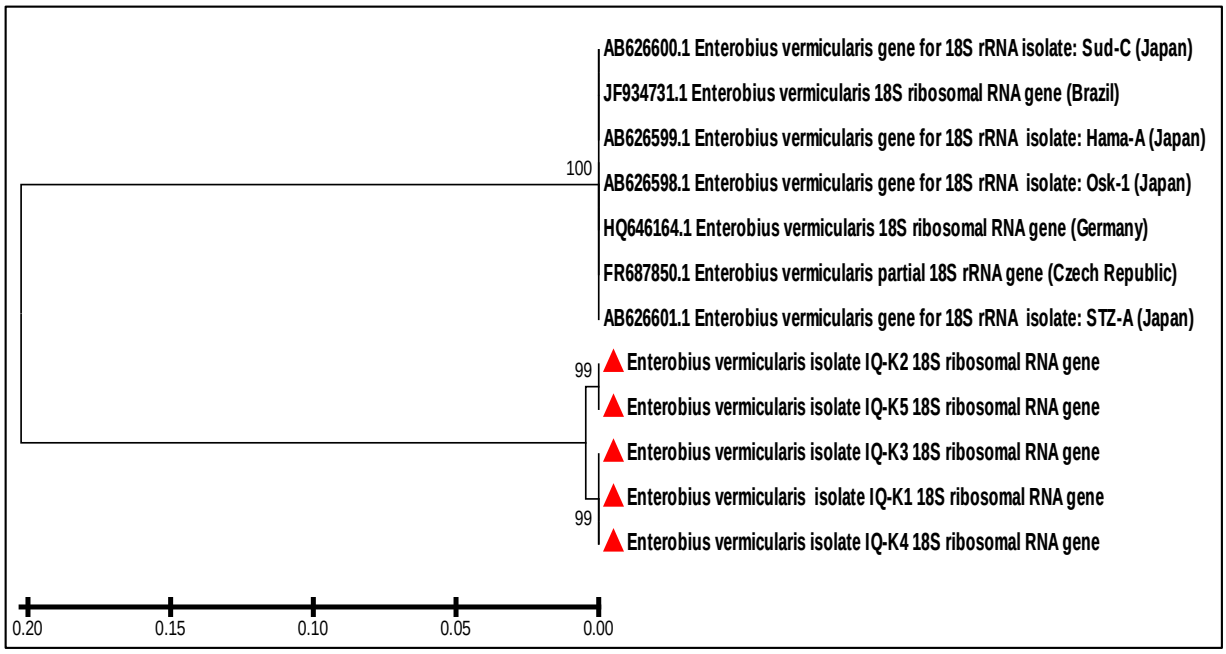

Figure 3: The Phylogenetic Tree Analysis

Indian Journal of Natural Sciences www.tnsroindia.org.in ©IJONS

Vol.8 / Issue 49 / August /2018 *International Bimonthly* *ISSN: 0976 – 0997*

RESEARCH ARTICLE

Anti-Bacterial Evaluation of Biocomposite Coated Dental Implant after Immersion in Glycopeptide

Hanan Khalaf [1]*, Basima Hussien [2] and Thair L ALzubaidi [3]

[1] ,[2]Department of Prosthodontics, College of Dentistry, University of Baghdad, Iraq.
[3] Department of Accelerators, Directorate of Research & Nuclear Applications, Iraqi Atomic Energy Commission IAEC, Baghdad, Iraq.

Received: 29 Apr 2018 Revised: 27 May 2018 Accepted: 28 June 2018

*Address for correspondence
Hanan Khalaf
Department of Prosthodontics,
College of Dentistry,
University of Baghdad, Iraq.
E-mail: hanan6851@yahoo.com

ABSTRACT

Prevention of surgical local infections at an early stage of implantation is greatly required for the success of implants in dentistry and orthopedics. A unique method to prevent bacterial infections is the local employment of antibacterial agents. Therefore, a great focusing on antimicrobial peptide (AMP) coatings on implant was directed to this project. The aim of this study is to evaluate the antibacterial effectiveness of Niobium oxide (Nb2O5) \polyethylene glycol (PEG 3500) biocomposite coating after immersion in the antimicrobial peptide (glycol peptide vancomycin) against bacteria involved in surgical infections of the dental implant (*S.aureus* and *E.coli*).Nb2O5\ PEG biocomposite coating was deposited on the surfaces of CPTi discs, using an RF magnetron sputtering method. Surface roughness was assessed using atomic force microscope. Antibacterial activity against *S.aureus* and *E.coli* was assessed in vitro using minimum inhibitory concentration (MIC) and agar disc diffusion tests. RF magnetron sputtering produced rough biocompatible coatings on titanium substrate. The collected data were analyzed with ANOVA test ($p< 0.05$). Biocomposite coating after immersion in the antimicrobial peptide (glycopeptide: vancomycin) reduced the growth of all examined bacterial in comparison to the unimmersed samples (control sample) after three incubation intervals (24,48and 72h) . AMP was effective against the bacterial pathogens tested *(S.aureus and E.coli*) at (2% and 6%) concentrations.

Key Words: Poly Ethylene Glycol, Niobium Oxide, RF Magnetron Sputtering, Antimicrobial Peptide, Antibacterial Tests.

INTRODUCTION

Commercially pure titanium (CPTi) and titanium alloys have been applied for dental implant treatment due to their sufficient mechanical properties, low density, and biocompatibility. Infection and implant failure are considered major clinical problems. [25] The characters of implant surface influenced the response of the bone enclosing it. The rough surface implant as found -by Beagle's histological observations on dogs- demonstrated that osseointegration can be obtained in a 6-week period with rough surfaces. The topography of implant surfaces affects biological responses after implant insertion ranged from protein attachment to bone remodeling around the implant. These processes are enhanced by surface roughness permitting faster bone implant attachment and make insertion of the prosthesis within shorter time intervals.[16,17,26,27] Different methods of improving the surface roughness are applied such as plasma sputtering. The RF magnetron sputtering produced thin coatings with great purity having elemental composition is approximate to that of the sputtering target.

Thin films possess high adhesion to underlying substrates.[1,2,27] Osseointegration could be impaired by multiple factors including infection of implantation site. Bacterial colonization of dental implants can lead to inflammatory reactions which prevent osseointegration. The major pathogens caused surgical infection and bone resorption are Gram-negative anaerobes and Gram+ positive aerobes. Staphylococcus constitutes two-thirds of all pathogens in implant infections and they are the main causative pathogen of bone infection (osteomyelitis), which lead to destruction of bone and of osseointegration. [28]. The causative pathogens for surgical infection come from the patient's endogenous flora. The most common organisms isolated from surgical infection are *Staphylococcus aureus*, coagulase-negative staphylococci, Enterococcus spp. and *Escherichia coli*. Various patient-related and procedure-related factors affect the degree of surgical site infection.[26] Different methods to reduce infection have been introduced like production of bioactive surfaces that either kill bacteria or inhibit their adhesion to implant surfaces thus create aseptic implantation site and promote bone healing and reduce dental implant failure. [28, 29]

Poly (ethylene-glycol) (PEG) is widely applied in drug delivery. It is the most commonly used protective coating material for drug delivery and is covalently bound to proteins and has also been applied as a carrier for hydrophobic drug molecules to enhance their aqueous solubility or dissolution characteristics .[30] cationic antimicrobial peptides (AMPs) have been examined in the last decades. It has been shown that different AMPs exhibit great antimicrobial efficiency against both Gram-positive and Gram-negative bacteria. [11, 12]

MATERIALS AND METHODS

Sample Preparation

Circular discs (6 mm diameter and 5 mm thickness) were prepared from CPTi grade 2 (Orotig Srl , company Italy) Each CPTi disc was grinded with silicon carbide paper started from 400 , 1200 and 2300 grits grain size using a rotative grinding and polishing machine at 250 rotations per minute (rpm) for 2 minutes. The specimens were cleaned ultrasonically in ethanol and deionized water for 20 min. at 25°C to obtain smooth mirror surface ,then the discs were washed with water and dried in an oven at 100°C for 15 minutes and stored in a desiccator. Five discs were prepared for each experimental group (n=5).

Preparation of Niobium Oxide, Polyethylene Glycol Composite Target

Biocomposite target (Nb2O5 \ PEG compound) was prepared by mixing Nb2O5 with PEG powders in proportion of 70 wt.% Nb2O5 and 30 wt.% PEG powder in electric mixer for 3 hours , then the selected weight of mixture (20 g) was mixed with 20ml of distilled water in hot stirrer for 3 hours at 70° C , the homogenous mixture was dried in oven

at 60°C for 24 hours , then the mixture was molded in stainless steel mold (50 mm diameter, 3mm thickness) under 8 tons pressure for 2 minutes to obtain the composite target .

RF Magnetron Sputtering

Radio frequency sputtering was performed in a vertical chamber under the following conditions (power= 50 w. , pressure \ p1 = 4.9 × 10^{-4} torr , p2 = 1.8 × 10^{-2} torr, temperature =40 °C , distance = 10 cm , time = 3 hours) to obtain Nb2O5 \ PEG biocomposite coating, figure 1. Atomic force microscopy (AFM) was performed for investigation surface morphology and roughness of biocomposite coating deposited on the substrate. This analysis provides high-resolution 3D data of the Nb2O5 \PEG biocomposite coated surface.

Bacteriological Tests

Minimum Inhibitory Concentration (MIC test)

MIC test was applied to evaluate the antibacterial effect of tested agents (PEG and AMP) against Gram +ve bacteria (*Staphylococcus aureus*) and Gram-ve *bacteria* (*Escherichia coli*)**.**
MIC test involves the following procedures

Preparation of McFarland Standard

A 0.5 McFarland standard is prepared by mixing 0.05 mL of 1.175% barium chloride dihydrate (BaCl2•2H2O) with 9.95 mL of 1% sulfuric acid (H2SO4), the standard was kept in sterile screw cap tubes and used to adjust the turbidity of bacterial suspensions .[6]

Preparation of Nutrient Broth

Nutrient broth (HIMEDIA) was prepared by dissolving 13 grams of the medium in one liter of distilled water according to manufacturer instructions. The medium was dispensed into clean containers and sterilized in autoclave at 121°C and 15 pounds \ $inch^2$ for 15 minutes. [24]

Bacterial activation

Single colony was carried with sterile loop and transferred to nutrient broth and incubated at 37 °C for 24 hrs. With a sterile loop, the activated bacteria were cultured by streaking on nutrient agar and incubated at 37° C for 24 hrs. to promote bacterial growth.

Preparation of Bacterial Suspension

A loop full from activated bacteria are carried with a sterile loop and transferred to normal saline, the suspension turbidity was adjusted to be equal to that of a 0.5 McFarland standard and to perform MIC test, the turbidity was adjusted visually and by Spectrophotometer. [10]

Preparation of Mueller-Hinton Broth

21 grams of medium (HIMEDIA) was suspended in one liter of distilled water according to manufacturer instructions. The medium was dispensed into clean containers and sterilized in autoclave at 121°C and 15 pounds \ inch^2 15 minutes .This medium used for MIC test.

Preparation of Positive and Negative Controls

Positive and negative controls were prepared for comparison with a minimum inhibitory concentration of tested agents. Positive control represented by adjusted bacterial growth in Mueller-Hinton broth and the negative control represented by Mueller-Hinton broth without bacteria, figure 2.

Preparation of Stock Solution of Antimicrobial Glycol Peptide (vancomycin)

Percentage concentration was applied to prepare ten concentrations of AMP**.** In this method, the amount of the solute (AMP) is expressed in grams per 100 ml of the solution. Thus, a 10 % solution of AMP means 10 grams of AMP powder is dissolved in 100 ml of water.

$$\% (W \setminus V) = \frac{\text{Mass solute (g)}}{\text{Volume solution (ml)}} \times 100$$

MIC procedure involves serial dilutions of AMP from (10% -1%) , 9% concentration was prepared by adding 9 ml of stock solution of AMP to 1 ml of Mueller-Hinton broth. Dilutions were preceded till 1% by addition of 1 ml of stock solution of AMP to 9 ml of Mueller-Hinton broth to reach the final volume V2 which is equal to ten milliliter, this dilution was performed by applying the following equation: [31]

C1 V1 = C2 V2

V1: volume of stock solution
V2: final volume after dilution
C1: initial concentration of stock solution
C2: concentration of dilute sample
After that 1% (0.1 ml) of bacterial suspension was added to each tube contain the media with identified concentration of AMP, the tubes were incubated at 37 °C to evaluate the minimum inhibition concentration (MIC) against *S.areus* and *E.coli* .

Preparation of Stock Solution of Poly Ethylene Glycol (PEG)

100 g of PEG was weighed and dissolved in 100 ml of distilled water (w \ v %) using hot magnetic stirrer for 10 minutes till all particles are completely dissolved to obtain homogenous stock solution (100%). MIC procedure started with preparation of 10 serial dilutions having concentrations of 100% -10 %, 90 ml of stock solution of PEG was added to 10 ml of mueller- hinton broth to obtain 90% concentration and continue the dilution till reach the final concentration of 10% by applying the following formula:[31] **C1 V1 = C2 V2** After that 1% of bacterial suspension was transferred to each tube contained the media with identified concentration of PEG, the tubes were incubated at 37 °C to evaluate the minimum inhibition concentration (MIC) against *S.areus* and *E.coli*

Agar diffusion test (Kerby- Bauer test)

This test was performed to assess the antibacterial effect of AMP against *S. aureus* and *E.coli* .Mueller-Hinton agar was prepared by suspension of 38 grams of media in one liter of distilled water according to manufacturer instructions. The activated bacteria were inoculated on Mueller-Hinton agar separately by streaking method (Mat streaking) using sterile swab for even distribution of the bacteria, waiting for 5 minutes then the CPTi discs (biocomposite coated sample: with and without AMP immersion) are inserted within the prepared wells (6 mm diameter and 5 mm depth) on Mueller-Hinton agar by sterile cork borer and the petri dishes were incubated at 37° C for 24 hrs to promote bacterial growth. The diffusion of AMP from biocomposite coated discs was examined by measuring the inhibitory zone. After 24, 48 and 72 hrs incubation periods.

Statistical Analysis

Statistical analysis of the results was performed with Statistical Package for Social Sciences (SPSS); all data were analyzed as mean ± standard deviation. AVOVA test was used to detect the significant differences at ($p < 0.05$).

RESULT

It was appeared that RF magnetron sputtering increased surface roughness of the biocomposite film, the mean value of surface roughness was 298 nm as shown in figure 3.

Minimum Inhibitory Concentration (MIC test) of PEG 3500

MIC test exhibited no antibacterial activity regarding all concentrations of PEG (3500) against against *S.aureus* and *Ecoli* , all the tubes containing nutrient broth with activated bacteria and the tested concentrations of PEG (100%-10%) remained turbid indicated the existence of bacterial growth in comparison to negative control represented by Mueller-Hinton broth and positive control represented by bacterial growth, figure 4.100% polyethylene glycol exhibited non antibacterial activity against *Ecoli* and *S.aureus* on Mueller-Hinton agar , figure 5 .

Minimum Inhibitory Concentration of Antimicrobial Glycopeptide (AMP)

Following series of dilutions, an obvious antibacterial activity of AMP was observed against *S.areus* at concentration of 2%, while 6% concentration was effective in preventing *E.coli* growth, while the nutrient broth contained the lower concentrations remain turbid indicated the existence of bacterial growth in comparison to negative control represented by Mueller-Hinton agar broth and positive control represented by standardized bacterial growth. No colony growth of *S. aureus* at (2 % AMP) and *E.coli* at (6% AMP) was observed on Mueller-Hinton agar, figure 6A,B and figure 7A,B .

Agar Diffusion Test (Kerby- Bauer Method)

The biocompsite coat after immersion in AMP demonstrated antimicrobial efficiency against the microorganisms tested in certain concentrations. Biocomposite coated CPTi discs after immersion in 2% AMP revealed larger inhibition zone diameter (mean value 31.5, 27.6 and 22.4mm) against *S. aureus* in comparison to un immersed biocomposite disc (control) at 24, 48 and 72h incubation intervals. Higher concentration of AMP (6 %) produced clear inhibition against *E.coli* (mean value 22.5, 20.4 and 18.7mm) in comparison to control sample at 24,48 and 72h incubation intervals , (Table1 and 2) showed the descriptive mean and standard deviation and inferential analysis of AMP against the tested microorganisms. AMP has a highly significant anti bacterial activity against the tested bacteria especially at 24h in comparison to 48 and 72 h incubation intervals, this finding explained the slow diffusion

of AMP from the coated Ti disc and long last antibacterial effectiveness of AMP against *S. aureus* and *E.coli*, (fig.8 and fig.9).

DISCUSSION

RF Magnetron Sputtering

RF-magnetron sputtering affect the features of precipitated films , this technique form a dense, uniform coating with great adhesion and control the thickness and composition of the formed film[1,5,13,18] Niobium oxide enhanced surface roughness of CPTi substrate , this advancement of surface texture is needed to increase surface area on the implant surface and increase bone-to-implant attachment after the implant placement .[18,27] The surface topography of the biocompsite coatings has a significant effect in dental implant-tissue attachment and osseointegration .RF-magnetron sputtering permits formation of porous scaffolds with the complex structure. This coating morphology contribute to enhanced bone growth mechanisms.Rough implant surface participated in drug retention and act as a local drug delivery device which promote accelerated osseointegration and wound healing processes .[8,9,11]

Poly Ethylene Glycol (3500)

Polyethylene glycol (PEG) was used in this study for production of macro porous, scaffold surface structure; polyethylene glycol (PEG) is a polymer of choice in local drug releasing systems. [22] The results indicated that PEG (3500) enhances implant surface roughness which is an important factor to increase bone cells attachment and promote osseointegration. in addition PEG improve drug delivering and releasing to peri implant area to inhibit any microbial infection that participate in dental implant failure .[22]
This environment is helpful in establishing aseptic surgical field in dental implantation; drug releasing may extend longer depending on drug adsorption and infection intensity.

Antibacterial Efficiency of Biocomposite Film

Identification the spectrum of action of any antimicrobial agent is required for infection control which is important in all medical and biological fields especially in surgical procedures where the contact between the microorganisms and the living tissues might be of high risk. Agar diffusion test revealed no inhibition of bacterial growth for all tested concentrations of plyethylene glycol (PEG 3500),this finding is in agreement with (Rupp etal, 2018),(Triveni etal,2015)and(Albrektssonetal,2003)[21,28,31] who detect antimicrobial action of concentrated PEG 400, 1000. The inhibition zone data showed that 2% antimicrobial glycopeptide (AMP) was effective in preventing the growth of *S.aureus* when compared with the control discs. While the growth of *Ecoli* was inhibited at high concentration (6%) of AMP for upon three incubation periods. This result agree with (Emily *etal*,2010) who found that vancomycin is a glycopeptide that has a unique mode of action inhibiting the second stage of cell wall synthesis of susceptible bacteria and also alters the permeability of the cell membrane and selectively inhibits ribonucleic acid synthesis. *E. coli* are Gram-negative bacteria which own a cell wall that consists of an outer membrane containing lipopolysaccharides, a periplasmic space with a peptidoglycan layer, and an inner, cytoplasmic membrane. These bacteria are resistant to antimicrobial agents' .Such property enables *E. coli* to grow under all conditions and cause infection.[24] Surface of dental *implant* present suitable environment for bacterial attachment and formation of biofilm.The effectiveness of antibacterial dental implant coating is a promising finding and plays an important role in preventing bacterial colonization, implantation site infection and enhance osseointrgration around dental implant which is a very important factor to reduce dental implant failure .[25,29]

CONCLUSION

RF magnetron sputtering yielded thin and rough PEG-Nb2O5 biocomposte film deposited on CPTi substrate that held glycopeptide (vancomycin). Localized antimicrobial peptide revealed great antibacterial activities especially at 2% concentration against Staphylococcus aureus and at 6% concentration against Escherichia coli regarding the three incubation intervals. No antibacterial growth inhibition was noticed with the PEG at all selected concentrations.

REFERENCES

1. Kuo-Yung Hung , Hong-Chen Lai and Hui-Ping Feng (2017) . Characteristics of RF-Sputtered Thin Films of Calcium Phosphate on Titanium Dental Implants. Coatings. 7(126),2-10.
2. Alex Bunkera(2012) .Poly(ethylene glycol) in drug delivery, why does it work, and can we do better. Physics Procedia . 34 , 24 – 33.
3. Anisha A. D'souza &Ranjita Shegokar,(2016). Polyethylene glycol (PEG) a versatile polymer for pharmaceutical applications. Journal Expert Opinion on Drug Delivery . 13(9), 1257-1275.
4. Anna Zykova, Vladimir Safonov, Anna Yanovska, Leonid Sukhodub and Renata Rogovskaya (2015) Formation of Solution-derived Hydroxyapatite Coatings on Titanium Alloy in the Presence of Magnetron-sputtered Alumina Bond Coats. The Open Biomedical Engineering Journal. 9, 75-82.
5. Aronov AM, Pichugin VF, Eshenko EV, Riabtseva MA, Surmenev RA and Tverdokhlebov SI (2008) .Thin calcium-phosphate coatings produced by high frequency magnetron sputtering and prospects for their use in biomedical engineering. Med Tekh. 3,18-22.
6. Andrews JM (2001). Determination of minimum inhibitory concentrations. J Antimicrob Chemother. .48 (1) ,5-16.
7. Babita Yeshwante, Sonali Patil, Nazish Baig, Sonali Gaikwad4,Dr.Anand Swami and Mrunal Doiphode. (2012) Dental Implants- Classification, Success and Failure –An Overview. IOSR-JDMS. 14(5),1-8.
8. B. Bechinger, S.-U. Gorr (2016). Antimicrobial Peptides. Mechanisms of Action and Resistance. Journal of dental research. 96 (3), 254-260. [Thomson]
9. Buxadera-Palomero , Canal C2, Torrent-Camarero , Garrido B3, Javier Gil and Rodríguez (2015).Antifouling coatings for dental implants: Polyethylene glycol-like coatings on titanium by plasma polymerization. Biointerphases .10(2). 029505. doi: 10.1116/1.4913376.
10. C Valgas, S.M. De Souza, E.F.A. Smânia. (2007) Screening methods to determine antibacterial activity of natural products. Braz. J. Microbiol. 38(2) , 369-380.
11. Gabriele Ceccarelli, Rossella Presta, Laura Benedetti, Maria Gabriella Cusella De Angelis, Saturnino Marco Lupi, and Ruggero Rodriguez y Baena (2017). "Emerging Perspectives in Scaffold for Tissue Engineering in Oral Surgery," Stem Cells International, vol. 2017, Article ID 4585401,11pages.
12. Emily Hart ,Kristy Azzopardi ,Heng Taing ,Florian Graichen, Justine Jeffery,Roshan Mayadunne ,Malsha Wickramaratna, Mike O'Shea Brunda Nijaga and Rebecca Watkinson (2010). Efficacy of antimicrobial polymer coatings in an animal model of bacterial infection associated with foreign body implants .Journal of Antimicrobial Chemotherapy. 65(5) , 974–980.
13. Ellmer K, Welzel T (2012) . Reactive magnetron sputtering of transparent conductive oxide thin films: Role of energetic particle (ion) bombardment. J Mater Res.27(5),765–779.
14. FrancescaVeronesia,GianlucaGiavaresiab,MilenaFiniab,GiovanniLongoc,Caterina Alexandraloannidud and AnnaScotto d'Abuscod etal (2017). Osseointegration is improved by coating titanium implants with a nanostructured thin film with titanium carbide and titanium oxides clustered around graphitic carbon. Materials science and engineering. 70(1), 264-271.[Elsevier]
15. Guo CY, Tang AT, Matinlinna JP (2012). "Insights into surface treatment methods of titanium dental implants." J Adhesion Sci Technol 26,189-205.
16. Godoy-Gallardo , Mas-Moruno , Fernández-Calderó, Pérez-Giraldo , Manero JM and Albericio F, etal (2014).Covalent immobilization of hLf1-11 peptide on a titanium surface reduces bacterial adhesion and biofilm formation. Acta Biomater.10(8),3522-34.

17. Hengchong Shi, Haiyu Liu, Shifang Luan, Dean Shi, Shunjie Yan, Chunmei Liu, Robert K. Y. Li and Jinghua Yin(2016). Effect of polyethylene glycol on the antibacterial properties of polyurethane/carbon nanotube electrospun nanofibers, RSC advances. 6 (23), 18737 – 19637.
18. Ivanova AA, Surmeneva MA, Surmenev RA and Depla D (2015). Influence of deposition conditions on the composition, texture and microstructure of Rf-magnetron sputter-deposited hydroxyapatite thin films.Thin Solid Films. 591(B), 368–374.(scopus)
19. James C.Gumbart, MorganBeeby,Grant J. Jensen and BenoîtRoux(2014) . Escherichia coli Peptidoglycan Structure and Mechanics as Predicted by Atomic-Scale Simulations. PLoS Comput Biol .10(2). (https://doi.org/10.1371/journal.pcbi.1003475)
20. Ulbricht J, Jordan R, Luxenhofer R(2014). On the biodegradability of polyethylene glycol, polypeptoids and poly(2-oxazoline). Biomaterials. 35(17),4848-61. [Elsevier]
21. Rupp F, Liang L, Geis-Gerstorfer J, Scheideler L, Hüttig F (2018) .Surface characteristics of dental implants: A review. Dent Mater,34(1),40-57
22. Matteo Albertini, Marc Fernandez-Yague, Pedro Lázaro, Mariano Herrero-Climent, Jose-Vicente Rios-Santos and Pedro Bullon (2015). Advances in surfaces and osseointegration in implantology. Biomimetic surfaces, Med Oral Patol Oral Cir Bucal. 2(3), 316–325.
23. Marta Ribeiro, Fernando J. Monteiro, and Maria P. Ferraz (2012). Infection of orthopedic implants with emphasis on bacterial adhesion process and techniques used in studying bacterial-material interactions. Biomatter. 2(4), 176–194.
24. Mounyr Balouiri, MoulaySadiki, Saad Koraichi Ibnsouda (2016) .Methods for in vitro evaluating antimicrobial activity: A review. J. Pharmceutical analysis. 6 (2) , 71-79.
25. Owens CD1, Stoessel K. J (2008) .Surgical site infections: epidemiology, microbiology and prevention.Hosp Infect. 70 (2) ,3-10.
26. Roman Surmenev, Alina Vladescu, Maria Surmeneva, Anna Ivanova, Mariana Braic and Irina Grubova (2017). Radio Frequency Magnetron Sputter Deposition as a Tool for Surface Modification of Medical Implants[Internet] .8th ed. Chapter 12,213-248.
27. Rama Krishna Alla , Kishore Ginjupalli , Nagaraja Upadhya , Mohammed Shammas , Rama Krishna Ravi and Ravichandra Sekhar (2011).Surface Roughness of Implants:A Review.Trends Biomater. Artif.Organs.25(3), 112-118
28. Triveni Mohan Nalawade, Kishore Bhat, and Suma H. P. Sogi (2015). Bactericidal activity of propylene glycol, glycerine, polyethylene glycol 400, and polyethylene glycol 1000 against selected microorganisms. J Int Soc Prev Community Dent. 5(2), 114–119.
29. Varun Dahiya, Pradeep Shukla, Shivangi Gupta(2014). Surface topography of dental implants: A review . journal of dental implant. . 4 (1) , 66-71.
30. Watanakunakorn C (1984).Mode of action and in-vitro activity of vancomycin.JAntimicrob Chemother.14 ,7-18.[Pubmed]
31. Albrektsson T, Berglundh T, Lindhe J. Osseointegration. .Historic background and current concepts (2003) .Clinical Periodontology and Implant Dentistry–, 6th ed. Wiley Blackwell . Chapter 33, 809 – 820.

Table 1: The Antimicrobial Effect of 2% AMP Against *S. aureus* (Inhibition Zone Diameter in mm)

Descriptive Statistics					Mc by Bonferroni
time	Mean	SD	F	Sig.	
24h	31.500	1.732	42.610	0.000 HS	24 X 48=0.037
48h	27.600	1.782			24 X 72=0.002
72h	22.400	1.140			48 X 72=0.028

Table 2: The Antimicrobial Effect of 6% AMP against *E.coli* (Inhibition Zone Diameter in mm)

2					Mc by Bonferroni
time	Mean	SD	F	Sig.	
24h	22.500	1.500	21.419	0.001 HS	24 X 48=0.109
48h	20.400	.548			24 X 72=0.021
72h	18.700	.447			48 X 72=0.031

Figure 1: Biocomposite Coated Disc

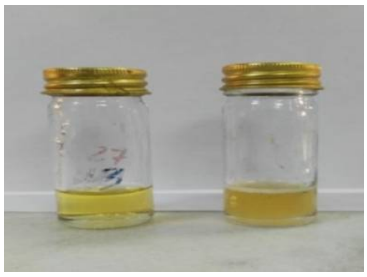

Figure 2: Negative and Positive Controls for Comparison in MIC Test

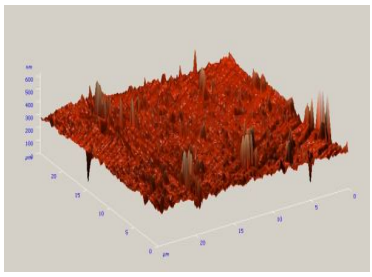

Figure 3 : (3 D) Micrograph Exhibit Roughness of Biocomposite Coat

Figure 4 : Minimal inhibitory concentration for polyethylene glycol

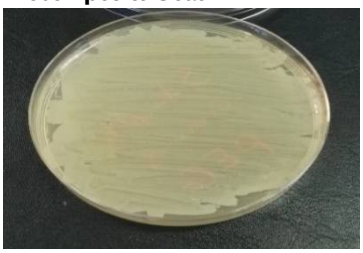

Figure 5: 100% polyethylene glycol exhibited non antibacterial against *Ecoli* and *S.aureus*

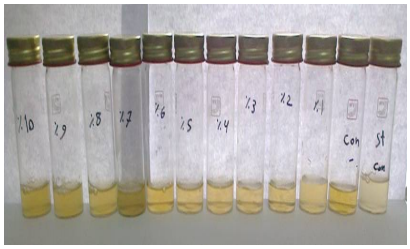

Figure 6A : 2 % MIC of AMP against *S aureus*

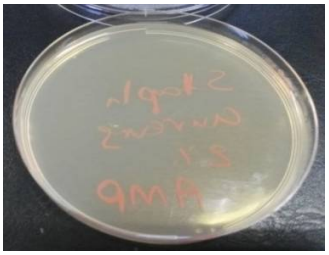

Figure 6B : No colony growth of *S. aureus* at 2 % AMP

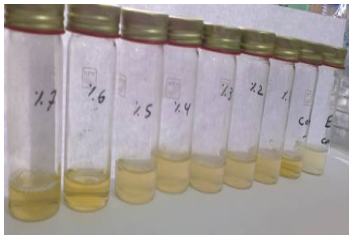

Figure 7A : 6% MIC of AMP against *Ecoli*

Figure 7B : No colony growth of *E.coli* at 6 % AMP

Figure 8: Inhibition zone against *S.aureus* at 24h incubation time

Figure 9: Inhibition zone against *E.coli* at 24h incubation time

Indian Journal of Natural Sciences www.tnsroindia.org.in ©IJONS

Vol.8 / Issue 49 / August /2018 *International Bimonthly* *ISSN: 0976 – 0997*

RESEARCH ARTICLE

Molecular Detection of *C. jejuni* in Chicken Meat Samples in the Qadisiyah Province, Iraq

Hind Hamzah Abdulhussein* and Abbas Mayar Hezam

Department of Biology, College of Science, University of AL- Qadisiyah, Iraq.

Received: 23 Apr 2018 Revised: 25 May 2018 Accepted: 28 June 2018

*Address for correspondence
Hind Hamzah Abdulhussein
Department of Biology,
College of Science,
University of AL- Qadisiyah, Iraq.

ABSTRACT

Chicken meat is viewed as the essential wellspring of disease with Campylobacter spp. in people. A sum of 50 chicken meat (thigh and bosom meat) tests from naturally butchered chicken at retail outlets in business sectors in the AL-Qadisiyah region, Iraq from January to May 2018. The outcomes exhibit a high commonness rate of *C. jejuni* in chicken thigh meat tests 23 out of 50 tests (46 %), trailed by chicken bosom meat 12 out of 50 tests (24 %). RT-PCR focusing on the species particular harmfulness quality cad f and hip O quality particular for *C. jejuni*.

Key words: - Molecular, detection, Campylobacter.

INTRODUCTION

Campylobacter spp. are a noteworthy reason for bacterial gastroenteritis around the world (1). The moderately low infective measurements, the conceivably genuine sequelae (1), and additionally the relationship between certain Campylobacter destructiveness qualities and the example of clinical contamination (2), affirm the significance of this zoonotic disease as a noteworthy wellbeing peril. Customary symptomatic strategies using a mix of culture and biochemical testing require that speculated stool examples are refined on particular agar at 42ºC under microaerophilic conditions for up to 72 h before a negative report is issued. Just culture plates with settlements demonstrating trademark Campylobacter morphology and oxidase inspiration are accounted for as *Campylobacter spp*. Advance recognizable proof to the species level requires different tests, including development temperature inclinations, anti-infection affectability to cephalothin and nalidixic corrosive, and biochemical tests. The sodium hippurate hydrolysis response is the main biochemical test used to separate *Campylobacter jejuni* and *Campylobacter coli*. The expanded and monotonous nature of these techniques has invigorated research into atomic demonstrative methodologies. A few laborers have explored the use of multiplex PCR for Campylobacter recognition and speciation (3, 4) with these conventions being connected to confines from unadulterated societies. In any case, the utilization of multiplex PCR on bacterial provinces implied that ordinary societies were as yet required for the underlying recognizable proof. To assess the multiplex approach straightforwardly on stool examples (5) falsely spiked stool

examples with microscopic organisms. Be that as it may, just two reports have depicted the immediate use of a multiplex convention on stools acquired from patients with enteritis (3) and both utilized groundworks focusing on the ceuE quality. Different mixes of family particular and species specific qualities, and in addition mixes of species-particular successions of ceuE or lpxA qualities, have been connected in multiplex conventions (6 ,7). The general point of the present work was to explore the commitment of chicken as potential wellsprings of *C. jejuni* contaminations in people at Wasit Province. This point was accomplished by utilizing regular and atomic devices to research the event of *C. jejuni* in chicken examples.

MATERIALS AND METHODS

Samples Collection

An aggregate of 50 tests of chicken meat (thigh and breast meat) tests were acquired from naturally butchered chicken at retail outlets in business sectors in the AL-Qadisiyah region, Iraq between January to May 2018. Twenty-five grams from each chiseled chicken meat (thigh and bosom) were aseptically exchanged to a sterile blender containing 225 ml of Preston improvement juices for homogenization of the example (8).

Biochemical Identification of Bacteria

0.1 ml of the juices was streaked onto adjusted Campylobacter particular agar base Cefoperazone Charcoal Desoxycolate Agar (mCCDA) (Oxoid, CM 0739). The plates were then brooded at 42ºC for 48 hours under microaerophilic conditions. Suspected provinces were purged on blood agar plates and subjected to biochemical ID utilizing catalase test, oxidase test, urea hydrolysis test, hydrogen sulfide (H2S) generation, citrate usage test and fast hippurate hydrolysis test (9).

Molecular Identification of Bacteria

DNA extraction from the biochemically recognized disengages was performed by the producer rules utilizing Bacterial DNA Extraction Kit (Spin-section) (BioTeke Corporation, China). The continuous test based PCR (qPCR) responses were utilized independently for the affirmation of *C. jejuni* biochemically distinguished secludes. Species-particular preliminaries and TaqMan test sets focusing on hipO quality particular for *C. jejuni* (3). The groupings of hipO groundworks and test are: Cj-F1 forward: 5'- TGCTAGTGAGGTTGCAAAAGAATT-3', Cj-R1 switch: 5'-TCATTTCGCAAAAAAATCCAAA-3' and Cj-FAM probe: 5'-ACGATGATTAAATTCACAATTTTTTTCGCCAAA-3'. (Table-1).

Each qPCR measure utilizing preliminaries and tests particular for *C. jejuni*, was done by (QuantiTect® Probe RT-PCR units Qiagen). Each qPCR response contained 12.5 µl of 2x QuantiTect Probe RT-PCR Master Mix (containing HotStart Taq® DNA polymerase, QuantiTect Probe RT-PCR support [Tris-Cl, KCl, (NH4)2SO4, 8 mM MgCl2], dNTP blend including dUTP, ROX™ detached reference color and 8 mM MgCl2), 0.1 units AmpErase [Uracil N-glycosylase] (Qiagen), 500 nM of pertinent groundworks and 500 nM of important test and 5 µl DNA format. Nuclease free water was added to a last volume of 25 µl. Non layout DNA and positive controls of *C. jejuni*. The response conditions were 50ºC for two minutes to actuate UNG, 95ºC for 15 min then 40 cycles at 94ºC for 15 sec.s and 60ºC for 60 sec took after by plate read for fluorescence securing.

RESULT

Prevalence of *C. jejuni* in Chicken Samples

The commonness rates of *C. jejuni* in chicken meat tests gathered from business sectors in the AL-Qadisiyah domain. The event of *C. jejuni* was recognized by bacteriological examination and biochemical examination. The outcomes exhibit a high commonness rate of *C. jejuni* in chicken thigh meat tests 23 out of 50 tests (46 %), trailed by chicken breast meat 12 out of 50 tests (24 %) (figure-1**).**

Molecular Identification

The molecular confirmation by real time PCR was connected just to bacteriology and biochemically *C. jejuni* detaches. The outcomes exhibit that rate of *C. jejuni* in chicken thigh meat tests 6 out of 23 tests (26 %), trailed by chicken breast meat 2 out of 12 tests (16 %) (figure-2).

Statistical Analysis

The measurable investigation was performed utilizing SAS (Statistical Analysis System - rendition 9.1) (10).

DISCUSSION

Campylobacter species, basically *C. jejuni* is perceived as imperative bacterial specialists of gastroenteritis in human (11, 12) and household creatures particularly poultry, domesticated animals and partner creatures (13). Poultry and poultry items are viewed as a typical and principle wellspring of Campylobacter disease to people (14). A world study evaluated the pollution of chickens with *Campylobacter spp*. to be around 58% (15). Oven corpses could be cross-tainted with *Campylobacter spp*. by fecal substance or ingest (16), so the utilization of undercooked poultry items and direct contact with live poultry or their defecation are the conceivable hazard pathways for human contaminations (17). In this study groundworks against two qualities of *Campylobacter spp*. counting cad F (family particular harmfulness quality), hip O (hippuricase quality for *C. jejuni*) were utilized. These qualities and groundworks have been considered autonomously and provided details regarding by different specialists and every one of them, particularly the cad F quality, are exceedingly moderated among detaches of various sources (18, 19, 20, 21, 22). The objectives of this review were to distinguish and to separate *C. jejuni* and to decide the recurrence of Campylobacter gastroenteritis in chicken meat in the Qadisiyah Province, Iraq utilizing PCR. Poultry are presented to *Campylobacter spp*. Right off the bat at cultivates level because of deficient biosecurity measure, optional at showcase outlets because of defilement of remains amid gutting and singing, thirdly amid capacity (23). Nations utilizing pluck-shop based markets have higher defilement rates of *Campylobacter spp*. from poultry than nations utilizing current handling plants (24). Manual butchering and gutting lead to fecal pollution of cadavers, which thusly might be in charge of expanded quantities of *Campylobacter spp*. in poultry meat (24). The danger of chicken meat sullied with *Campylobacter spp*. isn't just because of the utilization, yet in addition because of the exchange of the microbes display in chicken parts to hands, kitchen utensils and to other nourishment either straightforwardly or by means of cutting sheets (25). The outcomes point to the appropriateness of the PCR based assays as touchy techniques for fast and direct recognition and concurrent speciation of Campylobacter spp. The outcome demonstrates that *Campylobacter spp*. were disengaged from chicken thigh meat tests 23 out of 50 tests (46 %), trailed by chicken bosom meat 12 out of 50 tests (24 %) are Similar to (26) and (25) detailed the confinement of *Campylobacter spp*. from 31% of bosom meat and 47.9% of chicken legs, individually. The recognizable proof and separation of *C. jejuni* and *C. coli* is viewed as dangerous in light of the fact that it just relies upon a solitary phenotypic test in light of the hydrolysis of hippurate (27). Hence, atomic distinguishing proof strategies have been portrayed as a contrasting option to the off base, tedious, biochemical phenotypic techniques (3). Be that as it may, the ongoing improvement of constant PCR expelled the

need to control PCR items after enhancement to diminish cross-sullying (3). The single duplicate quality hip O quality (benzoglycine amidohydrolase) is in charge of the hippurate movement which separates *C. jejuni* from other *Campylobacter spp*. (28). The outcome demonstrate that rate of *C. jejuni* in chicken thigh meat tests 6 out of 23 tests (26 %), trailed by chicken bosom meat 2 out of 12 tests (16 %) were affirmed by qPCR. These outcomes fortify the speculation that in spite of the fact that hippurate hydrolysis test is generally used to separate *C. jejuni* from different species, *C. jejuni* hippurate negative strains and false positive strains have been disengaged (29). Moreover (28) and (3) announced that around 10% of *C. jejuni* segregates neglect to hydrolyze hippurate under research facility conditions, bringing about misclassification of these secludes as C. coli. Also, the hippurate hydrolysis measure is reliant upon the inoculums size of the bacterium, which implies that the examine can't recognize low level of hippuricase item (30). In this manner, the discovery of the quality by PCR rather than the phenotypic identification of the hippuricase item are viewed as a solid elective strategy for the segregation of *C. jejuni* separates (31).

CONCLUSION

Poultry dealing with amid butcher and destruction significantly affects the danger of poultry meat sullying instead of capacity temperature.

ACKNOWLEDGMENTS

Creators earnestly wish to recognize the individuals from the Laboratory of the College of Science, University of AL-Qadisiyah for supporting.

REFERENCES

1. Moore JE, Corcoran D, Dooley JS, Fanning S, Lucey B, Matsuda, M, McDowell, DA, Me´ graud F, Miller BC and other Authors. 2005. Campylobacter. Vet Res 36, 351–382.
2. Al-Mahmeed A, Senok AC, Ismaeel AY, Bindayna KM, Tabbara, KS and Botta, GA. 2006. Clinical relevance of virulence genes in Campylobacter jejuni isolates in Bahrain. J Med Microbiol 55, 839–843.
3. LaGier MJ, Joseph LA, Passaretti TV, Musser KA and Cirino, NM. 2004. A real-time multiplexed PCR assay for rapid detection and differentiation of Campylobacter jejuni and Campylobacter coli. Mol Cell Probes 18, 275–282.
4. Klena JD, Parker CT, Knibb K, Ibbitt JC, Devane PM, Horn ST, Miller WG and Konkel ME. 2004. Differentiation of Campylobacter coli, Campylobacter jejuni, Campylobacter lari, and Campylobacter upsaliensis by a multiplex PCR developed from the nucleotide sequence of the lipid A gene lpxA. J Clin Microbiol 42, 5549–5557.
5. Persson S and Olsen KE. 2005. Multiplex PCR for identification of Campylobacter coli and Campylobacter jejuni from pure cultures and directly on stool samples. J Med Microbiol 54, 1043–1047.
6. Jensen AN, Andersen MT, Dalsgaard A, Baggesen DL and Nielsen EM. 2005. Development of real-time PCR and hybridization methods for detection and identification of thermophilic Campylobacter spp. in pig faecal samples. J ApplMicrobiol 99, 292–300.
7. Gebreyes WA, Thakur S and Morrow WE. 2005. Campylobacter coli: prevalence and antimicrobial resistance in antimicrobial-free (ABF) swine production systems. J Antimicrob Chemother 56, 765–768.
8. Kiss I. 1984. Testing methods in food microbiology. AkademiaKiado, Budapest, Hungary.
9. Nachamkin I. 1999. Campylobacter and Arcobacter. In Muray, P. R., Baron, E. J. et al.(Eds). Manual of clinical microbiology, p. 716-726. Washington, D. C: ASM press.
10. SAS. SAS/STAT Users Guide for Personal Computer. Release 9.13.SAS Institute, Inc., Cary, N.C., USA.2010
11. Konkel ME, Gray SA, Kim BJ, Garvis SG, Yoon J.1999. Identification of the enteropathogens Campylobacter jejuni and Campylobacter coli based on the cadF virulence gene and its product. J Clin Microbiol. 37(3):510–7.
12. Persson S, Olsen KE. 2005. Multiplex PCR for identification of Campylobacter coli and Campylobacter jejuni from pure cultures and directly on stool samples. J Med Microbiol. 54(Pt 11):1043–7.

13. Aquino MH, Regua Mangia AH, Filgueiras AL, Teixeira LM, Ferreira MC, Tibana A. 2001. Use of a multiplex PCR-based assay to differentiate Campylobacter jejuni and Campylobacter coli strains isolated from human and animal sources. Vet J. 163(1):102–4.
14. Humphrey T, O'Brien S and MadSen M. 2007. Campylobacter spp. as zoonotic pathogens: a food production perspective. International Journal of Food Microbiology 117: 237–257.
15. Suzuki H and Yamamoto S. 2009. Campylobacter contamination in retail poultry meats and by-products in the world: a literature survey. The Journal of Veterinary Medical Science 71 (3): 255–261.
16. Mead GC, Hudson WR and Hinton MH. 1995. Effects of changes in processing to improve hygiene control on contamination of poultry carcasses with Campylobacter. Epidemiology and Infection 115: 495–500.
17. Anderson J, Horn BJ Gilpin BJ. 2012. The prevalence and genetic diversity of Campylobacter spp. in domestic backyard poultry in Centerbury, New Zealand. Zoonosis and Public Health 59 (1): 52-60.
18. Abu-Halaweh M, Bates J, Patel BK. 2005. Rapid detection and differentiation of pathogenic Campylobacter jejuni and Campylobacter coli by real-time PCR. Res Microbiol. 156(1):107–14.
19. Al Amri A, Senok AC, Ismaeel AY, Al-Mahmeed AE, Botta GA. 2007. Multiplex PCR for direct identification of Campylobacter spp. in human and chicken stools. J Med Microbiol. 56(Pt 10):1350–5.
20. Nayak R, Stewart TM, Nawaz MS. 2005. PCR identification of Campylobacter coli and Campylobacter jejuni by partial sequencing of virulence genes. Mol Cell Probes. 19(3):187–93.
21. Linton D, Lawson AJ, Owen RJ, Stanley J. 1997. PCR detection, identification to species level, and fingerprinting of Campylobacter jejuni and Campylobacter coli direct from diarrheic samples. J Clin Microbiol. 35(10):2568–72.
22. Wang G, Clark CG, Taylor TM, Pucknell C, Barton C, Price L, et al. 2002. Colony multiplex PCR assay for identification and differentiation of Campylobacter jejuni, C. coli, C. lari, C. upsaliensis, and C.fetus subsp. fetus. J Clin Microbiol. 40(12):4744–7.
23. Ellis-Iversen J, Jorgensen F, Bull S, Powell L, Cook A J and Humphrey TJ. 2009. Risk factors for Campylobacter colonization during rearing of broiler flocks in Great Britain. Preventive Veterinary Medicine 89 (3-4): 178-184.
24. Parkar SFD, Sachdev D, deSouza N, Kamble A, Suresh G, Munot H, Hanagal D, Shouche Y and Kapadnis B. 2013. Prevalence, seasonality and antibiotic susceptibility of thermophilic Campylobacter spp. in ceca and carcasses of poultry birds in the "live-bird market". African Journal of Microbiological Research 7 (21): 2442-2453.
25. Guyard-Nicodème M, Tresse O, Houard E, Jugiau F, Courtillon C, El Manaa K, Laisney M and Chemaly M. 2013. Characterization of Campylobacter spp. transferred from naturally contaminated chicken legs to cooked chicken slices via a cutting board. International Journal of Food Microbiology 164 (1): 7–14.
26. Luu QH, Tran TH, Phung DC and Nguyen TB. 2006. Study on the prevalence of Campylobacter spp. from chicken meat in Hanoi, Vietnam. Annals of the New York Academy of Science 1081: 273–275.
27. Steinhauserova I, Ceskova J, Fojtikova K and Obrovska I. 2001. Identification of thermophilic Campylobacter spp. by phenotypic and molecular methods. Journal of Applied Microbiology 90: 470–5.
28. Englen MD, Ladely SR and Fedorka-Cray PJ. 2003. Isolation of Campylobacter and identification by PCR. Methods in Molecular Biology 216: 109–121.
29. Nayak R, Stewart TM and Nawaz MS. 2005. PCR identification of Campylobacter coli and Campylobacter jejuni by partial sequencing of virulence genes. Molecular and Cellular Probes19 (3): 187-193.
30. Linton D, Lawson AJ, Owen RJ and Stanley J. 1997. PCR detection, identification to species level, and fingerprinting of Campylobacter jejuni and Campylobacter coli direct from diarrheic samples. Journal of Clinical Microbiology 35: 2568–2572.
31. Slater ER and Owen RJ. 1997. Restriction fragment length polymorphism analysis shows that the hippuricase gene of Campylobacter jejuni is highly conserved. Letters in Applied Microbiology 25: 274–278.

Table 1: List of Primers that used in PCR amplification

PCR	Primer	Sequence	
Cycle	hipO	F	TGCTAGTGAGGTTGCAAAAGAATT
		R	TCATTTCGCAAAAAAATCCAAA

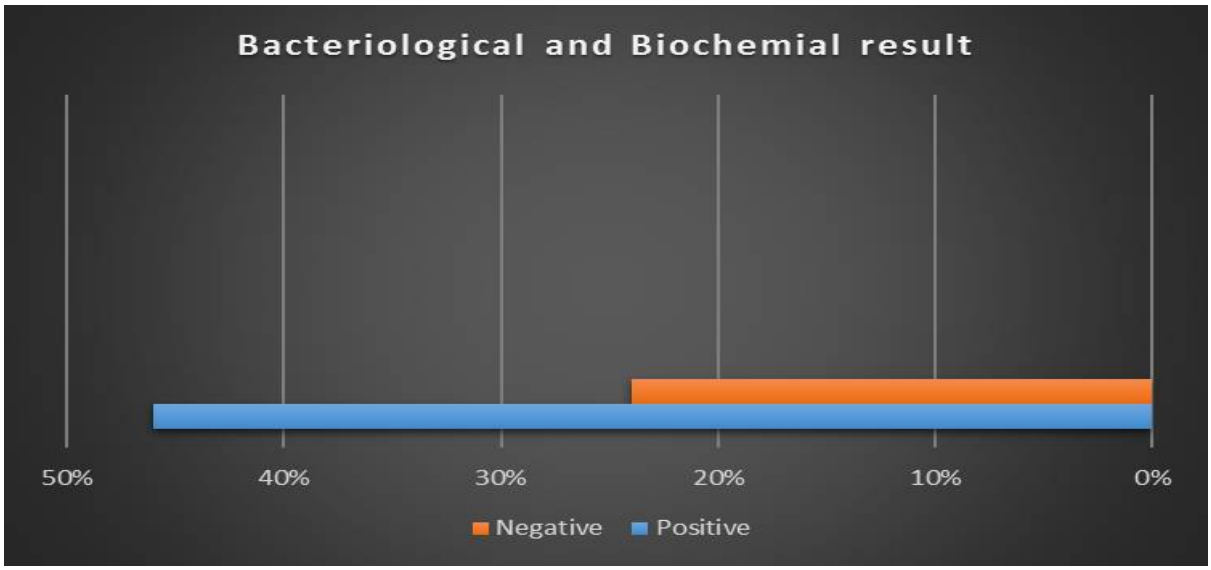

Figure 1: - The Result of Bacteriological and Biochemical Test

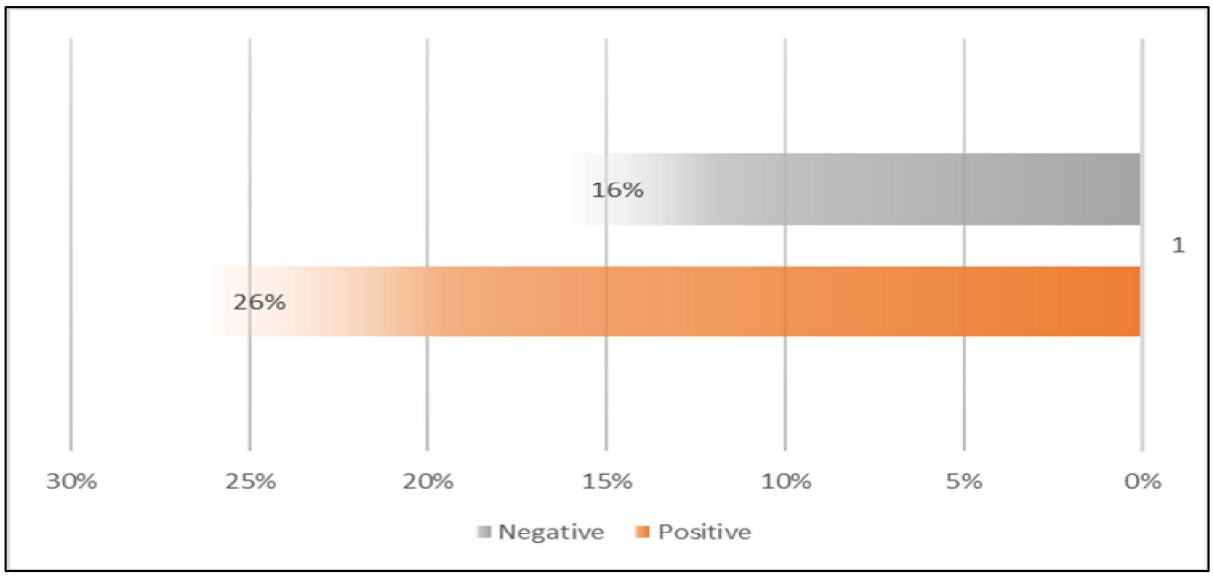

Figure 2: - The Result of Molecular Test

Indian Journal of Natural Sciences www.tnsroindia.org.in ©IJONS

Vol.8 / Issue 49 / August /2018 *International Bimonthly* *ISSN: 0976 – 0997*

RESEARCH ARTICLE

The Value of Coronary Artery Calcium Score and Coronary Artery Computed Tomographic Angiography in Coronary Artery Disease

MousaQasim Hussein[1]*, Ali Hussein YahyaAlsara[2] and Noor Hamza Abdulkhdhur Al- khuzaie[3]

[1]Assistant Professor, Consultant Physician, Department of Medicine, Al Kindy Medical College, University of Baghdad, Baghdad, Iraq.
[2]Senior House Officer, Department of Internal Medicine, Al-Kindy Teaching Hospital,Al-Rusafa Heath Directorate ,Baghdad, Iraq
[3]Specialist Doctor, Dakuk General Hospital, Kirkuk Health Directorate, Kirkuk, Iraq

Received: 02 May 2018 Revised: 01 June 2018 Accepted: 03 July 2018

*Address for Correspondence
Dr.MousaQasim Hussein
Assistant Professor,
Consultant Physician,
Department of Medicine,
Al Kindy Medical College,
University of Baghdad, Iraq.
Email:drmusaqassim2016@gmail.com

ABSTRACT

Computed tomography calcium scoring is a technique that is sensitive in identifying and quantifying calcified atherosclerotic plaques. Recent guidance from the National Institute of Clinical Excellence proposes the use of Computed tomography calcium scoring in patients with stable chest pain who have low likelihood of coronary artery disease. It was recommended that patients with low likelihood risk of ischemic heart disease (10-30%) have a Computed tomography calcium scoring and if the score is 0, they can be considered to have non-cardiac chest pain. However, there is controversy regarding relationship of absent calcification with significant coronary artery disease and its prognostic value.Objective: To assess the role ofthe calcium score as a predictor for the coronary artery disease.Patients and methods:A cross sectional study included 96 patients suffering from chest pain attending Ibn-Alnafeesand Baqubah Teaching Hospitals, during 6 months (April tillOctober 2017), were divided according to gender , age group , risk factors of IHD. Results: This study demonstrated that calcium score and the biochemical markers (lipid profile&glucose level), have highly significant association with occurrence of coronary artery disease ($p<0.001$) and have also asignificant correlation between calcium score and dyslipidemia ($p<0.001$) according to the riskfactor taken. Calcium score have significant correlation with the age, weight &lipid elements $p<0.001$, which reflectstheincreasingincidence of the coronary artery disease with age and obesity.There are no gender differences in occurrence of coronary calcium calcification. The smoker have significant correlation between the Ca^{++} score and the coronary artery disease inaddition to

that there is more strong correlation if there is association between smoking & diabetesmellitus same thing apply to the lipid markers in this group (p<0.001).Coronary computed tomographic angiography with +ve result show very high significant correlation withcalcium score (p<0.001).The study showed that Computed tomography calcium can predict ischemic heart disease among chest pain patients with a sensitivity =71% , specificity =95%.Conclusion:We can use Computed tomography calcium scoring as predictor of ischemic heart disease.

Keywords: Coronary Artery, Calcium Score, tomographic angiography

INTRODUCTION

Coronary Artery Disease (CAD), in other term, coronary heart disease (CHD), is one of the most killers and common silent diseases contributing high morbidity and mortality worldwide [(1)]. Atherosclerosis is a diffuse disease that affects many arteries of the body not just the coronary arteries. In the early stages, it causes changes in the walls of the arteries with increases in cholesterol content and scar tissue. In later stages, it causes plaques that thicken the wall of the artery and in some cases it cause narrowing of the center of the artery so that the flow of blood is gradually reduced. At this stage, calcium is generally present in the plaques [(2)]. Coronary artery calcium is typically present in direct proportion to the overall extent of atherosclerosis, although typically only a minority (approximately 20%) of plaque is calcified [(3)].

Coronary artery calcification is an independent risk factor for coronary heart disease, with even low coronary calcium scores doubling the risk of coronary events [(4)].Therelativeriskassociated with coronary calcification is greater than that associated with established factors, such as smoking, hypertension and diabetes mellitus[(5)]. Thus, the presence of coronary artery calcification is not only indicative of atheromatous plaque disease, but its progression may correspond with cardiovascular event rates[(5)].The availability of a noninvasive technique to detect coronary calcification makes it possible to obtain direct information on the presence of atherosclerosis in the coronary arteries.The sum of the area and density weightings across the coronary arteries is the unit less calcium score originally defined by Agatston and colleagues. Other quantification methods are available, including a calcium volume determination and mass score [(3)].As a non-invasive measure of overall coronary artery disease burden Coronary Artery Calicum testing is a clinically useful screening test for coronary atherosclerosis[(6)].

Cardiac CT is a fast developing technique. In 10 years, it developed from an investigative tool into a clinical reality (2). The latest innovations provide fast coverage with >64 slice detectors, high spatial resolution with 0.5 mm slice thickness, high temporal resolution with <100 ms in hardware, and higher contrast resolution with the forthcoming dual-energy solutions [(7)]. Now, multi-detector computed tomography (MDCT) scanners are available; they enable the simultaneous acquisition of 64 slices per rotation[(7)]. The clinical impact of the new technology lies in the improvement in image quality in terms of both spatial and temporal resolution. The improvement in spatial resolution is useful for:

- It increases the ability to visualize small-diameter vessels (e.g. the distal coronary branches) [(8)].
- It increases the ability to quantify calcium in that it reduces blooming artefacts [(8)].
- It enables the reduction of blooming artefacts in stents and therefore enables the visualization of the stent lumen.
- It improves the definition of the presence of coronary plaques and better quantifies their characteristics (volume, attenuation, etc.).

CT easily identified the coronary calcium because the roentgen graphic attenuation of calcium is much higher compared with that of the surrounding tissues [(9)]. Histologic studies have shown that a Computed Tomography tissue density of greater than or equal to 130 HU is highly correlated with calcified coronary plaques (10).

The extent of coronary calcium correlates with the overall atherosclerotic plaque burden (i.e., presence of calcific and non-calcific atherosclerosis), although the calcific plaques constitute only 20% of the total coronary plaque burden [(11,12)]. So, the presence of coronary calcium is evidence of the presence of coronary atherosclerosis. CT coronary calcium screening is generally not recommended for asymptomatic individuals at low or high risk of cardiovascular disease. Calcium screening may be useful for intermediate-risk individuals in whom a low calcium score suggests an actual low risk, whereas those with a high calcium score (>400) should be reclassified to high risk, justifying intensive modification of risk factors [(13)].

Aim of the Study

To test the value of calcium score as a predictor for the coronary artery disease.

MATERIALS AND METHODS

A cross-sectional study was conducted at IbnAlnafees Hospital and Baqubah Teaching Hospital, the study extended for 6 months from April tillOctober 2017. The study included 180 patients who visited the internal and cardiac clinic at Ibn al-Nafis Hospital and Baqubah Teaching Hospital (100 patients from Ibn al-Nafis Hospital and 80 patients from Baqubah Hospital). They were selected according to the clinical signs and symptoms (all patients selected were suffering from chest pain), whether they had a history of illness or risk factors or without. Blood tests were conducted as well as the work of ECG for all patients. Some patients were excluded because of the lack of the required standards for study (non-cardiac, musculoskeletal, Gastroesophageal reflux, pain in the thoracic vertebrae). The selected patients (suffering from chest pain and IHD was expected (central chest pain, discomfort or breathlessness, precipitated by exertion or other forms of stress, relieved by rest)) [(62)].subjected to present study andthese selected patients were divided intomany groups according to the riskfactors.

All patients underwent a case historyquestionnaire and the questionnaire included sociodemographic data (age, gender, smoking) and medical history (hypertension, diabetes mellitus), and patient was sent for biochemical investigations (RBS, lipid profile including total cholesterol (TC), high-density lipoprotein (HDL), Triglycerides (TGs) and LDL.Determination of LDL: LDL=Total cholesterol – (HDL+TG/5) Determination ofVLDL: VLDL= TG/5 ECG (TMTand Echo study were done for negative ECG). CT coronary artery calcium score and CTAngiography (CTA) was done for all patients.

The Exclusion Criteria

1. Patient with history of coronary artery bypass graft and/or prior stent placement,
2. Patient unable sustain a breath holds for at least 15 to 20 seconds. (Because CAC measurement required breathe holding for at least 15 sec).
3. Patient with history of renal impairment(contrast induced nephrotoxicity)
4. Patient with history of any allergic reaction to contrast agent

CT coronary angiography was performed with a 64-slice scanner (Aquillon 64, V4.51 ER 010, Toshiba Medical Systems, Tochigi, Japan) with retrospective ECG gating. Before Multi-Slice CT angiography, a non-contrast CT was acquired to measure calcium score according to the Agatston method. Slice thickness was 0.3- 0.5 mm. Calcium score was categorized in to two categories [(14)]

1. low risk (less or equal to 100) (0:very low, 0-10:low ,11-100 moderate)
2. high risk (more than 100) (101-400:moderately high, more than 400 :very high) for coronary artery calcifications

The result of CTA was divided in to (normal and abnormal or diseased arteries). The CT examination was performed in a calm and comfortable atmosphere (e.g., lights were dimmed, and the staff speak quietly), avoiding anything that might affect the patient's heart rate, because a constant rate is crucial for diagnostic quality and accuracy. On the day of the test the patient must not take caffeine (no coffee, tea, caffeinated soft drinks or chocolate) and must not smoke. And should also not exercise immediately prior to the test. It is recommended that the patients arrive 30 minutes prior to their appointment.If the pulse rate is high,advice to take a tablet (Beta-blocker) to lower the heart rate. CT Coronary Artery Calcium Scoring is performed just like a normal CT scan. It takes about 10 – 15 minutes. The patients asked to lie on their back on the CT table. The radiographer (the medical imaging technologist performing the test) will place electrocardiogram (ECG) leads on the chest. And the examiner asked the patients to breathe in and hold their breath several times while the machine takes the images. The CT scanner assesses the heart beat and calculates when it wants to take the scans.

Coronary calcium scoring, unlike CT coronary angiography; is always performed by using prospective triggering with 3mm slice collimation without contrast administration and reduce radiation exposure by allowing exact determination of the scan range required for subsequent CT coronary angiography (from about 1 cm above to 1 cm below the coronaries). The clinical benefit of calcium scoring is not in detecting or ruling out coronary artery disease, but in risk stratification of individual patients. In regarding CTAngio, for venous access, an upper extremity vein (antecubital vein of the right arm) and a 20-gauge IV canula was used.

Ethicalconsideration

The research proposal was approved by agreement of scientific and ethical committee of the Iraqi Board for Internal Medicine, and scientific and ethical committee in MOH. A written consent was approved from all studied patient after full explanation of the aim of the study and tailing the patient that the collected data will be used for scientific purposed and insure confidentiality of data use.

Statistical Analysis

Data were introduced in to personal computer, IBM SPSS V. 23 were used in statistical management of the collected data. Descriptive statistics were displayed using tables.Analytic statistics were presented through usage of Chi square test, Fisher Exact and Spearman correlation.Kruskal-wallis test was used to find out significance of differences between CAC and the diseased arteries because the data of CAC among affected arteries was not normally distributed by using of SHAPIRO-WILK test. P.V. < 0.05 was considered as significant level marker.

RESULT

This cross sectional study included 96 patients with IHD , 68 (70.8%) of them were male patients , 58 (60.4%) of them their age more than 50 years , 52 (54.2%) of them have normal weight (BMI less than 25) , 51 (53.1%) of them are smoker , 57 (59.4%) of them were HT , DM were found among 67 (69.8%) of patients , total cholesterol was increased in 56 (58.3%) , TG were found to be elevated among 59 (61.5%) , HDL decrease in 58 (60.4%) , both LDL and VLDL increase in 58 (60.4%) , CTA was found to be abnormal in 76 (79.2%) , and CAC was found to be high risk in 55 (57.3%) as shown in table (3).

Table (4) shows the association between different studied variables and CAC. It revealed that significant association were found between age, weight, smoking, HT, DM, lipid profile (TC , TG , HDL , LDL , VLDL) and CAC that are represented by p – value =<0.001.

Table (5) shows the correlations betweensociodemographics and lipid profile variables and CAC. In regarding the correlations between age, CAC, HT and TC there is strong correlations between them .In regarding the correlations weight, CAC, age, HT and TC. In regarding the correlations between smokings, CAC, age, HT, TC and TG there is strong correlations between them. And the same correlation present related to the HT. In regarding the correlations between DM, CAC, lipid profile (TC, HDL, VLDL) there is strong correlations between them .and lastly there is no correlation between gender and CAC.

Table (3.4) Revealed that CAC was found to be highest among patients suffered from LAD disease (mean ±SD {220.41±159.94}), followed by RCA disease (mean ± SD {204.08±150.26}), and lowest CAC was found among patients suffered from LCX disease (mean ±SD {120.6±98.77}), it was provided that there was significant statistical differences between means of CAC and types of artery disease provided by Kruskal-Wallis Test

Table (7) Revealed that the most sever lesion (subtotal) were found among 14 patients in which the mean CAC was the highest (mean ±SD {475.8571±35.16960}, mean rank =71.21), while the lowest lesion severity(no critical) were found among 9 patients with (mean ± SD {31.6667±16.69581}, mean rank =6.94), it was clear that the most sever lesion was found in patients got hieghest CAC ,while the least sever lesion was found among patients with lowest CAC and this differences is statistically significant (p value =0.001) provided by Kruskal-Wallis Test.

Table (8)revealed that CAC and CTA were significantly associated. P value less than 0.001.CAC can be used as a diagnostic test in comparism with CTA .with Sensitivity = 71.1% Specifity = 95% ,as shown in table 8.

DISCUSSION

In regard to the age distribution and sex, the coronary calcium score is highly associated withelderly age that is agree with study of Lloyd-Jones et al.,[16]who said that there is marked increase in the incidence and prevalence of CVD with advancing age.There is no gender differences in occurrence of coronary calcium that is not agree with the results obtained byHoffet al.[17]who reported that there is gender differences in occurrence of coronary calcium support the association of CAC with coronary atherosclerosis and underline the importance of age- and gender-specific reference points for CAC scoring [17].With respect to the weight,there is a strong relation to the Ca^{++} score in our study there is a link between calcium score and obesity or over weight that is agree with the study of Julian and Marsh[18]. Regional body fat distribution has an important influence on metabolic and cardiovascular risk factors.

Many prospective studies have shown that increased abdominal (visceral) fat accumulation is anindependent risk factor for CAD, hypertension, stroke, and type 2 diabetes (DM2) [19] .Regarding lipid profile, from our study we can conclude that correlation between lipidparameters, weight and Ca^{++} score for the patients strongly significant correlation.That is consider the most important step for forming the atherosclerosis that predisposing for CAD .this fact in our study was improved and agree with study done by Carr and Brunzell[19]whoshowed that, the changes in lipid metabolism seen with abdominal fat accumulation have been well characterized and include hypertriglyceridemia, reduced HDL cholesterol, and increased numbers of small, dense LDL particles. Concerning hypertension, from our study we can conclude that correlation between hypertension and Ca^{++} score for the patient's strongly significant correlation.

This fact in our study was improved and agree with study done by Framingham Heart Study,[20]they said that, even high-normal blood pressure (defined as a systolic blood pressure of 130-139 mm Hg, diastolic blood pressure of 85-89 mm Hg, or both) increased the risk of cardiovascular disease 2-fold, as compared with healthy individuals[20]. With reference todiabetes mellitus, in this group there are 67 patient out of 96 that is mean 69.8 %are diabetic patient most of them aretype 2 diabetes mellitus so weconclude that there is a strong correlationbetween Ca^{++} Score, age and the lipid profile indiabetic patient.Numerous cross-sectional studieshave documented that patients withdiabetes have a

higher prevalence andextent of coronary calcium than nondiabeticpatients [21]. Recent study suggested that CACscoring may be superior to establishedcardiovascular risk factors for predictingsilent myocardial ischemia and shorttermcardiovascular outcomes amongstable, uncomplicated type 2 diabeticpatients [22].Patients with diabetes are consideredto be in the highest risk categoryaccording to the Adult Treatment Panel III guidelines [22,23].
Therefore, there is a clear clinical need to detect CAD at an early stage in DM patients who are at risk of both fatal and non-fatal cardiac events before the onset of symptoms [24].

As for smoking , the data obtained from smoker patients group which account 51 for Smoker and ex-smoker (53.1%) and non-smoker about 45 patients out of 96 patients (46.9%). this data show the strong correlation of the VLDL , TC , and Ca^{++} score (p 0.000) ,that is explain how the smoking have strong influence on the CAD by playing important role in deposition of the Ca^{++} in the coronary arteries and through strong correlation with VLDL, our results agree with the results obtained by Yanbaeva et al.[25]who reported that Endothelial dysfunction is mainly caused by diminished production or availability of NO. It has been demonstrated that the serum concentration of nitrate and nitrite, metabolic end-products of NO, is significantly decreased in smokers relative to that in nonsmokers. Although most of smoking-induced changes are reversible after quitting, some inflammatory mediators like CRP are still significantly raised in exsmokers up to 10 to 20 years after quitting, suggesting ongoing low-grade inflammatory response persisting in former smokers [25] Our study also reveal important results that explain the strong correlation between the diabetes and the smoking since there is significant increase in the lipid parameters level and Ca^{++} score in diabetic and smoker patients more than those who are non-smoking but non diabetic, that is agree with study done by Yanbaeva et al. [25]. Besides inflammation, proposed potential mechanisms by which smoking increases the risk of cardiovascular pathology include several other pathways: vascular endothelial dysfunction, systemic hemostatic and coagulation disturbances, and lipid abnormalities [25].

Withregard to the coronary computed tomographic angiogram, our study a prove there is moderate significant correlation in between CAC and CTA measurement (R= 0.542, P value less than 0.001). it also showed that using CAC instead of CTA can catch CAD among patient suffered from chest pain with sensitivity = 71% and specificity =95% and this goes with what had been found by Greenland et al.,[26] which said that the Electron-beam computedtomography (EBCT) and multi-detector computed tomography (MDCT) are theprimary fast CT methods for CAC measurement at this time. With regard to differences between means of calcium score according to affected arteries, our study revealed that CAC was found to be highest among patients suffered from LAD disease (mean ± SD {220.41±159.94}), and this not agree with the study ofKadhim et al.[27]as they found that the RCA stenosis was significantly more prevalent among the abnormal CTA group. With reference to the distribution of cases according to calcium score and severity of the arterial lesion, it was clear that the most sever lesion was found in patients got highest CAC, while the least sever lesion was found among patients with lowest CAC and this differences is statistically significant (p value =0.001),and this agree with the study of Kadhimet al.[27]who confirmed that themost sever lesion was more prevalent in patients with highest CAC.

CONCLUSION

Measurement of coronary artery calcification is useful & sensitive mean to the early diagnosis of the CAD.The monitoring of the lipid profile is of great importance during the evaluation and care of CAD patients. Smoking, DM show significant correlation between each of them and increase CAC score, so quitting smoking and prevention or at least good control of DM may play role in prevention of increasing CAC which in turn prevent CAC.

REFERENCES

1. Hadaegh F, Harati H, Ghanbarian A et al. Prevalence of coronary heart disease among Tehran adults: Tehran Lipid and Glucose Study East Mediterr Health J. 2009 Jan-Feb;15(1):157-66.

2. Hoffmann U, Brady TJ, Muller J. Use of New Imaging Techniques to Screen for Coronary Artery Disease. Circulation. 2003; 108: e50-e53
3. Allen J. Taylor ,Cardiac Computed Tomography -BRAUNWALD'S HEART DISEASEA Textbook of Cardiovascular Medicine. Vol I 9thed, pp365-366
4. Pletcher MJ, Tice JA, Michael P, Browner WS. Using the coronary artery calcium score to predict coronary heart disease events: a systematic review and meta-analysis. Arch Internal Medicine. 2004;13:1285–1292. doi: 10.1001/archinte.164.12.1285.
5. Raggi P, Cooil B, Shaw LJ, Aboulhson J, Takasu J, Budoff M, Callister TQ. Progression of coronary calcium on serial electron beam tomographic scanning is greater in patients with future myocardial infarction. Am J Cardiol. 2003;13:827–829. doi: 10.1016/ S0002-9149 (03) 00892-0.
6. Sangiorgi G, Rumberger JA, Severson A, et al. Arterial calcification and not lumen stenosis is highly correlated with atherosclerotic plaque burden in humans: a histologic study of 723 coronary artery segments using nondecalcifying methodology. J Am CollCardiol. 1998;31:126–133. doi: 10.1016/ S0735-1097 (97) 00443-9.
7. Law WY, Yang CC, Chen LK, et al. Retrospective gating vs. prospective triggering for noninvasive coronary angiography: assessment of image quality and radiation dose using a 256-slice CT scanner with 270 ms gantry rotation. AcadRadiol. 2011;18:31–39
8. Agatston AS, Janowitz WR, Hildner FJ, et al: Quantification of coronary artery calcium using ultrafast computed tomography. J Am CollCardiol 1990; 15:827-832
9. Kachelriess M, Kalender WA. Electrocardiogram-correlated image reconstruction fromsubsecond spiral computed tomography scans of the heart. Med Phys. 1998; 25:2417–2431.
10. Bacha F, Edmundowicz D, Sutton-Tyrell K, Lee S, Tfayli H, Arslanian SA. Coronary artery calcification in obese youth: what are the phenotypic and metabolic determinants?. Diabetes Care. 2014 Sep. 37(9):2632-9.
11. Rumberger JA, Simons DB, Fitzpatrick LA, et al: Coronary artery calcium area by electron-beam computed tomography and coronary atherosclerotic plaque area. A histopathologic correlative study. Circulation 1995; 92:2157-2162.
12. O'Rourke RA, Brundage BH, Froelicher VF, et al: American College of Cardiology/ American Heart Association Expert Consensus document on electron-beam computed tomography for the diagnosis and prognosis of coronary artery disease. Circulation 2000; 102:126-140
13. Greenland P, Bonow RO, Brundage BH, et al; Society of Atherosclerosis Imaging and Prevention; Society of Cardiovascular Computed Tomography: ACCF/AHA 2007 clinical expert consensus document on coronary artery calcium scoring by computed tomography in global cardiovascular risk assessment and in evaluation of patients with chest pain: A report of the American College of Cardiology Foundation Clinical Expert Consensus Task Force (ACCF/AHA Writing Committee to Update the 2000 Expert Consensus Document on Electron Beam Computed Tomography) developed in collaboration with the Society of Atherosclerosis Imaging and Prevention and the Society of Cardiovascular Computed Tomography. J Am CollCardiol 2007; 49:378-402.
14. Cademartiri F.Casolo, G.; Midiri, M., editors. Clinical applications of cardiac CT. New York: Springer; 2012. Calcium score and coronary plaque; p. 121
15. Cury, R. C., et al. .CAD-RADS: Coronary Artery Disease – Reporting and Data System.: An Expert Consensus Document of the Society of Cardiovascular Computed Tomography (SCCT), the American College of Radiology (ACR) and the North American Society for Cardiovascular Imaging (NASCI). Endorsed by the American College of Cardiology. J Am CollRadiol2016;13(2 PtA): 1458 – 1466
16. Lloyd-Jones D, Adams R, Carnethon M, et al. Heart disease and stroke statistics--2009 update: a report from the American Heart Association Statistics Committee and Stroke Statistics Subcommittee. Circulation. 2009 Jan 27;119(3):e21–181.
17. Hoff JA, Chomka EV, Krainik AJ, et al. Age and gender distributions of coronary artery calcium detected by electron beam tomography in 35,246 adults. Am J Cardiol 2001;87:1335–9.
18. Julian B, Marsh M D. Lipoprotein Metabolism in Obesity and Diabetes: Insights from Stable Isotope Kinetic Studies in Humans.Nutrition Reviews, 2003; 61(11): 363–375.

19. Carr MC, Brunzell JD. Abdominal Obesity and Dyslipidemia in the Metabolic Syndrome: Importance of Type 2 Diabetes and Familial Combined Hyperlipidemia in Coronary Artery Disease Risk, The Journal of Clinical Endocrinology & Metabolism, 2004; 89(6) 1: 2601–2607. https://doi.org/10.1210/jc.2004-0432
20. Vasan RS, Larson MG, Leip EP, et al. Impact of high-normal blood pressure on the risk of cardiovascular disease. N Engl J Med. 2001 Nov 1. 345(18):1291-7.
21. Raggi P, Shaw LJ, Berman DS, Callister TQ. Gender-based differences in the prognostic value of coronary calcification. J Womens Health (Larchmt) 2004;13:273– 83.
22. Raggi P, Shaw LJ, Berman DS, Callister TQ: Prognostic value of coronary artery calcium screening in subjects with and without diabetes. J Am CollCardiol 2004, 43:1663-1669.
23. Executive Summary of The Third Report of The National Cholesterol Education Program (NCEP) Expert Panel on Detection, Evaluation, And Treatment of High Blood Cholesterol In Adults (Adult Treatment Panel III). JAMA. 2001;285:2486-2497.
24. Andreini D, Pontone G, Bartorelli AL, Agostoni P, Mushtaq S, Antonioli L, Cortinovis S, Canestrari M, Annoni A, Ballerini G, Fiorentini C, Pepi M. Comparison of the diagnostic performance of 64- slice computed tomography coronary angiography in diabetic and nondiabetic patients with suspected coronary artery disease Andreini et al. Cardiovascular Diabetology 2010, 9:80,
25. Yanbaeva DG, Dentener MA, Creutzberg EC, Wesseling G, MD, Wouter EFM, . Systemic Effects of Smoking. Chest 2007; 131:1557– 1566.http://dx.doi.org/10.1378/chest.06-2179
26. Greenland P, Bonow RO, Brundage BH, Budoff MJ, Eisenberg MJ, Grundy SM, Lauer MS, Post WS, Raggi P, Redberg RF, Rodgers GP, Shaw LJ, Taylor AJ, Weintraub WS, Harrington RA, Abrams J, Anderson JL, Bates ER, Eisenberg MJ, Grines CL.ACCF/AHA 2007 Clinical Expert Consensus Document on Coronary Artery Calcium Scoring By Computed Tomography in Global Cardiovascular Risk Assessment and in Evaluation of Patients With Chest Pain. A Report of the American College of Cardiology Foundation Clinical Expert Consensus Task Force (ACCF/AHA Writing Committee to Update the 2000 Expert Consensus Document on Electron Beam Computed Tomography).Journal of the American College of Cardiology.2007; 49(3):378-402.
27. KadhimMA, Wassan A.K. Al – Saadi , Ghassan H. Hadi:Prevalence of Coronary Artery Disease in Symptomatic Patients with Zero Calcium Score Undergoing Coronary CTAngiography, Iraqi JMS 2015; Vol.13(3)

Table 1: Standardized Categories for the Coronary Artery Calcium Score (Cac)[14]

Agaston score	Calcium score categories	Propabilitysignifigant CAD	Cardiovascular risk
0	Absent	Very unlikely (<5%)	Very low
1-10	Minimal	Very unlikely (<10%)	Low
11-100	Mild	Mild or minimal coronary stenosis likely	Moderate
101-400	Moderate	Non obstructive CAD ,high likely .obstructive CAD possible	Moderately high
>400	Extensive	High likelihood of significant coronary stenosis (>90%)	High

Table 2: The CAD-RADS Classification of Coronary Artery Disease: [15]

Classification	Maximal Stenosis	Interpretation
CAD-RADS 0	0%	No CAD (non critical)
CAD-RADS 1	1 – 24%*	Minimal non-obstructive(non critical)
CAD-RADS 2	25 – 49%	Mild non-obstructive(non critical)
CAD-RADS 3	50 – 69%	Moderate stenosis(intermediate)
CAD-RADS 4	A: 70 – 99% orB: Left Main >50% or 3-vessel ≥ 70%	Severe stenosis(critical, and between 90-99% regard as subtotal)
CAD-RADS 5	100%	Total coronary occlusion

Table 3:The Frequency Distribution of Studied CAD Patients According to Different Variables

		Count	Column N %
Gender	MALE	68	70.8%
	FEMALE	28	29.2%
Age	=>>50	58	60.4%
	<50	38	39.6%
Weight	Normal	52	54.2%
	Increased	44	45.8%
Smoking	SMOKER	51	53.1%
	NO	45	46.9%
HT	HT	57	59.4%
	NO	39	40.6%
DM	DM	67	69.8%
	NO	29	30.2%
TC	Increase	56	58.3%
	Normal	40	41.7%
T.G	Increase	59	61.5%
	Normal	37	38.5%
HDL	Decrease	58	60.4%
	Normal	38	39.6%
LDL	Increase	58	60.4%
	Normal	38	39.6%
VLDL	Increase	58	60.4%
	Normal	38	39.6%
CTA	Abnormal	76	79.2%
	Normal	20	20.8%
CAC	High risk	55	57.3%
	Low risk	41	42.7%

CAD=coronary artery disease, HT=hypertension, DM= diabetes mellitus, TC=total cholesterol, CAC= Coronary artery calcium score , CTA= contrast enhanced computed tomographic angiography

Table4: Association Between CAC and Different Variables in CAD Patients

		CAC				Sig
		High risk		Low risk		
		Count	Row N %	Count	Row N %	
Gender	**MALE**	39	57.4%	29	42.6%	0.985
	FEMALE	16	57.1%	12	42.9%	
Age	**=>>50**	55	94.8%	3	5.2%	<0.001
	<50	0	0.0%	38	100.0%	
Weight	**Normal**	48	92.3%	4	7.7%	<0.001
	Increased	7	15.9%	37	84.1%	
Smoking	**SMOKER**	48	94.1%	3	5.9%	<0.001
	NO	7	15.6%	38	84.4%	
HT	**HT**	54	94.7%	3	5.3%	<0.001
	NO	1	2.6%	38	97.4%	

DM	**DM**	53	79.1%	14	20.9%	<0.001
	NO	2	6.9%	27	93.1%	
TC	**increase**	53	94.6%	3	5.4%	<0.001
	Normal	2	5.0%	38	95.0%	
T.G	**increase**	52	88.1%	7	11.9%	<0.001
	Normal	3	8.1%	34	91.9%	
HDL	**decrease**	51	87.9%	7	12.1%	<0.001
	Normal	4	10.5%	34	89.5%	
LDL	**increase**	51	87.9%	7	12.1%	<0.001
	Normal	4	10.5%	34	89.5%	
VLDL	**increase**	51	87.9%	7	12.1%	<0.001
	Normal	4	10.5%	34	89.5%	

CAD= coronary artery disease, CAC= Coronary artery calcium score, TC=total cholesterol, HT=hypertension, DM= diabetes mellitus

Table 5: Spearman Correlation Between CAC,CTA, Socio Demographic and Lipid Profile Variables In CAD patients

		CAC	CTA	Gender	Age	Weight	Smoking	HT	DM	TCl	T.G	HDL	LDL	VLDL
CAC	CC	1.000	.542**	.002	.937**	.770**	.793**	.915**	.670**	.893**	.787**	.765**	.765**	.765**
	Sig.	.	.000	.985	.000	.000	.000	.000	.000	.000	.000	.000	.000	.000
CTA	CC		1.000	.179	.529**	.455**	.495**	.516**	.500**	.503**	.332**	.529**	.529**	.581**
	Sig.			.082	.000	.000	.000	.000	.000	.000	.001	.000	.000	.000
Gender	CC			1.000	.043	.054	.224*	.076	.077	.108	.198	.137	.137	.184
	Sig.				.678	.604	.028	.463	.456	.293	.053	.184	.184	.073
Age	CC				1.000	.837**	.862**	.979**	.720**	.958**	.847**	.826**	.826**	.826**
	Sig.					.000	.000	.000	.000	.000	.000	.000	.000	.000
Weight	CC					1.000	.770**	.814**	.670**	.876**	.775**	.794**	.752**	.752**
	Sig.						.000	.000	.000	.000	.000	.000	.000	.000
Smoking	CC						1.000	.881**	.655**	.900**	.843**	.776**	.776**	.819**
	Sig.							.000	.000	.000	.000	.000	.000	.000
HT	CC							1.000	.703**	.936**	.827**	.805**	.805**	.805**
	Sig.								.000	.000	.000	.000	.000	.000
DM	CC								1.000	.732**	.598**	.766**	.581**	.766**
	Sig.									.000	.000	.000	.000	.000
TC	CC									1.000	.894**	.871**	.871**	.871**
	Sig.										.000	.000	.000	.000
T.G	CC										1.000	.760**	.760**	.760**
	Sig.											.000	.000	.000
HDL	CC											1.000	.739**	.782**
	Sig.												.000	.000
LDL	CC												1.000	.739**
	Sig.													.000
VLDL	CC													1.000
	Sig.													.

CAC= Coronary artery calcium score , CTA= contrast enhanced computed tomographic angiography
CAD=Coronary artery disease, CC= correlation coefficient, sig=significance, HT=hypertension, DM=diabetes mellitus

Table 6:Kruskal-Wallis Test showed differences between means of calcium score according to affected arteries

Artery	N	Calcium score			SIG
		Mean	SD	Mean Rank	
LAD	46	220.41	159.94	36.22	0.005
LCX	5	120.60	98.77	21.80	
RCA	12	204.08	150.26	34.08	
LAD+RCA+LCX	4	399.00	110.35	61.25	
LAD+RCA	7	383.00	90.71	59.29	
LAD+LCX	4	385.00	54.04	59.25	
Total	78	243.69	159.74		

Table 7 :Kruskal-Wallis Test Showed Distribution of Cases According to Calcium Score and Severity of the Arterial Lesion

	N	CAC score	Mean± SD	Mean rank	Artery lesion
No critical	9	0-10	3.16±1.66	6.94	4 of them with LCX, 3 with LAD ,2 with RCA
Intermediate	18	11-100	83.61±40.27	17.72	1 of them with LCX, 13 with LAD ,4with RCA
Critical	37	101-300	285.29±80.72	46.01	20of them with LAD , 3 with RCA,7with comp of (LAD+RCA) , 4 with comp of (LAD+RCA+LCX),3 with comp of (LAD+LCX),
Subtotal	14	301-550	475.85±35.16	71.21	10 of them with LAD , 3with RCA,1 with comp of (LAD+LCX)
Total	78		243.69±159.74		

Table 8: Association Between CAC and CTA Among CAD Patients

		CT angio N=98					
		Abnormal N=76			Normal N=20		
		N	C N %	R N %	N	C N %	R N %
CAC Total	High risk N=55	54	71.1%	98.2%	1	5.0%	1.8%
	Low risk N= 41	22	28.9%	53.7%	19	95.0%	46.3%
Sensitivity=71.1 %, specificity =95%							

Indian Journal of Natural Sciences www.tnsroindia.org.in ©IJONS

Vol.8 / Issue 49 / August /2018 *International Bimonthly* *ISSN: 0976 – 0997*

RESEARCH ARTICLE

Toxicopathological Changes in Internal Organs of Albino Mice after Treatment with Sodium Nitrate

Riyam Ibrahim Mustafa[1]*, SalemaLafta Hassan[2] and FalahMuosaKadhim[3]

[1]Department of Pathology and Poultry Diseases, University of Baghdad, Baghdad, Iraq.
[2]Department of Physiology, Biochemistry and pharmacology, University of Baghdad, Baghdad, Iraq.
[3]Collage of Veterinary Medicine, University of Baghdad, Baghdad, Iraq.

Received: 01 May 2018 Revised: 31 June 2018 Accepted: 03 July 2018

*Address for correspondence
Riyam Ibrahim Mustafa
Department of Pathology and Poultry Diseases,
University of Baghdad,
Baghdad, Iraq

ABSTRACT

The present study aimed to investigate the the toxic effect of Sodium Nitrate on the histological status of internal organ of male mice. This study was carried out at College of Veterinary Medicine Baghdad, for six weeks. Forty adult males Swiss albino mice, aged 8 weeks, were divided into four equal groups. 1st group (G1) was administrated orally with drinking water with (0.1 LD_{50}) of sodium nitrate daily for 6 weeks, 2nd group (G2) was administrated sodium nitrate as 1st group and at the same time vitamin E (15 I.U./kg) with diet for 6 weeks, 3rd group (G3) was administrated of sodium nitrate as 1st group and at the same time inoculated by I/P with 0.4 ml Brucell.Rev1 vaccine two doses, two weeks interval, 4th group (G4) was considers as control negative group.All animals were euthanized and pieces of liver, kidney and testis were taken for histopathological examination. Results showed that the toxic effect of Sodium Nitrate in the liver characterized by mild to moderate hydropic degeneration that was characterized by swelling of hepatocytes was seen especially at the pericentral regions of liver besides congestion in the portal vein and blood sinusoids. The microscopic section of the kidney showed congestion of glomerular capillaries with swelling in the glomerular cells, besides degenerative changes in renal tubules. Histopathological examination of testes showed testicular degeneration with absence of spermatids and spermatogenic cells in semeniferous tubules, and absence of epididymal sperm reserve. To avoid its harm on human, the use of sodium nitrate should be expertised.

Keywords: Histopathology, liver, kidney , Testis, Sodium nitrate, Vit E, Brucella vaccine Rev 1, I.U., WHO.

INTRODUCTION

Sodium nitrate is a white solid very soluble in water. It is readily available source of the nitrate anion (NO_3^-), which is useful in several reactions carried out on industrial scales for the production of fertilizers, pyrotechnics and smoke bombs, glass and pottery enamels, food preservatives (esp. meats), and solid rocket propellant. Nitrate ions are also produced from nitric oxide. When taken with food, they are readily absorbed from the small intestine is partially converted to nitrite by oral bacteria and by stomach acids, helping to reduce gastrointestinal tract infection (Combs, 2000). Sodium nitrate is also used in conjunction with calcium nitrate and potassium nitrate for heat storage and heat transfer in solar power plants**.** (Kuravi, *et al.,* 2013).Absolute net tubular reabsorption of NO-3 showed linear relationship with filtered loads, with no evidence of transport maximum. These data show that, in the absence of additions from intrarenal sources, urinary excretion rates of nitrate increases progressively in response to increases in its circulating levels without exhibiting transport maximum but with progressive decreases in fractional reabsorption**.** (Godfrey and Majid, 1998).

Approximately 60% of oral nitrate is excreted in urine. Bacterial or endogenous metabolism probably accounts for the remainder. Minor part is excreted in sweat (IPCS, 1996)**.** Nitrates produce methemoglobinemia when they are changed into nitrites under the influence of bacterial proliferation of reductase held in plants. It happens with spinach and carrot soup **(**European Chemicals Bureau 2000)**.** Approximately 25% of the ingested nitrate is secreted in saliva and about 20% of the nitrate of the salivary secretion is then converted into nitrite by microorganisms in the oral cavity. So, for normal individuals, about 5–7% of the ingested nitrate can be detected as nitrite in saliva (Chan, 2011 and Pannala *etal* .2003).

Methemoglobinemia, which may even lead to death. Newborns very sensitive to this type of pathology, also known as "blue baby syndrome".unlike adults who have more protection against the low pH of the stomach reduction of nitrate to nitrite by bacteria Nitrites, which are much more unstable than nitrates, react with the haemoglobin of red blood cells to form methemoglobin. The presence of nitrite can also involve the formation of various N-nitroso compounds (nitrosamines and nitrosammides) by reaction with secondary amines and amides present in the food. It has been shown that this occurs both with nitrites ingested and with those present in the saliva (Pannala et al., 2003; Speijers and Van Den Brandt, 2003)

MATERIALS AND METHODS

Forty adult male Swiss Albino mice and aged 8 weeks and weighed range (20-25g), supplied from animal house of the College of Vet. Med. University of Baghdad was used in present study. They were housed and maintained in a conventional animal facility, with controlled conditions of temperature (20 ± 5ºC). The animals were fed on special formula of food pellets and given water *ad libitum*. Throughout the experiments, each group of mice was housed in plastic cage containing hard-wood chip as bedding. The bedding was changed continuously to ensure a clean environment. The experiment is University of Baghdad College of Veterinary Medicine Department of pathology and poultry.

Experimental Design

Forty adult males Swiss Albino mice, aged 8 weeks, were divided into four groups. 1St group(1) was administrated orally with drinking water with (0.1 LD50) of sodium nitrate daily for 6 weeks, 2nd group(2) was administrated sodium nitrate as 1st group and at the same time vitamin E (150 I.U./kg) with diet for 6 weeks, 3rd group(3) was administrated of sodium nitrate as 1st group and at the same time inoculated by I/P with 0.4 ml Brucella Rev1 vaccine two doses, two weeks interval,4th group(4) was considers as control negative group.

Median lethal dose (LD_{50}):-

"Up-and-down" method.(Dixon, 1980).was used for determination of median lethal dose **(LD_{50})** of Sodium Nitrate which fifty albino mice weighed (20-25) gm were used in this study in whichSodium Nitrate was prepared at concentration 27 mg / ml by dissolving powderSodium Nitrate in distilled water. The volume of doses was calculated according to animal weight, Sodium Nitrate was given orally to the animals at range of doses (2800) mg /kg B.W and the difference in doses was (400mg / kg B.W) . LD50 was calculated after 24 hours observation of lethality in the dosed animals. The LD_{50} is calculated by using the equation in Appendix- 1

Dixon Method

Dixon, (1980) calls for dosing individual animals in sequence singly at 24-hour intervals, with the initial dose set at "the toxicologist's best estimate of the LD_{50}." Following each death (or moribund state) the dose was lowered; following each survival, it was increased, according to prespecified dose progression factor If death followed an initial direction of increasing doses of 10-20 % or survival followed an initial direction of decreasing dose with the same ratio, five additional animals according to outcome Up & down were tested following the same dose adjustment pattern and then testing was ended. The LD_{50} was calculated by using the following equation:

LD_{50}= xf + kd.
LD_{50}=Median lethal dose.
Xf =The last dose administrated.
K = factor value from appendix.
D = difference between dose levels.
O =Symbol of survival animal after24hours of dosing.
X =Symbol of dead animal within 24 hours of dosing
LD_{50}=2800+(-0.154*400)
LD_{50}=2738.4 mg/kg B.W
1/10 LD_{50}=273.84 mg/kg B.W

Brucellin preparation

This Ag was used for immunization animals Prepared according to (Saleh, 1999) as follow:

1. The *Brucellamelitensis*vasccine life attenuated.
2. Add 30x10^9*Brucellamelitensis* with 15 ml PBS.
3. The solution suspension sonication: the universal tube that contained *Brucellamelitensis* suspension was put in cold environment (ice) and placed in the ultra-sonicator (type Karl Klob – Germany) with 2 minutes intervals between them, for 30 minutes in alkindi company to production of vaccines and veterinary medicines.
4. The suspension was centrifuged in cold centrifuge at (10000 rpm/4c° / /30 min) then the supernatant was taken in sterile method.
5. The supernatant was filtered by Millipore filter 0.22nm.
6. The sample sonicated was tested by culture.
7. The supernatant considered the Brucillin and the protein concentration were evaluated by biuratprocedure.
8. The Brucillin diluted to become 0.5 mg/ml PBS, and stored in -20° till use and injection of mice 0.1 ml in pad foot.

Histopathology

Pieces of testes, liver and kidney were fixed in 10% normal buffer formalin for 72 hours for routine histopathological examination(Luna, 1968).

RESULT

Histopathological changes of animals treated with sodium nitrate. The main lesions in the liver characterized by mild to moderate hydropic degeneration that was characterized by swelling of hepatocytes especially at the pericentral regions of liver besides congestion in the portal vein and blood sinusoids (Figure 1). The examined liver showed dilated central vein congestion.As well as The centrilobular area showing marked sinusoidaldilatation with sporadic cell necrosis and kupffer cellprolifration (Figure 2);the portal area showing marked bileduct hyperplasia, increased number of bile ductules, ovalcell hyperplasia, portal congestion and mononuclear cellsinfiltration (Figure 3).

The microscopic section of the kidney showed congestion of glomerular capillaries with swelling in the glomerular cells, besides degenerative changes in renal tubules, focal fibrosis and infiltrated with .number of inflammatory cells (Figure 4) at the medullary portion.Histopathological examination of testes showed testicular degeneration with absenceof spermatids and spermatogenic cells in semeniferous tubules (Figure 5).Histopathological changes of animals treated with sodium nitrate plus of vitamin E administration. The main lesions in the liver characterized by proliferation of kupffers cells, lymphocytes aggregation around central veins, portal veins and bile duct in portal area(Figure 6). The microscopic section of the Kidney showed congestion with dilatation of glomerular capillaries filled bowman's space (Figure 7). Histopathological examination of testes showed areas of semeniferous tubular degeneration with vacuolations; as well as showed few numbers of spermatogenic cells and spermatids (Figure 8).

Histopathological changes of animals treated with sodium nitrate and at the same time immunized with $1x10^8$brucella Rev1 vaccine two doses, two weeks interval. The main lesion in liver characterized by marked aggregation of mononuclear cells particularly lymphocytes around central vein and proliferation and hypertrophy of kupffers cells (Figure 9). The main lesion of the kidney showed hypercelullar of urinary glumeruli with mononuclear cell between renal tubules (Figure 10). A few mononuclear cells aggregations around in the interstial tissue. Histopathological section in the testis of immunized animal at 6 weeks post- treated with sodium nitrate showed vaculardegenration and absence of epididymal sperm and marked inflammatory cells aggregation between the tubules (Figure 11). In kidney showed vacuolar degeneration of renal tubular epithelium with invaded with a number of red blood cells (Figure 12).Histopathological changes of animals of 4^{th} group was considers as control negative group. There were no significant macroscopic findings.

DISCUSSION

The pathological lesions in examined organs in group treated with NaNO3 may be attributed to nitrates is oxidation products and ready sources of NO, that NO reacts rapidly with superoxide to form highly reactive peroxynitrite ($ONOO^-$) such products may increase lipid peroxidation (LPO) which can be harmful to different organs including liver and kidney (Chow and Hong, 2002; Hassan *et al*., 2009); Rocha *et al*., 2012). The liver is liable to injury by a variety of causes and its injury may lead to profound metabolic disorders. Liver injury induced by chemicals has been recognized as one of the most toxicological problems (Cohen, 1982).These results are in accordance with (Sharma*et al*., 2008), attributed the dilatation of the blood sinusoids to the direct toxic effect of the toxin leading to their dilatation. Moreover exhibited sinusoidal congestion as a result of which the radial orientation of the hepatic cords was lost.

Hepatocellular necrosis is probably due to the direct attached of the cell membranes by the hepatotoxin or by interacting with some specific components of the metabolic pathways leading to the alteration of their structure and function (Klatskin and Conn, 1993). As well as dilatation of the central vein and sinusoids, degenerative changes in periaciner zone, beside hyperplasia, hypertrophy and detachment of epithelium lining of the bile duct with mononuclear cell infiltration also recorded by(Mondal*et al*., 1999) In addition to ,(Malte and Tienush, 2013). Reported marked bile duct hyperplasia, increased number of bileductules, oval cell hyperplasia, another study hypothesized

the sodium nitrite inducing vasodilation via nitricoxide (NO) activation of the cyclic guanosine monophosphate (cGMP) signaling pathway in vascular smooth muscle cells. Periportal hepatocellular vacuolation and necrosis were observed similar findings were described by (Zeenat and Phil, 2010). The microscopic examination of the Kidney revealed massive necrobiotic changes of renal tubules that ranged from vacuolization and swelling to necrosis of epithelial lining associated with accumulation of proteinaceouseosinophilc cast in collecting tubular lumina All renal alterations are attributed to sodium nitrite inducing hypoxia with the subsequent free radical formation that inducing tissue changes including renal tissue (Kim et al., 2002);(Manassaram, et al., 2007).

Histopathological examination showed testicular degeneration with absence of spermatids and spermatogenic cells in semeniferous tubules and absence of epididymal sperm reserve, alterations in seminiferous epithelium so after sodium nitrate treatment the changes are due to the effect of sodium nitrate.induced hemic hypoxia on the male reproductive system arecontroversial. Male rats (Farias *etal*., 2005b) and rhesus monkeys (Saxena,1995) subjected to hypobaric hypoxia showed atrophy of germinal epithelium with Sertoli cell replacing spermatogonia as well as spermatogenic arrest at the end of the third week of exposure.(Petrova and Ormandzhieva, 2012).reported hypoxia is induce oligoasthenospermia with reduced motility, reduction of the total number of motile sperm and an increase of abnormal or immature spermatozoa. In animal models (rat, mouse, guinea pig, rabbit, monkey, sheep), it has been shown that hypobaric hypoxia induces partially reversible quantitative changes such as decrease in semen volume, sperm count and sperm motility As well as low thyroid hormone concentrations have also been reported to affect semen quality (Chandrasekher*et al.,* 1985).

We noticed moderate lesions in the internal organs of animals feeding with vitamin E adminstration post- treatment, these observations may be indicate that that vitamins with antioxidant activity protect soft tissues against damaging effect of free radicals which produced as a result of heavy metals toxicity (Hamadoche*et al*., 2012). Moreover, it has been reported that the co-administration of vitamins combined with chelating agents may have better beneficial role and protective effects against lead intoxication (Flora *et al.,* 2012). As well as Vitamin E acts as a radical scavenger, delivering an H atom to free radicals.At 323 kJ/mol, the O-H bond in tocopherols is about 10% weaker than in most other phenols. (Lide, 2006). This weak bond allows the vitamin to donate a hydrogen atom to the peroxyl radical and other free radicals, minimizing their damaging effect. Thus generated tocopheryl radical is relatively unreactive but revert to tocopherol by a redox reaction with a hydrogen donor such as vitamin C. (Traberet *al.,* 2011). As it is fat-soluble, it is incorporated into cell membranes, which are protected from oxidative damage by vitamin E.

The pathological lesions in examined organs in immunize animals there were mononuclear cells aggregation around blood vessels, in addition to lymphoid tissue hyperplasia due to proliferation of lymphocytes, this result may indicate that Ags stimulate proliferation of lymphocytes and may give an indication that good immune responses were elicited these study agree with (Singh et al., 2012) who observed a greater persistence of immune stimulation in animals vaccinated with S19, evidenced by prolonged IFN-ɣ, MHC Class II+CD4+ cells and CD4+ memory cells response, both vaccination regimens were able to evoke a significant IFN-ɣ response after vaccination and revaccination. In addition to(Levine2010) who reportedbrucellosis vaccines is an appealing method of immunization since vaccination should stimulate the mucosal immune system to eliminate brucellae before they become systemic and possibly should stimulate the systemic immune compartment to prevent dissemination into host tissues

CONCLUSION

In conclusion, Sodium Nitrate possesses toxic effect for spermatogenesis, liver and kidney baranchymia in mice. Therefore, application of sodium nitrate should be limited to designed program.

ACKNOWLEDGMENT

The authors are grateful to the Department of Pathology and Poultry Science,College of Veterinary Medicine, Baghdad University, Iraq.

REFERENCES

1. Chan, T.Y.K. (2011). Vegetable-borne nitrate and nitrite and the risk of methaemoglobinaemia. Toxicology Letters, 200, 107–108. doi:10.1016/j.toxlet.2010.11.002
2. Chandrasekher, Y.M.K.; Holland, M.J.; D'Occhino.andSetchell, B.P. (1985). Spermatogenesis, seminal characteristics and reproductive hormone levels in mature rams with induced hypothyroidism and hyper-thyroidism. J. Endocrinol., 1005:39–46.
3. Chow, C.K. and Hong, C.B. (2002). Dietary vitamin E and selenium and toxicity of nitrite and nitrate.Toxicology, 180 (2):195–207.
4. Cohen, M.S. (1982). Special aspects of prenatal and pediatrics pharmacology.Basic.Clin.Pharmacol., 60: 701-706.
5. Combs, G.F. (2000). Food system based approaches to improving micronutrient nutrition, the case for selenium CrossRefBiofactors., 12 :39-43.
6. Dixon, W.J. (1980). Efficient analysis of experimental observations. Ann. Res. Pharmacol. Toxicol. 20: 441-462.
7. European Chemicals Bureau; IUCLID Dataset.(2000) Potassium nitrate. CD-ROM edition., 7757:79-1.
8. Farias, J.G.; Bustos, E.; Obregón, P.J.; Tapia, E.; Gutierrez, A.; Zepeda, C.; Juantok, G.; Cruz, G.; Soto, J.; Benites. and Reyes, J.G. (2008). Time course of endocrine changes in the hypophysis-gonad axis induced by hypobaric hypoxia in male rats.J.Reprod. Dev., 54: 18–21.
9. Flora, G.; Gupta, D. and Tiwari A. (2012). Toxicity of lead: a review with recent updates. Interdiscip.Toxicol. 5 47–58.
10. Godfrey, M. and Majid, D.S. (1998). Renal handling of circulating nitrates in anesthetized dogs. Am J Physiol Renal Physiol., 275: F68–F73.
11. Hamadouche, N.M.; Slimani and Aoues, A. (2012). Beneficial effect of administration of vitamin C in amelioration of lead hepatotoxicity. Nat. Sci. Biol. 4 (3), 7-13.
12. Hassan, H.A.; El-Agmy, S.M.; Gaur, R.L.; Fernando, A.; Raj, M.H.G and Ouhti, t.A. (2009).In vivo evidence of hepato- and reno-protective effect of garlic oil against sodium nitriteinduced oxidative stress.Int J BiolSci 5(3):249-255.
13. International Programme on Chemical Safety(IPCS); (1996). Nitrates and nitrites. Poisons Information Monograph., G016:
14. Kim, H.J.; Chang, W.K.; Kim, M.K.; Lee, S.S. and Choi, B.Y. (2002). Dietary factors and gastric cancer in Korea:Case-control study. Int. Jr. of Cancer, 97: 531-535.
15. Klatskin, G. and Conn, H. (1993).Histopathology of the Liver.Vol. 1, Oxford Univ. Press, Oxford and New York.
16. Kuravi, S.; Trahan, J.; Goswami, D.Y.; Rahman, M.M. and Stefanakos, E.K. (2013).Thermal energy storage technologies and systems for concentrating solar power plants.Prog Energy Combust Sci., 39: 285-319.
17. Levine, M. M. (2010). Immunogenicity and efficacy of oral vaccines in developing countries: lessons from live cholera vaccine. BMC Biol. 8:129–139.
18. Lide, D.R.; ed. (2006). CRC Handbook of Chemistry and Physics (87th ed.). Boca Raton, FL: CRC Press. ISBN., 0-8493-0487-3.
19. Luna, L.G. (1968). Manual of histologic staining methods of the armed forces institute of pathology, 3rd edn.McGrawHill, New York, NY.
20. Manassaram, D.M.; Backer, L.C. and Moll, D.M. (2007). A review of nitrates in drinking water: maternal exposure and adverse reproductive and developmental outcomes, Cien. Saude Colet. 12, pp. 153–163.
21. Mondal, D.B.; Pandey, N.N. and Charan, K. (1999). Effects of prolonged low nitrite intoxication in goats.IndianVet. J. 76: 800-803.

22. Pannala, A.S.; Mani, A.R.; Spencer, J.P.E.; Skinner, V.; Bruckdorfer, K.R.; Moore, K.P. and Rice-Evans, C. A. (2003).The effect of dietary nitrate on salivary, plasma, and urinary nitrate metabolism in humans. Free Radical Biology and Medicine, 34, 576–584. doi:10.1016/S0891-5849(02)01353-9.
23. Petrova, E. and V. Ormandzhieva.(2012). Hypoxia and the male reproductive system.Andrologia, 21 (1): 7–14.
24. Rocha, B.S.; Gago, B.; Barbosa, R.M.; Lundberg, J.O.; Radi, R. and Laranjinha, J. (2012).Intragastric nitration by dietary nitrite: implications for modulation of protein and lipid signaling. Free RadicBiol Med., 52(3):693-8.
25. Saleh, H.M. (1999). Immunological evaluation of the locally produced Brucillins in the sheep infected with Brucella and immunized with RevIvaccine.Msc. Thesis. Vet. Med. Coll. Bagh. Univ.
26. Saxena, D.K. (1995). Effect of hypoxia by intermittent altitude exposure on semen characteristics and testicular morphology of male rhesus monkeys. Int. J. Biometeorol., 38: 137–140.
27. Sharma, R.K.; Singh, B.andSahoo, A. (2008).Exploring feeding value of oak (Quercusincana) leaves: nutrient intake and utilization in calves.Livest. Sci., 118 (1/2): 157-165.
28. Singh, R.; Basera, S.S.; Tewari, K.; Yadav, S.; Joshi, S. and Singh, B. et al. (2012). Safety and immunogenicity of Brucellaabortus strain RB51 vaccine in cross bred cattle calves in India. Indian J ExpBiol 50: 239–242.
29. Speijers, G.J.A. and Van Den Brandt, P.A. (2003, July 21). Nitrate (and potential endogenous formation of N-nitroso compounds).[Online]. (WHO Food Additives Series Retrieved from http://www. inchem.org/documents/jecfa/jecmono/v50je06. Htm.
30. Traber, M.G.; Stevens, J.F. and Stevens. (2011). Free Radical Biology and Medicine – Vitamins C and E: Beneficial effects from a mechanistic perspective". Free Radical Biology and Medicine. 51 (5): 1000–1013.
31. Ulrike, B.H.; Malte, K. and Tienush, R. (2013).Free radicals, oxidative stress and antioxidants in human health and disease. J. Am. Oil Chem. Soc., 75: 199-212.
32. Zeenat, F.Z. and Phil, D. (2010).Periportal necrosis in rat liver exposed to sodium nitrite-induced hypoxia. Res. J. Anim. Vet. Sci., 5(2): 111-116.

Table (1) up and down value of LD_{50}(Dixon, 1980)

Initial dose mg/k.g B.W	Final dose mg/k.g B.W	ifferences between doses mg/k.g B.W	Number of animals	Out come after 24 hours
2000	2800	400	5	KOOOO

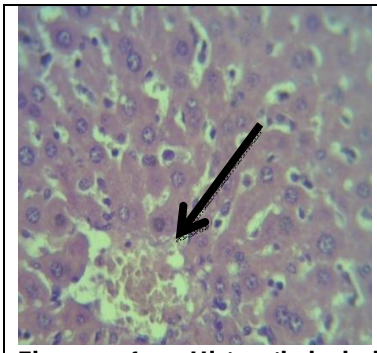

Figure 1: Histopathological section in the liver of animal treated with sodium nitrate showing swelling of hepatocytes was seen especially at the pericentralregions of liver (black arrow), H and E stain 40X.

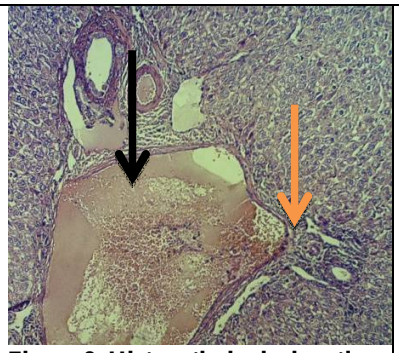

Figure 2:.Histopathological section in the liver of animal treated with sodium nitrate showing hepatic vessls marked dilation and congestion (black arraw) with moderate perivacular infiltration (orange arraw)accompained with cellular individualization of some hepathocyte (H & E X40)

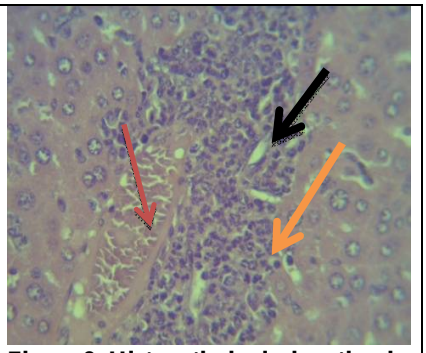

Figure 3: Histopathological section in the liver of animal treated with sodium nitrate showing marked bile duct hyperplasia(black arraw), increased number of bile ductules, oval cell hyperplasia, portal congestion and mononuclear cells infiltration (orangearraw) H & E X40

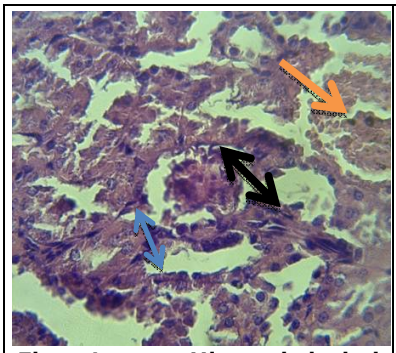

Figure4: Histopathological section in the kidney of of animal treated with sodium nitrate showing dissolution in the cortex highly vacuolated glomerular tuft (black arraw) hemorrhagic area (orange arraw) and inflammatory cells infiltration (blue arraw) periglomerular oedema and degeneration of epithelial cells lining in the renal tubule). H & E X40

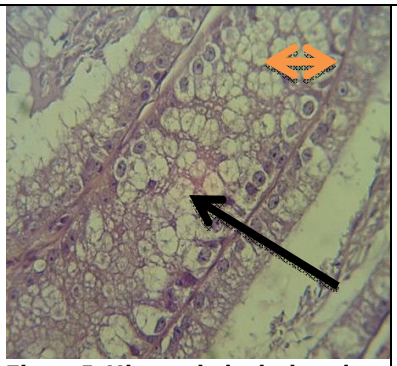

Figure 5: Histopathological section in the testis of animal treated with sodium nitrate showing areas of semeniferous tubular degeneration with vacuolations (orange arrows); absence of spermatogenic cells and spermatids (black arraw), H and E stain 40X.

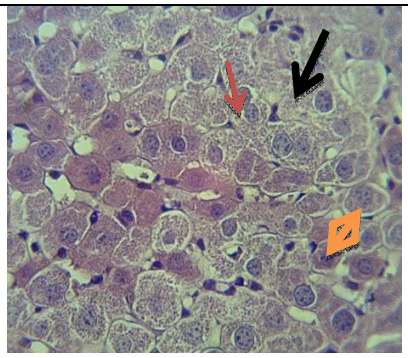

Figure 6:Histopathological section in the liver of animal treated with sodium nitrate plus of vitamin E administration showing degenerated hepatocytes(black arraw), the anucleated others(orangearraw) and proliferation of kuffer

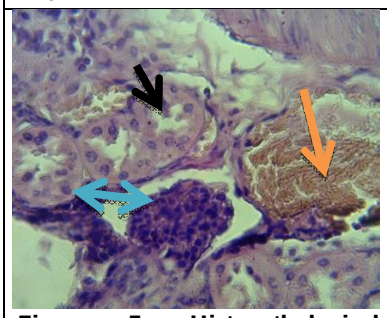

Figure 7: Histopathological section in the kidney of animal treated with sodium nitrate plus of vitamin E administration showing mild vacuolar degeneration of renal tubular epithelium (black arraw) with infiltrated mononuclear cells between renal tubules and around glomerula with Buman space (blue arraw) ,in addition to inflammatory cells in the lumen of renal tubules and haemorrhge(orangearraw), H and E X40.

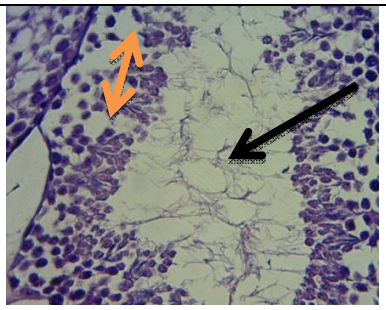

Figure 8:Histopathological section in the testis of animal treated with sodium nitrate plus of vitamin E administration showed semeniferous tubular degeneration with vacuolations (orangrarraw); as well as showed few number of spermatogenic cells and spermatids (black arraw), H and E X40.

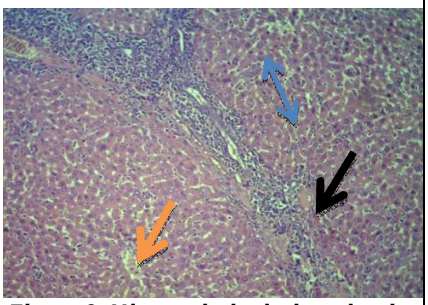

Figure 9: Histopathological section in the liver of immunized animal at 6 weeks post- treated with sodium nitrate showing mononuclear cells aggregation in the portal area (black arraw), lumen of dilated central vein (orange arraw) and sinusoids (bluearraw), H and E stain10X.

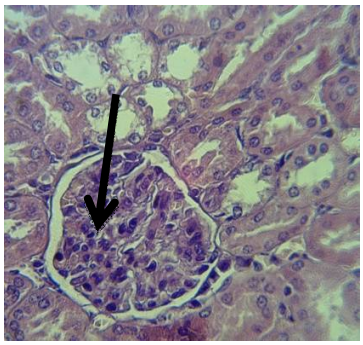

Figure 10: Histopathological section in the kidney of immunized animal at 6 weeks post- treated with with sodium nitrate showing marked inflammatory cells aggregation around glomerula with Buman space (black arraw), H and E stain 40X

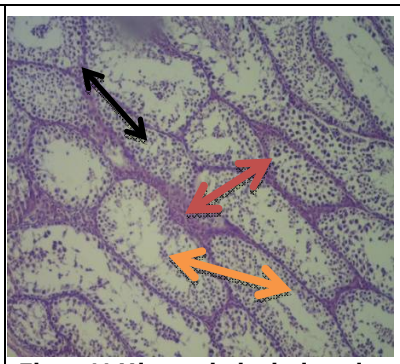

Figure11:Histopathological section in the testis of immunized animal at 6 weeks post-treated with sodium nitrate showing mildvaculardegeneration (black arraw) and few number of epididymal sperm (orange arraw) and marked inflammatory cells aggregation between the tubules(redarraw,) H&E stain 40X.

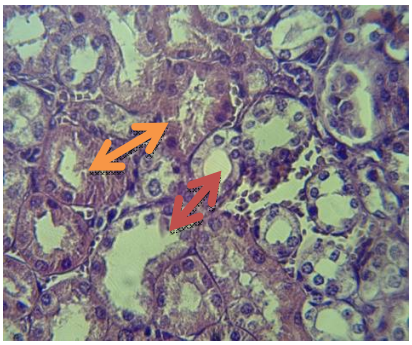

Figure12:Histopathological section in the kidney of immunized animal at 6 weeks post- treated with sodium nitrate showingcloudy swelling of renal tubular epithelium(black arraw); invaded with a number of red blood cells(orangearraw) and infiltration of inflammatory cell between renal tubule (red arraw),H&Estain x40.

Indian Journal of Natural Sciences www.tnsroindia.org.in ©IJONS

Vol.8 / Issue 49 / August /2018 *International Bimonthly* *ISSN: 0976 – 0997*

RESEARCH ARTICLE

Study Spectral Indices of Land Cover Around Al-Shari Lake and Produce Mapping by Using Remote Sensing Technique

Abdulrahman B. A[1]*, Fouad K. Mashee[2] and Sabah N. Kadim[3]

[1]Atmospheric Science Department, College of Science AL- Mustanseriya University, Iraq.
[2]Remote sensing unit, College of Science, University of Baghdad, Baghdad, Iraq.
[3]Atmospheric Science Department, College of Science AL- Mustanseriya University, Iraq.

Received: 04 May 2018 Revised: 03 June 2018 Accepted: 05 July 2018

*Address for Correspondence
Abdulrahman B. A
Atmospheric Science Department,
College of Science,
AL- Mustanseriya University, Iraq.
Email: Abdrahman29@yahoo.com

ABSTRACT

Remote sensing techniques were used to monitoring and classify the land cover for Al-shari lake region, to execute this goal in search applied Landsat satellite imagery used in study simultaneous decade periodic. After obtaining Landsat satellite images and performing some digital image processing for the purposes required by the research, the Supervised Classification technique was applied to the satellite images depending on the visual interpretation and geographical maps of the study area by using GIS 10.5 and ERDAS IMAGINE 2014. Six classes within the study area were identified, during the extended period (1996-2017) in winter and summer, are represented by high density arable land and permanently irrigated, low density arable land mixed with fallow land, sand dunes and rocks, abandoned land and saline, Sand plains and water bodies in order to verify the accuracy of the classification results, the values of the spectral indices were calculated of which (NDVI, SAVI, NDWI). The results showed In winter season high density arable land and permanently irrigated formed 13.0% and increased to 13.3% in 2017.Low density arable land mixed with fallow land formed 54.5% in 1996 and decreased to 51.6% in 2017 and in summer season high density arable land formed 4.8% in 1996 and increased to 5.5% in 2017. Low density arable land mixed with fallow land formed 48.8% in 1996 decreased to 21.8% in 2017. In winter sand dunes and rocks formed 7.7% in 1996 and increased to 14.6% in 2017. Abandoned land and saline formed 0.8% in 1996 increased to 2.8% in 2017. Sand plains formed 23.0% in 1996 decreased to 19.1% in 2017 and in summer sand dunes formed 6.7% in 1996 and increased to 18.8% in 2017. Abandoned land and saline formed 2.0% in 1996 decreased to 1.9% in 2017. Sand plains formed 36.9% in 1996 increased to 50.1% in 2017. Water bodies in winter formed 1.0% in 1996 and decreased to 0.8% in 2017 and in summer formed 0.9% in 1996and increased to 1.9% in 2017.

Key word: Al-shari Lake, Landsat satellite, RS, GIS, ERDAS, Spectral indices.

INTRODUCTION

Several studies have been conducted to monitor changes in land cover, Through the use of some means of assistance, including remote sensing [1]. The use of remote sensing and GIS techniques is an effective means of detecting desertification processes, including changes in natural vegetation cover, land use and soil [2]. One way to monitor the extent of change in the natural resources of land use and land cover is to use satellite images [3], these satellite images consist of columns and rows in the form of small squares clustered alongside It is called the cell or pixel Each cell has a number representing the amount of radiation reflected from the surface area of the Earth represented by this cell, information is collected in the form of several spectral bands by special sensors [4]. Land cover refers to all monuments on the surface, whether industrial or natural, such as buildings, lakes, trees, water and crops, a measure of the change in the surface of the earth due to the physical and human environment [5]. The basic idea in the use of remote sensing techniques in land cover classification is based on changes in the radiation values reflected from the surface received by the sensor. These changes are due to different land cover type and its association with certain factors such as different weather conditions, differences in sun angle or soil moisture variation [6]. In this study, a number of spectral indicators were used for the purpose of diagnosing and determining the nature of land cover in the study area. Some of them helped isolate certain elements from each other with high accuracy.

MATERIALS AND METHODS

Study Area

The study area is located in northern Iraq in the province of Salah al-Din near Beji town, between 35.00°N and 34.45°N latitudes and 43.60°E and 44.50°E longitudes. It is bordered by the Tigris River on the western side and Hamrin Hills on the east and north-east side either on the south and south-east, the Alaiden River is bounded by it. The most important natural phenomena in the region is the existence of Lake Shari and the presence of sand dunes, the climate of the region is a desert climate, as the summer Strong dryness and high temperature. The rain in the study area is very low and volatile. The region is economically important as its people practice agriculture, especially grains such as wheat, barley and maize, depending on the style of irrigation agriculture [7]. and the figure (1) show the study area location

Data Source and Processing

Four satellite images were used in this study, obtained from Landsat 5 and Landsat 7 satellites which carry sensors (TM, ETM+) respectively. These images obtained from USGS website [8]. They were taken in different dates in the summer and another in winter as shown in the table (1). Some processors have been performed using GIS 10.5 and ERDAS Version 14.00.0. Such as the geometric correction was done using the image to image method, depending on another satellite image that is highly accurate and known geographic coordinates, so that all the features have known coordinates and have a projection system that is similar to the corrected image used in the debugging process and radiometric correction was performed using ERDAS Version 14.00.0. by converting the data to Radiation units are known to facilitate comparison of data. Then it was merging of many bands of satellite images to produce new colored image (RGB) for both sensors (TM, ETM+) and spectral bands were merged (NIR, Red, Green) as shown in the table (2).

Satellite image analysis

After the composites of spectral bands and Satellite images processing we do some analysis on satellite image:

Classification Processes

The classification is the most important step in digital image processing, as it is the ultimate goal of these processes. Information is obtained from the image after adjustments, where it can be defined as an organizational means of aggregating similar categories that is, the process of converting the image into an objective map containing information about the phenomena in the area to be categorized, where the pixels are distributed to groups or categories according to the digital number spectrum standards of these pixels [9]. The classification process can be divided into two parts,

Supervised Classification

This method of classification requires the presence of training samples for each type expected in the area under study. In this way, each unit of image is classified on the basis of its proximity and its compatibility with the training samples in terms of spectral response and some statistical calculations.

Unsupervised Classification

This type of classification lack training sample and we do not need prior information about the study area and does not require knowledge of the number of land covers, but algorithms are used to group image elements with similar spectral properties in the form of spectral classes [10], the Supervised Classification technique was applied to the satellite images .six classes within the study area were identified, representing three types of land cover (vegetation, soil, water) for years (1996-2017) in summer and winter, are represented by high density arable land and permanently irrigated, low density arable land mixed with fallow land, sand dunes and rocks, abandoned land and salines, Sand plains and water bodies (Rivers and canals) each class is given a specific color for the purpose of distinguishing it. The following figures illustrate the process of supervised classification, The following table 3 and figure 6 illustrates the areas of land covers was Classified In (Km^2).

Spectral Indices

Some spectral indices have been used to identify the land cover patterns prevailing in the study area and for specific species to overcome some overlap between land cover types that exhibit close values of spectral reflectivity, particularly between Low density arable land and high density arable land. The spectral indices used are:

Normalized Difference Vegetation Index (NDVI)

It is used for the purpose of diagnosing, identifying and removing the condition of overlap between the vegetation class and the other types of land covers, which are often overlapping where it is the most accurate method of digital processing of satellite images in the presentation of vegetation. It is based on the fact that plants have high reflectivity in the range of near-infrared wavelength and low reflectivity in the range of red wavelength. It represents the ratio of the difference between the spectral reflections at the near- infrared wavelength and red wavelength on their total, is represented by the following equation [11]:

NDVI= (NIR-red) / (NIR+ red) ……..…..... (1)

Results are displayed in the following images below, shown figure 7 and 8.
The area of vegetation cover was calculated in each image taken, as the table 4 show.

Soil Adjusted Vegetation Index (SAVI)

Developed by Huete at the University of Arizona, United States, in the late 1980s. The idea was to have a global model for monitoring soil and determination of variation in vegetation from remotely sensed data it is similar to Normalized difference vegetation index but with addition of adjustment factor (L) and its value can vary between 1.0 for low vegetation densities, 0.5 for intermediate densities, and 0.25 for high densities, it is represented by the following equation:

SAVI= (NIR-red) / (NIR+ red+ L). (1+L) **…….** (2)

Where;

L=0 the NDVI = SAVI.

Results are displayed in the following images below, shown figure 9 and 10. The following table 5 and figure 11 shows land covers areas in each image taken.

Normalized Differences Water Index (NDWI)

The NDWI was concluded using the same principle (NDVI) where the spectral reflectivity of the water is high in the range of the green wavelength (0.52-0.60 µm) and low in the in the range of near-infrared (0.76-0.90 µm). The values of have a range of (+1 to -1). Negative values are an indicator of the absence of water covers in the area, while positive values are indicators of the presence of water cover. It is used for water body mapping and drought monitoring and it is sensitive to change in water content. (NDWI) is represented by the following equation, [11]:

NDWI = (green - NIR) / (green + NIR) ……, (3)

Results are displayed in the following images below, shown figure 12 and 13.

The area of water bodies was calculated in each image taken in the table 6.

CONCLUSION

The process of identifying and detecting the change in land cover is important in monitoring changes and developments in land cover and determining the factors affecting them. Show through the analysis of Satellite images Clear changes in land cover area during twenty years between (1996-2017) which included changes in vegetation and water as well as soil. Where the results showed the area of agricultural land in winter is greater than its area in the summer. In winter season high density arable land and permanently irrigated formed 1203.5 Km^2 and increased to 1228.1 Km^2 in 2017.Low density arable land mixed with fallow land formed 5039.2 Km^2 in 1996 and decreased to 4770.8 Km^2 in 2017 and in summer season high density arable land formed 445.3 Km^2 in 1996 and increased to 507.3 Km^2 in 2017. Low density arable land mixed with fallow land formed 4506.4 Km^2 in 1996 and decreased to 2018.5 Km^2 in 2017. Either barren land with natural vegetation we note that there is no regularity in their areas due to human and climatic interaction. In winter sand dunes and rocks formed 713.5 Km^2 in 1996 and increased to 1345.5 Km^2 in 2017. Abandoned land and saline formed 181.9 Km^2 in 1996 increased to 175.8 Km^2 in 2017. Sand plains formed 2123.2 Km^2 in 1996 decreased to 1767.7 Km^2 in 2017 and in summer sand dunes formed 617.6 Km^2 in 1996 and increased to 1737.1 Km^2 in 2017. Abandoned land and saline formed 181.9 Km^2 in 1996 decreased to 175.8 Km^2 in 2017. Sand plains formed 3409.2 Km^2 in 1996 increased to 4627.3 Km^2 in 2017. Water bodies which include rivers and canals were different clearly in its areas; they rely on water releases from the main sources of Turkey and Iran. These differences reflect the nature of the climatic conditions and lack of rainfall that led to drought as well as a decrease in the amount of water from the main sources represented by Iran and Turkey. In winter formed 88.3in 1996 and decreased to 86.3in 2017 and in summer formed 78.6 Km^2 in 1996and increased to 172.9 Km^2 in 2017.

REFERENCES

1. Jumaili, Meshaal Mahmoud Fayyad. 2012. Study of vegetation and water cover changes in Ramadi district using remote sensing technologies and GIS. Anbar Journal of Agricultural Sciences, Vol. 10, No.1
2. Albaluwi, K. and L. Kumur. 2013.Using remote sensing to detect, model and map desertification: A review. Food, Agriculture and Environment Vol.11 (2): 791-797
3. Ismail, A. S., Dhahi, K.Z., Sabar A., 2012. The use of digital processing and geographic information systems in the diagnosis of soil units for the West of Makhoul in the province of Salah al-Din. Tikrit University Journal of Agricultural Sciences. Vol. 12, No. 1.
4. Hassan, E. M., 2007. "Digital Image Processing in Remote Sensing", Research Center, College of Engineering, King Saud University, Riyadh, Saudi Arabia.
5. Lillesand, T., and R. W. Kiefer., 2000. "Remote Sensing and Image Interpretation", forth Edition. John Wiley and Sons, New York, USA.
6. Ali, J. T., Ali H. T. and Qassim M. S., 2015. Identification of desertification zones using remote sensing technology and GIS in Muthanna Governorate . Kufa Journal of Agricultural Sciences Vol.7. No.1
7. Al janabi, M. H., 2008. "hydrochemistry of the unconfined aquifer and the relationship of unsaturated zone sediments on ground water quality in Tikrit-Samara", PhD Thesis, Department of geology Science, College of Science, University of Baghdad.
8. http://earthexplorer.usgs.gov.
9. Hassan, E. M., 2007. "Digital Image Processing in Remote Sensing", Research Center, College of Engineering, King Saud University, Riyadh, Saudi Arabia.
10. Mohammed, W., 2013. "Introduction to Remote Sensing and its Applications" Department of Environmental Architecture, College of Architecture and Planning, University of Dammam, Dammam, Saudi Arabia.
11. Khalaf, I. A., Jassem K. 2013. Calculation of NDVI values and plant evidence to assess the degradation status of pasture lands using remote sensing techniques. Tikrit University Journal of Agricultural Sciences. Vol.13. No.1.

Table (1): Information on the Images of Landsat (5 and 7) Used in the Study.

Rank	Satellite type	Date	Sensor	Resolution
1	LANDSAT-5	19/3/1996	TM	30
2	LANDSAT-5	11/8/1996	TM	30
3	LANDSAT-7	17/3/2017	ETM+	30
4	LANDSAT-7	21/8/2017	ETM+	30

Table (2): composites bands of satellite Image (RGB).

Resolution	TM and ETM+	Color
30	Band-4	NIR
30	Band-3	Red
30	Band-2	Green

Table 3: Areas of Land Covers in (Km^2).

Date of image	High density arable	Low density arable	Sand dunes and rocks	Abandoned land and saline	Sand plains	Rivers and canals	sum
19/03/1996	1203.5	5039.2	713.5	71.3	2123.2	88.3	9239.0
11/08/1996	445.3	4506.4	617.6	181.9	3409.2	78.6	9239.0
17/03/2017	1228.1	4770.8	1345.5	40.6	1767.7	86.3	9239.0
21/08/2017	507.3	2018.5	1737.1	175.8	4627.3	88.3	9239.0

Table 4: Areas of Vegetation Cover Extracted From NDVI for Images in (Km²).

Date of image	Area of vegetation cover in (Km²).
19/03/1996	2138.3
11/08/1996	588.4
17/03/2017	1555.6
21/08/2017	600.3

Table 5: The Calculated Land Covers Extracted From SAVI Images in (Km²).

Date of image	Dense vegetation	Low vegetation	Water
19/03/1996	105.9	3187.1	93.8
11/08/1996	59.9	492.1	70.4
17/03/2017	85.2	2463.4	90.6
21/08/2017	98.5	714.4	158.2

Table 6: Area of Water Bodies Extracted From NDWI for Images in (Km²).

Date of image	Area of water bodies in (Km²).
19/03/1996	136.9
11/08/1996	70.8
17/03/2017	145.2
21/08/2017	154.2

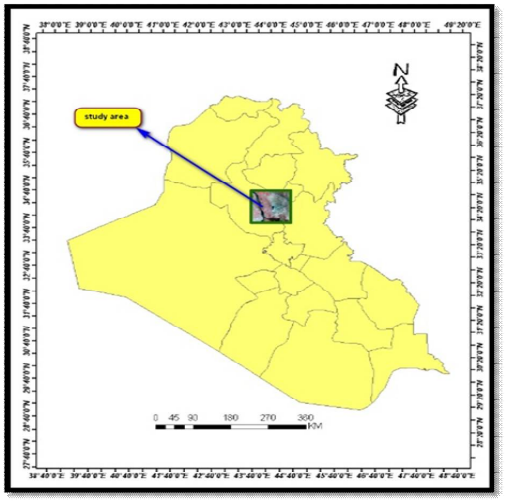

Figure (1): Location of Study Area

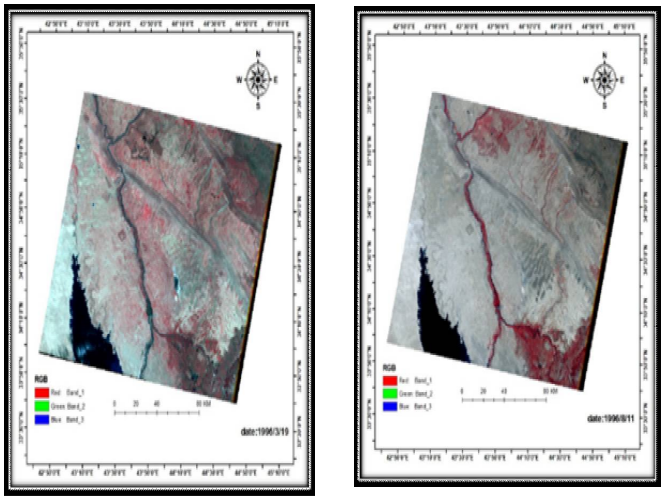

(a) **(b)**

Figure 2: (a) Color composite image of 1996 for study area in winter season in march, (b) Color composite image of 1996 for study area in summer season in august.

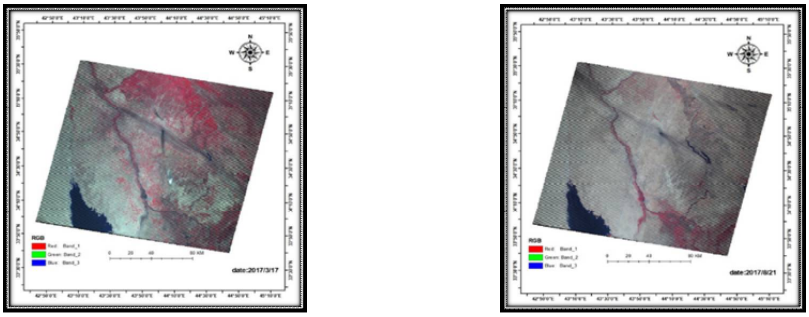

(a) **(b)**

Figure 3: (a) Color composite image of 2017 for study area in winter season in march(b) Color composite image of 2017 for study area in summer season in august.

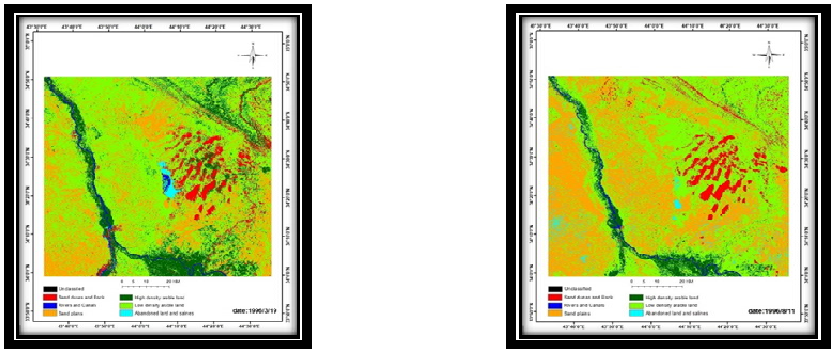

(a) **(b)**

Figure 4: (a) Applying supervised classification on image(1996) for study area in in march (b) applying supervised classification on image (1996) for study area in august

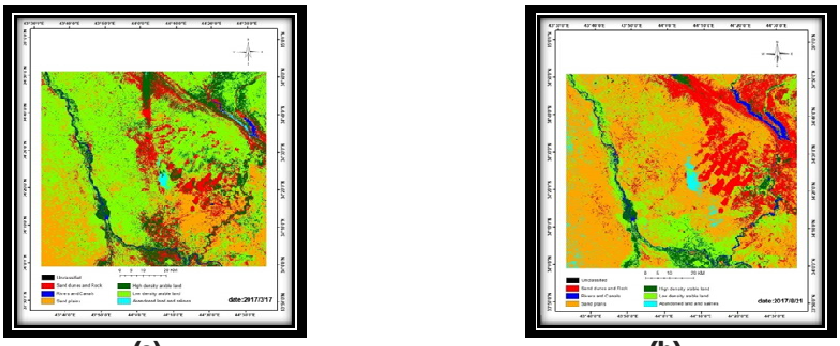

(a) **(b)**

Figure 5: (a) Applying supervised classification on image (2017) for study area in in march (b) applying supervised classification on image (2017) for study area in august.

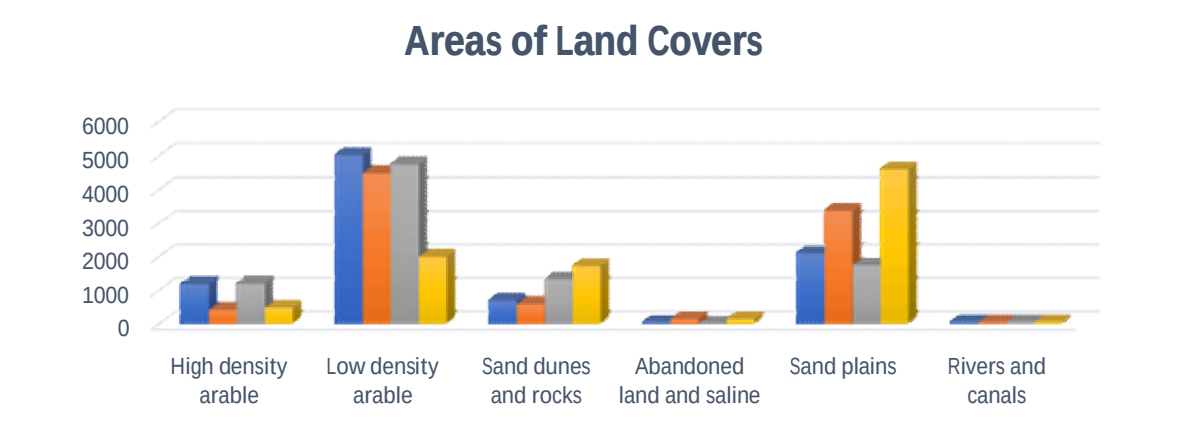

Figure 6: The temporal variation in the areas of land covers during the years of study using supervised classification

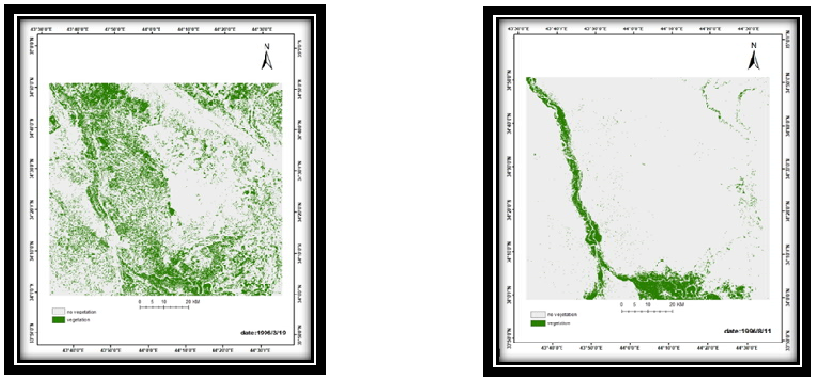

(a) **(b)**

Figure 7: (a) NDVI images on (1996) for study area in March (b) NDVI images on (1996) for study area in august

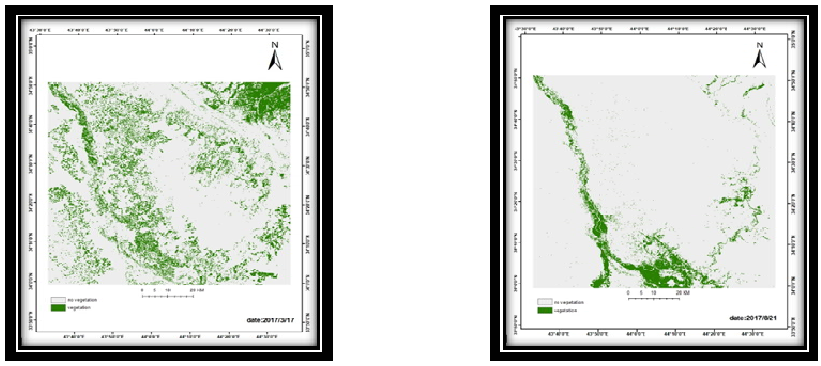

(a) **(b)**

Figure 8: (a) NDVI images on (2017) for study area in March (b) NDVI images on (2017) for study area in august.

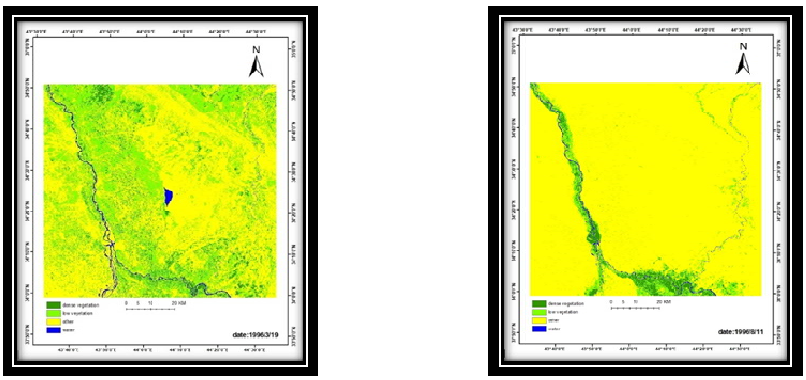

(a) **(b)**

Figure 9: (a) SAVI images on (1996) for study area in March (b) SAVI images on (1996) for study area in august

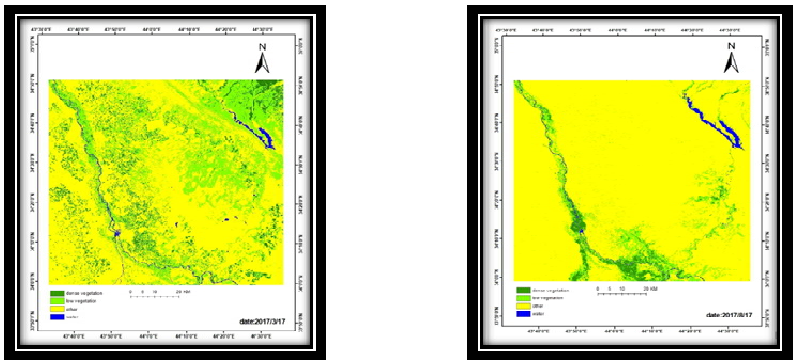

(a) **(b)**

Figure 10: (a) SAVI images on (2017) for study area in march (b) SAVI images on (2017) for study area in august

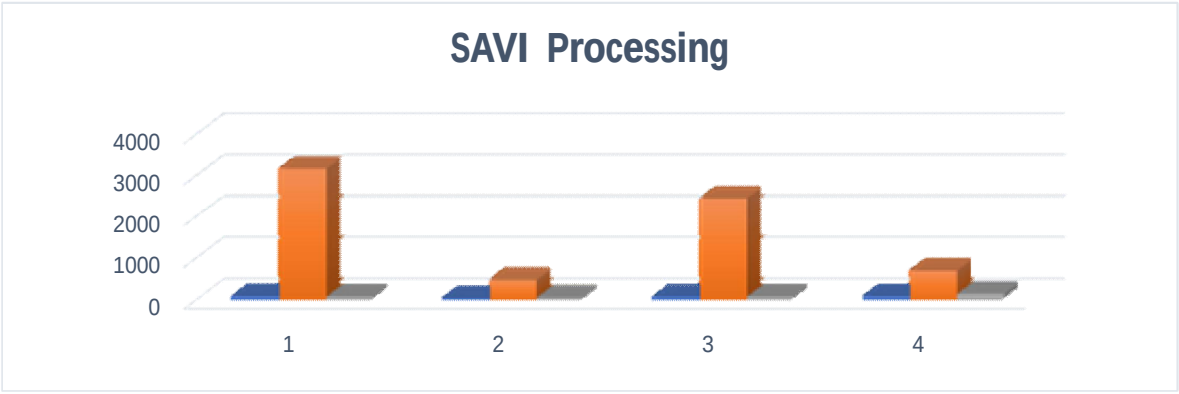

Figure 11: The temporal variation in the areas of land covers during the years of study using SAVI guide.

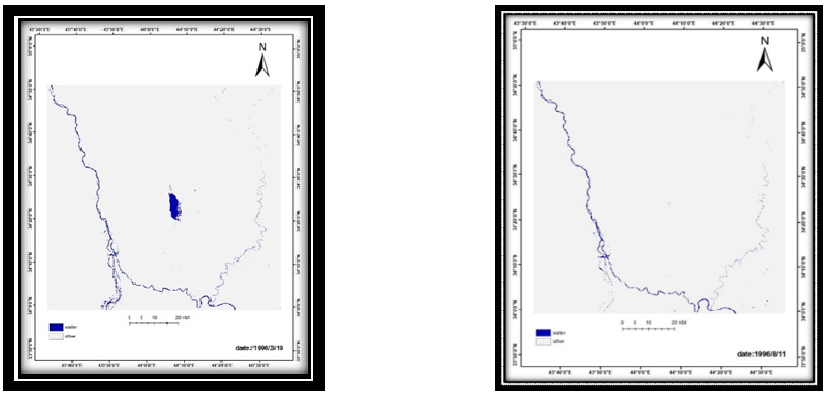

(a) **(b)**

Figure 12: (a) NDWI images on (1996) for study area in march (b) NDWI images on (1996) for study area in august.

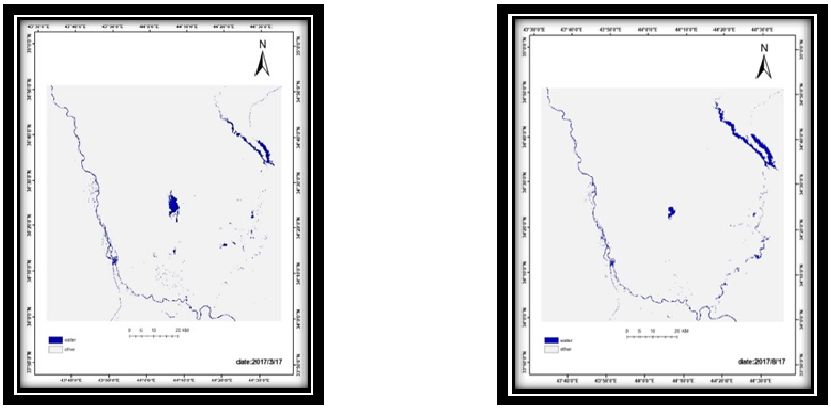

(a) **(b)**

Figure 13: (a) NDWI images on (2017) for study area in march (b) NDWI images on (2017) for study area in august.

Indian Journal of Natural Sciences www.tnsroindia.org.in ©IJONS

Vol.8 / Issue 49 / August /2018 *International Bimonthly* *ISSN: 0976 – 0997*

RESEARCH ARTICLE

Phylogenetic Study of Camel Trypanosomiasis in AL- Najaf Province, Iraq Based on Microscopic Examination and PCR

Jihad T. Aboed[1]*, Azhar Ali Faraj[2] and Ilham A. Khalaf[3]

[1,2]Department of Parasitology, College of Veterinary Medicine, University of Baghdad, Baghdad , Iraq.
[3]Al-Razi Center for Research and Diagnostic Kits, Ministry of Industry and Minerals, Baghdad, Iraq.

Received: 04 May 2018 Revised: 05 June 2018 Accepted: 07 July 2018

***Address for Correspondence**
Jihad T. Aboed
Department of Parasitology,
College of Veterinary Medicine,
University of Baghdad,
Baghdad, Iraq.

ABSTRACT

The present study, *Trypanosomaevansi* was detected and identified in local camels in AL-Najaf province in Iraq by microscopic examination then confirmed by molecular diagnosis for *T.evansi* using a polymerase chain reaction technique (PCR).This Study is conducted during the period from November 2016 to May 2017 in different areas of AL-Najaf province. A total of 210 blood samples are collected from camels different ages and sexes.Resultsshowed infection rate was higher in adults than young was 15.86% and 7.69% respectively. While the infection rate according to sex was differentiated, it was higher among females than males, it was16.37% and 9.57% respectively. The rate of infection was variation during the months, high infection rate was in May and April and November, it was 30%, 23.33% and 20% respectively. The rate of infection by use the PCR was 90%, molecular assay can be utilized as a powerful sensitive tool for the detection of *T.evansi* in camels, and as a superior substitute to the conventional technique, phylogenetic tree analysis of *T.evansi* has been disclosed in this study.The first study for molecular technique of*Trypanosomaevansi* in camels in Iraq.

Key word: *Trypanosomaevansi,* PCR, phylogenetic tree, Camels, Iraq.

INTRODUCTION

Trypanosomiasis (surra) is a major vector-borne disease of camels caused by protozoan parasites *Trypanosomaevansi* (Moghaddaret al., 2009). The disease transmitted mechanically by the bites of haematophagous flies (tabanids and stomoxes), is endemic in Africa, Asia, South American (Eyob and Matios, 2013). Camel trypanosomiasis is an acute, chronic disease of camel leading to anemia, intermittent high fever marked , progressive loss of body weight , pale mucous a occasionally abdominal odema and death. It causes economic losses as a result of reduced productivity and

abortion in all age groups of pregnancy period (Tadesseet al., 2012). *T.evansi* is usually detected by microscopically examination (wet blood film , stained blood smears and buffy coat examination) and serological tests, however, microscopically observation requires skilled techniques and has poor sensitivity , the serological tests yield false positives and negatives result of*T.evansi* antigenic variation and it cannot differentiate between treated case and infected (Sonia et al., 2015). Consequently, there is a need more sensitive diagnostic test, therefore a molecular technique, especially polymerase chain reaction (PCR) has been developed in order to overcome the problems faced with conventional and serological techniques. The study was designed to detection of *T.evansi* in Camels in AL-Najiaf province by using conventional (wet film and stained blood) and molecular methods.

MATERIALS AND METHODS

Specimens Collection

This study is conducted during the period from November 2016 to May 2017 in different areas of AL-Najaf province. A total of 210 blood specimens are collected from camel's different ages and sexes. Five ml of blood sample were collected from the Jugular vein or during the slaughtering of animals and kept in tubes containing anti-coagulant (EDTA). All samples were transferred in cooling conditions to the laboratory to conduct the necessary tests to determine the infection with *T.evansi.*

Microscopic Examination

Blood smears examined for detection of parasite between red cells under light microscopy by X100 oil-immersion (Chaudhri and Gupta, 2003).

DNA Extraction and PCR assay

Extraction of DNA from 100 bloodSpecimenscollected, Genomic DNA of *T.evansi*isolate was extracted by using (tissue and blood DNA extraction kit Geneaid. USA) according to manufacturer's instructions, primer were used in this study were obtained from IDT company (18sRNA). These primers were prepared according to the information of the company (Table.1).

Statistical Analysis

Statistically analyzed by Chi-square tests for significance using SPSS 15 version.

RESULTS

Prevalence of *T.evansi* Cases According to age

The microscopic examination showed that *T.evansi* between red blood cell of infected camels figure (1). The percentage of infection was showed that among (210) *T.evansi* suspected cases were examined microscopically 13.33%were given positive result.The major of *T.evansi* cases were among the older Camels (> 3 years) which recorded the highest percentage 15.86%while the lowest 7.69%were the young's (< 3 years) with significant P<0.05 differences between the rate of infection, camels(Table 2).

Prevalence of *T.evansi*according to Sex

The result showed that revealed significant P<0.05 differences between the rate of infection, the major of *T.evansi* cases were amongfemale which recorded the highest percentage 16.37%. While the lowest percentage 9.57%were the male (Table2).

Prevalence of *T.evansi* Cases According to Months

The results showed that high positive case in May, April (2017) and November (2016), infection rate was 30%, 23.33% and 20% respectively. and the lower infection rate in December (2016), January and March (2017). There is no infection in February (Table3).

Prevalence of *T.evansi* Cases by Using PCR Amplification

The result showed thatPCR analysis of the DNA isolated from 100 blood samples has high rate of infection with *T.evansi* (90%) (figure2).

Sequence alignment of 18s RNA Gen

Amplification and sequence analysis of 18s 540 bp of the rRNA gene of each isolate was successfully achieved. A BLAST search of the sequenced *T.evansi* 18s RNA Gen fragment (540 bp).The results of the 16SrRNA gene sequence analysis were summarized in figures(3,4) Table (4), indicating the number and location of mutations, and showed that there were 7 mutations in 10 samples in this gene. More than one mutation was recorded in each sample and this may have different effects. In the type of genetic code; and then change in amino acids at translation.

Phylogenetic analysis of the 18s gen

To study the sequences recorded in this study .The sequences with the strains recorded in the databases were described using the Bio Edit program. The evolutionary relationship was also plotted using molecular sequences with the sequences recorded in the 18SrRNA databases using the MEGA 6.06 program. The gene is suitable for the development of evolutionary relationships by using sequencing in the determination of cluster relationships, because of the variation in single gene sequences (18SrRNA) can extend between 0.1.

Analysis ofphylogenetic the 18s gen sequences by Neighbor-Joining tree method, revealed 18s RNA, 29J 18Srna, 7J 18sRNA and 37J 18sRNA was closely related to gather in one branch. While 6J 18s RNA and 39J 18sRNA in one branch. Also 36J 18sRNA. 38J 18sRNA .and 35J 18sRNA associated to gather. While 8J 18sRNA alone in one branch. These findings are in agreement with those of (GenBank Accession Number KY114579.1) for *T. evansi* isolated from India,(GenBank Accession Number JN896755.1 and JN896754.I)for *T. evansi* isolated from Iran respectively and (GenBank Accession Number AB551922.1 and AB551921.1) for *T. evansi* isolated from Egypt respectively. The results of present study different fromisolate of China (GenBank Accession Number KU552346.1).Japan (GenBank Accession Number D89527.1).Thailand (GenBank Accession Number AY912271.1) and Sudan (GenBank Accession Number LC149491.1 and LC199490.1).

DISCUSSION

Parasitic diseases have severely hindered development of livestock production in many Countries; trypanosomiasis is the most widely distributed. The bulk of these diseases are caused by vector-borne Protozoa. Transmission of blood parasites could take place at any time by biting flies which was noticed in large numbers (Barghashet al., 2014).

The present study recorded that rate of infection by *T.evansi* in Camels examined by microscopic examination using Giemsa stain was 13.33% agree with previous study in Iraq by Awkati and AL-Katib (1972) when they recorded the rate of infection was 11%. The studies in others countries also recorded different results by using microscopic examination included 2.1% in Iran by Khosraviet al (2015), 6% in Sudan Ali et al., (2011) and 0.7% In Pakistan (Tehseenet al.,2015). Difference in above results may be attributed to differences of environmental and climatic conditions, number of samples was examined, methods used in their diagnosis, density of vectors and poor animals health. With regard to the effect of age on trypanosomiasis, there was considerable variation in values within age using blood film, the results of present study showed that the highest rate of infection in adult camels more three years was 15.86%, while the lowest rate in young camels less than three years was 7.69%. The results agree with study in Egypt done by Sobhyet al., (2017) was recorded 25.8% prevalence infection in adult camels compared with young animals, it was 14.6%and in Saudi Arabia AL-Salameenet al., (2016) was recorded 17.5% in adults and 4% in young. The high infection rates in the in adult camels may be due to heavy stress through their use for transportation of goods, poor management, immune status of animals which depressed with progressive in age and infection with disease that may predisposed to *T.evansi* (Sobhyet al., 2017).

The results of present study showed that the percentage of infection in females was 16.37higher than in males was 9.57%. The results agree with Bhutto et al., (2010) in Pakistan, recorded 15.79% in females while in males the rate of infection was 9.84 %. Also agree with Barghashet al., (2014) was recorded 23.6% in females and the lower rat was in males 14.7%. The high prevalence of trypanosomiasis in females may be due to exposure to stresses factor causes immune depression such as pregnancy and lactation period and also used to carried heavy things during migration from one thing from one place to another agree with (Bhuttoet al., 2010 and AL-Salameenet al., 2016).

Prevalence of trypanosomiasis increase during the months, *T.evansi* was observed high in May, April and November,infection rate was 30%, 23.33% and 20% respectively, then the infection rate was decrease during March, December, January and February the infection rate was 10%, 6.66%, 3.33% and 0% respectively. Agree with Elbalkemyet al., (2016) was detected seasonal variation, the results showed that at summer, spring, winter and autumn 61.8%,58.7%,31.3% and27.2% respectively of the examined camels. The highest prevalence of *T. evansi* during months of spring could be due to the increased activity of the vector during these seasons. The obtained data demonstrated that summer followed by spring was the most favorable season for the prevalence of *T.evansi* infection.This might be related to a higher risk of camels' exposure to *T.evansi* infection due to the increased density of vector populations at this time of the year coincides with (Barghash, 2005).

In present study using PCR technique showed that the rate of infection with *T.evansi* was 90% out of 100 blood samples. The result of this study was agree with Ali et al., (2011) was recorded 90% in Sudan. Also in Egypt (Ashour*et al.,* 2013). And disagree with El Wathiget al., (2016) who was recorded 25% in Saudi Arabia by using PCR. The first registration on *T. evansi* genotypes in camels in Iraq. Ten samples selected randomly and send to Macrogen, Inc. (Seoul, South Korea).A partial sequence of Iraqi isolates of 18s RNA gene was identical to the *T. evansi* sequences recoded from India (GenBank Accession Number KY114579.1),Egypt(GenBank Accession Number AB551922.1 and AB551921.1) and Iran (GenBank Accession Number JN896755.1 and JN896754.I) but varied similarity was seen when aligned with China (GenBank Accession Number KU552346.1), Japan (GenBank Accession Number D89527.1), Thailand (GenBank Accession Number AY912271.1) and Sudan (GenBank Accession Number LC149491.1 and LC199490.1). *T. evansi* sequences.

Phylogenetic analysis exhibited sequence divergence between *T.evansi* from Iraq and ten selected globally from GenBank. Molecular analysis, based on ribosomal gene sequences, is essential for phylogenetic analyses and determination of taxonomic identities of trypanosomes Phylogenetic trees based on different regions of rRNA analyzed in the present study were informative to infer phylogenies and relatedness of the Iraqi isolates. Based on 18S sequences, Iraqi isolates were clustered with those of *T. evansi* retrieved from Genbank. Were agreement with identical to *T. evansi* sequences from Egypt (GenBank Accession Number AB551922.1 and AB551921.1),India

(GenBank Accession Number KY114579.1) and Iran (GenBank Accession Number JN896755.1 and JN896754.I). There is no, similarity was seen when aligned with the isolate of China (GenBank Accession Number KU552346.1), Japan (GenBank Accession Number D89527.1), Thailand (GenBank Accession Number AY912271.1) and Sudan (GenBank Accession Number LC149491.1 and LC199490.1).

The rapprochement has taken place as a result of commercial trade in animal trade with other countries and also the wide host range of the parasite. Agree with (Mahmoud *et al* .,2013).The mutations occurred as a result of the biological and environmental conditions and lack of interest by the owners and veterinarians, this mutations which led to increase pathogenicity of *T.evansi* agree with (Carnes et al., 2015). describing that higher infection rate of *T. evansi* in Iraq showed the found of higher levels of intra-specific genetic variability of *T. evansi*while decrease genotype variability would be present in low endemic trypanosomiasis areas as a result of the elimination of virulent trypanosome strains agree with (Nakayimaet al ., 2012 and Abou El-Naga et al ., 2012). *T.evansi* is described as presenting genetic variability occur according to geographical distribution agree with (Barghashet al., 2016).Conclusions, this first study forPCR phylogenetic analysis of*T. evansi* in camels in theIraq. Phylogenetic analysis of 18S rRNA gene sequence of *T. evansi*isolate of Iraqian origin showed a close relationship to global isolates from Egypt, India and Iran. There is no sequences information for any 18S rRNA gene of *T. evansi*available from Iraq other than the sequence reported here.

REFERENCES

1. Abou El-Naga,TR; Barghash, SM; Abdel-Hafez, HM:Ashour AA; Salama M.S : Evaluation of (RoTat 1.2-PCR) assays for identifying Egyptian *Trypanosomaevansi* DNA. ActaParasitol.Globalis. 2012; 3: 01-06.
2. AliNOM; Croof H I MN; AbdallaHS: Molecular diagnosis of *Trypanosomaevansi* infection in *Camels dromedaries* from Eastern and Western regions of the Sudan, Emir. J. Food Agric. 2011; 23: 320-329.
3. AL-Salameen MA; BabikerIA; HousawiFM; El Hassan EM: The Effect of Camel (*Camelusdromedarius*) Sex and Age on Susceptibility to Blood Parasites Infection in AL-Ahsa Province of Saudi Arabia. J Vet SciAnim Husb.2016; 4: 2348-9790.
4. AshourAA; Abou El-NagaTR; BarghashSM; SalamaMS: Detection of *Trypanosomaevansi* DNA in naturally and experimentally infected animals using TBR1 & TBR2 primers, Experimental. Parasitol. 2013; 134: 109–114 .
5. AwkatyAJ;AL_katib GM:Trypanosomiasis in domestic animals of Iraq.J .Egyp. Vet. Med .Ass.1972; 32:203_206.
6. Barghash SM; Abou El-Naga T R; El-Sherbeny E A ;Darwish AM: Prevalence of *Trypanosomaevansi* in Maghrabi Camels (Camelusdromedarius) in Northern-West Coast, Egypt using Molecular and Parasitological Methods. ActaParasitol Glob.2014; 5: 125-132.
7. Barghash SM: Molecular Studies on *TrypanosomaEvansi* Infecting Camelsand Other Susceptible Animals in Egypt (M.Sc. thesis). Ain Shams Univ., Egypt.ActaParasitol Glob.2005;5: 125-132.
8. Barghash SM; DarwishAM; Abou-ElNaga TR: Molecular Characterization and Phylogenetic Analysis of *Trypanosomaevansi* from Local and Imported Camels in Egypt. J PhylogeneticsEvol Biol. 2016;4: 169_187.
9. Bhutto B; GadahiJA; ShahG; DewaniP; ArijoAG: Field investigation on the prevalence of trypanosomiasis in camels in relation to sex, age, breeds and herd size. Pak Vet J.2010;30: 175-177.
10. Carnes J; Anupama A; Balmer O; JacksonA ; Lewis M : Genome and Phylogenetic Analyses of *Trypanosomaevansi* Reveal Extensive Similarity to *T. brucei* and Multiple Independent Origins for Dyskinetoplasty. PLoSNegl Trop Dis. 2015; 9:333_345.
11. Chaudhri SS; Gupta SK: Manual of General Veterinary Parasitology. 1st edition .department of Vet .Parasit.College of Vet. Sci. Haryana Agicultural University India. 2003;Pp:46-47.
12. El WathigM; Faye B; Thevenon S; Ravel S ; Bossard G: Epidemiological surveys of camel trypanosomosis in Al-jouf, Saudi Arabia based on PCR and ELISA Emirates Journal of Food and Agriculture.2016; 28: 212-216.
13. Elbalkemy F A; Menazi A M; Selim A M; Wahba AA and El-Shazly YA:Seroprevalence of Camel (Camelusdromedarius) Trypanosomiasis, with special Reference to Gene Sequencing of Trypanosomaevansi in Sharkia Governorate, Zagazig Vet.2016; J. 44: 187-195.

14. EyobE; Matios L: Review on camel trypanosomosis (surra) due to *Trypanosomaevansi* Epidemiology and host response. Parasitology Department, Yabello Regional Veterinary Diagnostic Laboratory, Ethiopia. J. Vet. Med. And Anim. Heal.2013; 5: 334-343.
15. Khosravi A; Parizi M H; Bamorovat M; ZarandiM B;Mohammadi MA : Prevalence of *Trypanosomaevansi* in camels using molecular and parasitological methods in the southeast of Iran,J Parasit Dis. 2015; 39:422–425.
16. Mahmoud M; Elhaiga – Ahmed I; Youssefb; Amal K ; El-GayarcS: Molecular and parasitological detection of *Trypanosomaevansi* in Camels in Ismailia, Egypt J.Vet Par. 2013;198 : 214– 218.
17. MoghaddarN; Diantpour V: Distribution pattern of *Trypanosomaevansi*in camels (*Camelusdromedarius*) in Iran. J Camel Pract Res.2012; 16:73–75.
18. Nakayima J; Nakao R; Alhassan A; Mahama C; AfakyeK: Molecular epidemiological studies on animal trypanosomiases in Ghana. Parasit Vector. 2012; 5: 217.
19. Sazmand A; Eigner B;Mirzaei M; Hossein S; Timoghaddam H; Harl J; Duscher, G G; FuehrerHP; Joachim A: Molecular Identification of Hemoprotozoan Parasites in Camels (*Camelusdromedarius*) of Iran. Iran J Parasitol.2016;11: 4.568-573.
20. SobhyHM; BarghashSM; BehourTS; Razin E A: Seasonal fluctuation of trypanosomiasis in camels in North-West Egypt and effect of age, sex, location, health status and vector abundance on the prevalence. B J. B A S. 2017;6 : 64–68.
21. Sonia T; Nusrat J; Muhammad FQ; Marc D; Mirza, IS;Stijn D ; Philippe. B: Parasitological, serological and molecular survey of *Trypanosomaevansi* infection in dromedary camels from Cholistan Desert, Pakistan. Parast .Vect. 2015; 8: 415_433.
22. Tadesse A; Omar A; Aragaw K; MekbibB; Sheferaw D: A study on camel trypanosomosis in Jijiga zone, Eastern Ethiopia. J Vet Adv. 2012;2:216–219
23. Tehseen S; Jahan N; Qamar, M F;DesquesnesM;ShahzadM I; Deborggraeve S;BüscherP;Parasitological, serological and molecular survey of *Trypanosomaevansi* infection in dromedary camels from Cholistan Desert, Pakistan. Parasit Vector J. 2015; 8, 415.

Table (1): The Primers with their Sequences and Product Size

Primers	Primer sequence (5′ to 3′)		Product size (bp)	References
18S	F	GCG AAA CGC CAA GCT AAT AC	540	(Sazmand*et al* .,2016)
	R	ACG GCA CAA AAC TAC GTG		

Table (2): Showed Effect of Age on Infection by Microscopically Examination

Age	Total number	Positive	%
Young's(< 3 years)	65	5	7.69%
Adults (> 3 years)	145	23	15.86%
Total	210	28	13.33%
Chi-Square (χ^2)	---	---	4.0392 *

* (P<0.05).

Table(3):Showed rate of Infection According to Sex by Microscopically Examination.

Sex	Total Number	Positive	%
Male	94	9	9.57%
Female	116	19	16.37%
Total	210	28	13.33%
Chi-Square (χ^2)	---	---	4.015 *

* (P<0.05).

Table(4): Showed Rate of Infection During the Months by Microscopically Examination.

Months	Total number	Positive	%
November(2016)	30	6	20%
December	30	2	6.66%
January(2017)	30	1	3.33%
February	30	0	0%
March	30	3	10%
April	30	7	23.33%
May	30	9	30%
Total	210	28	13.33%
Chi-Square (χ^2)	---	---	9.021 **

* (P<0.05).

Table (5): Substitution of Amino Acid Sequence of 18SrRNA Gen in *T. evansi* isolated from Different Camels and Accession number of Local Isolates

Strain	Wilde type	Mutant type	Change in amino acid	Accession number
7 J-18s RNA	CAT	CCT	I /L	LC331314
	TGT	TGC	V / A	
	AGT	AAT	V /I	
	ACA	AAC	H / Q	
8 J-18s RNA	AAT	AAC	M / T	
	GAA	CAA	G / S	
	GGG	GAG	S / N	
	TAG	TAA		
6 J-18s RNA				LC331313
26 J-18s RNA	CAT	CCT	I /L	LC331316
	TGT	TGC	V / A	
	AGT	AAT	V /I	
	ACA	AAC	H / Q	
29 J-18s RNA	CAT	CCT	I /L	LC331317
	TGT	TGC	V / A	
	AGT	AAT	V /I	
	ACA	AAC	H / Q	
35J-18s RNA				LC331318
36 J-18s RNA	CAT	CCT	I /L	LC331319
37 J-18s RNA	TGT	TGC	V / A	LC331320
	AGT	AAT	V /I	
	ACA	AAC	H / Q	
38 J-18s RNA	CAT	CCT	I /L	LC331321
39 J-18s RNA				LC331322

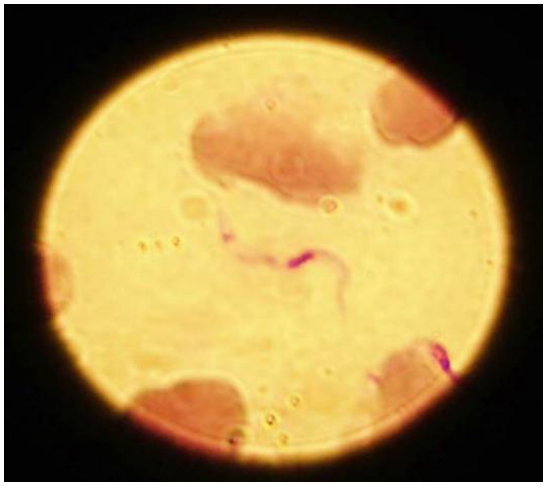

Fig (1):*T.evansi* show between camel red blood cells (X 100).

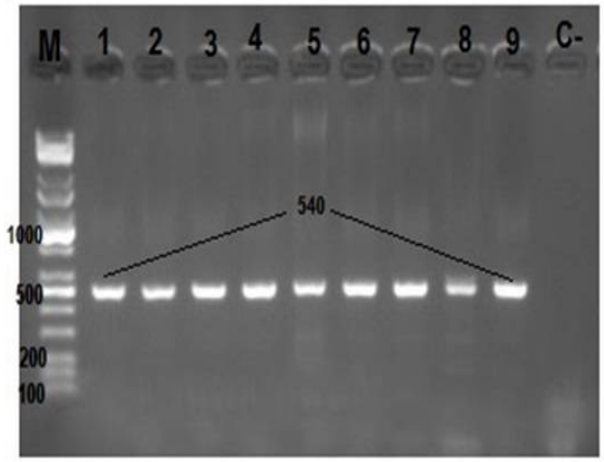

Fig (2): Gel electrophoresis of PCR product of *18s (*540bp), for*T.evansi*using 2% agarose gel at 6volt/ cm for 1 hour. Lane 1- 9: PCR product positive for 18s genes, C- : control negative, M: 1000-bp DNA marker.

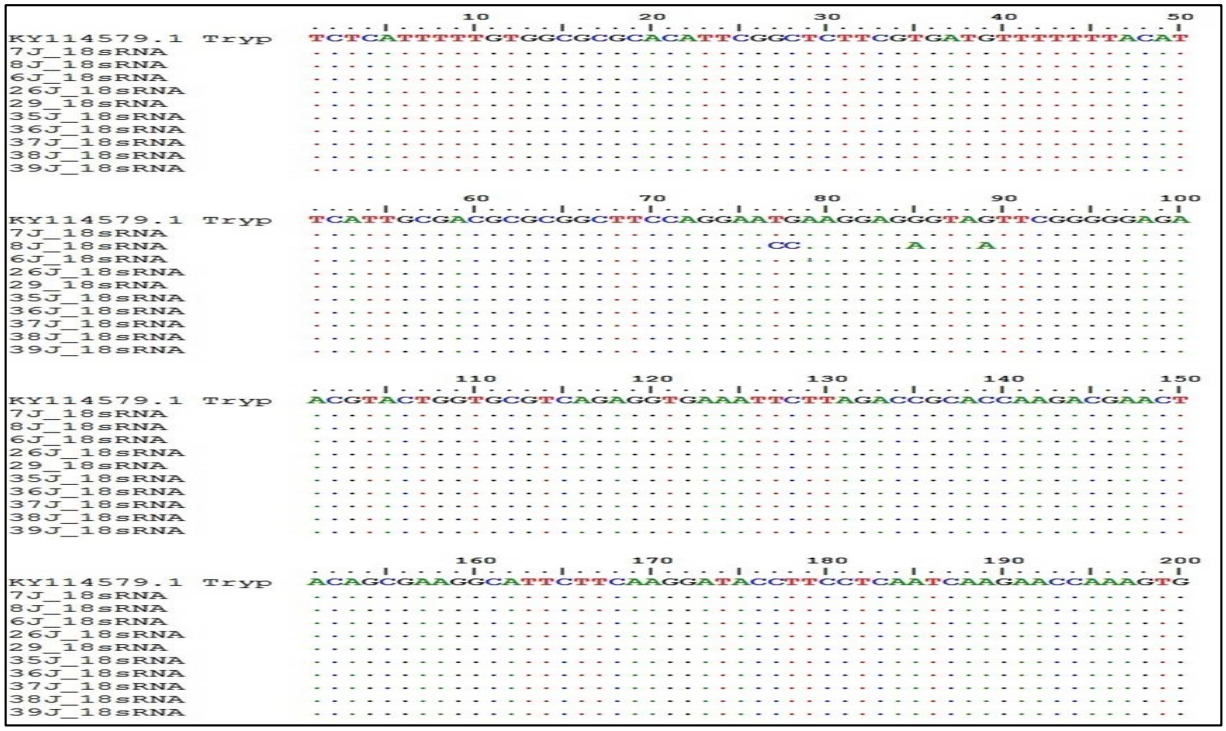

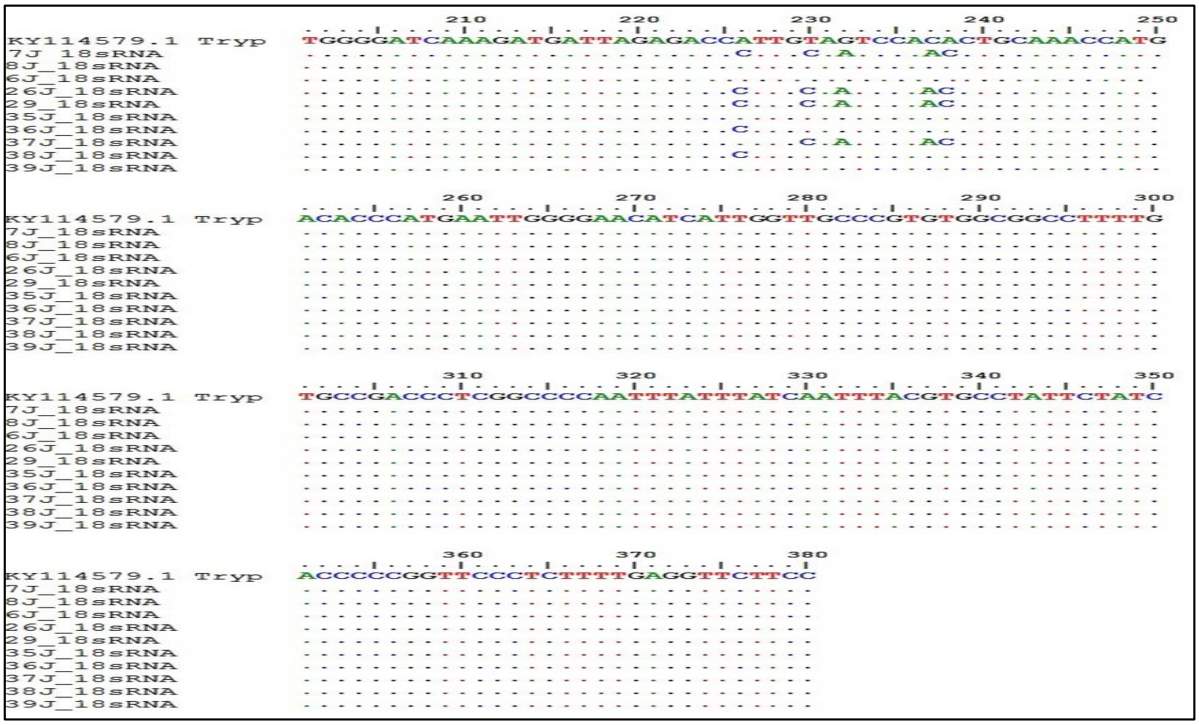

Fig (3): Molecular alignment of partial 18SrRNA DNA sequences of 10 Iraqi strain of T. evansi including reference strain of *T. evansi* recorded in GenBankacc. No (KY114579.1)

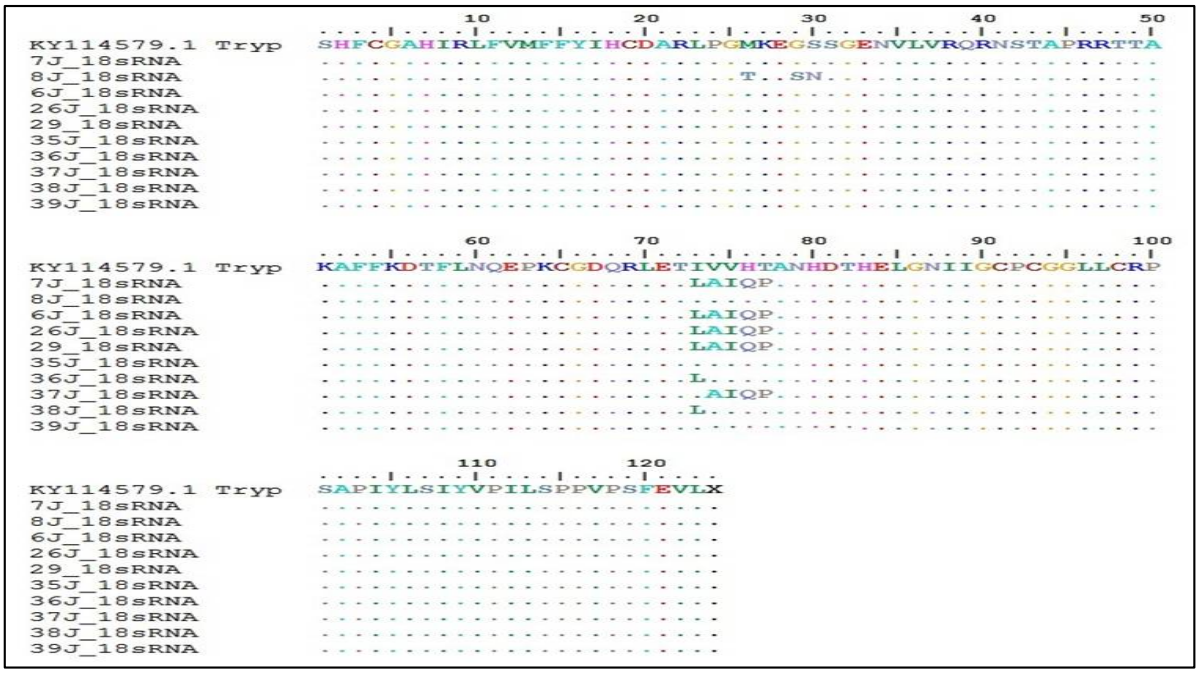

Fig (4): Alignment of partial 18srRNA peptide sequences (showing the mutations) from 10 Iraqi strains including the reference strain acc. No. KY114579.1.

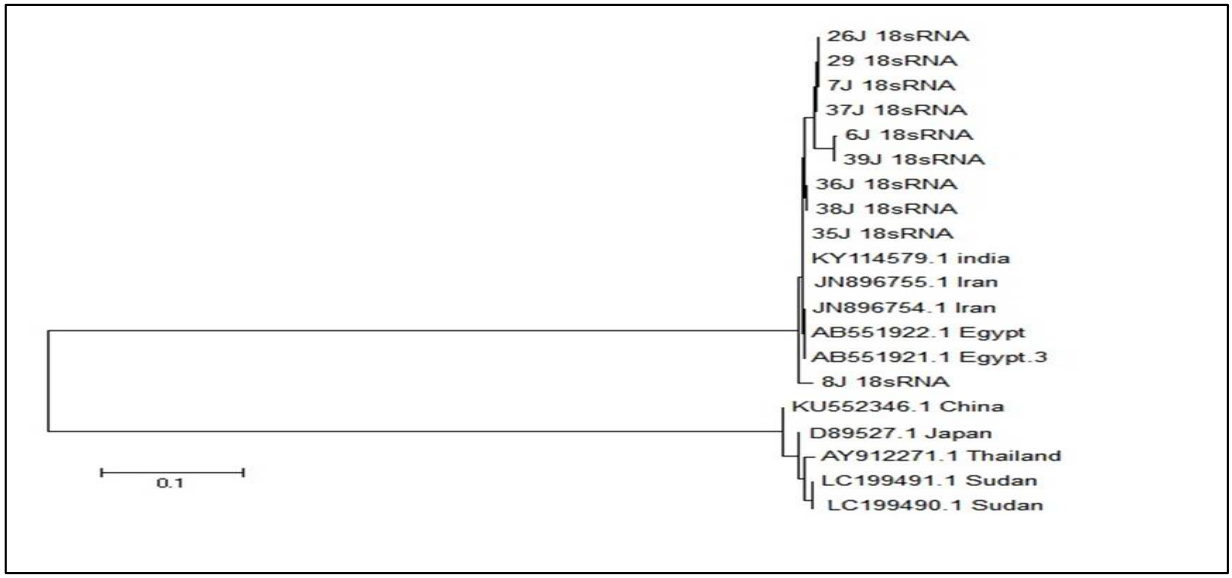

Fig (5): Phylogenetic analysis of the *18SrRNA* sequence of Iraqi isolates and sequences of strains reported from different parts of the world (available in public database; GenBank, EMBL and DDBJ), Neighbor-joining tree was built using bootstrapping with 1000.

Indian Journal of Natural Sciences *www.tnsroindia.org.in ©IJONS*

Vol.8 / Issue 49 / August /2018 *International Bimonthly* *ISSN: 0976 – 0997*

RESEARCH ARTICLE

The Pathological Changes of Internal Organs Causing by Nitrate Ion Experimentally in Mice

Zainab R. Zghair[1]*Salma S.AL- Anni[2] and Eman K. Khalel[3]

[1]Zoonosis Unit, College of Veterinary Medicine, University of Baghdad, Baghdad, Iraq.
[2]Ministry of science and Technology, Environment & Water office, Baghdad, Iraq.
[3]Public Health Department, Fallujah College of Veterinary Medicine, Baghdad, Iraq.

Received: 09 May 2018 Revised: 07 June 2018 Accepted: 10 July 2018

*Address for Correspondence
Zainab R. Zghair
Zoonosis Unit,
College of Veterinary Medicine,
University of Baghdad,
Baghdad, Iraq.

ABSTRACT

Twenty white mice, 7-8 week olds were randomly divided into two groups each group contain ten in both sexes, and treated with nitrate ion dissolved in distilled water (D.W) to prepare doses one of them 0.25 gram/10 ml. of D.W as follows: First group was administrated orally o.3 ml of nitrate ion (concentration was 0.25gm/10ml) daily for one month. Second group was administrated orally 0.3 ml of distilled water (D.W) daily for one month as control group. After day 30 post administration all animals were sacrificed, the results revealed that liver enzymes increased from normal values. Histopathological sections of some internal organs of animals that treated with nitrate ion appeared in lung hemorrhage filled the alveoli and infiltration of alveolar macrophage and infiltration of inflammatory cells like macrophage around the blood vessels showed in liver. hyperplasia of goblet cells of intestine, destruction of the villi and infiltration of inflammatory cells in the lamina propria, Necrosis in interstitial tissue in spleen, kidney appeared dilatation of urinary space , degeneration of the epithelia of renal tubules.

Key word:. Vessels, hemorrhage, lamina propria,

INTRODUCTION

Nitrate is a problem as a contaminant in drinking water due to its harmful biological effects. Methemoglobinemia can occure with high concentrations, and have been cited as a risk factor in developing gastric an intestinal cancer. Although there have been studies performed attempting to link nitrate consumption to various illnesses, only

methemoglobinemia, (also infant cyanosis or blue-baby syndrome) has been proven to result from ingestion of water containing high nitrate concentrations (Kross, 1993).Nitrogen constitute like (Nitrite, Nitrate and Ammonia) a core group of aquatic pollutants and concentrate in the tissues causing alteration at various functional levels of the organisms not only accumulate in water and sediment (Vutukuru *et al.,* 2005).Nitrite concentrations are comparable in the liver after nitrite intoxication. the high methaemoglobin values neither cause a cerebral hypoxic state nor alter the mitochondrial function in this organ; thus, anemic hypoxia damages the brain less than the liver(Arillo *et al.,* 1984). pathological lesions in pancreas of treated with nitrate ion revealed the exocrine region and islets of Langerhans with damaged due to necrosis, and congestion of blood vessel.(AL- Anni *et al.,* 2016),so this study was aimed to the pathological changes of some internal organs by nitrate ion.

MATERIALS AND METHODS

Nitrate Ion Preparation

Nitrate ion dissolved in distilled water (D.W) to prepare doses one of them 0.25 gram/10ml. of D.W

Experimental Design

twenty white mice, 7-8 week olds were randomly divided into two groups each group contain ten in both sexes, and treated as follows:

1. First group was administrated orally o.3 ml of nitrate ion (concentration was 0.25gm/10ml) daily for one month.
2- Second group was administrated orally o.3 ml of distilled water (D.W) daily for one month as control group. After day 30 post administration all animals were sacrificed, blood were collected for measurement of GOT, GPT and histopathological changes examination according to (Luna,1968).

RESULTS

The total of GOT and GPT for infected and control groups with nitrate ions 0.25g/10 ml showed that increased of GOT and GPT (23,28) respectively of infected group compared with second group which represent as control group. Histopathological sections of some internal organs of animals that treated with nitrate ion appeared in lung hemorrhage filled the alveoli and infiltration of alveolar macrophage and lymphocytes as in (fig.1), liver showed granulation of cytoplasm of hepatocytes and infiltration of inflammatory cells like macrophage around the blood vessels (fig.2) Hyperplasia of goblet cells of intestine in (fig3), destruction of the villi (fig.4) and infiltration of inflammatory cells in the lamina propria as macrophage and neutrophil as in (fig.5). Necrosis in interstitial tissue in spleen (fig.6), kidney appeared dilatation of urinary space, infiltration of inflammatory cells in the renal paranchyma, degeneration of the epithelia of renal tubules (fig.7). heart showed accumulation of amyloid between myocardial fibers as in (fig.8).Table 1: show the total of GOT and GPT for infected and control groups with nitrate ions 0.25g/10 ml

DISCUSSION

Nitrite is a natural component of the nitrogen cycle, its well documented toxicity to animals due to presence in the environment is a potential problem (Jensen, 2003). Nitrate was perceived as a purely harmful dietary component which causes infantile methaemoglobinaemia, carcinogenesis and possibly even teratogenesis (Santamaria, 2006). The concentration was given to mice 0.25gm/10ml daily for one month, so the acute oral toxicity of nitrate to laboratory animals is low to moderate. Median lethal doses (LD50 values) of 1600–9000 mg of sodium nitrate per kilogram of body weight have been reported in mice (Speijers *et al.,* 1989). Elevated of liver enzymes as GOT and GPT indicated to the influence of nitrate ions on liver function and detoxification of nitrate ions to a complex substance

that causing lesions in liver and other internal organs. In our study showed the effect of nitrate ions on internal organs like kidney, and Hook, (1990) expression that it is the predominant organ involved in the regulation of extracellular volume and control of electrolyte and acid-base balance and major sites of foundation of hormones that influence systemic metabolic functions. And Panday *et al.* (1997) observed that morphological changes in kidney damage. Hypertrophy and Vacuolation of the epithelial cells lining, proximal convoluted tubules, shrinkages in the glomeruli resulting in dilation of Bowman's space, necrotic changes in Liza paresis exposed to lead and agree with our results. Damage kidney such as disintegration of glomerulus, shrinkage of Bowman's capsule, vacuolation formed around the capsule, enlargement of tubular lumen and distal and proximal tubules Mohanta *et al.* (2010).

Histopathological of intestine showed infiltration of inflammatory cells in the lamina propria as macrophage and neutrophil and this agree with Santamaria,(2006) who said that nitrate metabolites may produce a number of health effects, itself is relatively non-toxic. studies suggest that nitrate is actually a key part of the bodies' defenses against gastroenteritis.Histopathological sections of lung showed hemorrhage filled the alveoli and infiltration of alveolar macrophage and lymphocytes in liver appeared granulation of cytoplasm of hepatocytes and infiltration of inflammatory cells like macrophage around the blood vessels, in spleen showed necrosis in interstitial tissue and in the heart the lesion was accumulation of amyloid between myocardial fibers. So nitrate ions can cause all these lesions and effect on their functions, in the same times when the nitrate ions effect on kidney and there are another studies support the result, other organs also may infected, and this inspection in our study, and other research proved that the same dose of nitrate ions can cause pathological lesions in pancreas showed the exocrine region and islets of Langerhans with damaged due to necrosis, while the second group was infected with nitrate ion showed the exocrine region and islets of Langerhans with necrosis and congestion of blood vessel (AL- Anni *et al.,* 2016).

REFERENCES

1. Abdel-Tawwab, M., M. A.A., Abbass, F.E., (2007) A. Growth performance and physiological response of African catfish, Claries gariepinus (B) fed organic selenium prior to the exposure to environmental copper toxicity. Aquaculture 272(1-4), 335-345.
2. Arillo A., Gaino E., Margiocco C., Mensi P., Schenone G.(1984): Biochemical and ultrastructural effects of nitrite in rainbow trout: Liver hypoxia as the root of the acute toxicity mechanism. Environmental Research,34, 135–154.
3. Hook, J.B., (1980) Toxic responses of the kidney. In: Toxicology-the basic science of poisons. Doull, J., Klaassen C.D., Amdur, M.O., (Eds.), Casarett and Doull's McMillan publishing Co.Inc., New York. Pp.232-245.
4. Jensen F.B. (2003): Nitrite disrupts multiple physiological functions in aquatic animals. Comparative Biochemistry and Physiology, Part A, 135, 9–24.- Kross, B. C., Hallberg, G. R., Bruner, R., Cherryholmes, K., and Johnson, K. J., (1993), The Nitrate Contamination of Private Well Water in Iowa, American Journal of Public Health, v. 83, p. 270-272.
5. Luna, L.G. (1968).Manual of histological staining methods of the Armed Forces Institute of Pathology .3rd Ed. Mcgrow-Hill Book Company. New York.
6. Mohanta, M.K., Salem, M.A, Saha, A.K., Hasan, A., Roy, A.K., 2010.Effects of tannery effluents on survival and histopathological changes in different organs of cannas punctatus. Asian J.Exp Biol.Sci.1 (2), 294-302.
7. Pandey, A.K., George, K.C., Mohamed, M.P., 1997, Histopathlogical alternations in the gill and kidney of an estuarine mullet, Liza parsia, Caused by sub lethal exposure to lead (Pb). Indian J.Fish.44 (2), 171-180.
8. Salma S.AL- Anni, Zainab R. Zghair, Mohanad D. Al- jaboore, Eman K. Khale (2016). Histopathological study of nitrate ion effect on pancreas experimentally in laboratory mice. Bas.J.Vet.Res.Vol.15,No.4, p.:3.461.- Santamaria, P. (2006), Nitrate in vegetables: toxicity, content, intake and EC regulation. J. Sci. Food Agric., 86: 10–17. doi: 10.1002/jsfa.2351
9. Speijers GJA et al. (1989) Integrated criteria document nitrate; effects. Appendix to RIVM Report No. 758473012. Bilthoven, National Institute for Public Health and the Environment) (RIVM Report No. A758473012).

10. Vutukuru, S.S., (2005) acute effects of hexavalent chromium on survival, oxygen consumption, hematological parameters and some biochemical profiles of the Indian major carp, Labeo rohita. Int.J. Environ. Res. Public Health.2(3), 456-462.

Table 1: show the total of GOT and GPT for infected and control groups with nitrate ions 0.25g/10 ml

Groups	GOT	GPT
First group	23	28
Second group	18	21

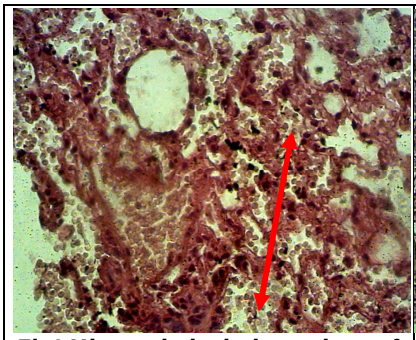

Fig1:Histopathological section of lung of one animal that treated with nitrate ion showed hemorrhage filled the alveoli and infiltration of alveolar macrophage andlymphocytes(↔)(H&EX400).

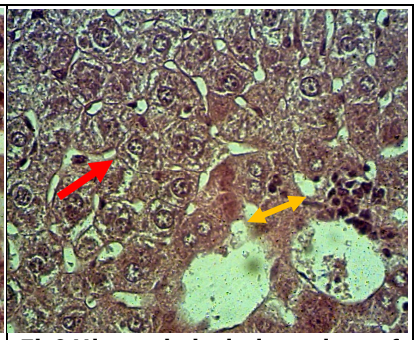

Fig2:Histopathological section of liver of one animal that treated with nitrate ion showed granulation of cytoplasm of hepatocytes (⟶) and infiltration of inflammatory cells like macrophage around the blood vessels (↔)(H&EX400).

Fig3:Histopathological section of intestine of one animal treated with nitrate ion showed hyperplasia of goblet cells(⟶) (H&EX400).

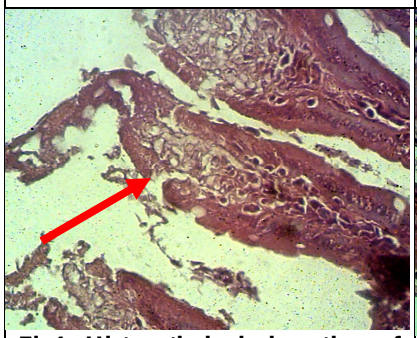

Fig4: Histopathological section of intestine of one animal that treated with nitrate ion showed destruction of the villi (⟶) (H&EX400).

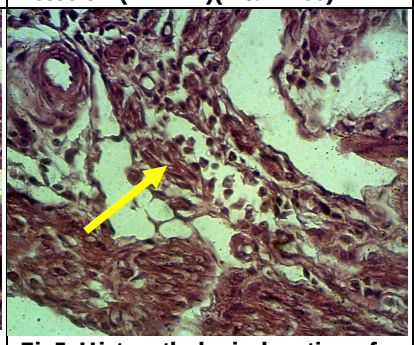

Fig5: Histopathological section of intestine of one animal that treated with nitrate ion showed infiltration of inflammatory cells in the lamina propria as macrophage and neutrophil (⟶) (H&EX400).

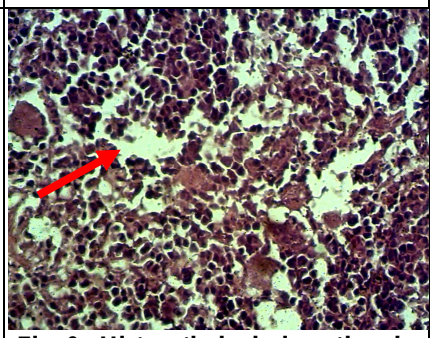

Fig 6: Histopathological section in spleen of one animal treated with nitrate ion showed necrosis in interstitial tissue (⟶) (H&EX400).

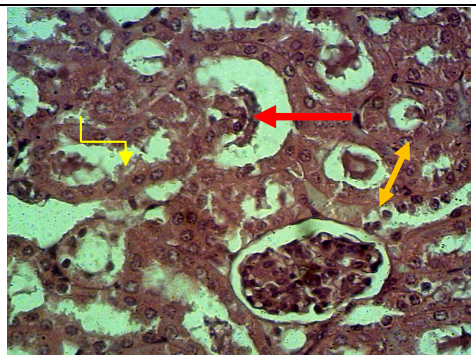

Fig7:Histopathological section of kidney of one animal treated with nitrate ion showed dilatation of urinary space (⟶), infiltration of inflammatory cells in the renal paranchyma (↘↗), degeneration of the epithelia of renal tubules (↳). (H&EX400).

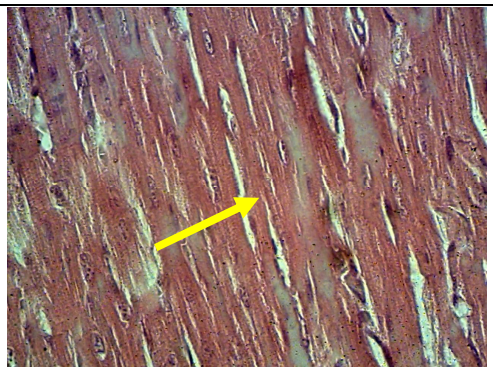

Fig8: Histopathological section of heart of one animal treated with nitrate ion showed accumulation of amyloid betweenmyocardial fibers (⟶), (H&EX400).

Indian Journal of Natural Sciences www.tnsroindia.org.in ©IJONS

Vol.8 / Issue 49 / August /2018 *International Bimonthly* *ISSN: 0976 – 0997*

RESEARCH ARTICLE

TiO_2 Enhanced Sensing Performance of Zn:TiO_2 Thin Films

Sahar M.Naif* and Bushra A.Hasan

Department of Physics, College of Science, University of Baghdad, Baghdad, Iraq.

Received: 08 May 2018 Revised: 11 June 2018 Accepted: 09 July 2018

***Address for Correspondence**
Sahar M.Naif
Department of Physics,
College of Science,
University of Baghdad,
Baghdad, Iraq.
Email: saharmohammed212@gmail.com

ABSTRACT

Thin films of ZnO:TiO_2 were deposited on different substrates like glass and c-Si using spray pyrolysis method .The structures and morphology of the prepared samples films were cheeked using X-ray diffraction and atomic force microscope. Gas sensing measurements provided from resistance measurement in the absent and exposure to NO_2 gas. The results showed that good enhancement of sensitivity take place after doping with tin oxide. Maximum sensitivity obtained at 9% doping ratio and operating temperature 200^{o}C.

Key word:. Films, ZnO: TiO2, microscope, measurements, samples

INTRODUCTION

Thin-film zinc oxide continues to attract attention because of its low toxicity and its many applications in solar cell technology [1] and as thin-film gas sensors [2 4], Due to these properties ZnO is a promising material for electronic or optoelectronic applications such as solar cells (anti-reflecting coating and transparent conducting materials), gas sensors, liquid crystal displays, heat mirrors, surface acoustic wave devices etc. [5.6], light emitting diodes(LED's), laser systems [7] and transparent electrodes [8], The direct optical energy gap of 3.3eV for ZnO is large enough to transmit most of the useful solar radiation. Further, abundant availability of ZnO in nature makes it less expensive and its sharp UV-cut-off makes it desirable in many applications [9]. Many techniques have been employed to produce zinc oxide, sputtering [10], metal organic chemical vapor deposition [11], sol gel [12] and spray pyrolysis [13,14], pulsed laser deposition [15] have deposited high quality ZnO films. Among these techniques, spray pyrolysis has proved to be a simple and inexpensive method, particularly useful for large area applications. The SPD is essentially the same film processing technique as so-called pyrosol technique, in which a source solution is sprayed on a heated substrate to be deposited as films. In other words, when source solutions is atomized, small droplets splash and vaporize on the substrate, and leave dry precipitates in which thermal decomposition takes place [16]. In

this paper, we report ZnO film formation from a Zinc Acetate dehydrate (Fisher Scientific, India) by chemical Spray Pyrolysis deposition technique and studies of several structural and optical parameters of ZnO films.

MATERIALS AND METHOD

Preparation of an aqueous solutions of Titanium(III)chloride $TiCl_3$and zinc chloride with concentration of 0.1M at (3%,5%,7%,9%) ratios by dissolving in distilled water and stirred with a magnetic stirrer for 15 minute. The spraying apparatus was manufactured locally in the department laboratories. In this technique, the prepared aqueous solutions were atomized by a special nozzle glass sprayer at heated collector glass fixed at thermostatic controlled hotplate heater. Air was used as a carrier gas to atomize the spray solution with the help of an air compressor with pressure (7 Bar) air flow rate (8 cm^3/sec) at room temperature. The glass substrates were cleaned with distilled water followed by ethanol in ultrasonically cleaner and then dried. The temperature was maintained at 250 C during spraying , The distance between the substrates and spray nozzle was kept at (30 ±1 cm), number of spraying (100) and time between two spraying (10 sec). The X-ray diffraction (XRD) data of the prepared films were taken using CuKα with radiation of wavelength λ =1.5406Å, current =15mA, voltage = 30 kV and scanning speed = 2 deg /min) over the diffraction angle range 2θ=20-80 at room temperature .The average crystallite size (D) was estimated using the Scherrer equation as follows [17]

$D=0.9\lambda/\beta \cos\theta$ …….. (1)

where λ, β, and θ are the x-ray wavelength, the full width at half maximum (FWHM) of the diffraction peak and Bragg's diffraction angle respectively. The surface distribution of ZnO: TiO_2 thin films were measured using a scanning probe microscopy (CSPM5000) instrument. D.C conductivity was calculated using equation (2)

$$\sigma_{D.C} = \frac{1}{\rho} \quad \text{…….. (2)}$$

$\sigma_{d.c.}$: The conductivity of the films , ϱ: The resistivity of the films

Activation energies can be calculated from the plot of ln σ versus 1000/T according to equation [18]:

$$\sigma = \sigma_0 \exp(\frac{-E_a}{k_B T}) \text{ …..…… (3)}$$

Where σ_o is the minimum electrical conductivity at 0 °K, E_a is the activation energy which corresponds to (E_g/2) for intrinsic conduction, T is the absolute temperature and k_B is Boltzman's constant equal to (8.617×10^{-5} eVK^{-1}) . By taking (Ln) of the two sides of equation (3)

$Ln\sigma = Ln\ \sigma_0\ (-E_a/k_BT)$ …….. (4)

From the slope of ln σ against 1000/T graph, the activation energy can be found:

$E_a = k_B$. Slope ……..…… (5)

Hall measurements are used to distinguish whether a semiconductor is n or p – type

From the Hall coefficient equation, the carrier's concentration of the semiconductor, and the carrier type, can be determined from the sign of R_H such that:

$$R_H = \frac{-1}{n.q} \text{ For n-type ……..... (6)}$$

$$R_H = \frac{1}{p.q}$$ For p-type ..... (7)

Where R_H: Hall coefficient.

The Structure and Mechanism of ZnO for Gas Sensing Behavior there are two basic functions which a gas sensor consist of. These are receptor functions and transducer functions. Receptor function includes the recognition the chemical substance, whereas transducer function converts the chemical signal into electrical signals.This section deals with the structural properties favoring receptor functions of ZnO responsible for gas sensing behavior. ZnO has many different structural forms and shapes grown under different growth conditions. Wurtzite is the most favored form of ZnO at ambient conditions thermodynamically. The lattice constant parameters of wurtzite ZnO are :a=3.2490 Å and c=5.2070 Å with two interconnecting hexagonal close- packed (hcp) sub-lattices in hexagonal lattice of Zn^{2} and O^{2-} involving sp^3 covalent bonding [19] .

RESULTS AND DISCUSSION

The XRD patterns of pure ZnO and doped with TiO_2 in different ratios (3%,5%,7%,9%) are shown in Figure(1). Table (1) showed that crystallite size increases as Titanium oxide introduced to the host material (zinc oxide). The crystallite size then decreases as a result of the broadening in the diffraction peaks take place as a result of increasing of pore walls thickness and upward shifts (relaxation of strain) .

Atomic Force Microscopy (AFM)

Figure 3 shows the Atomic force microscopy (AFM) images for ZnO: TiO_2 thin films with different doping ratios (3%,5%,7%,9%) deposited on glass substrate. AFM parameters contain average diameter, average roughness and peak-peak value for these sample have been shown in Table (2). These tables illustrates reduction in average diameter up to 5% followed by increment and finally return to reduced by increasing of doping ratio.

The Electrical Measurements

D.C Conductivity

Figure(4) shows the variation of Ln(σ) with reciprocal temperature. It is obvious that there are more than one conduction mechanism and hence more than one activation energy. Table (3) shows there are two activation energies can be observed for the pure and doped samples with, 3%,5%,7%,9%. It is clear that the conductivity increased as TiO_2 was added to the host material. This result is expected since the increases the density of charge carriers. From other side the activation energy at low temperature denoted by E_{a2} increases by increasing of doping ratio (although the reduction was not in systematic manner). This take place as result of reduction of crystal size as seen from X-ray diffraction and table 1.

Hall Effect Measurements

Table(4) show the type of charge carriers, concentration (n_H) and Hall mobility (μ_H), have been estimated from Hall measurements for un-doped ZnO and doped with TiO_2 films at different concentration.Hall measurements show that all these films have a negative Hall coefficient (n-type charge carriers), this is attributed to following two reasons .The number of electrons excited above the conduction band mobility edge is larger than the number of holes excited below the valance band mobility edge. The life time of free electrons excited from negative defect state is higher than

the life time of free holes excited from positive defect state.The charge carriers density increases five orders of magnitude by increasing of doping ratio.

Gas Sensing Measurement

NO_2 Sensing Mechanism for ZnO: TiO2 Films

The thin films specimens are examined for gas sensing using NO_2 with concentration of 25 ppm at different operation temperature beginning from room temperature (30°C) up to 250°C Figures from (5) to (9) show the variation of resistance as a function of time with on/off gas valve.The results show that the sensitivity of the gas sensors thin films increases with the increase of the operating temperature especially for high doping ratios i.e. 0, 5, 7, and 9%. it is clearly observed that 5% doping ratio produced best sensitivity values at all operating temperatures. Maximum sensitivity value (780) was obtained for ZnO thin films doped with 9% TiO_2 at a temperature of (473K) which is called the optimal temperature. The increase and decrease in the sensitivity indicates the adsorption and desorption phenomenon of the gas.

CONCLUSION

Crystal size increases by increasing of doping ratio, Doping has no effect on the type of conductance of the prepared films, Doping ratio has no effect on the high temperature activation energy while has well pronounced effect on the law temperature activation energy, Maximum sensitivity obtained at the lowest crystal size belonged to ZnO thin films doped with 9% TiO_2 at optimal temperature of (473K).

REFERENCES

1. Thin Film Solar Cells, edited by K. L. Chopra and S. R. Das ~Plenum, New York, 1983, p.607.
2. Chopra, K.L., Major, S., Pandya, D.K., 1983. Thin Solid Films 102, 1.
3. Muller, J., Weissenrieder, J.S., 1994. J. Anal. Chem. USSR 349, 380.
4. Lin, F.C., Takao, Y., Shimizu, Y., Egashira, M., 1995. J. Am. Ceram. Soc. 78, 2301.
5. Bose, S., Barua, A.K., 1999. J. Phys.D: Appl. Phys. 32, 213.
6. Kim, H., Gilmore, C.M., 2000. Appl. Phys. Lett. 76, 259.
7. Szarko, J.M., Song, J.K., Blackledge, C.W., 2005. Chemical Physics Letters, 404, 171 -176.
8. Ootsuka, T., Liu, Z., Osamura, M., 2005. Thin Solid Films, 476, 30 34.
9. S., P.P., Tewari, S., Nath, R.K., 2007. Cryst. Res. Tec hnol. 42, 723 729.
10. S. So, Choon-B. Park, 2005. Journal of Crystal Growth 285, 606.
11. Tan, S.T., Chen, B.J., Sun, X.W., Hu, X., Zhang, X.H., Journal of Crystal Growth 281,571.
12. Y. Kim, W. Tai, Su-Jeong Shu, 2005. Thin Solid Films 491, 153.
13. Ashour, A. Kaid, M.A., El-Sayed, N.Z., Ibrahim, A.A., 2005. Applied Surface Science In Press.
14. Martins, R., Igreja, R., Ferreira, I., Marques, A., Pimentel, A., Gonçalves, A., Fortunato, E., 2005. Materials Science and Engineering B 118, 135.
15. Dikovska, A.Og., Atanasov, P.A., Vasilev, C., Dimitrov, I.G., Stoyanchov, T.R., 2005. JOptoelectron. Adv. Mater. 7, 1329.
16. M.Okuya, K. Nakade, 2004. Journal of Photochemistry and Photobiology A:Chemistry 164, 167-172.
17. J. Q. Xu, Q. Y. Pan, Y. A. Shun and Z. Z. Tian, "Grain Size Control and Gas Sensing Properties of ZnO Gas Sensor," Sensors and Actuators B: Chemical, Vol. 66, No. 1-3, pp. 277-279,July 2007.
18. P. Kireev, "Semiconductor Physics " ,Moscow: MIR publishers, (1978).
19. R. Kumar, G. Kumar, A. Umar, Zinc oxide nanomaterials for photocatalytic degradation of methyl orange: a review. Nanosci. Nanotechnol. Lett. 6(8), 631–650 (2014). doi:10.1166/nnl.2014.1879

Table .1 The XRD Out Put of ZnO: TiO2 Thin Films Deposited with Different Doping Ratios

TiO_2%	2θ (Deg.)	FWHM (Deg.)	d_{hkl} Exp.(Å)	G.S (nm)	Hkl	d_{hkl} Std.(Å)	Phase	Card No.
Pure	34.2938	0.1730	2.6128	48.1	(002)	2.6035	Hex. ZnO	96-901-1663
3%	34.4538	0.1840	2.6010	45.2	(002)	2.6035	Hex. ZnO	96-901-1663
5%	34.4548	0.1890	2.6010	44.0	(002)	2.6035	Hex. ZnO	96-901-1663
7%	34.4617	0.1560	2.6092	53.3	(002)	2.6035	Hex. ZnO	96-901-1663
9%	34.4627	0.1650	2.6092	50.4	(002)	2.6035	Hex. ZnO	96-901-1663

Table(2) AFM Measurements for Thin Films at Different Sno_2 Doping Ratios

TiO_2 %	Average diameter (nm)	Average roughness (nm)	r.m.s roughness (nm)	Peak –Peak (nm)
0	105.70	9.19	11.1	61.4
3	103.7	4.14	4.97	21.3
5	92.61	4.06	4.67	20
7	82.61	4.02	4.64	16.1
9	68.61	1.18	1.44	6.8

Table (3): D.C Activation Energies, their Temperature Ranges for Pure Zno and Doped With Different Ratio of TiO_2

TiO_2%	E_{a1} (eV)	Range (K)	E_{a2} (eV)	Range (K)	σ_{RT} ($\Omega^{-1}.cm^{-1}$)
0	1.073	283-363	0.186	363-473	0.104
3	1.070	283-363	0.165	363-473	0.1325
5	1.065	283-364	0.156	363-474	0.1821
7	1.055	283-363	0.152	363-473	0.2909
9	1.022	283-363	0.139	363-473	0.7228

Table(4): Hall Measurements Results of ZnO :TiO_2 Thin Films at Different Doping Ratios

$Tio_{2(\%)}$	σRT (Ω-1.cm1)	RH (cm^3/Coul)	nH ×10^{15} (cm^3)	Type	μH(cm^2/V.sec)
0	0.2132	-3859	4.402	n	822.73
3	0.2467	-1226	5.961	n	302.45
5	0.3448	-1121	6.617	n	286.52
7	0.5787	-600	7.833	n	247.22
9	0.698	-588	9.744	n	210.424

Table.5: Sensitivity as a Function of Operating Temperature to NO_2 Gas for Pure ZnO and Doped with TiO_2 at Different Concentrations Deposited On n-Si

Operating Temp.(K)	Sensitivity				
	doping ratio of TiO_2				
	0%	3%	5%	7%	9%
R.T	5.9	31	750	2.98	2.7
373	6.25	60	266.6	7	47.36
473	39.2	13.1	121.62	112.5	780
523	29.8	13.2	260	600	550

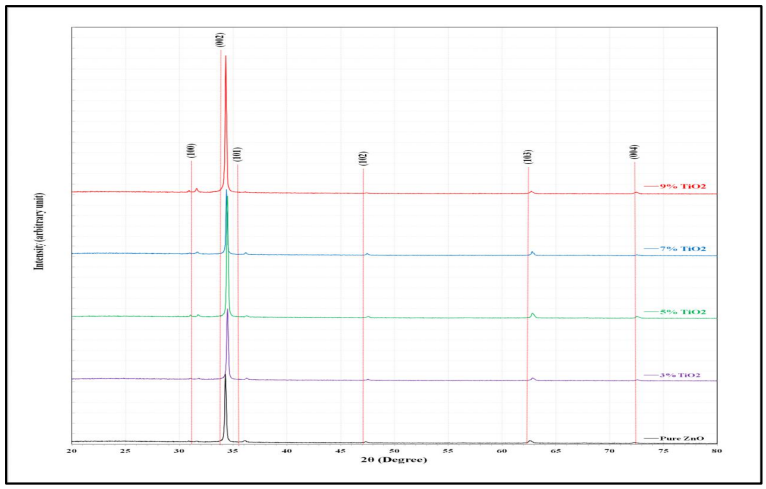

Figure.1: XRD Patterns of ZnO: TiO_2 Thin Films Deposited With Different Doping Ratios.

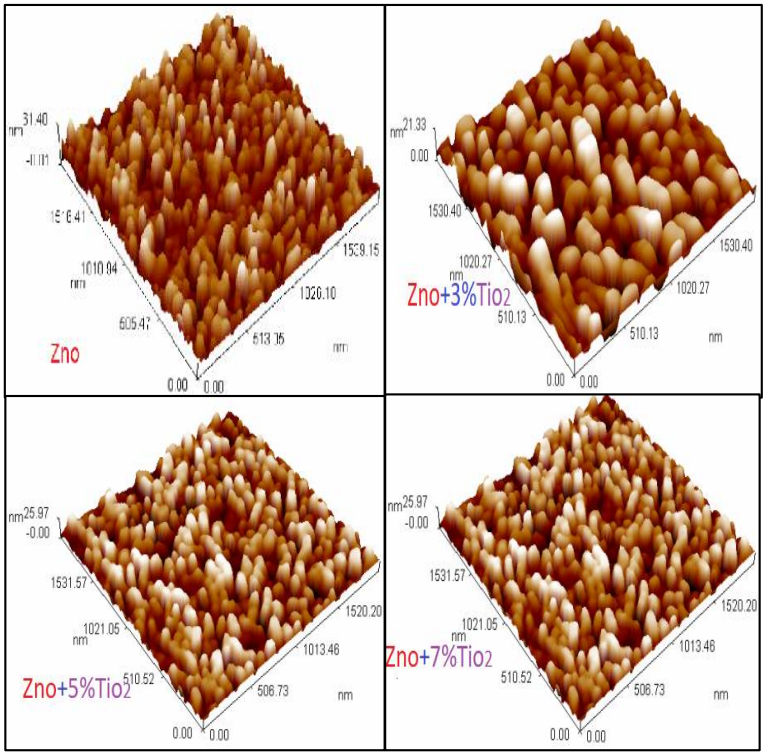

Figure .2: AFM images of ZnO: TiO2 Thin Films Deposited with Different S_nO_2 Doping Ratios

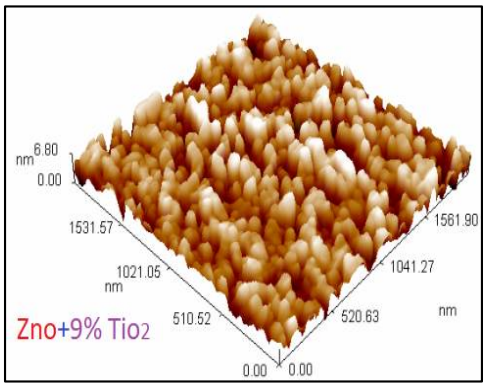

Figure .3: AFM images of ZnO: TiO2 thin films deposited with different S_nO_2 doping ratios

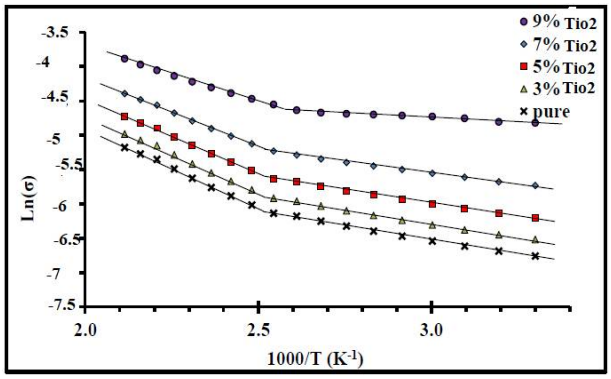

Figure (4): Plot of ln (σ) vs. 1000/T of un-doped ZnO and doped with different ratio of TiO_2.

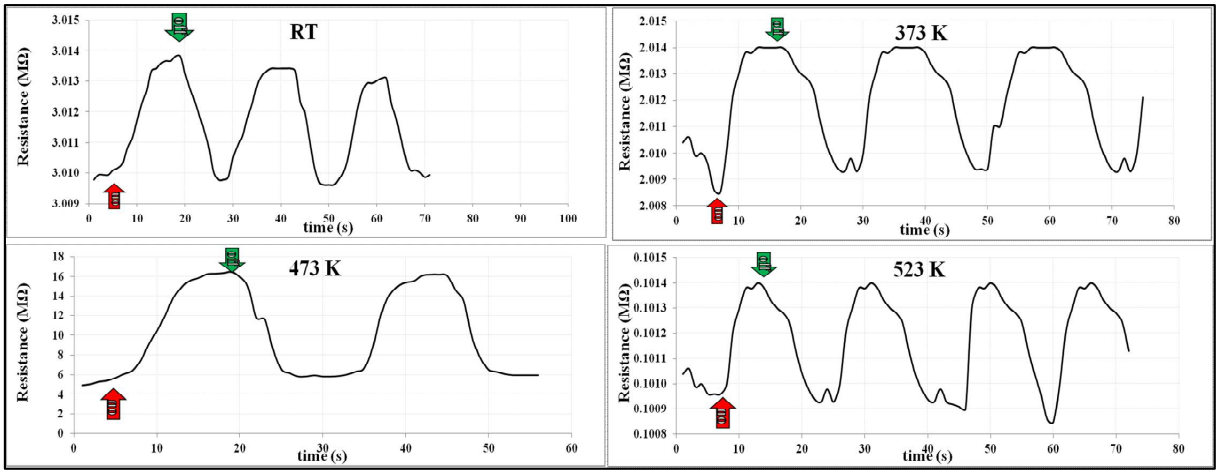

Figure.5: Variation of Resistance with Time for Pure ZnO Films as NO_2 Gas Sensor

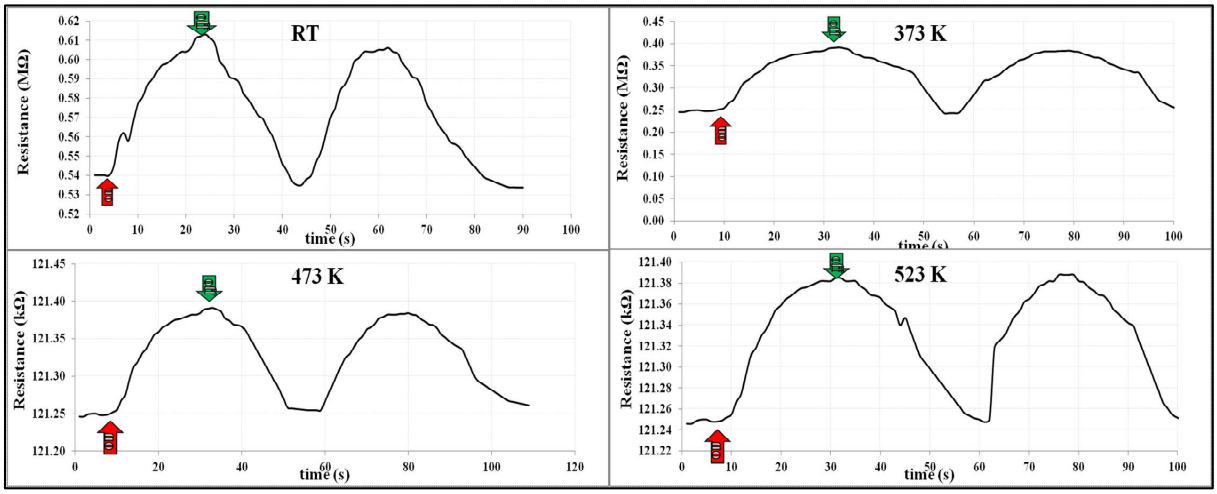

Figure 6: Variation of Resistance with Time for 3% TiO_2 Doped ZnO films as NO_2 gas sensing

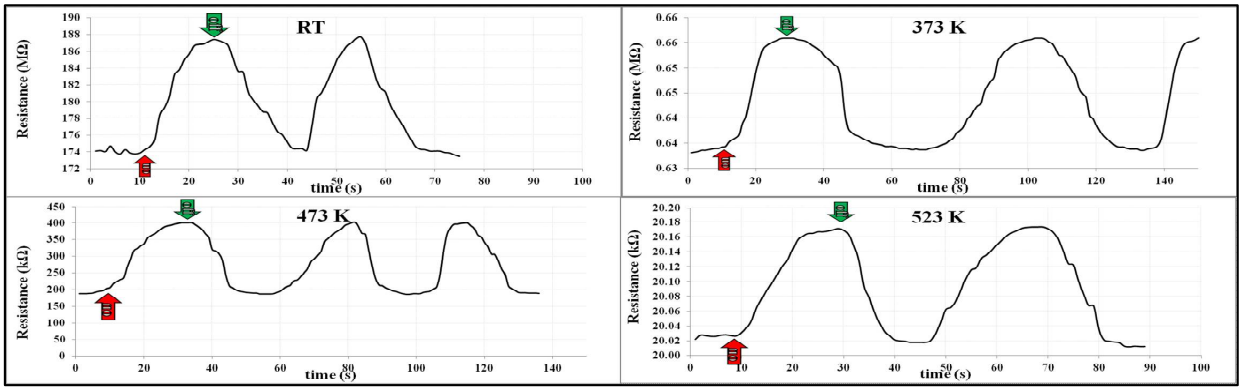

Figure.7: Variation of Resistance with time for 5%TiO_2 Doped ZnO Films as NO_2 Gas Sensor

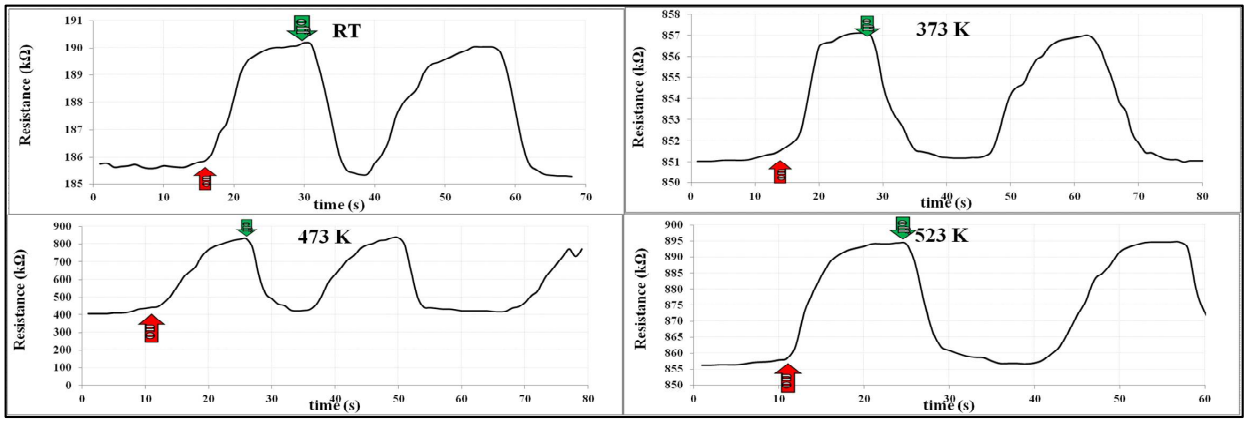

Figure.8: Variation of Resistance with Time for 7% TiO_2 Doped ZnO Films as NO_2 Gas Sensor.

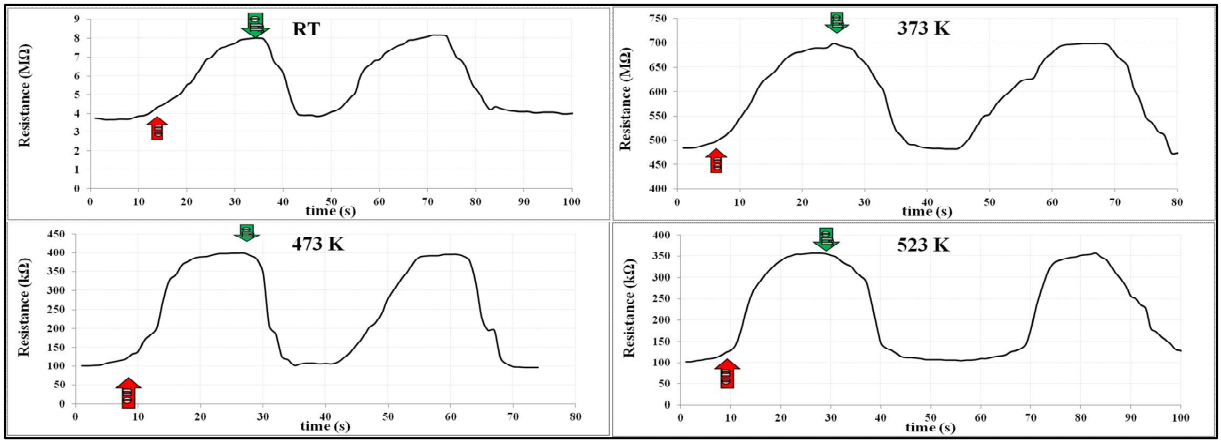

Figure 9: Variation of Resistance with Time for 9% TiO2 Doped ZnO Films as NO_2 Gas Sensor

Indian Journal of Natural Sciences *www.tnsroindia.org.in ©IJONS*

Vol.8 / Issue 49 / August /2018 *International Bimonthly* *ISSN: 0976 – 0997*

RESEARCH ARTICLE

Eastern Shore Board of India Tsunami Safe?

Deepak Bhattacharya*

C/o Sri Radha Krishna, Kedar Gouri Road, Bhubaneswar, Odisa, India.

Received: 24 May 2018 Revised: 28 June 2018 Accepted: 30 July 2018

***Address for Correspondence**
Deepak Bhattacharya
C/o Sri Radha Krishna,
Kedar Gouri Road,
Bhubaneswar, Odisa, India.
Email: oddisilab1@dataone.in

ABSTRACT

The southern shore boards of India (south of Krishna delta) have adversely been effected by Tsunami. The eastern shore board of India is longer in stretch; year round high productive; densely populated; loaded with strategic cum civil engineering infrastructure; and beach based cultural heritage. High coastal waves have been reported. Long period IMD data; geographic, orogrpahic field study and laws of physics are relied upon. Are not tsunami. Are sea surges; innately of meteorological cum astronomical cum hydrological etiology. Tsunami has a seismic etiology, large depth dimension and long scope propagation. Apart from being in the lee of the coral islands, other wave propagation cancellation factors are also at work, year round-along the eastern shore board of India. Haldia-Dhamara-Paradeep-Gopalpur-Vishakhapatnam, are tsunami safe ports. Ganga sagar, Puri, Konarak are beach based safe centers of cultural heritage related activities. Bhitarkanika and the Chilika are tsunami safe natural heritage and for marine amphibian mass nestling. Historical evidence also concurs. The eastern shore board of India, posits as paradise for sea-bath related activity; for the investment banker; for the related engineering services; and employment generation.

Key Words: Tsunami safe; Eastern shore board of India; Meteorological event; Gravity waves; historically vetted; Multi-disciplinary study.

INTRODUCTION

The eastern shore board of India is year round productive; densely populated; is flat and low lying; and is loaded with engineered infrastructures; of great antiquity, included. Tsunami adversely effects. D. Bhattacharya [1] has been studying and reporting various aspect of Tsunami. In 2007 there were numerous press reports indicating repeated occurrences of tsunami or tsunami like situation off the Odisa coasts. The local vernacular news report between 09 and 12-09-2007 [2,3,4] were also associated with photographs of shore erosion, sea wave intrusion in various

segments in various time, sand deposition on the marine drive extending between Puri to Konarak (Odisa) and lot of hue and cry, etc. The entire rim of the Bay of Bengal {BoB} has numerous vital coastal and maritime related infrastructures. From coastal engineering perspectives, the eastern shore board ranges from Haldia {Ganga mouth} to the Krishna mouth. We visited the sites, did field survey and eye witness interview. We used IMD resources [**5**] and have examined the facts and have found that the {news} reported events were not tsunami. This is 1st time original report. It arises out of Bhattacharya & Panigrahi's presentation in the AHI seminar [6]

Pressure was same also at 14-30 hours IST, on all reported days. Bhubaneswar (20°16′N//85°50′E) is on the same meridian and only 0.67^0 to the north of Puri {N↔S}. Bhubaneswar has a decadal avg. surface level pressure of the order 999 hPa in Sep., while at Puri, it is 1007 hPa. There is an atmospheric (natural) gradient from the sea towards the land, in a northerly direction. So too was during the event period. At Puri between 06/09/07 and 19/09/07 pressure difference occurred by an order of 5hPa between the selenic waxing and waning phases respectively; while the variation from the long period average was only of the order 2hPa {insignificant}, the deviation when compared to that of Bhubaneswar {data not shown} posits as large. Interesting indeed.

Pressure was same also at 14-30 hours IST, on all reported days. The latitudinal difference between Berhampur and Gopalpur is of the order 0.02^0 and the longitudinal difference is of the order 0.06^0 {insignificant}. Berhampur has a decadal avg., surface level pressure of the order 999 hPa in Sep., and Gopalpur has 997 hPa. This means, Berhampur is towards the south-west of Gopalpur on sea {SW↔NE}, and both the station are meteorologically isotrophic {long period average basis}, were so too during the event period. At Gopalpur there was a variation by an order of 7hPa between the selenic phases. And that, it was an increase by an order of 12hPa from the long period average. At either station the pressure was similar, and such phenomenon was consistent for 12hrs, {2-30 to 14-30hrs}. Tsunami events are short.

Juxtaposing T-I with T-II we observe that, deviation from the long period average was steeper at Gopalpur {not at Puri}. So, the sea to land pressure gradient was along an E→ W axis inclined along Gopalpur → Puri shore line which have a meridonial separation of only 1^0. During the Puri-Konarak event period, high waves were not reported off the shores off Gopalpur or from any of the Ganjam beaches, which are contiguous to Puri district. And, it was spring tide period. This suggests the operation of some hitherto unknown forces {met phenomena}, which portends risks for the beach/shore based engineering structures; ongoing investments; and anthropogenic activity, along with an opportunity for enquiry.

Our Fig.-1a is the global SST anomaly {SST-a} on 13-09-2007 [7]. In monochrome, the light coloured regions are the warm and the deeper shade are the cold SST-a regions, respectively. It shows warm SST-a extending over the entire northern regions of the BoB. We may note a small area (pocket) south east of Gopalpur indicating cold SST-a. Cold SST-a signifies down-welling of water and downdraft of the ocean-atmosphere couple. Warm SST-a signifies upwelling of water and updraft of the ocean-atmosphere couple {turbulent sea}. It is well known that during Sep., period, the BoB has a strong north bound coastal current [8]. It means water that was sinking off the coast of north Andhra was upwelling to the north of Gopalpur. Thus SST-a also offered shore wave up-regulating sea hydrological conditions around the event window and the geographic domain. However, the events in question ranged over a short scope of the shore line (<10Km span). SST-a variation cannot inflict such well directed, narrow band sea surge.

Cloud Picture

Our Fig.-1b is a satellite image [9]. It is of the BoB dt.11/09/2008, at 00 UTC, in IR range. It shows a depression extending over the entire northern regions of the BoB with part inland ingression. Therefore, a depression was concurrently in decay motion >500Km afar north of Puri. The system has no coverage of the Odisa coasts, and clear sky condition is noted specially over Puri & Gopalpur, during the event period. The IMD, categorises any sea located weather system as a 'depression' when it has 2 close isobars {2hPa apart}; 3 close isobars makes a 'deep depression;

and with 4-7 close isobars, a 'cyclone' [10]. The IMD also issues a DC-1 as the first signal when a 'depression' has already formed and is located at about 500 nautical kilometers from port. This is a 'general alert' signal for ships on sail in the high seas. Not for shores; beaches jetties & ports. The IMD had logically therefore not issued any warning. An gradient of 12hpa works out to 6 close isobar conditions. Such steep abrupt gradient is highly atypical and merits enquiry. Ultra high sea waves under fair weather a condition was logically mistaken as, tsunami.

Concurrent Seismic Activity

We also raise the question if any seismic activity had occurred during this period? We note, that, as per GDACS's report [11], there was a sea located earthquake near Bengakullu (Sumatra, Indonesia,), of 7.5 Richter intensity (duration not noted), at a depth of 10 km., at 03:35:29 UTC on 13/09/2007 i.e., 16-40 IST of 12/09/2007. Mini (harmless) non-tsunamis waves were reported from various regions, with propagation being away from the eastern sea board of India. In relation to our T-I & T-II we also note that IMDs recordings were done 2 hours pre and 10 hrs post this seismic event. We also note that the narrow band beach wave phenomena were between Sep., 8thnight and the wee hours of the 12th. Hence the Bengakullu event had no connection with the Puri beach events. We [see Ref 6 & 32] have presented that the Odisa- north Andhra coast is in the lee of the Andaman coral Islands {barrier}. The instant case bears out our theory, that, tsunamis do get filtered {down-turned} due to coral barrier reef phenomena.

All this clearly brings out the fact, that such atypical phenomena have remained un-reported and un-co-related. That, there is a need to explain {attempt} the underlying physics and the mechanics. Condition 5-i to 5-v seeks to address such objectives.

It shows that, the Puri-Konarak region: (a) extends out into the sea geomorphologically and geologically as a 'sand fan' due to the delta building process; (b) this shore-line is tangential to the meridians. It is known that during the Indian Monsoon period, the Hadley's Cell lyses [13] in the Indian Ocean region, preceded by large flow of ocean water into the BoB (ref.8).The flow being more or less meridonial. And the Gopalpur-Konarak shore line is tangential to the meridians. It is well known that sea/waves/stream flow exert highest thrust at tangential locations. However sub-marine shore waters always act as formidable boundary due to Kelvin type submerged long waves, propagating sea wards {posits as a cancellation mass against any incoming submerged wave}; specially off shores having convex architecture with short shelf {alike Puri-Konarak sand fan}. Shore surface waves have an opposite flow. And, shore waves are superficial members. Co-incidence of numerous meteorological phenomena during inter-annual month, results in the weakening of such boundary in any location resulting in the (direct) projection of the sea's tangential thrust on to the beaches in a narrow manner, even causing inundation and erosion. Projection of the tangential thrust of the sea on to the beaches and weakening of the coastal fluid boundary are limited to inter-annual-periods, when the coastal currents also tend to change their direction of flow in the BoB and in the Arabian Sea.Historically the sea surface condition a month pre spring Equinox is most placid. Therefore, meteorologically caused sea surge of variable amplitude will be normal events along Puri-Konarak shore-line at spring tide during autumn Equinox period. Yet it does not satisfactorily explain the well directed, narrow band phenomena.

Bhattacharya & Kara [14] have presented that the stretch between Gopalpur and Puri {grossly} is inclined in a SW-to-NE axis {100km}, and that the land mass of Puri juts out into the sea by an order of nearly 1^0 {100km} of geo space {Fig.-2}.This contributes in year round tangentiality of the incident sea-atmosphere couples; heightened sea breeze and foam crested curving breakers off the Puri beach. This is because, the atmospheric pressure acts as a burden on the liquid surface and transfers the thrust along a supra hydraulic pathway. Therefore, the monsoon period coastal sea currents and the sea-atmosphere couples {weather systems} are also more incident onto this shore line.

At Gopalpur the local shore is inclined in a SE-to-NW axis (oop. Of SW-to-NE axis), hence monsoon period coastal current {S→N} is not incident on to Gopalpur beach. This acts as wave size limiting (down regulating factors) along the Gopalpur beach.Whereas, the coastal current during north east monsoon period {N→S} is more incident, which

causes waves of higher amplitude at Gopalpur than those at Puri during the same period. In other words, annually, Puri beach will have higher wave size during south-west monsoon period, and Gopalpur will have higher wave size during north east monsoon period. Any deviation is likely to be misinterpreted by the uninformed. Under such ideal conditions, if it be spring tide period coupled with a selenic alignment having a beach-line tangent trajectory, along with an wide domain covering atmospheric depression in the rear (turbulent sea); up-welling sea hydrology, thence tidal bore type wave conditions will prevail even though the local weather may not be cyclonic. All this has not been considered pre to this report.

In Fig.2 the white parabolic lines represent erstwhile sand bars and their direction of propagation. These bars give to the Puri-Konarak region, its unique sandy geomorphology. Thus we see here a case of a unique couple formed between orography ↔ geomorphology. Due the jutting out type orography the Sun is viewable from rise to set at Puri sea beach, round the year [15]. This has added great value to the beaches. Using Sat. image {geo-stationary; visible range}, Fig.-3 graphical explains that the globe is inclined towards the true NE, and that, the event domain remains alignment with the sun at its True East position at rise {00 UTC} during autumn Equinox (© Dundee Uni. Sat. Centre). The horizontal is the ecliptic and marks the true E ↔ W. Hence the globe's inclination (positional astronomy) is also a factor in the year round diurnal view of the Sun from rise to set.

Condition 5-ii

Fig.-4 gives the schematic impression {elevation} of the shore board ranging between 500 - 1500 Mts., inland from the spring tide line at swell [ref. No. 32].The cross section is imagined {L to R} running from village Charinala- through Sri Jagannath temple into outer see.The sand bar {locally known as *luni bandha*} measures between 5-15 Mts., in height from that of the level at village Charinala. Atop such natural sand-bar {that also span the entire sand fan}is the schematic location of the man made apex heritage structure {*sri mandira*}.

Annual alteration in flow direction of the coastal currents also results in 'dumping of the long shore drift' {sand} on the beaches and in the eventual making of the coastal sand bars due to synergic wind action (see ref.14), which double up as an effective physical barriers [16]. And which, in turn, assists coastal Kelvin waves due heightened shelf gradient. Additionally, our considered theory is that, there is a one way relationship between the meteorologically caused coastal shore waves and the hydraulically caused sub-marine Kelvin waves. In other words, an up-regulation in the superficial shores waves {turbulence} is followed by an up-regulation of the coastal Kelvin as part of compensatory mechanism via the delayed action mechanism. *Interalia* it means up-regulation of the Kelvin waves will coincide with quaternary phases of the moon {also marked by placid sea yet with drowning deaths, with bodies missing}. They form a couple. Such couple additionally imparts limitations to wave size. A run away atypical high intensity, large sized numerous waves along a narrow band {as that of the reported events} is beyond the regular working mechanics of such couple. It thus had to be explored and discussed.

Condition 5-iii

When a depression decays, the fluid injection pathways of that system infract and fail. The moisture mass thence get effected by gravity and tend to fall [17].Such phenomena has been articulated as 'gravity waves'. Fig.-5a is that of the gravity waves in the Arabian Sea {Indian peninsula is to the right, waves are west inclined} as recorded on 15-11-2011 [18]. We have taken cue from it and have identified a similar condition. Fig. 5b is the IR image of the BoB on 10-09-2007 [19] It suggest radial type gravity waves in the very domain of our interest along with a decaying weather system to its north and west. The gravity wave (CSST, Fig-6) regions are marked by glistening mini wavelets on the sea surface. This is due to non uniform and non synchronous energy conservation cum transfer of gravity (as is embedded in the free falling compressible fluid) into non-compressible fluid (sea) that has great depth dimension i.e., high opposite force. Moreover, at lower atmospheres, the gravity waves become asymmetric due to meteorological boundary layer effect. Collision of asymmetric compressible fluid into static, non-compressible fluid (sea) does not

cause any piston effect nor generate any 'shock', which is the hall mark at point of benthic subduction that causes tsunami. In other words, atmospheric gravity waves cannot cause tsunami (neither up-regulate; nor down-regulate a tsunami that be in propagation mode). However, it can result in the generation of synchronous hydraulic waves at supra. The quantum of the gravity embedded into such free falls at near shore locations will reflect near linearly in wave amplitude. Our considered view is that 'gravity waves', was the principle up-regulating cause factor for the reported events.

Discussion for 5-i to 5-iii

As a depression germinates in the outer sea, the barometric pressure over the inter-tidal zone is relatively higher than in the outer sea/system location. The shores get to be placid due to seaward outbound surface skimming wind. This down regulates wave formation at point of injection of atmospheric thrust as in experimental models in Fluid mechanics [20]. Fig.-6 is an imaginary cross section covering the domain between Haldia-Puri towards Chitagong - Rangoon. Position WSST is the region of upwelling cum updraft of the ocean-atmosphere couple marked by ↑ arrows. UAD indicates the atmospheric turbulence cum atmospheric bridge connecting the depression with moisture sourcing regions.The bridge phenomena was discussed by us in 2006 & again in 2007 [see Ref 6 & 25]. It is alike the dipole phenomena [21]. Position CSST is the region of down draft cum down welling cum gravity wave phenomena of the ocean-atmosphere couple marked by ↓ arrows. Arrows along the sea surface mark the transfer of the horizontal component of the (additionally induced) thrust along the surface, towards the shore.

This is apart the sea breeze, which also has similar mechanics, and is surface skimming. Moreover, additionally at locus CSST the cold water sinks and pushes up the warm water at about point SLC. There is (possibility) mixing of warm sea surface water of synoptic scale. Principles of fluid mechanics states that when two fluid masses having contrasting hydrodynamic and hydrothermic property mix, they cause super elevation [22]. In Fig-5b we can note super elevation in. Further, due to the inclined continental shelf thinning of the fluid mass happen in this zone (marked as SS), counter thrust is low, and, Newton's 2nd Law of motion is dominant in place of the 3rd Law of motion. At the same time, synergistic astronomical gravity (marked as FM) further assists an hyper swell and fold enlarges the available space, for the more buoyant and dynamic fluid to occupy. The local sea surface attains an ultra heightened head; higher dynamics; and as a swelled and enlarged body surges forward towards the shore, as a unidirectional flow comprised of longitudinal waves of large breadth dimension (*locus* SS). Such phenomena can occur under clear sky conditions in fair weather. We find that the {reported} phenomena is an interplay involving, meteorology, positional astronomy, fluid mechanics and orography, which we have tried to graphically explain in Fig.-6.

Condition 5-iv

Bhattacharya & Ramancharala [23] have discussed wave propagation caused by meteorite strike on solid phase and sea bottom seismic subduction caused tsunami waves. We now consider in brief the underlying physical process {physics cum mechanics} of a tsunami. A tsunami may have (i) draw down phenomena as was the case in the Fukishima event of 03-2011 (ii) the typical leaping wave having giant architecture, as being operated as per some howitzer barrel action as was the case at Karikel on 26-4-12. Herein, we consider only No. (ii) For topical levity. For the generation of a Tsunami there has to be an active tectonic fault line of sea bottom *locus*, where occurs sub-duction, whence from germinates a compression as the product of piston effect. This compression packs hyper energy (dynamic inertia) and stands apart distinguished from the rest of the fluid bed {sea bottom liquid} that is in static inertia. Equilibrium must happen. So the energy band will move towards the point of least physical resistance *i.e.,* the surface. Post surfacing the energy band will travel as a sub-submerged wave and will also veer off the deep sea because they will have more firm boundaries and opposite thrust of higher order, and hence the wave will sail towards the nearest shore lines that also have relatively wider continental shelf [*note-i*].Thus the tsunami etiologically is a sub-marine wave and is different from that of shore waves. A tsunami wave also has much more packed energy.

In-Sea Cancellation

Figure 7 schematically explains the known paths of tsunami propagation in the BoB. Literally it pertains to the disastrous tsunami event of 26/12/2004. The thick black line represents the sub-duction active zone [24]; the arrows represent the lines of tsunami wave propagation as observed at event 26-12-2004. The Coral Islands (>100 in numbers) shield the eastern shore-board of the Indian peninsula that is approximately to the north of 15°+Lat. They act as barrier reef phenomena. South of such latitudinal divide, the beaches (Coromandal coast) had experienced the 12/2004 tsunami. North did not.

Furthermore, the regions that are apparent to the seismic line (yet are not to the lee of the Coral Islands) have perennial rivers with large discharges. These discharges are cold and are also loaded with silt (suspended solids). The sea's clear, saline, warm higher specific gravity fluid gets admixed with the river's cold, lighter, yet sand-silt loaded mass. This causes (gross) change in the current potential in either fluid masses leading to precipitous alteration in inertia in either fluid mass (i) inflicting an angular dive down of the incoming sea waves (ii) load shedding (suspended solids), that additionally also acts as a wall for dispersion of the energy as in the incoming submerged sea wave, thereby down-regulating/canceling effectively. Such cancellation do not occur with tide as because it is a supra member. In Fig.-7, one of the arrows is incident onto the Konaseema district {offshore oil gas bed new find zone}. This ray however is also loosely filtered by the coral barrier reef. During event 12/2004 the river mouth regions (to the north of Krishna south delta); of Godavari; Konaseems; Hoogly-Padma had precisely experienced an 'absence' of sea-surges, although the Karaikel coast (immediate south of Krishna mouth) registered 'howitzer barrel action' phenomena and (record) wanton loses.While, the neighbouring Visakhapatnam-Chilika-Vitar kanika-Dhamara are (additionally) directly in the lee of the coral islands.

The Hoogly-Padma shorelines have a more high discharge (any period). Hence this zone had completely cancelled the tsunami episode of 12/2004. Thus, the eastern sea-board of India, to the north of 15° Lat., is tsunami safe. Therefore, the Konarak-Kalingapatna shore-line has historically attracted high rise, load structured building exercises measuring >45 meters in height and cultural concentrations. This stretch also has the characteristic shore dunes (colloquially known as '*luni bandha'*) made of fine sand. It may be relevant to discuss further, that, the extant 'historical load structures' on the shore-line also suggests absence of catastrophic tsunamis and or disastrous seismic activity for at least on a time scale of millennia [25]. Which is why, the entire delta-coastal belt of Mahanadi-Chilika flood plains (*upataka*) is a veritable store of on-surface, intact, maritime archaeology [26-28]. This also additionally suggests non devastation by any past events of tsunami. In other words, the southern section of the shore line of the eastern shore board of India (south of Krishna delta) are not tsunami safe.So also is the western shore board of Bangladesh and Myanmar. Thus the Indian engineers and related engineering services have domain specific cut out jobs for the entire BoB rim nations.

Heritage Perspective

Historical facts and heritage practices have to us also provided inspiring leads and links. They need to be discussed in brief for topical levity. Among the various politico-cultural communities that habitated the eastern shore board of India, the natives of the Dhamara-Paradip-Puri-Gopalpur-Visakhapatnam/Gopal-patna-Konaseema region were known as 'kalingans'- a prakrit-sanskrit phone that means 'cleaver & intelligent' [29], and the geography as heart land Kalinga.Bhattacharya [30-33] has adduced a series of archaeology related enviable maritime assets; and hydraulic devices and their science and engineering, datable to *c.*650-1450 A,D. Majumdar [34], has proven that pre to Chola period (*c.* 10th A.D.) the erstwhile mighty Kalinga empire was bi-partite. That, one part of such erstwhile empire was in the S E archipelago; wherein even to this date the royal families go by the epithet 'kalingan princes/dynasty'. So, alike the Nordic, the kalingiyas too were a maritime society [35]. And, they have passed no stories whatsoever about sea caused deluge; giant/leaping waves or sea ingression. This has inspired the author to look beyond the apparent.Albeit there is prophecy (c.16th A.D.) in the local vernacular [36].

On any beach, the fluid flows back as a thin film ground hugging flow to form the next wave (beach side).This is 'back wash'. It is also the apron of the (part feed stock) swell that makes the next wave. It has lower velocity than the 'wash up', post splash. The back wash is the under current. On Puri-Konarak beaches such-under current ranges between 3-7 mts. only. The inter-wave regions widen towards the sea; have increasingly depth of the fluid; and reducing under current (selenic phase & alignment dependant). At swell, such 'depth', enlarges. The inter-region reduces at tide, and widen at ebb. It is the depth of the fluid that makes everything buoyant (more because sea water has higher specific gravity), including causing death by drowning only of the non-initiated {and not the under current}. At ebb, the 2nd inter-region is marked by distinctly clear water. The 1st inter-wave region is also the most populated bathing stretch. It is also relatively shallow (knee deep); turbulent; with rapid reversal (*i.e.,* next wave forms and breaks) phenomena. The bottom sandy surface of the wave breaking regions are marginally deeper (waist deep) due to scouring, than the wave build up regions (knee deep), due to load shedding/sedimentation. In other words, the inter-wave regions experience sedimentation due to weak under current (low Reynolds phenomena), which is why, the entire span of the breaker zone has an undulating bottom (dimensions keep altering). All this restricts any long scope out flow (at surface or at bottom).Facilitates sea bath and annual mass nestling by amphibians of various types.

On the Puri-Konark beaches, following the break (beach side wave splash), the wash-up is relatively much stronger and of longer scope than the wash back. However, the beaches being inclined at an average of 15^0 to the sea level, the velocity of the wash back is flow length cum volume dependant (also mixing length dependant if the fluid mass of 2 continuous/contiguous splashes mingle during wash-up). During the two inter-annual periods beach wash and consequent are weak (placid sea). At Puri a month pre to spring equinox and while at Gopalpur a month post autumn equinox the long shore phenomena is virtually non existent, and beach wash is also weakest (inter space of the long shore phenomena is widest at either beach bar and formation mechanics is in up-regulation mode). This limits wave size and also results in early attainment of the splash threshold of the next wave. As and when, a miss-match occur {randomly happens} in the timing, a larger wave with a strong 'wash-up' materializes. This however does not compare with the wave size of the reported events.

Again, as compared to all other beaches along the same latitude with a similar size of sea-front, at Puri the pneumatic thrust in the wash ups is higher, at any hour of the day, throughout the year. This results in the floatsam/off balance bather being washed up the beaches, and not being dragged in. This makes sea bathing safe and exhilarating. All these (over-time) have conjointly resulted in the region becoming a choice sea-shore tourist/religion related bather's destination, since *c.*12th A.D., which is the historical date of the great Hindu religious heritage structure 'Sri Mandira' (apex shrine) being built in the locale, and pan India Hindus [*note-ii*] gravitating to these beaches for ritualistic bath(s). Among other mass participation based rituals, baths have historically been uniting the Hindus, across India. The beaches along the western and southern shore boards of the Indian peninsula have no such (comparative) wave phenomena, nor bath rituals. Save & except Goa (c.17th onwards) the southern-western beaches also do not have any similar geomorphology or orography (the underlying main causes). Due to such benign beach conditions in Odisa the Olive Ridley [37] and the Horse Shoe Crab [38], which also are docile amphibians cum inefficient swimmers, select these beaches for mass nestling (natural selection).

The selection of these beaches by the docile ancient species may also have the precedent cum inspiration factor for the anthropogenic mass-bath rituals. Furthermore, Odisa has large rivers (sans similar mass festivals). Yet the natives of Odisa have adopted sea beach baths. So we may (considerately) aver that mass beach baths are conscious societal decision, and is vital to the caption context. Bathers drown primarily due to (i) intoxication (ii) psychological shock; and not due to wave action or under current. It is noted that tsunami effected beaches are also home to frogs; such as Bengakallu which in Odia-Prakrit is 'Benga-kulla' (frog shore). Froga are conspicuous by absence along the Puri-Konark beaches whereupon millions of pan-India Hindus congregate for mass beach baths. Puri is the Hindu's apex religious heritage site, and Konarak is UNESCO-World heritage site; separated by 20kms along the same shore line. At Puri, the Trinity's mobile representative {*chalanti pratima*} visits the beaches, on every new moon, at high tide

period. This apart, the Puri beaches have numerous other bath rituals ranging the full *luni* year. At Konarak (Chandrabhaga beach), is held the very special bath festival (as different from weekly/ monthly/ trimester rituals as are at Puri, and elsewhere) beckoning the pan-India Hindu. It is known as the *Magha saptami buda* (dip of the 7th of February; waxing; neap tide; absence of 'long shore' phenomena), whence, an amber Sun (made more splendid by stage-to-stage changing refraction due to the variously stratified sea mist) rises with the moon at zenith. All this becauses moderate swell; surf crested mild breakers; higher volume beach wash with lazy back wash; with the under-current being at annual least.

Whole large joint families take this annual ritualistic dip, including children – starting the wee hours (camp and cook on the beaches). The Chandrabhga *Magha saptami buda* (wee hour event in arm sea water) is associated with good-health/therapeutic effect/recovery from chronic\debilitating ailments related to the osteo; dermis and the musculature. This mass beach bath is the 'heritage health bath' of India. It is an east facing event. It is preceded by the *Ganga-sagar mela* (Ganges-Sea confluence congregation; south facing event), held along the same shore board, pre dating by two weeks, also moored to the luni calendar, yet celebrates the phenomena of northward precession of the Sun. It is associated with '*moksha'* (deliverance). Such mass beach festivals (having psycho-&-physiological connections) are not associated with other shore-boards of India; nor are such events of mass nestlings. Culturally active shore-lines (logically) are also more susceptible to fear psychosis, and introspection on the part of the altruistic administrations. Hence our enquiry is also relevant from day-to-day administrative and revenue perspectives.

Economy and Employment Aspects

During this decade long study and quinquennial mss., drafting period it was also noted, that in many instances, modern roads and temporary commercial/service providing tenements; mobile and movable kiosks; and round the year small, casual, yet gainful employment generating units have mushroomed at the edge of the monsoon period highest, high tide line (insignificant compared to Euro-American coastal eco zone violations). Diffuse self employment and revenue are being generated on a sustained basis {union & provincial kitty}.The union of India and as well as her regional and local administration(s) have also been providing with fillip.In other words, anthropogenic presence and elements have approached the sea and not the other way round. Citing East India Company period survey records, done in 1840-41, by the English military Revenue Surveyor (Lt. H.L.Yhuillier) on empire building duty, who had used the then modern survey methods [39]; and more pre-datable 'pilgrim guides' (*jatri pati*), Bhattacharya [ref.32] has amidst engineers, shown, that, there has been no ingression of the sea during the last half-millennia, at Puri, Odisa, India. At Konarak, the sea has receded marginally.

All this, is historical cum geographical counter evidence. It is well known, that, in a over-populous nation (India), by building sea shore tourist infrastructure, the economy gains in terms of year round international, national tourist visit, stay-put, employment and cash flow with a benign cascade, particularly, as the shoreline has no known history of tsunami [40]. And, heritage tourism is potent anti-dote to recession. The mid-Atlantic submarine ridge & fault are prone to severe a seismic possibility – which makes tsunamis as transpiring candidates. In the USA commercial firms are allowed to construct building even over the shore sweep regions (Atlantic\Gulf face). This is not the case in India. The coastal people & coastal ecology & coastal economy shall stand to benefit.

CONCLUSION

Sea surge/tidal bore has a development period – are gradual events, associated with strong winds and, also offers a much wider window (alert) for the beach and shore dwellers to react (even sans any public warning system). Whereas, the tsunami does not. Tsunami has a seismic etiology. The depth dimension and the potential energy factor of it is many fold more than sea surges and tidal bores. The intermittent, high coastal tides and wash backs are not tsunami. They are sea surges. Sea surge is innately of meteorological cum astronomical cum hydrological etiology.

Gravity wave is one of the prime co-upregulator, for an atypical behaviour at beach head. Sea surges are superficial waves. In Sep., the eastern rivers were in high flood discharge mode. Round the clock, cancellation factors were present in high potency. Our considered view is that the Sep.8-11th shores waves off the coast of Puri-Konarak marine drive is not seismic genic. Haldia- Dhamara-Paradeep-Vishakhapatnam is tsunami safe ports; Ganga sagar–Digha-Chandbali-Konarak-Puri beach heritage culture and rituals are tsunami safe. So also the Bhitarkanika and the Chilika are tsunami safe natural heritage. In response to our self set enquiry, the answer gels as, 'Yes', the eastern shore board of India is tsunami safe for anthropogenic activity relating to (i) heritage, religious, tourism, leisure, recreation, etc., (ii) maritime infrastructure and related domains (iii) monsoon water harvesting (iv) posits as paradise for the investment banker and for the related engineering services (v) few thousands of millions of national currency can be invested for sustained profit, on projects/ plans of various gestation with exponential increase in permanent employment scope and house hold prosperity. It is also safe for wild life nestling. The long period IMD data is a versatile tool having relevance for multi-disciplinary usages. Such discussion about the mechanics and the underlying general laws of Physics in particular that because the coastal surges under fair weather conditions remained due un-till this work.

ACKNOWLEDGEMENT

This mss., is dedicated to Sri Amitav Bagchi (Sr. Gown) for his seminal support for me to move to Ravenshaw University (1976).Mr. S. K. Dastidar, both of Bhubaneswar helped me with wherewithal & psycho support for over a decade. Got delayed as falls & frivolous charges were levied against this author by; Arundhati; Swapna & Lipika; Pradeep (as prime abetment & tactical support) Subhasis, Debasis (physical attacks & assault), et.al., kept attacking physically & mentally (until Police & Courts stepped in & helped) – for Radha Krishna Sevasram properties; ransack and destroy. This Mss., in near completion stage on 17-3-2015 was availed from me by a New Delhi based person (cheat~withdrawn). Became untraceable thereafter. Meanwhile, the matter got reviewed concurrently and updated & submitted to IJONS, with thanks.

Notes

Note-I

The wider be the continental shelf, for longer scope the fluid burden acts as a thin film water body and Newton's 2nd law is more in operation. This acts as bed volume for better conservation of energy, and thereby attracts the tsunami.

Note-II

The term 'Hindu' is of Lama Etiology, and connotes unshakable\non-migratory. It is a non belittling term (human geography phone), never challenged even by the erudite scholarly Sanatanis. And, the ceaseless arrays of pan-indo mass festivals bear this out. Even the Muslims of India have picked it up, as compared to Muslims of other sub-continents; the native indo-musalman has more number of mass festivals (corollary info).

REFERENCES

1. Bhattacharya Deepak (D), 2008. "Tsunami Alarm : A Theoretical Model", International Research Symposium on Natural Hazards, Tsunami & Natural Hazard – 4th Asia Pacific Rim Universities, Uni..of California, Davis, USA, Proceedings, pp. 8-9.
2. "Tsunami Strikes Odisha Coasts", Translated from Odiya Vernacular daily. The Sambada, (10 Sep., 2007), p.1.
3. "Silent Tsunami Strikes Odisha", Translated from Odiya Vernacular daily The Dharitri, (11 Sep., 2007), p.1 & 4.

4. "Giant Waves Erodes Odisha Coasts", Translated from Odiya Vernacular daily The Samaya, (12 Sep., 2007), p.6.
5. India Meteorological Department, 30 yr. Data Book 1950-80, Govt. of India, New Delhi, 1995.
6. Bhattacharya, D. & R.C. Panigrahi, 2007. "Tsunami and Eastern Shore Board : Select Discussion", XXVI National Seminar on Hydrology, AHI, NEHU, Oct., Abstract No.5, pp.67-68.
7. http://www.osdpd.noaa.gov/data/sst/anomaly/2007/anomnight.9.13.2007.gif 11/09/2007, 00=00 UTC, IR range { courtesy : Dundee University Satellite Centre }.
8. Shetey, S.R., et.al., 1991. Continental Shelf Research, Vol.11, no.11, pp.1397-1408.
9. http://www.sat.dundee.ac.uk/geobrowse/geobrowse.php?sat=1&year=2007&month=9&day=11&slot=0&ch=2&size=1&grid=1 {courtesy : NOAA web site}.
10. Personal communication, S.K. Dastidar, Sr. Meteorologist, India Meteorology Society, Bhubaneswar.
11. Global Disaster Alert and Coordination System, http://www.gdacs.org/reports.asp?eventType=EQ&ID=30400&system=asgard&alertlevel=Green&glide_no=&location=IDN&country=Indonesia
12. Courtesy, India Meteorology Society, Bhubaneswar.
13. Bhattacharya, D. 2008. 'The Monsoon: Polygonal Box Experiment - A Model', *Hill Geographer,* XXIV, vol.1 & 2, 2008, pp.27-48.
14. Bhattacharya, D. & P.C. Kara, 2007. "Coastal Hydrology and Sand Bars : A Discussion", *XXVI National Seminar on Hydrology*, AHI, NEHU, pp.42-43.
15. Sun-rise to set are also viewable from Godavari and Krishna delta beaches.
16. Misra B. K. & Bhattacharya D., 2007. "Embankments and Coastal Hydrology Modification : Histo-Geographical Perspective", *XXVI National* Seminar, pp.40-41.
17. Kumar, K.N. & T. K. Ram Kumar, 2008. 'Characteristics Of Inertia-Gravity Waves Over Gadanki During The Passage of A Deep Depression Over The Bay Of Bengal', *Geophysical Resh Letters*, VOL. 35, L13804, 5 pp. doi:10.1029/2008GL033937.
18. Jeff Schmaltz, MODIS Land Rapid Response Team, NASA GSFC, Satellite : Aqua, http://modis.gsfc.nasa.gov/gallery/individual.php?db_date=2011-11-17
19. Meteosat VISSR (IODC) 057.0E Quicklooks, 10-09-2007 at 00=00 UTC, IR, 10.5 - 12.5 µm. Curtsey – Dundee University, Sat Receiving Centre.
20. Yuan, S. W. *Foundation of Fluid Mechanics*, Prentice Hall, New Delhi,1964, p.305.
21. Saji N H, et.al., 1999. A Dipole Mode In The Tropical Indian Ocean, *NATURE*, 401, pp.260-63. Doi : 10.1038/43854
22. Weerakoon, Tamai & Kawahara, 2003. *Proceedings of the Institute of Civil Engineers* [ICE], Mar., pp. 73-83.
23. Bhattacharya D. & P. Ramancharala, 2017. Journal of Geography & Natural Disasters, Vol. 7 (3), DOI: 10.4172/2167-0587.1000203.
24. Phil R. Cummins, 2007. Nature 449, 75-78, doi:10.1038/nature06088
25. Bhattacharya, D. *National Seminar on Earth Quake*, Institution of Engineers & Dept of Science & Technology, Bhubaneswar, 11-03-2006.
26. Bhattacharya, D. and Naik, P. C., 2007. '*Hydrology and Spacio-Temporal Aspects of Ancient River Dock*, *XXVI National Seminar on Hydrology*, AHI, NEHU, pp. 37-38.
27. Bhattacharya d, p.c. Naik, 2008. Lay out, hydrology & spacio temporal aspects of a possible ancient inland river dock : india, *utkal historical research journal, utkal uni.,* vol. Xxi, pp. 61-72.
28. Bhattacharya D, 2017. European Frigate Fort - Potagada ? Naval Heritage of India : A Hypothesis, *Journal of Odishan History*, Vol. XXIX, Dec. 2016, pp192-207.
29. V.S. Apte's, 1957. The practical Sanskrit English Dictionary, Ed. By Gode & Karve. Prasad Prakashan Poona, Voll. P. 547.
30. Bhattacharya, D. & Naik, P. C., 2008. "An Ancient Mariner's Compass", {international maritime journal} Pomorstvo, god. 22, br. 2, str. 221-243. WWW ~ : *hrcak.srce.hr/file/49124*
31. Bhattacharya, D. 2010. Indian Ancient Sciences, (Lap Lambert, Germany), ISBN 978-3-8443-2437-2.

32. Bhattacharya, D. 2011, **'**India's Irrigation Heritage: Select Perspectives', *Journal of The Institution of Engineers India, Architecture,* Vol.No.92, 18-04-2011, pp.28-37.
33. Bhattacharya D, 2012. Navigation Matters In Odisa Archaeology: Select Discussion, *Utkal Historical Research Journal*, Vani Vihar, Utkal Uni, Vol.XXV, pp.8-50.
34. Majumdar, R. C., 1986. *Suvarnadwipa* - Vol-I-pp-6, 17,30,31,33,39-87, 180, 181. Also see National Museum, Indian Navy Gallery, New Delhi.
35. Bhattacharya D, 2017. European Frigate Fort - Potagada ? Naval Heritage of India : A Hypothesis, *Journal of Odishan History*, Vol. XXIX, Dec. 2016, pp192-207.
36. Achyutananda Das.s 16th A.D., "Bhavisyata Maalika" (Panchasakha), https://en.wikipedia.org/wiki/Achyutananda
37. http://articles.timesofindia.indiatimes.com/2012-03-22/flora-fauna/31224741_1_olive-ridley-turtles-gahirmatha-beach-female-turtles
38. Bhattacharya D, 2012. A Discussion on Indian Indigenous LAL, *International Journal of Research Pharmacy,* Vol.3 (8), pp. 176-82 (sterling invention for india).
39. Sarat Ch. Mahapatra, 1994. Car Festival of Lord Jagannath Puri, (full book), Sri Jagannath Research Centre, Puri.
40. Bhattacharya, D. etal., 2009. INTROPMET, IMS, N Delhi, Book of Abstracts, p.144.

Table – I (Puri)

Date	Location (19°49′N//85°50′E)	Avg. Decadal hPa/Sep.	Selenic Phase	IMD station data on date	Hour
06/09/2007	Puri	1006-08	Dasami (waxing)	1004	02.30
07/09/07	-do-	-do-	Ekadasi "	1006	-do-
08/09/07	-do-	-do-	Dwadasi "	1008	-do-
09/09/07	-do-	-do-	Traiyadasi "	1009	-do-
10/09/07	-do-	-do-	Chaturdasi "	1009	-do-
11/09/07	-do-	-do-	New Moon "	1009	-do-
12/09/07	-do-	-do-	Pratipada(waning)	1008	-do-
19/09/07	-do-	-do-	Sasthi "	1006	-do-

Table – II (Gopalpur)

Date	Location (19°49′N//85°50′E)	Avg. Decadal hPa/Sep.	Selenic Phase	IMD station data on date	Hour
05/09/2007	Gopalpur	1000-04	Nabami (waxing)	1002	02.30
06/09/07	-do-	-do-	Dasami	1002	-do-
07/09/07	-do-	-do-	Ekadasi "	1004	-do-
08/09/07	-do-	-do-	Dwadasi "	1006	-do-
09/09/07	-do-	-do-	Traiyadasi "	1008	-do-
10/09/07	-do-	-do-	Chaturdasi "	1009	-do-
11/09/07	-do-	-do-	New Moon "	1009	-do-
12/09/07	-do-	-do-	Pratipada (waning)	1007	-do-
19/09/07	-do-	-do-	Sasthi "	1004	-do-
22/09/07	-do-	-do-	Dasami "	997	-do-

Fig. -1a

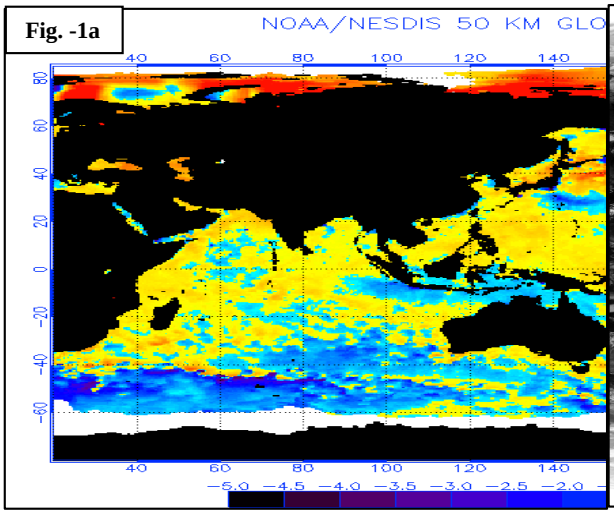

Fig. – 1b

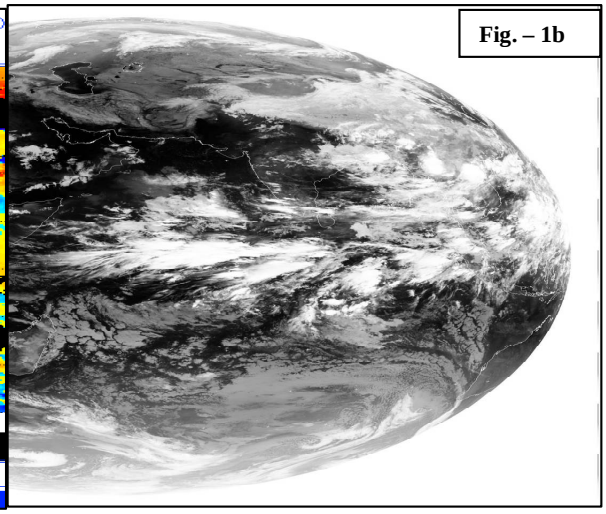

Fig.-1a is the global SST anomaly {SST-a} on 13-09- 007 **Fig.-1b is a satellite image**

Fig. - 2

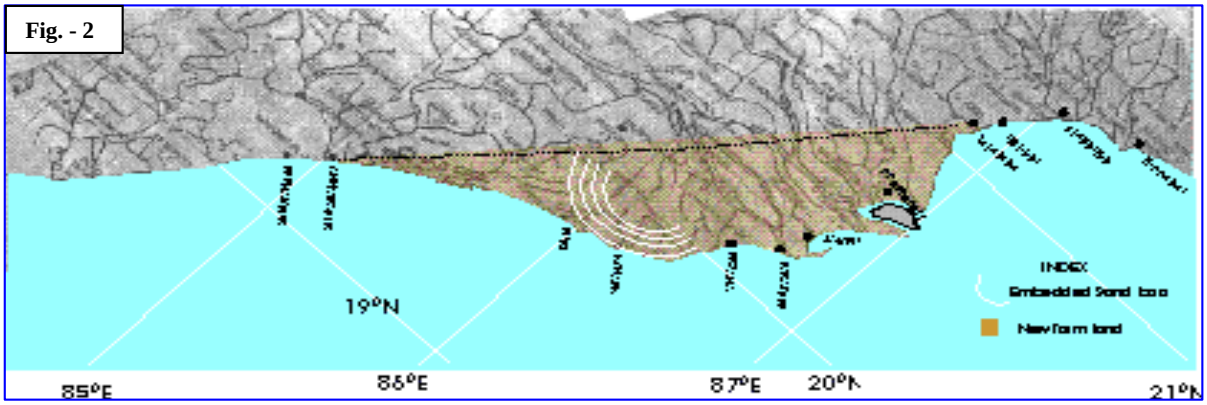

Figure 2 is a map of the focused domain, drawn at 1° grid

Fig. - 3

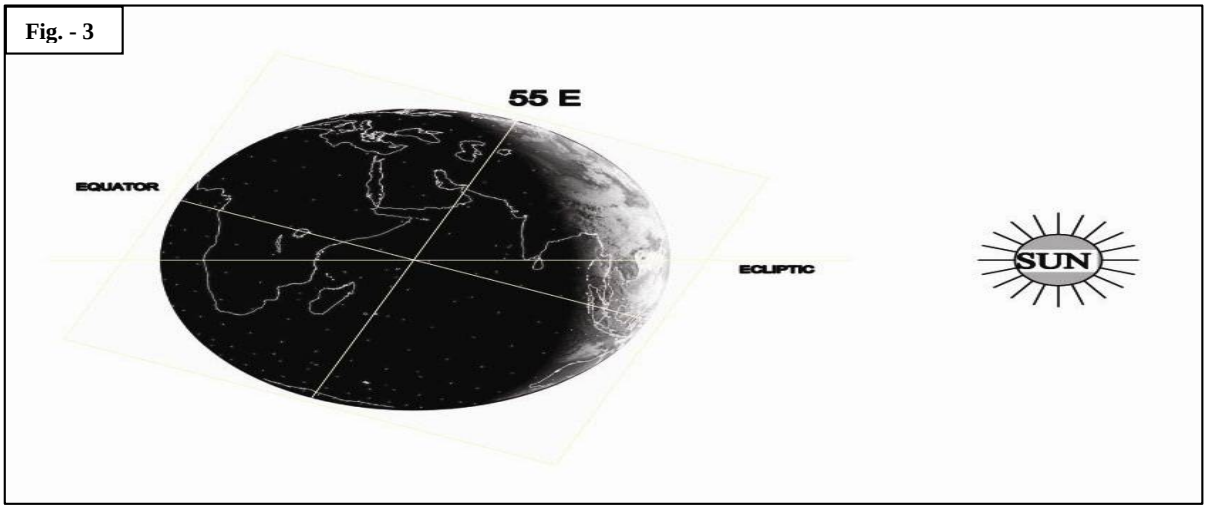

Fig.-3 graphical explains that the globe is inclined towards the true NE

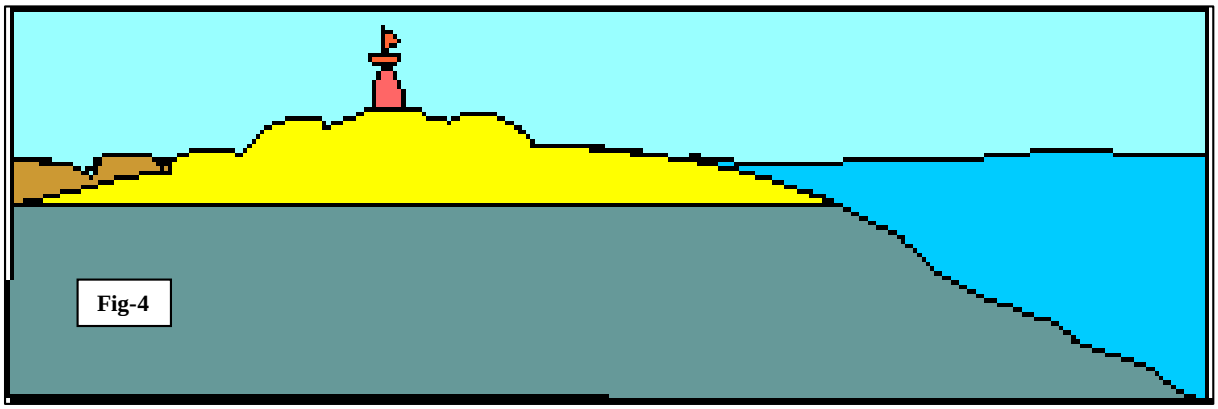

Fig.-4 gives the schematic impression {elevation} of the shore board ranging between 500 - 1500 Mts

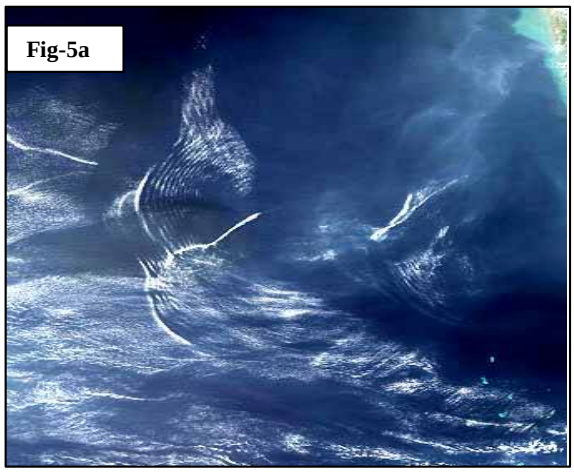

Fig.-5a is that of the gravity waves in the Arabian Sea

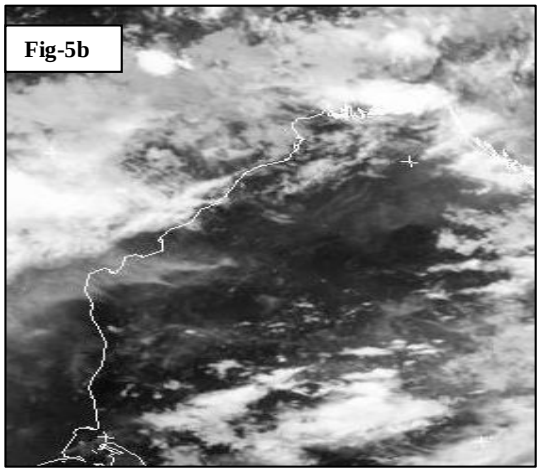

Fig-5b super elevation

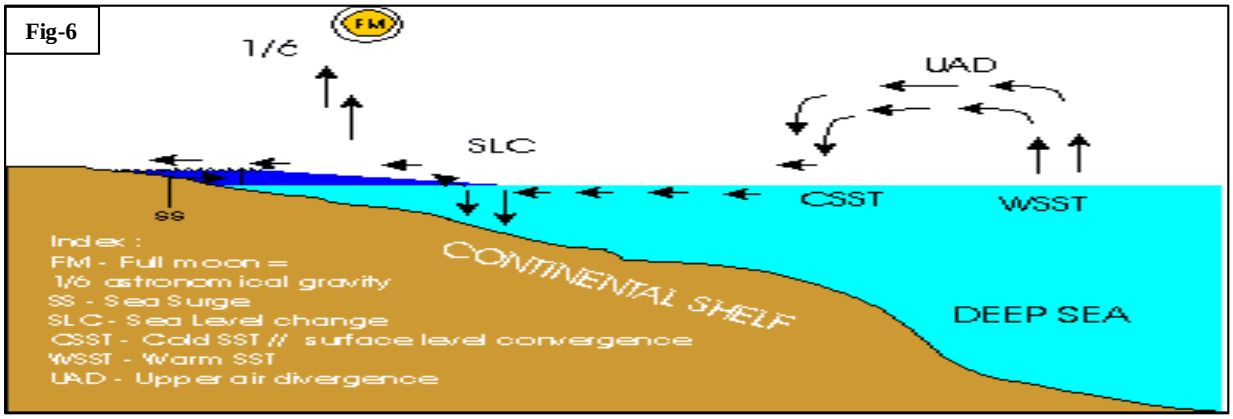

Fig-6 regions are marked by glistening mini wavelets on the sea surface

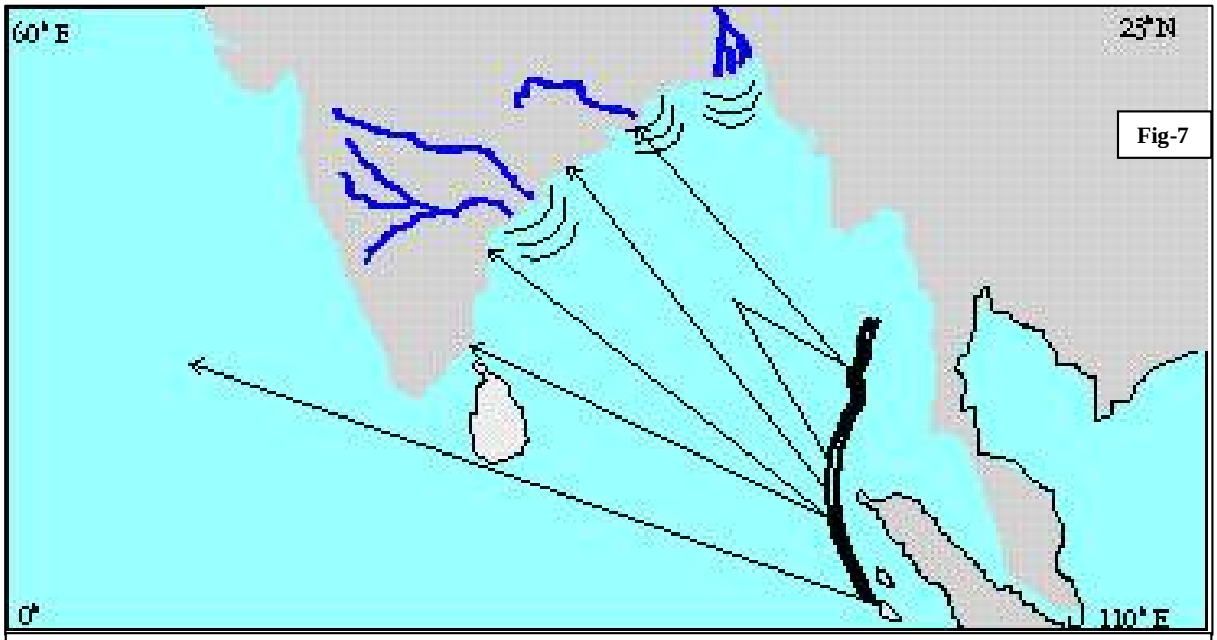

The eastern sea board of India is shielded by the coral islands which act as a barrier reef and the river discharge act as the cancellation masses.

Fig. 7 schematically explains the known paths of tsunami propagation in the BoB. Literally it pertains to the disastrous tsunami event of 26/12/2004.

Indian Journal of Natural Sciences www.tnsroindia.org.in ©IJONS

Vol.8 / Issue 49 / August /2018 *International Bimonthly* *ISSN: 0976 – 0997*

RESEARCH ARTICLE

Study the Level of Correlations between Hormones and Cholesterol, Blood Sugarin Polycystic Ovaries

Nidhal khaleefah Ahmed* and Ezeddin A. Albayyar

Department of Biology, Faculty of Sciences, University of Anbar, Al-Anbar, Iraq.

Received: 08 May 2018 Revised: 15 June 2018 Accepted: 19 July 2018

***Address for Correspondence**
Nidhal khaleefah Ahmed
Department of Biology,
Faculty of Sciences,
University of Anbar,
Al-Anbar, Iraq.
Email: daln87.na@gmail.com

ABSTRACT

Polycystic ovary syndrome (PCOS) causes ovulation disorder and infertility in female patients. This study is under taken to measure level of hormone (FSH, LH, testosterone and prolactin) and to see the relationship level of hormones with cholesterol and B. sugar. The result of this study was increase in level of testosterone, prolactin, LH and cholesterol in patients compared with control group and FSH is different in both study groups but remained within normal limit. Cholesterol was positive correlation with the level of hormones and negative correlated with blood suqer and PRL

Key Word: Polycystic Ovaries, Hormones, Cholesterol, Blood Sugar

INTRODUCTION

Polycystic ovary syndrome (PCOS) is one of the leading causes of endocrine-dependent infertility, with a prevalence of 6.5-10% among women of reproductive age **(1).**Polycystic Ovary Syndrome (PCOS) is a heterogeneous disorder as one of the leading causes of anovulatory infertility; It is believed that 5 - 10% of the reproductive-aged female population is living with polycystic ovary syndrome (2**)**. PCOS is often associated with obesity, mainly abdominal obesity **(**3**)** and insulin resistance **(**4**)**. The link between obesity and reproductive problems in women has been studied for a long time and is confirming by numerous epidemiological and clinical studies **(**5**)**. It hasbeen demonstrated that visceral fat is the most significant variable correlating with metabolic dysfunction in women with PCOS **(6)**. A recent review showed that visceral adipose tissue is involved in the secretion of various adipokines and vasoactive substances associated with an increased risk of metabolic and cardiovascular diseases One of the major biochemical features of PCOS is insulin resistance(7) accompanied bycompensatory hyperinsulinemia; that hyperinsulinemia produces hyperandrogenism of PCOS by increasing ovarian production particularly testosterone and by decreasing serum SHBGconcentration(8). The high levels of androgenic hormones interfere with the

pituitary ovarianaxis leading to increased LH levels, anovulation, amenorrhea, recurrent pregnancy loss andinfertility(9). Hyperinsulinemia has also been associated with high blood pressure and increasedclot formation and appears to be a major risk factor for the development of heart diseas andInsulin resistance effects 15-20% of women withPCOS leading to a number of comorbiditiesincluding metabolic syndrome, hypertension, dyslipidaemia, glucose intolerance, anddiabetes(10)

Mental health disorders including depression, anxiety, bipolar disorder and bingeeating disorder also occur more frequently in women with PCOS.Study was undertaken to assess the risk factors for women infertile women with polycystic ovarian syndrome resulting from physiological disorders and clinical ests.Demonstration of serum level of related hormones (Prolactin, Follicle Stimulating Hormone (FSH), Luteinizing Hormone (LH), Testosterone.Identification of LH/FSH ratio in women with PCOS.PCOS relationship with sugar, cholesterol.

MATERIALS AND METHODS

The study was conducted during the period from November 20016 to May 2017 at Abu Ghraib Hospital.The study of material consisted of a total number of 70 women in the reproductive age. Fifty patients with PCOS diagnosed by gynecologist aged between 18 to 40 years whose chief complaints were infertility and/or menstrual disturbances and /or clinical signs of hyperandrogenism (hirsutism and acne), and/or ultrasoundevidence of polycystic ovaries, with twenty healthy women regarded as control group aged between 17 to 45 years. All patients enrolled in the study fulfilled the following criteria:

Exclusion criteria

1. Patient's refusal.
2. History of recent administration of hormonal therapy.
3. Male factor infertility.

Each subject was involved to detailed clinical history. The patients group had undergone baseline investigations of PCOS.According to our including criteria, all patients were expected to have disturbed ovulatory function with chronic oligomenorrhea (cycle length more than 35 day; less than 9 cycle per year) or amenorrhea (cycle length more than 12 week) and typical appearance of polycystic ovaries by ultrasound (U.S) according to the criteria of Rotterdam consensus meeting 2003

Anthropometric data

Body Mass Index

All the subjects' height and weight were recorded using standard apparatus. Body mass index (BMI) was calculated by dividing weight (kg) by height (m2). Normal weight was defined as BMI < 25, Overweight as BMI between 25.0-29.9 and Obesity as BMI > 30.

Sample Collection and Storage

5 ml of venous blood samples was collected from healthy controls and women with PCOS after 12 hrs overnight fast. 1 ml of sample was taken in a tube containing anticoagulant and analysed for plasma glucose. 4 ml of sample was taken in a plain tube. After centrifugation at 3000 rpm for 10 minutes, the serum samples were incubated for 15 minutes at room temperature and analysed.

Methods of Biochemical Estimation

The control and patients with Polycystic ovary syndrome blood samples were analyzed for biochemical parameters by standard procedures as follows: Serum glucose was estimated by kit (Spinreact, Spain) ,Cholesterol in the serum was measured by enzymatic method, with the biomerux kit, France and serum folliclestimulating hormone ,luteinizing hormone,testosterone and Prolactin were estimated by ELISA method usin Human ELISA Kit ,Germany

Statistical Analysis

Data Analysis was performed using SPSS 16 Software. The differences between means were assessed by "t" test. Pearson's correlation coefficients among parameters were estimated.

RESULTS AND DISCUSSION

FSH and LH

In our study the mean value of FSH and LH in patients was 5.028±1.94 mIU/ml dnd7.02±4.18respectively, compared with control mean which equal to 7.41 ± 3.96 mIU/ml, 2.07 ± 2.18mIU/ml respectively. There was highly significant difference ($p<0.05$) between two groups, high level of LH and low level of FSH, may be due to enhanced pituitary sensitivity to GnRH stimulation or to increased pulse frequency of GnRH secretion. Aberrations in GnRH pulse frequency and inappropriate gonadotrophin secretion may also reflect an insensitivity of the GnRH pulse generator to the negative feedback effects of estrogens and progesterone (11). These results agreed with the results of Shi et al., (12) who considered that polycystic ovarian syndrome stems from a basic inability of the ovaries to produce hormones in the correct proportions. The pituitary gland senses that the ovary is not working properly and reacts by releasing abnormal amounts of Luteinizing Hormone (LH) and Follicle Stimulating Hormone (FSH). Both hormones are necessary for ovulation, the ovary to develop and release an egg.Meeket al., (**13)** said that a higher LH than FSH in the early part of the menstrual cycle is a hallmark of PCOS and seem that confirmation of an elevation in LH is very diagnostic of PCOS. The measurement of FSH will also permit the diagnosis of an occult ovarian failure where the FSH levels are particularly elevated

Regarding LH/FSH ratio there was a significant difference ($p<0.05$) between both study groups as the mean value of LH/FSH in the patients and control was 1.601±0.767, 0.874±0.44 respectively. The explanation of FSH ratio might be due either to primary central disorders involving GnRH secretion or secondary pituitary sensitization to GnRH by an abnormal feedback signals from ovaries as suggested by other studies (14). Estrogens were able to increase LH response to GnRH compared with FSH, mainly if unopposed by progesterone that might lead to absence of negative feedback mechanism on LH pulse frequency in response to different GnRH pulse patter (15) . This could explain the highest LH/FSH ratio in PCOS. Still there were controversies about the role of inhibin in preferential inhibition of FSH and not LH rendering elevated LH/FSH ratio in PCOS in general as mentioned by many studies. (16). studies were done in England during the few years ago find that 2.8 was taken as a cut – off value for detecting PCOS, same observation was noticed in 1989 in U.K (17)and this value was agreed with our study.

Prolactin

In our study the mean value of prolactin was 31.4±17.5 ng/ml was significantly ($P<0.05$) higherthan control mean which was equal to 18.75± 12.28ng/ml. The explanation of PRL level might be due to the central neurotransmitter dysregulation, which leads to abnormal gonadotropin output and abnormal ovarian function (18). Altered dopamine turnover could result in hyperprolactinemia, could also affect GnRH output, and therefore could be a common cause for both PCOS and hyperprolactinemia. However, the incidence of hyperprolactinemia among women with PCOS

should be higher if there is a common underlying neurotransmitter abnormality (12), Also Estrogen stimulates prolactin production. Persistently elevated estradiol levels are often found in women with PCOS and could result in mild prolactin elevation (19).This result is parallel with study of Torreand Falorni (20) who revealed that some women with PCOS had hyperprolactinemia .Mild hyperprolactinemia has been reported in 5 - 30% and is generally only 50% above the upper limit of normal.

Testosterone

The results of the present study showed that the mean level of testosterone hormone in patients with PCOS was1.19±0.39 ng/ml while in control group the level was 0.60±19 ng/ml. There was a significant difference (P<0.05) between patients and control regarding level of testosterone hormone. This may be due to the fact that an outer coat of the ovary and the tissue within the core of the ovary was thickened in women with PCOS. The thickened core contained theca cells which produce extra amounts of testosterone .The result of our study was in agreement with the finding obtained by Meek et al., (13) who suggests that ovarian theca cells in affected women with PCOS are more efficient at converting androgenic precursors to testosterone than the normal theca cells. Joham et al., (21) also found that PCOS women had a higher serum level of free Testosterone and this level was usually no more than twice the upper normal range

Blood sugar

In the study the level of Blood Sugar (BS) in patients with PCOS and control group was138.18±32.35 mg/dl and mg/dl 128.2±21.73 respectively. This indicates no significant difference between the groups. This may be due to the many lifestyle changes can pull someone out of the metabolic chaos of PCOS, and decrease her chances of developing co-morbidities such as diabetes, heart disease, hypertension, sleep apnea, anxiety, depression and infertility. This result agreed with study of Moran and Teede (22) who found no significant difference in the level of BS in both study groups (patient with PCOS and control, while in contrast with Insulin lowers the blood sugar by storing the glucose in cells. When this resistance goes on for a while, you have high insulin and high blood sugar. Al-Jumaili et al., (23) found that glucose increased in patients with PCOS than the control and suggest that degree of relativeness of patients with PCOS may be at high risk for diabetes.

Cholesterol in Polycystic Ovary Syndrome

In Our study, the mean level of Cholesterol in patients with PCOS was 225.80±42.79 ng/ml while in control group the level was199.15±36.46 ng/ml with significant difference (P<0.05). This may be due to the fact that Adipocyte secreted adipokines are strongly involved in the development of PCOS.A number of studies found that the evidence in lean women with PCOS is less clear-cut. Sami et al., (24) found that lean patients had significantly lower (HDL-CHO) Levels compared with control, this finding was confirmed by Coasta et al., (25), who compared a number of lean polycystic ovary syndrome patients with others body mass index matched controls and found a significant difference in high density lipoprotein cholesterol levels, which reflected insulin resistance rather than body mass index.

Correlations between Hormones and Cholesterol, Blood Sugar

Table (3.4) demonstrated theCorrelations between cholesterol and B. sugar with hormones (LH, FSH, Prolactin and Testosterone) The results obtainedthat cholesterol was highly significant positive correlation with LH and testosterone and positive correlation with FSH,while it was a highly significant negative correlated with blood sugar and negative Pearson correlated withPRL. B.suqer was highly significant negative Pearson correlated with IH ,FSH, PRL, Testosterone This may be due to s; Were subject to treatment by drugMetformin Metformin is insulin sensitizing drug that exert its effect by promoting peripheral glucose utilization and improving insulin sensitivity.

This result was in contrast with(26)suggested the blood sugar level was highly significant in patients with PCOS and the administration of glucose to hyperandrogenic women increases circulation of insulin and androgens and the administration of insulin to women with PCOS increased circulation androgens

REFERENCES

1. Azziz R, Woods KS, Reyna R, Key TJ, Knochenhauer ES, Yildiz BO., (2004) The prevalence andfeatures of the polycystic ovary syndrome in an unselected population. *J Clin Endocrinol Metab* 89:2745-2749.
2. Ardabili HR, Gargari BP, and Farzadi L.(2012) Vitamin D supplementation has no effect oninsulin resistance assessment in women with polycystic ovary syndrome and vitamin Ddeficiency.Nutr Res, 32(3): 195-201. 28.
3. Chen X, Jia X, Qiao J, Guan Y, Kang J.(2013) Adipokines in reproductive function: a link between obesity and polycystic ovary syndrome. J Mol Endocrin.;50:21–37*BJOG,* 113: 1203-9
4. Amato MC, Vesco R, Vigneri E, Ciresi A, Giordano C.(2015) Hyperinsulinism and polycystic ovary syndrome (PCOS): role of insulin clearance. J Endocrinol Invest. 38(12):1319–1326.
5. Jungheim ES, Travieso JL, Carson KR, Moley KH. (2012) Obesity and reproductive functions. Obstet Gynecol Clin North Am.;39:479–93.
6. Lord, J., Thomas, R., Fox, B., Acharya, U., & Wilkin, T. (2006). The central issue? Visceral fat mass is a good marker of insulin resistance and metabolic disturbance in women with polycystic ovary syndrome. BJOG: An International Journal of Obstetrics & Gynaecology, 113(10), 1203-1209.
7. Niţă C, Hâncu N, Rusu A, Bala C.(2011)Nutrition and triple major risk of abdominal obesity: type 2diabetes mellitus, cardiovascular diseases and cancer.Nutritional Therapy & Metabolism, 29: 55-69.
8. Chang, R. J., & Dumesic, D. A. (2019). Polycystic ovary syndrome and hyperandrogenic states. In *Yen and Jaffe's Reproductive Endocrinology (Eighth Edition)* (pp. 520-555).
9. Hart, R. J. (2016). Physiological aspects of female fertility: role of the environment, modern lifestyle, and genetics. *Physiological reviews*, *96*(3), 873-909.
10. Laakso, M., & Kuusisto, J. (2014). Insulin resistance and hyperglycaemia in cardiovascular disease development. *Nature Reviews Endocrinology*, *10*(5), 293.
11. Moran, L.and Teede.I.(2009). Metabolic features of the reproductive phenotypes of polycystic ovary syndrome. Human Reproduction Update ;15(4):477-488.
12. Shi X, Zhang L, Fu S, Li N. (2011)Co-involvement of psychological and neurological abnormalities in infertility with polycystic ovarian syndrome.Arch Gynecol Obstet.;284:773–
13. Meek, C.L.; Bravis, V.; Don, A.; Kaplan, F. (2013) Polycystic ovary syndrome and the differential diagnosis ofhyperandrogenism. Obstet. Gynaecol., 15, 171–176.
14. March WA, Moure VM, Willson KJ, Phillips DI, Norman RJ, Davies MJ. (2010) "The prevalence of polycystic ovary syndrome in a community sample assessed under contrasting diagnostic criteria". Hum Reprod. Feb, 25 (2), 544-551.
15. Herde MK, Geist K, Campbell RE, Herbison AE. (2011) Gonadotropin-releasing hormone neurons extend complex highly branched dendritic trees outside the blood-brain barrier. Endocrinology152(10):3832–41. doi:10.1210/en.2011-1228
16. Vahidroodsari F, Ayati S, Yousefi Z, Saeed S.(2010)Comparingserum follicle-stimulating hormone (FSH) level with vag-inal pH in women with menopausal symptoms. Oman MedJ;25:13.
17. Qu, F., Wang, F. F., Lu, X. E., Dong, M. Y., Sheng, J. Z., Lv, P. P., ... & Huang, H. F. (2010). Altered aquaporin expression in women with polycystic ovary syndrome: hyperandrogenism in follicular fluid inhibits aquaporin-9 in granulosa cells through the phosphatidylinositol 3-kinase pathway. *Human Reproduction*, *25*(6), 1441-1450.
18. Roland, A. V., & Moenter, S. M. (2014). Reproductive neuroendocrine dysfunction in polycystic ovary syndrome: insight from animal models. *Frontiers in neuroendocrinology*, *35*(4), 494-511.
19. Azziz R, Carmina E, Chen Z, Dunaif A, Laven JS, Legro RS, Lizneva D,Natterson-Horowtiz B, Teede HJ, Yildiz BO. (2016)Polycystic ovary syndrome.Nat Rev Dis Primers.;2:16057.

20. Torre, D. L., and Falorni, A. (2007). Pharmacological Causes of Hyperprolactinemia. Journal of Therapeutics and Clinical Risk Management, Vol. 3 (5), 929–951
21. Joham, A.E.; Palomba, S.; Hart, R. Polycystic Ovary Syndrome, Obesity, and Pregnancy. Semin. Reprod. Med. .Moran LJ, Misso ML, Wild RA, Norman RJ. (2016)Impaired glucose tolerance, type2 diabetes and metabolic syndrome in polycystic ovary syndrome: a system-atic review and meta-analysis. Hum Reprod Update 2010;16:347–63, 34, 93–101.
22. Moran, L.and Teede.I.(2009). Metabolic features of the reproductive phenotypes of polycystic ovary syndrome. Human Reproduction Update ;15(4):477-488.
23. Al-Jumaili, F. T., Naji, A. J., & Jasim, T. M. (2015). Evaluation of Some Biochemical Markers in Patient's with Polycystic Ovarian Syndrome. *Jornal of Biotechnology Research Center*, *9*(2), 37-45
24. Sami N, Ali TS, Wasim S, Saleem S.(2012) Risk Factors for Secondary Infertility among Women inKarachi, Pakistan. *PLoS ONE*, , 7(4): e35828. doi:10.1371/journal.pone.0035828.
25. Costa EC, de Sá JC, Mafaldo Soares EM, et al. (2012);Anthropometricindices of central obesity how discriminators of metabolic syndrome inBrazilian women with polycystic ovary syndrome.Gynecol Endocrinol.
26. De Pergola, G., Ciampolillo, A., Paolotti, S., Trerotoli, P., & Giorgino, R. (2007). Free triiodothyronine and thyroid stimulating hormone are directly associated with waist circumference, independently of insulin resistance, metabolic parameters and blood pressure in overweight and obese women. *Clinical endocrinology*, *67*(2), 265-269.

Table (1-3): Concentration of serum LH, FSH, and FSH: LH ratio & testosterone hormones in Polycystic ovarian syndrome and health groups

	Hormonal assay (m. + SE)				
	FSH (μIU/ml)	**LH (μIU/ml)**	**Testosterone (ng/ml)**	**LH:FSH ng/ml)**	**PRL ng/ml)**
patient	a 5.028±1.94	a 7.02±4.18	a 1.19±0.39	a 1.68 ±1.18	a 31.4±17.51
health	b 7.41 ±3.96	b 2.07 ±2.18	b 0.60± .19	b 0.32±0.35	b 18.75± 12.28

Table 4 Correlations between cholesterol and B. sugar with hormones (LH, FSH, Prolactin and Testosterone)

		FSH	LH	PRL	Testosterone	cholesterol
LH	Pearson Correlation	.551**				
PRL	Pearson Correlation	.348**	.363**			
Testosterone	Pearson Correlation	-.110-	.75**	.019		
cholesterol	Pearson Correlation	.163	.681**	-.425-**	.786**	
Sugar	Pearson Correlation	-.52-**	-.997-**	-.430-**	-.758-**	-.631-**

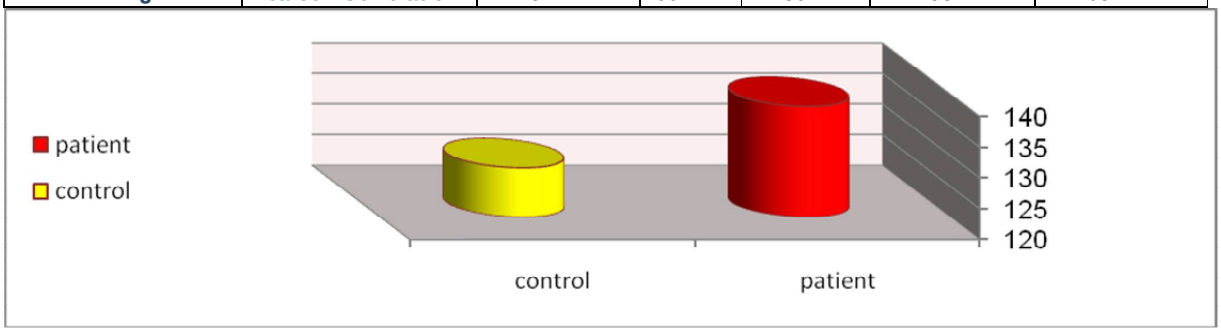

Figure (1-3): The level of blood sugar in patients with polycystic ovarian syndrome (PCOS) and control group

Indian Journal of Natural Sciences *www.tnsroindia.org.in ©IJONS*

Vol.8 / Issue 49 / August /2018 *International Bimonthly* *ISSN: 0976 – 0997*

RESEARCH ARTICLE

A Comparative Evaluation of Some Functions for the Analysis of Growth Curves Inmales and Females Ross 308 Broilers

Ahmed M. Al-Nedawi*

Department of Animal Production, College of Agriculture, University of Baghdad, Baghdad, Iraq.

Received: 20 May 2018 Revised: 23 June 2018 Accepted: 24 July 2018

***Address for Correspondence**
Ahmed M. Al-Nedawi
Department of Animal Production,
College of Agriculture,
University of Baghdad,
Baghdad, Iraq.

ABSTRACT

The present study was carried out to evaluate the validity of some non-linear functions (Richard, Weibull, Logistic, and Gompertz) for describing the growth curve of Ross 308 broilers under the condition of Iraq. A total of 72 broiler chicks (36 male and 36 female) were reared during the period from 15/10 to 27/11/2017. Results demonstrated that the differences in the body weight due to sex were significant ($P<0.05$) in the second, third, fourth, and fifth week, while the differences were not significant in the one day old and first week.The asymptotic weight was highest in the Gompertz (3215.8gm) and lowest in the Weighted Least Square (WLS) (2082.7gm) in males and similar results obtained in females. The corresponding estimations in females were 2388.1 and 1659.0 gm. The results of the four functions indicated that the WLS function is the best function for description the growth curve of the males and females followed by the Richards function.

Keywords: Growth models, Richard, Weibull, Logistic, and Gompertz, Ross 308

INTRODUCTION

The consumption of broiler is dominating the world poultry consumption as it represents about 70 percent of the total poultry meat consumption (Roenick, 1998). All breeders looking for the broilers with very fast grow along with a good quality carcass during the shortest time (Prince, 2002). The fasting broilers growth has apriority of concern because of its importance as an economic trait(Schulze et al., 2001).The growthcurve was subjected to study in different birds and animals because the knowledge of the growth curve has practical applications and will lead to increasing the economic revenue of the project. (Sabbioni et al., 1999; Abbas et al., 2014).The using of nonlinear functionsto fit the growth curve is very important as these functions will provide some parameters that could be used to describe the changes ingrowth pattern over time. Moreover, it will assist the breeders to predict the weight of animals at a specific age and to identify the stage that associated with the decreasing in growth rate (Tzeng and

Becker, 1981; Yakupoglu and Atil, 2001). Several functions have been applied in the broiler for instance: Logistic, Gompertz, Richards, Weighted Least Square (Yang et al., 2006; Topal and Bolukbasi, 2008; Moharrery and Mirzaei, 2014; Al-Samarai, 2015; Mohammed, 2015). Therefore, the objectives of the current study isto identify the best nonlinear function to describe the growth curve of Ross 308 broilers under the conditions of Iraq.

MATERIALS AND METHODS

The experiment was carried outin the poultry farm of the College of Agriculture/ University of Baghdad during the period from 15/10 to 27/11/2017. A total of 72chicks (Ross 308) (36 female and 36 males) purchased from a local commercial hatchery were enrolled in this study. Birds were housed in a floor pen withthe lighting regimen provided for 22 h per day. All birds were subjected to a vaccine against Newcastle disease and infectious bronchitis on the 10^{th}dayof age and against Gambaro disease at 17 days of age. The ingredient and the nutrient composition of the basal diet given to the birds are shown in Table 1. The drinking water and feed were supplied *ad libitum*. Birds were weighed at one day old and each week for 5 weeks.

The concentrated protein type Brocon-5 special W contain the following per kg:20%crude protein, 5%fat,2.2%fiber,4.2%Ca,4.68%P,3.85% Lysine, 3.7% Methionine, 4.12 Methionine+Cystine, 2.5%Na, 2107 ME (kcal/kg), 2000 IU vit A, 4000 IU votD_3, 500 mg vit E, 30 mg vit K_3, 15 mg vit B_1, 140 mg vit B_2 , 20 mg B_6, 10 mg Folic acid, 100 μgBiotin, 1 mg Fe, 100 mg Cu, 1.2 mg Mn, 800 mg Zn, 15 mg I, 2 mg Se, 6 mg Co,900 mg Antioxident.

Growth Curve Functions

The growth functions were applied to the weekly body weight. Five functions were used (Weighted Least Square (WLS), Richard, Weibull, Gompertz, and Logistic) to determine the best function that describes the growth curve of the broiler. The functions and their mathematical notations are shown in Table (2). In all functions, a is the asymptotic (mature) weight parameter, bis the scaling parameter (constant of integration) and cis the instantaneous growth rate (per day) parameter (Yang et al. 2006).

Statistical analysis

The differences of the means in weekly body weight between males and females were assessed using the un-paired t-test. $P<0.05$ is considered significant.All parameters estimated by the Levenberg-Marquardtmethod using NLIN procedure in the SAS program (SAS, 2010). Several criteria are used to determine the goodness of fit: Coefficient of determination (R^2), Mean square of error (MSE), Coefficient of correlation ®, Standard error (SE). The figures for the fitting of function were performed using CurveExpert 1.3.

RESULTS AND DISCUSSION

The results demonstrated that the differences in the body weight due to sex were significant ($P<0.05$) in the second, third, fourth, and fifth week, while the differences were not significant in the one day old and first week (Table 3). These differences could be attributed to that the males have a higher growth rate and this will lead to increase their opportunity to get feed as compared with females.The results of the estimated weekly body weight mean and the prediction means according to different functions used in this studyin the males Ross 308 broilers are shown in the table (4) and Fig (1). Table (5) illustrated the parameters estimated by the different functions in the males' broilers. All parameters were positive except the b and c for WLS function. The asymptotic weight was highest in the Gompertz (3215.8gm) and lowest in the Weighted Least Square (WLS) (2082.7gm) in males. Similar results were obtained by Al-Samari, (2015) who reported that the asymptotic weight was highest in the Gompertz function (2814 gm) and lowest

in the WLS (2088 gm) in the Ross 308 in Iraq. The ranking of functions in male broilers according to some accuracy criteria are as following: WLS, Richard, Weibull, Gompertz, and Logistic (Table 6). Concerning the fitting of the functions in females Ross 308 broilers, the results of the estimated weekly body weight mean and the prediction means according to different functions used in this study in the females Ross 308 broilers are shown in the table (7) and Fig (2). Results indicated that all parameters of the functions were positive except the b of WLS which was negative (-4.34). The asymptotic weight was highest in the Gompertz (2388.1gm) and lowest in the Weighted Least Square (WLS) (1659.0gm) in the females. The ranking of the functions due to some criteria showed that the WLS function was the better function as it has the highest R^2 (0.99993), r (0.99996) and lowest MSE (195.2), SE (6.77), whereas, the Gompertz function located in the last order as it has the highest MSE(337.0) and SE (18.36) along with the lowest R^2(0.99974) and r (0.99966).

The high estimates of R^2 in the present study are similar to other studies obtained by Kuhi et al., (2003) who used several functions such as Lopez, Richards, von Bertalanffy, Gompertz and logistic and showed that all these functions are suitable to fit the growth carve. In this regards, Tompić et al., (2011) found that R^2 of the Gompertz, Richards and Logistic function were ranged from0.988 to 0.995 in Ross 308 broiler. Regardless of the WLS, the present study showed that the Richard function was the best as compared with other function. This result agreed with other results obtained by Kuhi et al., (2003), Tompić et al., (2011) and Moharrery and Mirzaei, (2014). On the other hand, our results disagreed with results reported by Gous et al., (1999) and Santos et al., (2005) who confirmed that the Gompertzfunction is the best function for describing growth curve in the broiler. These differences among studies are expected because there are many factors could affect the results such as the breed, the period of the experiment, type of diet and sample size (Yalcin et al., 1997; Wang et al., 2004; Sun et al., 2006). In conclusion: the results of the fitting of the growth carve by the studied functions confirmed the validity of all these functions in males and females because of the differences in the criteria of accuracy are too little

REFERENCES

1. Abbas AA, Yosif AA, Shukur AM, Ali FH.Effectof genotypes, storage periods and feed additives in broiler breeder diets on embryonic and hatching indicators and chicks blood parameters. Sci. Agri. 2014;7 (1): 44-48.
2. Al-Samarai FR. 2015.Growth Curve of Commercial Broiler as Predicted byDifferent Nonlinear Functions.American Journal of Applied Scientific Research.2015;1(2):6-9.
3. Gous RM, Moran ET, Stilborn HR, Bradford GD, Emmans GC. Evaluation of the parameters needed to describe the overall growth, the chemical growth, and the growth of feathers and breast muscles of broilers. Poult Sci. 1999; 78:812-21.
4. Kuhi HD, Kebreab E, Lopez S. France J. Anevaluation of different growth functions for describing theprofile of live weight with time (age) in meat and egg strainsof chicken. Poultry Sci. 2003; 82: 1536–1543.
5. Mohammed FA. Comparison of three nonlinearfunctions for describing chicken growth curves. ScientiaAgriculturae. 2015; 9 (3): 120-123.
6. Moharrery A, Mirzaei M. Growth characteristicsof commercial broiler and native chickens as predicted by different growth functions. J Anim Feed Sci.2014; 23: 82–89.
7. Prince SH. Modeling the broiler performance undersmall-scales and semi commercial management condition.Dissertation, Port Elizabeth Technician, George Campus.2002.
8. Roenick WP. Poultry will overtake pig meat consumption. World Poult. 1998; 12(14): 14-16.
9. Sabbioni A, Superchi P, BonomiA, Summer A. BoidiG. Growth curves of Ostriches in northern Italy. Paperpresented in 50th EAAP Congress, Zorich, 1999; 22-26.
10. Santos AL, Sakomura NK, Freitas ER, Fortes CMS, Carrilho ENVM.Comparison of free range broiler chicken strains raised in confined or semi-confined systems.Rev. Bras. Cienc.Avicola. 2005; 7:85–92.
11. SAS Institute, 2010. SAS/STAT User's Guide, Version9.1.SAS Institute Inc., Cary, NC.USA.

12. Schulze V, Rohe R, Looft H, Kalm E. Genetic analysis of the course of individual growth and feed intake of group-penned performance tested boars. Arch. Tierz. Dummerstorf.2001; 44:139-156.
13. Sun GR, Zhu ZM, He DG, Gong SM, Shen HM.Development Regularity of Early Body-Weight and the Fitness of Growth Curve on Lai-Chuan cross Chicken. Chinese JAnim Sci.2006; 42: 10-12.
14. Tompić T, Dobša J, Legen S, Tompić N, Medić H. Modeling the growth pattern of in-season and off-season Ross308 broiler breeder flocks. Poultry Sci. 2011; 90, 2879–2887
15. Topal M, BolukbasiSC.Comparison of NonlinearGrowth Curve Models in Broiler Chickens. JAPR.2008; 34: 149-152.
16. Tzeng RY, Becker WA. Growth pattern of body andabdominal fat weight in male broiler chickens. Poultry Sci.1981; 60:1101-1106.
17. Wang DQ, Lu LZ, Ye WC, Shen JD, Tao ZR, Tao ZL, Ma FL, Chen YC, Zhao A,Xu J. Study on theGrowth Regularity of Jinyun Muscovy Duck. Zhejiang J AnimSci Vet.2004;6:3-5.
18. Yakupoglu C, Atil H. Comparison of growth curvemodels on Broilers. II. Comparison of models. Online J. Biol. Sci. 2001;7: 682-684.
19. Yang Y, Mekki DM, Lv SJ, Wang LY, Wang JY.Analysis of fitting growth models in Jinghai mixed-sex yellow chicken. Int. J. Poult. Sci. 2006; 5: 517-521.

Table 1: Nutrient composition of the basal diet of broiler (Ross 308)

Ingredients	Starter 1-10 day	Growth 11-24 day	Finisher 25-35 day
Cornmeal	10.1	12	16.5
Wheat	50	50	50
Soybean meal 48 c.p	30	26	21.4
concentrated protein(1)	5	5	5
Sunflower oil	2.9	5.2	5.3
Calcium carbonate	0.9	0.9	0.9
Dicalcium phosphate	0.7	0.5	0.5
Sodium chloride	0.2	0.2	0.2
Mineral-vitamin-premix	0.2	0.2	0.2
Total	100	100	100
Calculated chemical analysis			
CP%	23	21.25	19.4
ME (kcal/kg)	3003	3153	3200
L-Lysine %	1.26	1.1	1.0
DL-Methionine %	0.48	0.45	0.43
Cysteine%	0.36	0.34	0.31
Methionine + Cyst %	0.84	0.796	0.74
Arginine%	1.28	1.15	1
Ca %	0.85	0.80	0.78
Av. Phosphorus %	0.43	0.40	0.40

Table 2: The Growth curve functions

Function	Mathematical model
WLS	W= a/(1+exp(-b-c*age))
Richard	W= a / ((1 + c * exp(-b * age)) ** (1 / d))
Weibull	W=a - b * exp(-c * age ** d)
Logistic	W=a/(1+b*exp(-c*age))
Gompertz	W=a*exp(-exp(b-c*age))

Table 3: Means±SE of the weekly body weight in the males and females Ross 308 broilers

Period	Male	Female	P
1st day	41.16±0.65	39.66±0.53	0.08
Week 1	163.11±3.01	156.53±3.49	0.15
Week 2	427.50±6.89	384.58±6.03	<0.0001
Week 3	803.00±12.78	712.17±14.71	<0.0001
Week 4	1323.30±18.16	1122.80±26.93	<0.0001
Week 5	1739.80±29.30	1429.70±27.98	<0.0001

Table 4: The prediction of the males'weight (gm) during different age stages in Ross 308 broiler according to different functions

Age	Observed Weight	WLS	Richard	Logistic	Weibull	Gompertz
1day	41.16	35.31	52.12	68.13	48.01	35.31
Week1	163.11	156.54	162.31	171.59	156.6	156.54
Week2	427.5	424.54	411.8	401.69	416.25	424.54
Week3	803	828.28	823.13	813.06	825.48	828.28
Week4	1323.3	1296.07	1310.47	1325.02	1307.31	1296.07
Week5	1739.8	1749.43	1743.4	1737.85	1744.23	1749.43

Table 5: The estimated parameters of studied functions in males'Ross 308 broilers

Function	a	b	c	d
Weighted Least Square	2082.7	-4.50	-0.82	-
Richard	2490.2	0.65	8.43	0.43
Weibull	2297.0	2266.0	0.0075	2.92
Gompertz	3215.8	1.90	0.40	-
Logistic	2142.2	80.68	0.97	-

Table 6: Some accuracy criteria of the functions in the male Ross 308 broilers

Function	MSE	R^2	r	SE
Weighted Least Square	292.8	0.99991	0.99993	12.43
Richard	475.0	0.99983	0.99978	21.79
Weibull	498.3	0.99977	0.99977	22.32
Gompertz	519.8	0.99974	0.99965	22.79
Logistic	524.5	0.99972	0.99965	22.90

Table 7: The prediction of the female's weight (gm) during different age stages in Ross 308 broiler according to different functions

Age	Observed Weight	WLS	Richard	Logistic	Weibull	Gompertz
1day	39.66	57.76	49.55	63.37	45.95	33.98
Week1	156.53	151.12	152.14	159.01	148.13	148.31
Week2	384.58	361.33	376.29	366.7	380.29	388.51
Week3	712.17	723.26	726.01	719.24	727.08	728.94
Week4	1122.8	1132.24	1112.79	1125.18	1110.59	1099.73
Week5	1429.7	1421.06	1432.76	1427.53	1433.4	1438.76

Table 8: The estimated parameters of studied functions in female's Ross 308 broilers

Function	a	b	c	d
Weighted Least Square	1659.0	-4.34	1.02	-
Richard	1921.3	0.68	8.52	0.45
Weibull	1784.0	1755.1	0.0097	2.84
Gompertz	2388.1	1.87	0.42	-
Logistic	1702.3	68.92	0.98	-

Table 9: Some accuracy criteria of the functions in the female Ross 308 broilers

Function	MSE	R^2	r	SE
Weighted Least Square	195.2	0.99993	0.99996	6.77
Richard	243.5	0.99987	0.99983	15.60
Weibull	256.8	0.99978	0.99983	16.02
Logistic	316.1	0.99976	0.99968	17.77
Gompertz	337.0	0.99974	0.99966	18.36

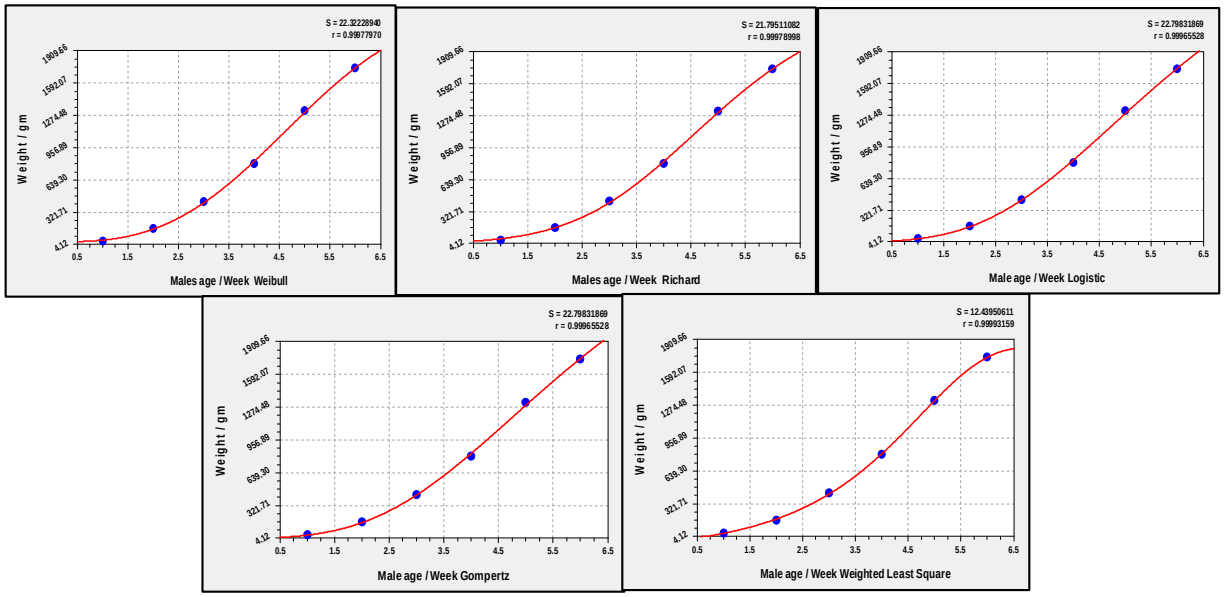

Figure 1: Fitting the growth carve of the males Ross 308

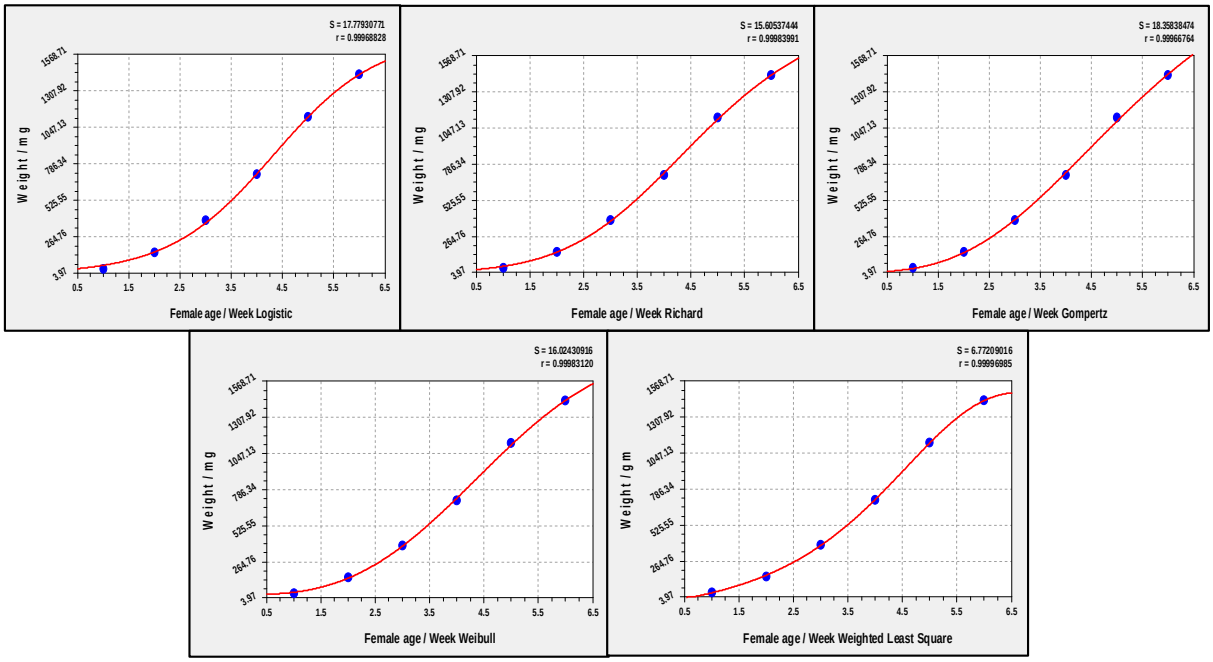

Figure 2: Fitting the growth carve of the females Ross 308

Indian Journal of Natural Sciences www.tnsroindia.org.in ©IJONS

Vol.8 / Issue 49 / August /2018 *International Bimonthly* *ISSN: 0976 – 0997*

RESEARCH ARTICLE

Study the Crystal Structure, Surface Morphology, and Antimicrobial Activity of Titanium Dioxide Nanopowders Prepared via a Sol-Gel Method

Ali Abdullah Fayyadh [1*], Abbas Fadhel Essa[2], Shatha Shammon Batros[3] and Zinah Shakir Shallal[4]

[1, 2] Department of Physics, College of Science, Wasit University Wasit, Iraq.
[3] Ministry of Science and Technology, Bagdad, Iraq.
[4]Department of Biology, College of Science, Wasit University, Wasit, Iraq.

Received: 20 May 2018 Revised: 23 June 2018 Accepted: 24 July 2018

[*]**Address for Correspondence**
Ali Abdullah Fayyadh
Department of Physics,
College of Science,
Wasit University,
Wasit, Iraq.
E-mail: alia224@uowasit.edu.iq

ABSTRACT

In this research, Titanium dioxide Nanopowders were prepared via the sol-gel method at alkaline medium (pH 9). TiO_2 Nanoparticles was prepared from Titanium (III) chloride ($TiCl_3$) and ammonium hydroxide (NH_4OH) as a precursor with 1:3 ratios. The manufactured TiO_2 Nanoparticles were studied and characterized by X-Ray Diffraction (XRD), Scanning Electron Microscope (SEM) , and Atomic Force Microscopy (AFM) .The antibacterial activity of the prepared specimens was indicated by the Kirby-Bauer disc method (KB testing). The outcomes demonstrated a very good antibacterial activity of TiO_2 Nanoparticles to microbe's strains: Gram positive *Staphylococcus aureus*, Gram negative *Pseudomonas aeruginosa*, and Gram negative *Escherichia coli*. The affectability of the tried microscopic organisms to TiO_2 Nanoparticles relies upon the crystalline type of the bearer TiO_2, density of unit cell, unit cell volume, particle size, and oxidation state.

Keywords: TiO_2 Nanopowders, sol-gel method, Antibacterial activity, particle size.

INTRODUCTION

Titanium dioxide, as well known as "Titania" and its chemical formula is TiO_2 (1). TiO_2 Nanoparticles have been of interest in a broad range of utilization such as photocatalysts and antimicrobial activity (2), dye-sensitized solar cells (3), a gas sensor (4), and Nano-medicine (5).Its photocatalytic characteristics have been used in different

Environmental applications to eliminate contaminants from both water and air **(6)**. TiO_2 Nanoparticles, in particular, has shown obvious-spectrum antibacterial activity against both Gram positive and Gram negative bacteria, where TiO_2 Nanoparticles working on inhibiting the formation of bacterial biofilms of Staphylococcus aureus, Escherichia coli, and Pseudomonas aeruginosa **(**7**)**. There are three types of TiO_2 crystalline phases which are brookite has an orthorhombic crystalline structure, anatase, and rutiles have a tetragonal crystalline structure. Only anatase and rutile phases show an excellent photocatalytic activity and antibacterial performance. In both structures, the Ti atom is circled by six oxygen atoms and every oxygen atom is circled by three atoms of Ti **(**8-9). The performance of TiO2 is greatly impacted via the crystalline structure, the morphology and the volume of the particles (10). TiO_2 Nanoparticles are of especially interest due to their especially volume-related properties. As the size, shape, and crystal structure of TiO_2 Nanoparticles change, not only does surface stability change but also the transformations between various phases of TiO_2 under compression and temperature **(**11**)**.TiO_2 Nanoparticles have been synthesized using different techniques such as hydrothermal (12), sonochemcal (13), solvothermal (14), reverse micelles (15), and sol-gel reaction for those applications. Latterly, the sol-gel method has been utilized in the preparation of TiO_2 Nanoparticles (16).

The sol-gel method is greatly used for the manufacture of TiO_2 Nanoparticles. The sol-gel method is a chemical method for the manufacture of nanomaterials beginning either from a chemical Sol or colloidal particles to create a linked network.Exemplary precursors are mineral alkoxides and mineral chlorides, which undergo hydrolysis and polycondensation reactions to generate a colloid, a system formed of solid particles (volume ranging from 1 nm to 1 µm) disbanded in a solvent. The solution results then towards the production of an inorganic consecutive network including a liquid phase (gelation)**(**17**)**. The sol-gel technique had additionally been utilized to prepared nanopowders at low preparation temperature have shown that by using the sol-gel method, controlled the size and narrow size apportionment of prepared powder can be achieved under optimized preparation condition **(18)**. In this research, TiO_2 Nanoparticles were synthesis via a sol-gel method at various calcined temperatures (300, 500, and 700°C). The influence of the calcined temperatures on the particle size and structure of the powders were studied. The results are characterized by X-Ray Diffraction (XRD) , Scanning Electron Microscopy (SEM) , and Atomic Force Microscope (AFM) . Finally, study the antibacterial activity of the intended TiO_2 Nanoparticles.

MATERIALS AND METHODS

Preparation of TiO_2 Nanoparticles

The sol-gel method was utilized to synthesize TiO_2 Nanoparticles. Titanium (III) chloride ($TiCl_3$) (99.9% Sigma Aldrich), and ammonium hydroxide (NH_4OH) (98% Sigma Aldrich) were utilized as the Titanium ancestor. 100 ml $TiCl_3$ solution was slowly added dropwise to 300 ml NH_4OH for 2hrs. The reaction was performed at 50 °C under strong stirring at 700 rpm for 2hrs, providing a final sol. At first, the mixture color is black and then becomes violet, after that changed to deep blue like a clear sky and then gradually turns to the white homogeneous solution. The pH of the resulting solution is measured and adjusting to the value 9. The solution was transformed to a gel by using ultrasonic bath device for 2hours. Finally, the gel was forcibly washed with distilled water many times for separating the contaminants (ammonia and chlorine ions). The gel was dried at (70°C) for 24h, the final powders were calcined at various temperatures (300, 500, and 700°C) for 1 hour in an ambient atmosphere, the powder transforms to TiO_2Nanoparticles in anatase phase. The resulting powders were squeezed as tablets with a diameter 10 mm.

Preparation of Bacteria for Sensitivity Test

Gram positive *Staphylococcus aureus*, Gram negative *Pseudomonas aeruginosa*, and Gram negative *Escherichia coli* it was used to performing the sensitivity test. The bacterial was subcultured on a rich medium like tryptic soy agar to activate it and incubated at 37 °C overnight for the sensitivity test. The bacteria were suspended in physiological

saline 0.85% and the turbidity of the suspension was compared with 0.5 McFarland turbidity standard tube which equal to (1×108 Colony Forming Unit /ml), McFarland was prepared according to MacFaddin (2000): (9.95 mL) of 1% sulphuric acid with 0.05 mL of 1.176%barium chloride dihydrate. (5mL) was a liquated into screw-capped tubes of the same size which were used in the procedure, the standard was stored in dark at room temperature and was vortexed prior to use. The bacterial suspension swabbed on the surface of "Muller Hinton agar" (the general media used for antimicrobial sensitivity test).TiO_2 tablets were distributed on the surface of the agar using sterilized forceps, this method termed disc diffusion method and the dishes were incubated at 37 °C overnight (18-24 hours) then the inhibition zone was measured in mm.

Characterization

The crystalline structure of TiO_2 powder examined by X-Ray Diffraction device model (Shimadzu-6000-XRD) manufactured in Japan records the intensity as a function of Braggs angle, with the following Specifications: Target is copper (Cu) with wavelength (λ=1.5406 °A), voltage (40 kV) and current (30mA). The scanning angle 2theta is changed in the range of (10-70) degree with a speed of (5 dig/min). The morphological surface study was conducted out using an atomic force microscope (SPM Ntegra NT – MDT) made in Russia. The SEM measurements are performed with a TESCAN VEGA 3, made by the Czech Republic.

RESULTS AND DISCUSSION

X-ray diffraction (XRD) analysis

Powder X-Ray Diffraction (XRD) analysis has been done to study the crystal structures, crystalline size, crystal density, and lattice parameter of the TiO_2 Nanoparticles prepared at different heat treatment. The primary formed structure observed at drying temperature 70°C is (NH_4Cl) as shown in fig.1.(a) The XRD pattern showed that this specimen has three sharp peaks 2θ angle at 32.743θ , 58.349θ, and 23.020θ with (101), (211), and (100) diffraction planes, respectively.It can be seen that very high percentage of (NH_4Cl) phase have sharp peaks. In addition, existence a small percentage of Ti which turns to TiO_2 as the calcined temperature increases. Fig.1. (b) Shows (XRD) analysis of calcined TiO_2 Nanoparticles at variouscalcined temperatures (300, 500, and 700°C).Anatase phase starts to appear at (300°C) calcined temperature. The peaks sharp become higher when calcined temperature increasing to (500 °C), and it remains at the same phase (i.e. anatase phase). Calcined temperature showed anatase-rutile mixed phase at (700°C). We named the predominant peaks linked with anatase (A) and rutile(R) phases.

The XRD pattern showed that the sample calcined at 300 °C has three sharp peaks 2θ angle at 25.317θ, 47.981θ, and 37.893θ with (101), (200), and (004) diffraction planes, respectively. The XRD pattern showed that the sample calcined at 500 °C has three sharp peaks 2θ angle at 25.290θ, 48.002θ, and 37.801θ with (101), (200), and (004) diffraction planes, respectively. The XRD pattern showed that the sample calcined at 700 °C has three sharp peaks 2θ angle at 25.306θ, 48.033θ, and 37.818θ with (101), (200), and (004) diffraction planes, respectively. The crystalline size of the prepared powders was determined by Debye Scherrer formula 1.

$$D = \frac{0.9\,\lambda}{\beta \cos\theta} \qquad \textbf{(1)}$$

Where, "D" is the crystallite size, "λ" is the wavelength of the incident X-ray beam, "θ" is the diffraction angle (Bragg's angle), and (β) is the Full Width at Half Maximum (FWHM)**(18)**. The distance between the crystalline levels was calculated by equation 2.

$$n\lambda = 2d\sin\theta \quad \textbf{(2)}$$

Where, "d"is the separation between atomic layers in a crystal, "λ" is the incident X-Ray wavelength, "θ" is the diffraction angle (Bragg's angle), and "n" is an integer representing the order of the diffraction peak **(**19-20**)**. The lattice parameters (a, b and c) were determined from the lattice spacing of Anatase (200) and (004) peaks by using the Bragg formula for the tetragonal lattice structure (a=b≠ c) using equation 3.

$$\frac{1}{d^2} = \frac{h^2 + k^2}{a^2} + \frac{l^2}{c^2} = \frac{4\sin^2\theta}{\lambda^2} \quad \textbf{(3)}$$

Ammonium chloride (NH_4Cl) has a cubic crystal structure **(21)**.The lattice constant was determined from the lattice spacing of NH_4Cl (101)peak by utilizing the Bragg equation for the cubic lattice structure (a=b=c) applying equation 4.

$$\frac{1}{d^2} = \frac{(h^2 + k^2 + l^2)}{a^2} = \frac{4\sin^2\theta}{\lambda^2} \quad \textbf{(4)}$$

Where, d is the spacing between the planes, (θ) is the diffraction angle (Bragg's angle),λ is the X-ray wavelength and (a, b and c) are the lattice parameters **(**22**)**. The volume of the unit cell for the specimens was determined by using the relation 5.

$$V = a^2 \times c \quad \textbf{(5)}$$

Where, V is the unit cell volume in cm^3, "a" and "c" are the lattice parameters.
The densities were determined by utilizing the formula 6.

$$\rho = \frac{FW \times Z}{V \times N_A} \quad \textbf{(6)}$$

Where, ρ is the density of unit cell (g/cm^3), FW is the formula weight, for anatase (FW= 79.89 gm/mol), and for NH_4Cl (FW= 53.49 gm/mol), Z is the number of unit cells, for anatase Z = 4, and Z=1 for NH_4Cl, V is the unit cell volume in cm^3 and N_A is Avogadro constant in per mol **(22**-23**)**. XRD analysis showed that when the calcined temperatures rise from 300 °C to 700 °C, the lattice parameters were slightly decreased, the FWHM decreases, and the average crystallite size increase. This outcome was also in good synchronized with the previous work**(24-25)**.Table1.Summarizes the structural properties of the specimen dried at (70 °C), and TiO_2 Nanoparticles synthesized at differentcalcined temperatures (300 °C, 500 °C, and 700 °C) for 1h and pH 9.

Scanning Electron Microscopy (SEM) Studies

Morphological, topography and crystallographic information of the obtained results for TiO_2 Nanoparticles were studied by the high-resolution Scanning Electron Microscopy (SEM) . Fig.2. Gives the surface morphology of the TiO_2 Nanoparticles for the sample dried at (70 °C) and calcined temperatures (300, 500, and 700°C) which shows the particle sizes become larger as the calcining temperature was raised.

Atomic Force Microscope (AFM) Studies

The topography, surface features, and the grain size of TiO_2 Nanoparticles were studied by using Atomic Force Microscope (AFM). Table 2.Summarizes the particle grain size, surface roughness, and root mean square measurements of the specimen dried at (70 °C), and TiO_2 Nanoparticles synthesized at various calcined temperatures (300, 500, and 700°C).For 1h and pH 9. It was observed when calcined temperatures increased from 300°C to 700°C the particles size increased. Fig. 3. Shows the Atomic Force Microscope (AFM): 2D and 3D images which described the surface topography of the TiO_2 Nanoparticles for the sampledried at (70 °C), and at calcined temperatures (300, 500, and 700°C). Fig. 4. Shows the Average Particle size range distribution for the dried sampleat (70°C), and calcined temperatures: (a) 300, (b) 500, and (c) 700°C.

According to the results, from the study of XRD, SEM, and AFM concluded that a raise in particle size of TiO_2 is linked with the rise in the calcining temperatures. After the calcining process, the crystals size raise because (OH) links are broken and crystals start to grow. This may happen due to the heat-induced TiO_2 collection and phase transmutation. The empirical determination concluded in this work provides for greater knowledge of the parameters that measure the increase of TiO_2 Nanoparticles while manufacturing with the sol-gel method. Also, the agglomeration grows bigger when the calcining temperatures are raised. It is seen that, in the raised calcining temperatures, the bigger particle size with unique topography is acquired for the specimen calcined at high temperatures. An addition of the temperature up to 700°C, the size grows higher than 300°C, and 500°C as well the agglomeration become great. The particle size grows larger as the calcining temperature was increased to 700°C, which described the influences of heat processing on the particle size of TiO_2 Nanoparticles. The thermic operation is needed to increase the crystallinity of amorphous powder. When TiO_2 Nanoparticles are calcined at a greater heat, crystal structure transmutations may happen. The phases (NH_4Cl, anatase, and anatase-rutile) are highly dependent on the method preparations, the species of the precursor and calcining statuses. Generally, the total transformation of NH_4Cl to anatase has been discovered to be formed at 300°C, and 500°C. The anatase-rutile transmutation has been notified to happen in 700 °C temperature. The SEM pictures demonstrate that utmost of the particles in spherical shape and influence of heat process on particle size was significant. The crystal growth becomes higher attributed to an increase in particle size with calcined temperature was raised from 300 °C to 700°C. The SEM and AFM result in an excellent agreement with XRD data.

Antibacterial activity of TiO_2 Nanoparticles

Based on the region of inhibition investigation, Table 3. Shows the region of microorganism's growth inhibition for *Staphylococcus aureus*, *E.coli*, and *Pseudomonas aeruginosa*. The diameter of the inhibition region was calculated in mm. It was observed that when calcined temperatures of TiO_2 increase (increasing of TiO_2 particles size) leads to the Zone of inhibition. Fig.5. shows the pictures of the region of growth inhibition for Staphylococcus aureus, E.coli, and Pseudomonas aeruginosa for a dried sample at 70 °C. Fig.6. shows the pictures of the region of growth inhibition for Staphylococcus aureus, E. coli, and Pseudomonas aeruginosa for TiO_2 Nanoparticles at calcined temperatures (a) 300 °C, (b) 500°C, and (c) 700°C.The mechanism of killing bacteria includes degeneration of the cell wall and cytoplasmic layer due to the generation of reactive oxygen kinds (ROK) like hydroxyl rebels and hydrogen peroxide. This firstly leads lost within a leak of cellular contents then cell lysis and perhaps followed by total mineralization of the organism. Contact between the cells of bacterium and TiO_2 may affect membrane permeability and this is lead to increased damage to all cell wall layers, allowing leakage of small molecules such as ions. Damage at this stage may be irreversible, and this accompanies cell death. Furthermore, membrane damage allows leakage of higher molecular weight components such as proteins, which may be followed by protrusion of the cytoplasmic membrane into the surrounding medium through degraded areas of the peptidoglycan and lysis of the cell. Degradation of the internal components of the cell then occurs, followed by complete mineralization. The degradation process may occur progressively from the side of the cell in contact with the TiO_2 nanoparticles.

CONCLUSION

TiO_2 Nanoparticles were prepared by utilizing the sol-gel technique. It is found that TiO_2 Nanoparticles is a viable material for antibacterial agents of gram positive *staphylococcus aureus*, gram negative *pseudomonas aeruginosa*, and gram negative *escherichia coli*. The structure and morphology were characterized using different techniques XRD, SEM, and AFM. From XRD characterization, the specimen dried at (70 °C) indicate NH_4OH phase with average crystallite size (47.806) nm, the specimen s calcined at 300 °C, and 500 °C indicate Anatase phase with average crystallite size (12.076) nm, and (17.366) nm, respectively. And the specimen calcined at 700 °C indicate (Anatase--Rutile) mixed phase with average crystallite size (28.77) nm. From the determination of SEM and AFM showed that an increment in particle size of TiO_2 Nanoparticles is associated with the increase in the calcining temperatures. It is found that the average particles size distribution ranging from (91.4 - 132.8) nm. It was observed that when calcined temperatures of TiO_2 Nanoparticles increased from (300 °C to 700 °C) the TiO_2 Nanoparticles size increased and the zone of inhibition diameter decreased.

ACKNOWLEDGEMENTS

This work was supported by solid state physics laboratory in Wasit University, college of science, physics department, and Ministry of Science and Technology, Materials Research Department.

REFERENCES

1. Zakarya SA, Kassim A, Lim HN, Anwar NS, Huang NM.Synthesis of titanium dioxide microstructures via sucrose ester microemulsion-mediated hydrothermal method. Sains Malaysiana. 2010; 39(6):975-9.
2. Zielińska-Jurek A, Wei Z, Wysocka I, Szweda P, Kowalska E.The effect of nanoparticles size on photocatalytic and antimicrobial properties of Ag-Pt/TiO_2 photocatalysts.Applied Surface Science. 2015; 353:317-325.
3. Kashyout AB, Soliman M, Fathy M. Effect of preparation parameters on the properties of TiO_2 nanoparticles for dye sensitized solar cells. Renewable Energy. 2010; 35(12):2914-2920.
4. BaiJ, Zhou B.Titanium dioxide nanomaterials for sensor applications. Chemical reviews. 2014; 114(19):10131-10176.
5. Galkina O.L, Sycheva A, Blagodatskiy A, Kaptay G, Katanaev V.L, Seisenbaeva G.A, et al. The sol–gel synthesis of cotton/TiO_2 composites and their antibacterial properties. Surface and Coatings Technology. 2014; 253:171-179.
6. Haider AJ, AL–Anbari RH, Kadhim GR, Salame CT. Exploring potential environmental applications of TiO_2 nanoparticles. Energy Procedia. 2017; 119:332-345.
7. Wang L, Hu C, Shao L. The antimicrobial activity of nanoparticles: present situation and prospects for the future. International journal of nanomedicine. 2017; 12:1227-1249.
8. Allen NS, Mahdjoub N, Vishnyakov V, Kelly PJ, Kriek RJ. The effect of crystalline phase (anatase, brookite and rutile) and size on the photocatalytic activity of calcined polymorphic titanium dioxide (TiO_2). Polymer Degradation and Stability. 2018; 150:31-36.
9. Malekshahi Byranvand M, Nemati Kharat A, Fatholahi L, Malekshahi Beiranvand Z. A review on synthesis of nano-TiO_2 via different methods. Journal of nanostructures. 2013; 3(1):1-9.
10. Hadjipanayis GC, Siegel RW, editors. Nanophase materials: Synthesis-properties-applications. Springer Science & Business Media; 2012.
11. Gopal M, Chan WM, De Jonghe LC. Room temperature synthesis of crystalline metal oxides. Journal of Materials Science. 1997; 32(22):6001-6008.
12. Tan Z, Sato K, Ohara S. Synthesis of layered nanostructured TiO_2 by hydrothermal method. Advanced Powder Technology. 2015; 26(1):296-302.

13. Mizukoshi Y, Makise Y, Shuto T, Hu J, Tominaga A, Shironita S, Tanabe S. Immobilization of noble metal nanoparticles on the surface of TiO_2 by the sonochemical method: Photocatalytic production of hydrogen from an aqueous solution of ethanol. Ultrasonics sonochemistry. 2007; 14(3):387-392.
14. Zhang Y, Zheng H, Liu G, Battaglia V. Synthesis and electrochemical studies of a layered spheric TiO_2 through low temperature solvothermal method. Electrochimica Acta. 2009; 54(16):4079-4083.
15. Inaba R, Fukahori T, Hamamoto M, Ohno T. Synthesis of nanosized TiO_2 particles in reverse micelle systems and their photocatalytic activity for degradation of toluene in gas phase. Journal of Molecular Catalysis A: Chemical. 2006; 260(1-2):247-254.
16. Maya Devi, Manas R. Panigrahi, and U. P. Singh. Synthesis of TiO_2 nanocrystalline powder prepared by sol-gel technique using TiO_2 powder reagent. Adv. Appl. Sci. Res., 2014; 5(3):140-145.
17. Nachit W, Touhtouh S, Ramzi Z, Zbair M, Eddiai A, Rguiti M, et al. Synthesis of nanosized TiO2 powder by sol gel method at low temperature. Molecular Crystals and Liquid Crystals. 2016; 627(1):170-175.
18. Roohollah A, Sousan R, Naghi P.A, Amin J. jk, Mohammad A. A systematic Investigation of Expermental Condition on the Particle Size and Structure of TiO_2 nanoparticles Synthesized by a Sol-Gel Method. Journal of Ceramic Processing Research. 2012; 13(2):164-169.
19. Bragg W.H, Bragg W.L. The Reflection of X-rays by Crystals. Proc. R. Soc. Lond.A. 1913; 88(605): 428-438.
20. Conrado A, Maria PG. Biomineralization and Biomaterials Fundamentals and Applications. 1st Ed. Sawston, Cambridge, UK: Woodhead Publishing; 2016.
21. Hazrati AM, Peters LK. Effect of temperature on the structure and density of ammonium chloride particles. Journal of Aerosol Science. 1981 Jan 1; 12(6):467-476.
22. Cullity B.D, Stock S.R. Elements of X-Ray Diffraction. 3rd Ed. USA: Pearson New International Edition; 2013.
23. Hussain S, Maqsood A. Influence of sintering time on structural, magnetic and electrical properties of Si–Ca added Sr-hexa ferrites. Journal of magnetism and magnetic materials. 2007; 316(1):73-80.
24. Sharmila J.S, Ramalingom S, Ravidhas C, Moses R.A. Effect of Calcined Temperature on Titanium Oxide Nanocrystallites in the Anatase Phase Synthesized By Sol-Gel Route. J. Appl. Phys. 2017; 9(4):32-39.
25. Yadanar W.M, Tun T.M, Wint Y.L. The Effect of Heat Treatment on Phase Transformation and Morphology of Nano-Crystalline Titanium Dioxide (TiO_2). Int. J. Sci. Technol. 2017; 6(6):293-299.

Table 1. Structural properties of the sample dried at (70 °C), and TiO_2 Nanoparticles synthesized at different calcined temperatures (300 °C, 500 °C, and 700 °C) for 1h and pH

Sample Calcined Temperatures (°C)	hkl	2 θ (Deg.)	FWHM (Deg.)	Crystalline size (nm)	d_{hkl}(Å)	Lattice parameters (Å)	Unit cell volume V (Å^3)	Density ϱ (g/cm^3)
Draying at (70 °C)	(101)	32.743	0.1869	46.25	2.73284	NH_4CL (Cubic) $a = b = c =$ 3.8648	57.7272	1.5386
	(211)	58.349	0.1863	50.99	1.58019			
	(100)	23.020	0.1833	46.18	3.3886			
(300 °C)	(101)	25.317	0.7191	11.82	3.51506	Anatase a = b = 3.7891 c = 9.5144	136.601	3.8847
	(200)	47.981	0.7292	12.45	1.89455			
	(004)	37.791	0.7333	11.96	2.37241			
(500 °C)	(101)	25.290	0.5209	16.32	3.51871	Anatase a = b = 3.7875 c = 9.5120	136.451	3.8889
	(200)	48.002	0.5733	15.84	1.89376			
	(004)	37.801	0.4397	19.94	2.37797			
(700 °C)	(101)	25.306	0.3019	28.16	3.51652	Anatase a = b = 3.7852 c = 9.5079	136.226	3.8953
	(200)	48.033	0.3010	30.17	1.89263			
	(004)	37.818	0.3136	27.98	2.3768			

Table 2. Surface roughness and root mean square measurements for TiO_2 Nanoparticles at pH 9 with different calcined temperatures

Calcined Temperature °C)	G.S (nm)	RMS (nm)	Surface roughness (nm)	Peak-to-peak (nm)
Draying at (70 °C)	91.4	29.479	23.222	199.645
(300 °C)	107.1	31.426	25.007	213.471
(500 °C)	119.4	33.711	26.858	232.816
(700 °C)	132.8	53.188	42.692	379.337

Table 3. Region of microorganism's growth inhibition

Bacteria type	Inhibition zone diameter (mm)			
	Draying Sample at 70 °C	Calcined temperature (300 °C)	Calcined temperature (500 °C)	Calcined Temperature (700 °C)
Staphylococcus aureus	13	51	42	37
E. coli	16	35	31	29
Pseudomonas aeruginosa	25	33	30	26

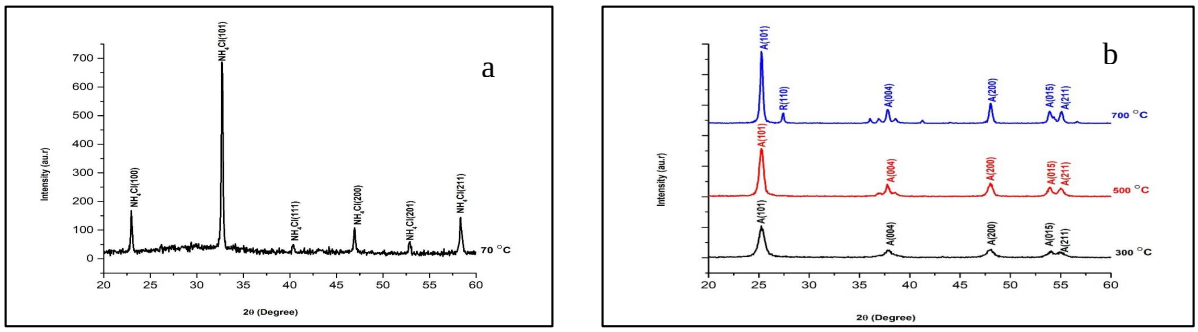

Fig.1. (a) XRD analysis of the primary formed structure (NH_4Cl) at drying temperature 70°C. (b) XRD patterns of TiO_2 Nanoparticles calcined temperatures (300, 500, and 700°C) A anatase and R rutile

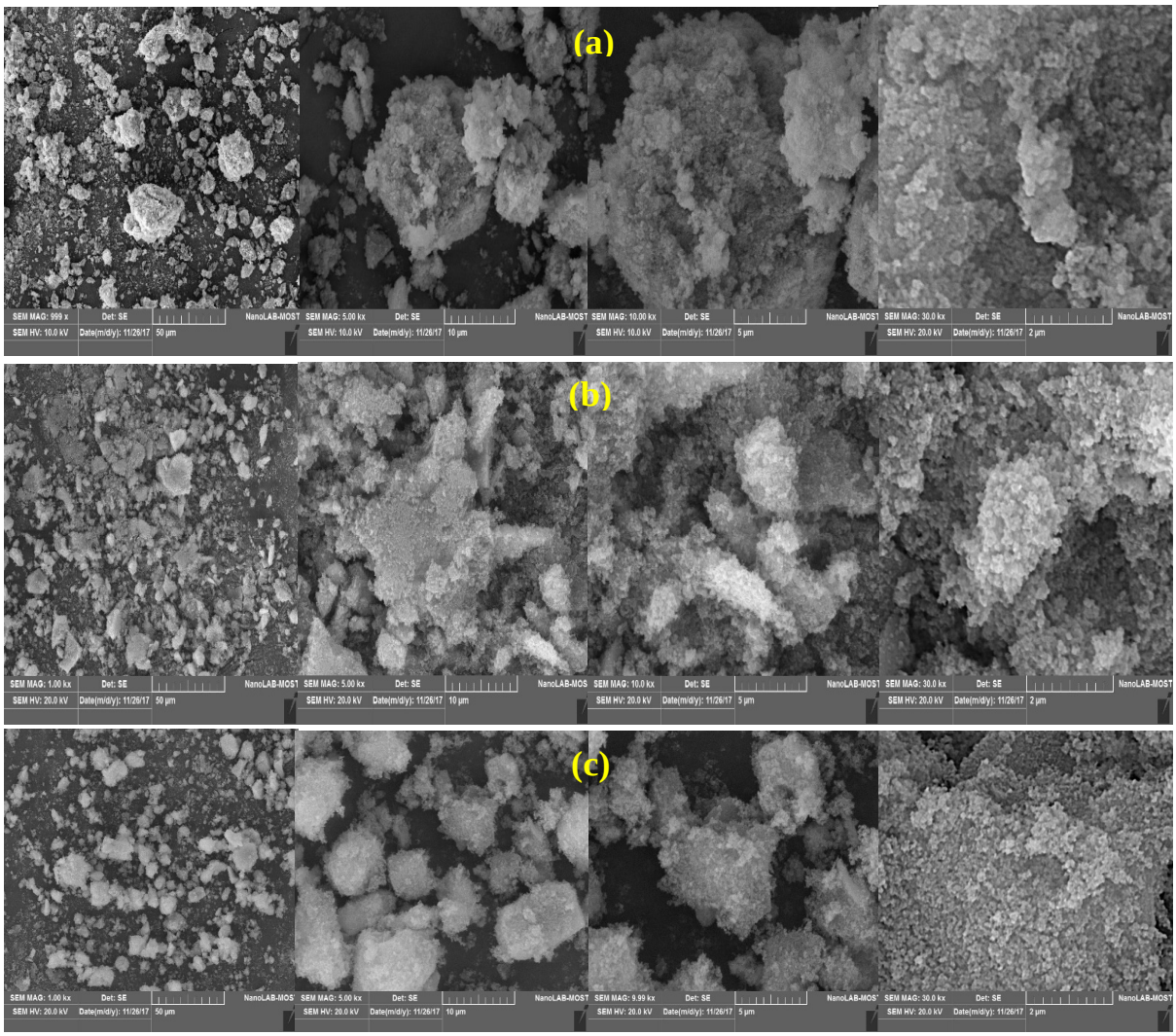

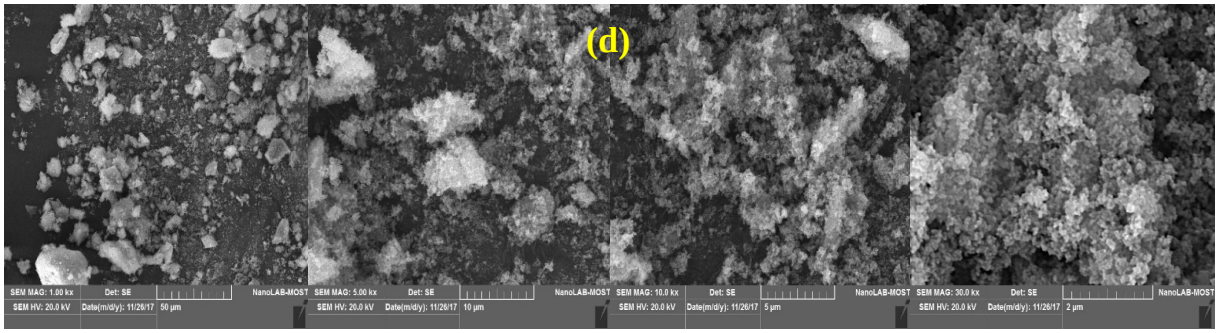

Fig. 2. SEM micrographs of (a) The sample dried at (70 °C) (NH_4Cl), TiO_2 Nanoparticles at calcined temperatures: (b) 300˚C, (c) 500 ˚C, and (d) 700˚C with four different magnifications 1.00kx, 5.00kx, 10.00kx and 50.00kx respectively (from the left to the right).

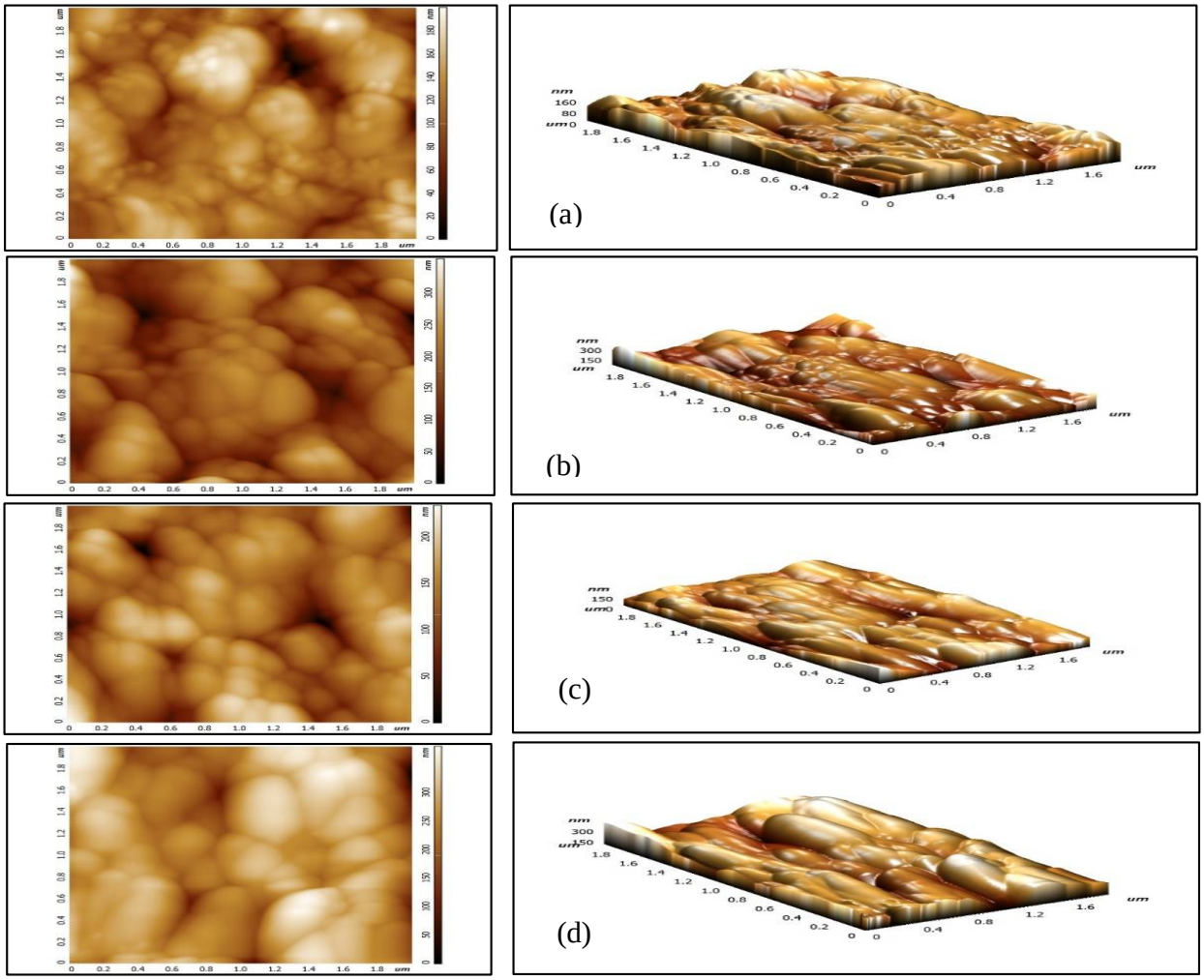

Fig. 3. AFM 2D and 3D images: (a) dried specimen at (70 ˚C), and TiO_2 Nanoparticles at calcined temperatures: (b) 300 ˚C, (c) 500 ˚C, and (d) 700 ˚C.

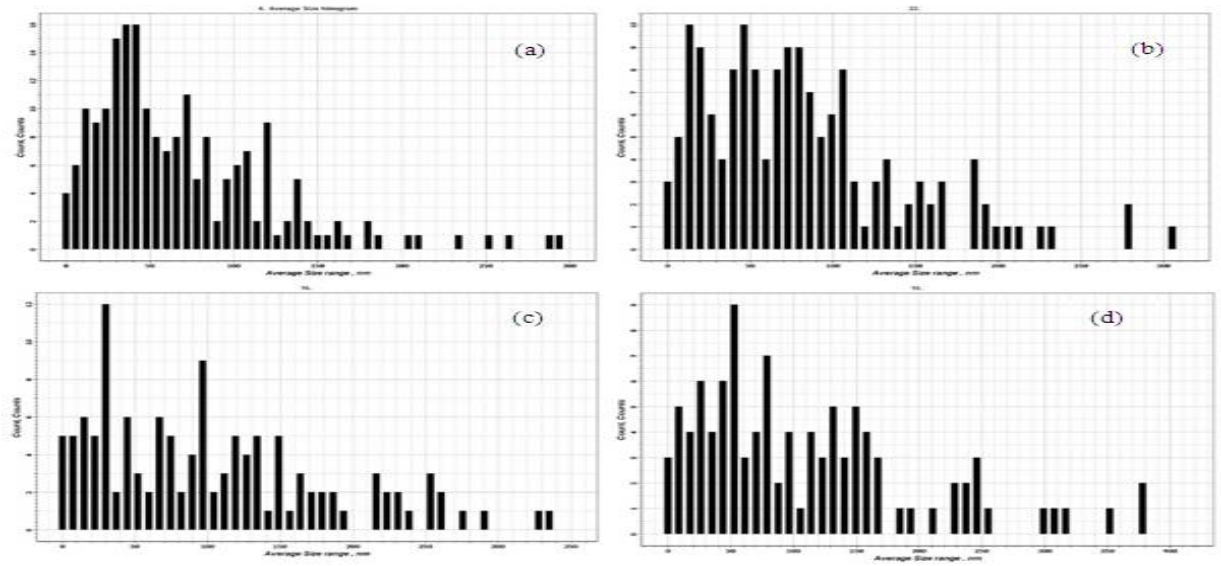

Fig. 4. Average Particle size distribution in nanometer scale histogram for (a) dried sample at (70 ^{O}C), and TiO_2 Nanoparticles at calcined temperatures: (b) 300 ^{O}C, (c) 500 ^{O}C, and (d) 700 ^{O}C.

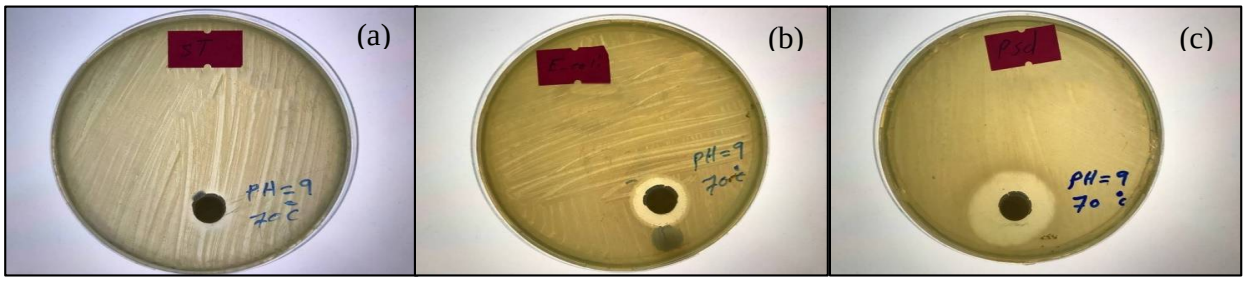

Fig. 5. Antibacterial activity of dried samples at temperature 70 ^{O}C at pH 9 against (a) Staphylococcus aureus, (b) E. coli, (c) Pseudomonas aeruginosa.

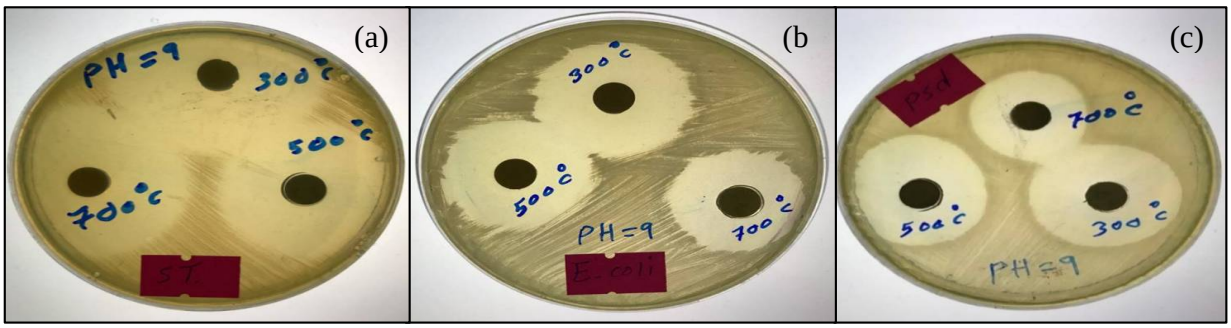

Fig. 6. Antibacterial activity of TiO_2 Nanoparticles of different calcined temperature (300 ^{O}C, 500 ^{O}C and 700 ^{O}C) at pH 9 against (a) Staphylococcus aureus, (b) E. coli, (c) Pseudomonas aeruginosa.